

Medical University of South Carolina

MEDICA

MUSC Theses and Dissertations

2014

Alveolar Epithelial Type II Cell Metabolism in Health, Hypoxia and Disease

Robyn Grayson Lottes

Medical University of South Carolina

Follow this and additional works at: <https://medica-musc.researchcommons.org/theses>

Recommended Citation

Lottes, Robyn Grayson, "Alveolar Epithelial Type II Cell Metabolism in Health, Hypoxia and Disease" (2014). *MUSC Theses and Dissertations*. 507.

<https://medica-musc.researchcommons.org/theses/507>

This Dissertation is brought to you for free and open access by MEDICA. It has been accepted for inclusion in MUSC Theses and Dissertations by an authorized administrator of MEDICA. For more information, please contact medica@musc.edu.

**Alveolar Epithelial Type II Cell Metabolism
in Health, Hypoxia & Disease**

by

Robyn Grayson Lottes

2014

A dissertation submitted to the faculty of the Medical University of South Carolina
in partial fulfillment of the requirements for the degree of Doctor of Philosophy in
the College of Graduate Studies.

Molecular & Cellular Biology & Pathobiology Program
Marine Biomedicine & Environmental Sciences
Department of Pediatrics

ACKNOWLEDGEMENTS

I am deeply indebted to the many people in my life who have helped me reach my goals, both professionally and personally. I am exceptionally grateful to my mentor, Dr. John Baatz, for providing outstanding training and a positive role model both in the lab and beyond. Special thanks is owed to Dr. Danforth Newton, who has been a kind and helpful colleague and friend and without whom this work would not have been possible. Thanks also to the members of my graduate committee who each in their own way have heavily influenced this work and my development as an independent scientist.

My sincere gratitude to Dr. Eric Lacy, Dr. Louis Guillette, and Ms. Taneisha Simpson of the MBES program for their unwavering support of my professional and personal growth; Dr. Carol Wagner and the Kellogg Vitamin D Study team for teaching me the science and art of clinical work; and Dr. Andrew Shedlock & the College of Charleston Biology Department for allowing me to join them for many wonderful semesters of teaching and learning. I also need to acknowledge my fellow students in the Marine Biomedicine & Environmental Sciences program: I have been lucky and proud to call you all my peers. Additional thanks to Dr. Ralph Saenz for the enduring inspiration to rock harder.

Finally, my deepest appreciation goes to my amazing, inspiring parents and my amazing, inspiring husband, who have been – and continue to be – my biggest cheerleaders and my breath of fresh air.

TABLE OF CONTENTS

ACKNOWLEDGEMENTS	ii
LIST OF FIGURES.....	vii
LIST OF TABLES	xi
KEY TO ABBREVIATIONS.....	xii
ABSTRACT.....	xvi
 CHAPTERS	
1. GENERAL INTRODUCTION.....	18
1.1 The pulmonary alveolar epithelium.....	19
1.2 Alveolar Epithelial Type II cells.....	22
1.3 Metabolic function of the lung.....	24
1.3.1 Lung tissue metabolism.....	24
1.3.2 ATII cellular metabolism	26
1.4 Lactate as a metabolic substrate.....	28
1.4.1 Cellular Lactate Consumption	28
1.4.2 Lactate metabolism in the lung.....	31
1.5 Pulmonary hypoxia.....	32
1.5.1 Clinical significance of decreased oxygen in pulmonary tissue	33
1.5.2 Cellular Response to Hypoxia: General.....	35
1.5.3 Cellular Response to Hypoxia: ATII Cells.....	38
1.6 Idiopathic Pulmonary Fibrosis.....	41
1.6.1 IPF overview.....	41
1.6.2 Alveolar Epithelial Cells in IPF.....	46
1.6.3 Pulmonary cell metabolism in IPF	51
1.6.4 Need for assessment of human IPF patient samples	54

1.7 Overall significance and specific aims	56
2. ATII CELLS HAVE AN OXIDATIVE, HIGHLY METABOLIC PHENOTYPE	60
2.1 Introduction.....	60
2.2 Results	63
2.2.1 ATII cells consume oxygen rapidly to fuel mitochondrial ATP production.....	63
2.2.2 ATII cells generate extracellular lactic acid.....	64
2.2.3 ATII cells maintain spare respiratory and spare glycolytic capacities.....	68
2.2.4 MLE-15 cells recapitulate ATII relative reliance on mitochondrial respiration.....	69
2.3 Discussion	72
3. CHRONIC HYPOXIA INDUCES METABOLIC ADAPTATION BY ATII CELLS	78
3.1 Introduction.....	78
3.2 Results	81
3.2.1 ATII cells maintain ATP homeostasis during long-term hypoxia.	81
3.2.2 Hypoxia suppresses oxidative metabolism in ATII cells. ..	81
3.2.3 Hypoxia does not enhance glycolytic function in ATII cells.	87
3.2.4 Hypoxia enhances ATII cell relative reliance on glycolytic metabolism.....	88
3.2.5 Hypoxia induces changes in ATII mRNA expression of genes associated with glucose metabolism.....	92
3.2.6 Hypoxia alters ATII metabolism to favor glycogen storage.....	92
3.3 Discussion	97

4. LACTATE SERVES AS SUBSTRATE FOR ATII CELL METABOLISM....	104
4.1 Introduction.....	104
4.2 Results	108
4.2.1 Culture in lactate alone induces a highly oxidative ATII cell phenotype.	108
4.2.2 Rapid respiration by mouse ATII grown in lactate is coupled to mitochondrial ATP production	109
4.2.3 Respiration is performed at maximal capacity in mouse ATII cells cultured in lactate.	110
4.2.4 Lactate availability alters glucose utilization.	115
4.2.5 Hypoxia suppresses ATII cell lactate respiration.	115
4.2.6 ATII cell lactate consumption and export are dependent on MCT function.	118
4.2.7 ATII cells express MCT1 in a non-hypoxia-inducible manner.	118
4.2.8 Lactate alone is sufficient to maintain ATP balance but not cell growth.....	119
4.3 Discussion	129
5. ATII CELLS IN IPF LUNG ADOPT A GLYCOLYTIC METABOLIC PHENOTYPE.....	137
5.1 Introduction.....	137
5.2 Results	142
5.2.1 ATII cells isolated from IPF lung have low overall metabolic function.....	142
5.2.2 ATII cells from IPF lung demonstrate a glycolytic phenotype.....	142
5.2.3 IPF ATII cells express high levels of LDH protein.....	148
5.2.4 Treatment of MLE-15 with myofibroblast-conditioned media or TGF β decreases LDH protein expression.	150
5.2.5 Neither TGF β -stimulated myofibroblast-conditioned media nor TGF β alter MLE-15 cell metabolism.	151
5.2.6 TGF β does not affect the response of MLE-15 to hypoxia.	151

5.2.7 Exposure of MLE-15 to myofibroblast-conditioned media or TGF β induces morphological change.....	156
5.2.8 Exposure to myofibroblast-conditioned media or TGF β induces expression of fibroblast and ATI cell markers in MLE-15.	156
5.2.9 Exposure of ATII to myofibroblast-conditioned media or TGF β specifically enhances SPC mRNA expression.	157
5.3 Discussion	162
6. CONCLUSION AND DISCUSSION: ATII CELL METABOLISM & METABOLIC CONTRIBUTION TO HYPOXIA-RELATED PULMONARY DISEASE	169
6.1 ATII cell metabolic phenotype & adaptation to hypoxia	170
6.2 Lactate shuttling in the alveolar epithelium.....	182
6.3 ATII metabolism in IPF lung	190
6.4 Targeting lactic acid production in treatment of IPF.....	201
6.5 Beyond IPF: A role for lactic acid in bronchopulmonary dysplasia.....	205
6.6 Final Comments	210
MATERIALS AND METHODS	212
APPENDICES	
A. OPTIMIZATION OF EXTRACELLULAR FLUX ASSAY.....	230
B. GLUTAMAX-FREE CONTROL FOR METABOLIC ASSAY OF CELLS CULTURED IN LACTATE.....	233
C. COMPLETE RESULTS FOR PCR ARRAY.....	235
LIST OF REFERENCES.....	238

LIST OF FIGURES

CHAPTER 1

Figure 1.1: The alveolar epithelium.....	21
Figure 1.2: Intercellular lactate shuttling.....	30
Figure 1.3: HIF1 and HIF2 regulate transcription of genes associated with overlapping but distinct roles in metabolism.....	39

CHAPTER 2

Figure 2.1: MLE-15 and primary ATII cells rapidly respire oxygen.....	65
Figure 2.2: Approximately half of oxygen consumption by ATII cells is coupled to mitochondrial ATP production.....	66
Figure 2.3: ATII cells have glycolytic function under ambient O ₂	67
Figure 2.4: ATII cells have significant mitochondrial and glycolytic reserve capacity.....	70
Figure 2.5: MLE-15 and primary ATII show similar relative reliance on oxidative versus glycolytic function.....	71

CHAPTER 3

Figure 3.1: Hypoxia and PHI exposure do not alter steady-state ATP concentration in ATII cells.....	83
Figure 3.2: Hypoxia and PHI suppress cellular respiration.....	84
Figure 3.3: ATII cells maintain mitochondrial reserve capacity in hypoxia.....	85
Figure 3.4: Hypoxia and PHI suppress basal do not affect coupling of oxygen consumption to mitochondrial ATP generation.....	86

Figure 3.5: Hypoxia and PHI do not increase extracellular proton production.....	89
Figure 3.6: Hypoxia does not alter cellular lactate generation in MLE-15 cells.....	90
Figure 3.7: Hypoxia and PHI do not impact ATII cell glycolytic reserve.....	91
Figure 3.8: Hypoxia and PHI promote intracellular storage of glycogen, which is consumed upon recovery in ambient O ₂	96

CHAPTER 4

Figure 4.1: Culture in lactate shifts ATII cells into a highly oxidative metabolic state.....	111
Figure 4.2: Inhibition of LDH reduces lactate-fueled respiration in MLE-15.....	112
Figure 4.3: ATII cells utilize lactate for mitochondrial ATP production.....	113
Figure 4.4: Mitochondrial respiration is performed at near-maximal rates in MLE-15 cells consuming lactate alone.....	114
Figure 4.5: Extracellular lactate concentration regulates glycolytic output.....	116
Figure 4.6: Exposure to hypoxia suppresses respiration of ATII cells cultured in glucose or lactate to a similar degree.....	117
Figure 4.7: MCT transporter function mediates export and import of lactic acid by MLE-15 cells.....	122
Figure 4.8: ATII cells express monocarboxylate transporter MCT1.....	123
Figure 4.9: <i>Mct1</i> expression is not hypoxia-inducible in ATII cells.....	124
Figure 4.10: <i>Mct1</i> expression by MLE-15 is increased by culture in lactate.....	125
Figure 4.11: Lactate alone is sufficient to maintain MLE-15 cell ATP homeostasis.....	126
Figure 4.12: Lactate alone is not sufficient to maintain cell growth in MLE-15 cells.....	128

CHAPTER 5

Figure 5.1: ATII cells isolated from IPF lung have low respiratory function compared to normal lung ATII.....	144
Figure 5.2: Glycolytic function of IPF ATII cells is maintained or elevated compared to control.....	145
Figure 5.3: ATII cells isolated from IPF lung maintain reserve respiratory and glycolytic capacity.....	146
Figure 5.4: ATII from IPF lung rely more heavily on glycolysis than control lung ATII cells.....	147
Figure 5.5: ATII cells from IPF lung express high levels of LDH protein.....	149
Figure 5.6: Treatment with myofibroblast-conditioned media or TGF β decreases LDH expression in MLE-15.....	152
Figure 5.7: Treatment with myofibroblast-conditioned media does not influence glycolytic or oxidative function in MLE-15.....	153
Figure 5.8: Treatment with TGF β does not influence glycolytic or oxidative function in MLE-15.....	154
Figure 5.9: TGF β treatment does not affect the MLE-15 metabolic response to hypoxia.....	155
Figure 5.10: Treatment with TGF β or myofibroblast media alters MLE-15 cell morphology.....	159
Figure 5.11: ATI and fibroblast marker gene expression is increased in MLE-15 exposed to myofibroblast-conditioned media or TGF β	160
Figure 5.12: Exposure to myofibroblast-conditioned media or TGF β increases <i>SPC</i> , but not <i>SPB</i> gene expression.....	161

CHAPTER 6

Figure 6.1: Hypothetical model of cellular metabolism in the alveoli in healthy and IPF lung tissue.....	195
--	-----

ADDITIONAL FIGURES

Methods & Materials Figure 1: Extracellular flux analysis using
Seahorse Bioscience XF technology.....218

Appendix Figure A.1: Optimization of FCCP concentration for XF assay.....231

Appendix Figure A.2: Optimization of Oligomycin A concentration for
XF assay.....232

Appendix Figure B.1: OCR in lactate-formulated media is not
significantly affected by the absence of Glutamax.....234

LIST OF TABLES

Table 1: Comparison of mouse ATII OCR values to other metabolic cell types based on previously reported data.....	77
Table 2: Hypoxia-dependent differential gene expression in MLE-15 cells.....	95
Table 3: Mouse cell plating densities used for extracellular flux assays.....	219
Table 4: Oligonucleotide primer sequences used in qPCR analyses.....	225
Table 5: Detailed results for glucose metabolism focused qPCR array using mRNA obtained from MLE-15 cultured in hypoxia versus ambient O ₂	235

KEY TO ABBREVIATIONS

AEC...alveolar epithelial cells
ALK...activin receptor-like kinase
AMP...adenosine-monophosphate
AMPK...AMP-activated protein kinase
AQP5...aquaporin 5
ATI...alveolar epithelial type 1
ATII...alveolar epithelial type 2
ATP...adenosine-triphosphate
BALF...bronchoalveolar lavage fluid
BPD...bronchopulmonary dysplasia
CF...cystic fibrosis
CHC... α -4-hydroxycinnamate
COPD...chronic obstructive pulmonary disease
DMOG...dimethylxalyglycine
DNA...deoxyribonucleic acid
ECAR...extracellular acidification rate
EdU...5-ethynyl-2'-deoxyuridine
EMT...epithelial-to-mesenchymal transition
EPO...erythropoietin
ER...endoplasmic reticulum
FBS...fetal bovine serum

FCCP...carbonyl cyanide-p-trifluoromethoxyphenylhydrazine
FFA ...free fatty acid
FSP...fibroblast-specific protein
GAPDH ... glyceraldehyde 3-phosphate dehydrogenase
GERD...gastroesophageal reflux disease
GLUT...glucose transporter
HAPE...high altitude pulmonary edema
HIF...hypoxia-inducible factor
HK...hexokinase
HPV...hypoxic pulmonary vasoconstriction
HRE...HIF response element
IL-1...interleukin 1
IL-13...interleukin 13
IPF...idiopathic pulmonary fibrosis
KGF... keratinocyte growth factor
LDH...lactate dehydrogenase
MCT...monocarboxylate transporter
MLE...mouse lung epithelial cell line
mTOR...mammalian target of rapamycin
MUC5B...mucin protein 5B
NADH ...nicotinamide adenine dinucleotide
NADPH...nicotinamide adenine dinucleotide phosphate

NDHF...normal human dermal fibroblasts

NOX4...NADPH oxidase 4

OCR...oxygen consumption rate

PDGF...platelet-derived growth factor

PDK...pyruvate dehydrogenase kinase

PFKL...phosphofructokinase

PGC1 α ...peroxisome proliferator-activated receptor gamma coactivator 1 α

PGK ...phosphoglycerate kinase

PGM...phosphoglucomutase

PHD...prolyl-hydroxylase

PHI...prolyl-hydroxylase inhibitor

PPR...proton production rate

Pro-col1a...pro-collagen 1a

qPCR...real-time quantitative polymerase chain reaction

RDS...respiratory distress syndrome

RNA...ribonucleic acid

RNAPII...RNA polymerase 2

ROS...reactive oxygen species

RPL13...ribosomal protein RPL13

SD ...standard deviation

SPB...surfactant protein B

SPC ...surfactant protein C

TCA...tricarboxylic acid

TGF β ...transforming growth factor beta

TLR...toll-like receptor

TNF α ...tumor necrosis factor alpha

TTF...thyroid transcription factor

UPR...unfolded protein response

VEGF...vascular endothelial growth factor

VHL...Von Hippel-Lindau E3 ubiquitin ligase

α SMA...alpha smooth muscle actin

ABSTRACT

ROBYN GRAYSON LOTTES. Alveolar Epithelial Type II Cell Metabolism in Health, Hypoxia and Disease. (Under the direction of JOHN E BAATZ, PhD).

Alveolar epithelial type II (ATII) cells constitute 50% of cells composing the alveolar epithelium and are essential to proper lung function. They are the primary producers of pulmonary surfactant, serve as progenitors capable of rapid self-renewal and differentiation, and play roles in immunity and fluid homeostasis, all of which require considerable energy investment. Given their many ATP-demanding functions, ATII cells are expected to be highly metabolically active; however, little is known about the fundamental metabolism of this critical cell type.

ATII cells are normally exposed to uniquely high oxygen concentrations. However, numerous lung diseases including idiopathic pulmonary fibrosis (IPF) lead to pulmonary hypoxia. The role of hypoxia has been extensively investigated in pathologies like cancer and heart disease but has received far less attention in pulmonary disease. Recent findings of lactic acid build-up in IPF lung suggest a role for altered cell metabolism, potentially related to hypoxia.

We investigate the hypothesis that hypoxia alters ATII metabolism, and that similar metabolic change occurs in IPF lung. ATII metabolism was characterized under ambient versus 1.5% O₂. Additionally, to understand possible contributions of ATII to lactic acid build-up in disease, the ability of

healthy cells to both produce and consume lactate was assessed. Extracellular flux analysis was performed to measure glycolytic and mitochondrial metabolism in a model cell line and ATII isolated from mouse and human lungs, and flux experiments were correlated with metabolite measurements and gene and protein expression.

This work demonstrates that ATII cells are highly metabolic and dependent on mitochondrial metabolism. Hypoxia suppresses ATII mitochondrial metabolism without concurrent change in glycolysis, despite enhanced enzyme expression. Similarly, ATII from IPF patient lung showed low mitochondrial function compared to control, while glycolytic output occurred at near-control rates or higher, generating a highly glycolytic phenotype. In both hypoxia-treated and IPF-derived ATII, reserve mitochondrial capacity was maintained. Additionally, we demonstrate that ATII consume lactate and that this ability is limited by hypoxia. Based on our findings, we propose a hypothetical model by which metabolic cooperation between ATII and other cell types is altered in IPF to favor enhanced lactic acid generation and reduced consumption.

CHAPTER 1. GENERAL INTRODUCTION

The cells that compose the pulmonary epithelium reside in a specialized physiological environment with significant implications for cellular metabolism. First, the lung is the best-oxygenated organ in the mammalian body, with healthy adult pulmonary tissue subjected to relatively oxygen concentrations of approximately 13% (or an alveolar pO_2 of approximately 104 mm Hg). Oxygen is a critical substrate for mitochondrial metabolism which is often an important factor determining cellular metabolic function, yet pulmonary cells have more oxygen readily accessible than cells of any other tissue. Second, the lung is the only organ apart from the heart itself that receives the full cardiac output on every circuit through the body. The full volume of the circulatory system passes through the lungs before being divided amongst the other organs, thus cells of the pulmonary tissue receive the full complement of circulating metabolic substrates from the heart. This creates a situation in which the local metabolic function of the lung has potential to globally influence circulating substrate and metabolite concentrations to which the rest of the body is exposed. Additionally, as the thin barrier between the external and internal environments across which gaseous substrate and waste are continuously exchanged, the cells of the pulmonary epithelium serve a number of energy-demanding functions that are absolutely

critical to the function and survival of the organism. Thus, a steady supply of cellular ATP must be available in order for pulmonary functions to be maintained. From this viewpoint, it is clear that cell metabolism is likely an important factor in determining lung function and potentially influences whole-body homeostasis. However, little is understood about the influence of pulmonary cellular metabolism in health and disease.

1.1 The pulmonary alveolar epithelium

In mammals, exchange of gases between the body and the environment is mediated by the lung and conducting airways, as well as muscoelastic structures of the thorax that physically move air through the respiratory passages. Each portion of the mammalian respiratory system serves a distinct function. The upper airways including the nasal passages and larynx serve primarily to filter incoming air of particulates and infectious agents; the trachea, bronchi and bronchioles conduct air to the heavily branched distal lung; and the alveolar ducts and saccular alveoli facilitate gas exchange between the blood and alveolar airspace. The pulmonary epithelium forms a specialized physiological barrier between the inside of the mammalian body and the external environment, and just as each anatomical region of the lung serves a distinct purpose, each region is lined by a distinct epithelial layer that facilitates specific function.

The alveolar epithelium forms the layer across which oxygen and waste gases are exchanged (Figure 1.1). Two distinct epithelial cell types compose the alveolar epithelium. Large, squamous alveolar epithelial type I (ATI) cells make

up approximately 50% of the cell population but 95% of the epithelial surface area, and serve as the primary mediators of gas exchange across the epithelial barrier. The other 50% of cells composing the alveolar epithelium are alveolar epithelial type II (ATII) cells, which do not play a direct role in gas exchange but instead serve many vital roles in lung function as the primary producers of pulmonary surfactant.

In addition to alveolar epithelial cells (AEC), fibroblasts and macrophages are major cell types composing the distal lung tissue. Pulmonary fibroblasts are found in the alveolar parenchyma, residing in the interstitial space outside of the alveolar sacs. Resident macrophages are present in the lung parenchyma in close association with the alveolar epithelium, where their function is to scavenge foreign material that makes it through the respiratory tract and into the alveoli, and to regulate local inflammatory responses.

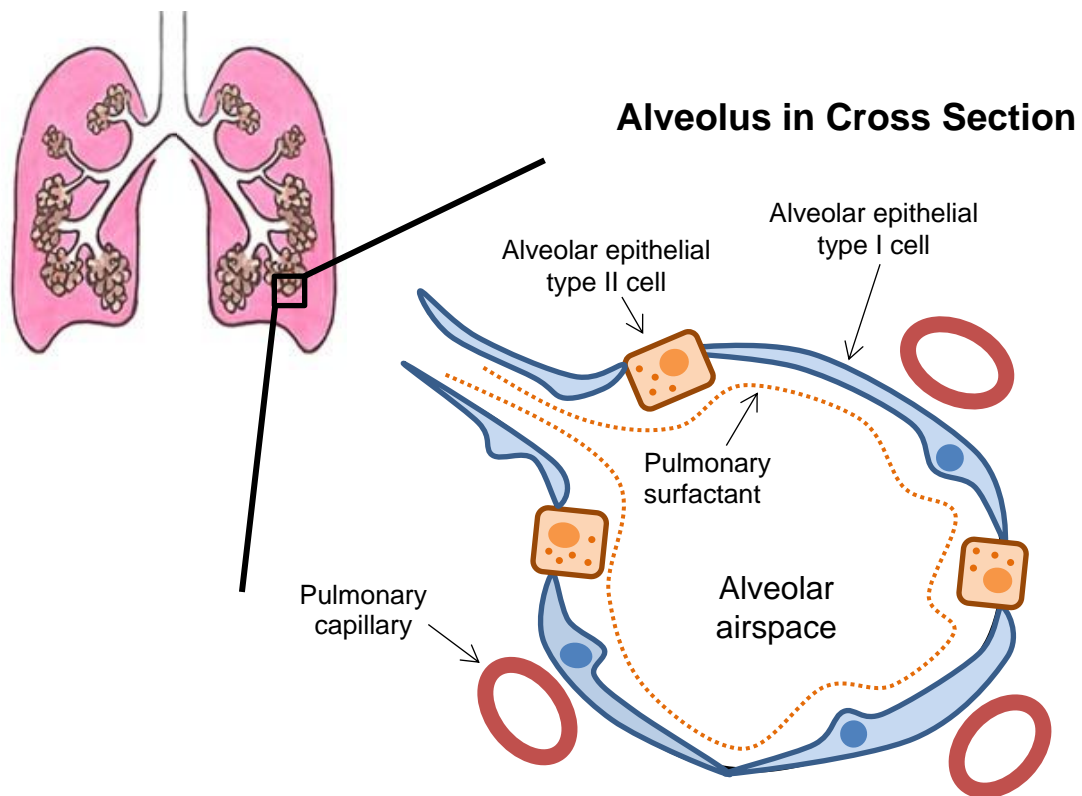


Figure 1.1: The alveolar epithelium. The alveolar epithelium is composed of ATI and AII cells. The large, window-like ATI cells serve as the passive barrier for gas exchange between the alveolar space and the fine network of capillaries that surrounds each alveolus. AII cells serve a wide variety of supportive functions, including production of pulmonary surfactant, that are essential for proper lung function (*see text*). Adapted from Camelo et al, 2014 (1).

1.2 Alveolar Epithelial Type II cells

ATII cells are the primary producers of pulmonary surfactant (2), a role that is absolutely essential in the maintenance of proper lung function. Surfactant is a mixture of proteins and phospholipid species that lines the alveolar epithelium. Its primary function is to reduce surface tension of the fluid coating the alveolar sac, an air-fluid interface which otherwise would collapse upon expiration and resist re-inflation. Surfactant proteins are synthesized in the ATII cell endoplasmic reticulum and packaged with phospholipids into intracellular lamellar bodies. Surfactant secretion is achieved through fusion of the lamellar body membrane with the apical cell membrane. Initially secreted as large aggregates from the lamellar body, surfactant in the extracellular space organizes into a complex, organized structure of tubular myelin and spreads across the air-fluid interface of the alveolar airspace to form a surface-active, monolayer film (3). The extremely hydrophobic surfactant proteins SP-B and SP-C are incorporated into surfactant and aid biochemically in organization of lipids into the interfacial monolayer and enhance the surface-active properties of the lipid mixture. Secreted surfactant is continuously recycled, in that a large portion of secreted surfactant is internalized and catabolized or re-organized into lamellar bodies. The processes of surfactant synthesis, transport, packaging, secretion, and recycling that are crucial for maintenance of homeostasis and proper lung function collectively require substantial energetic investment by ATII cells (4). Furthermore, surfactant plays a vital role in protecting the lung from foreign material such as bacteria. Surfactant proteins, as well as complete

surfactant itself, have properties that serve in innate immunity. SP-A and SP-D act as collectins that bind foreign antigens and promote phagocytosis by alveolar macrophages, cytokine production, and other innate immune cell responses. SP-C has been shown to negatively regulate innate immune response by interacting with and suppressing Toll-Like Receptors (TLR) in macrophages when engulfed with other surfactant components (5).

While generation of complete surfactant is perhaps the most characteristic function of ATII cells, they also have important roles in ion and fluid transport (6-8). Fluid clearance is particularly important for the alveoli, as accumulation of fluid in the airspace (pulmonary edema) greatly impairs gas exchange. Fluid transport is facilitated by ion transport across the epithelium, which in ATII cells is performed by sodium channels in the apical membrane and Na⁺/K⁺ ATPase ion pumps in the basolateral membrane.

Additionally, ATII cells serve as progenitor cells capable of repopulating the population of ATI cells following physical damage or stress (9). In this manner, they play a critical role in wound healing in the alveolar epithelium. While normal turnover of alveolar epithelial cells is relatively slow, when the epithelium is injured ATII cells multiply and differentiate rapidly to facilitate wound healing and re-establish an unbroken epithelial barrier.

Given the many ATP-consuming roles they continuously serve to facilitate lung function, ATII cells are expected to be highly metabolically active under normal physiological conditions. Thorough characterization of ATII cell metabolic function has not been performed.

1.3 Metabolic function of the lung

1.3.1 Lung tissue metabolism

Much of what is known about metabolism in the lung comes from tissue- and organ-level investigations conducted by providing isotopically-labeled metabolic substrates (10, 11). This was primarily accomplished by perfusing media containing labeled substrates through the pulmonary circulation of small mammals, known as the isolated perfused lung model. Following the innovation of this model which allowed researchers to quantitatively measure uptake and output of compounds across pulmonary circulation (12), a slew of investigations conducted in the 1970s and 1980s reported on the metabolism of glucose and other substrates by the lung parenchyma. Despite early assumption that the lung was a relatively passive tissue in terms of metabolic function, as an organ it was in fact found to be highly metabolic, with rates of glucose oxidation comparable to those observed in brain and heart (10).

Much of the original work was focused on glucose turnover to lactate, and multiple reports demonstrated net lactate generation from lung tissue perfused with glucose-formulated media, demonstrating that anaerobic glycolysis was performed in the lung under fully-oxygenated conditions (13). In perfusion studies, 40-50% of glucose-derived carbon ended up as monocarboxylate species lactate and pyruvate, with lactate production 10-fold higher than pyruvate (14). This measured rate of lactate generation via glycolysis was higher than rates measured in other tissues; for example, conversion to lactate accounts for only 20-25% of glucose consumption in the isolated, perfused heart (15).

However, further investigation demonstrated that despite the observation that the lung generates lactic acid and as a whole does not rapidly consume oxygen, oxidative metabolism is necessary to maintain energy balance in lung tissue (16), indicating that mitochondrial metabolism is a critical component of normal lung function.

Studies of whole lung metabolism expanded beyond glucose metabolism to investigate the use of other substrates for energy production. In particular, lactate was shown to be removed from pulmonary circulation and rapidly oxidized by lung tissues (11, 17, 18). This surprising finding suggested that while lactate is produced from glucose by the lung, it may also serve as an important metabolic substrate for lung cells. These observations are discussed in more depth in Section 1.4.

In addition to lactate and glucose, fatty acids are utilized by lung tissue. Only approximately 20% of free fatty acid taken up by the lung is oxidized to CO₂, indicating that a small percentage is actually used for mitochondrial energy production, with the remainder assumed to be used in synthetic reactions (19). Free fatty acid (i.e. palmitic acid) oxidation generates more ATP per mole than glucose, thus fatty acids could still be a significant source of energy for oxidative metabolism in the lung. However, the addition of palmitate to perfusion media in the perfused lung model was shown to have minimal impact on glucose oxidization, suggesting minimal contribution to whole lung energy production under *in vivo* conditions (20). Alanine, glycerol, and the ketone 3-hydroxybutarate have also been investigated but were shown to be used sparingly (11).

The impact of oxygen availability was a point of particular interest in early studies of lung metabolism. In a landmark study of pulmonary metabolism, Longmore and Mourning (21) investigated lung lactate production under ambient O₂ and hypoxic conditions. Similar to previous studies, they observed net lactate production in 21% O₂. Under hypoxic conditions, lactate production increased two-fold; however, using ¹⁴C-labeled glucose, they showed that the excess lactate was not a product of anaerobic glucose metabolism, suggesting instead that lactate was produced by non-glycolytic means, such as amino acid breakdown, in hypoxia.

1.3.2 ATII cellular metabolism

More than a decade after the many studies examining whole-lung metabolism of glucose and other substrates, Fox and colleagues performed similar ¹⁴C-labeled substrate studies, this time performed in isolated and cultured primary ATII cells from fetal rat lung. Of the measured substrates which included glucose, lactate, 3-hydroxybutyrate, and glutamine, glucose actually had the lowest rate of oxidation (22). Lactate was oxidized to carbon dioxide at a rate more than 20 times that of glucose, while other substrates showed intermediate rates of oxidation. Furthermore, lactate and glucose were shown to be metabolized via similar pathways, as reciprocal inhibition of oxidization occurred between the two when provided simultaneously. This same group investigated oxidization of these substrates in ATII cells compared to fibroblasts isolated from fetal lung and showed that ATII cells oxidized all measured substrates more

rapidly than fibroblasts (22). This was particularly true for lactate, which was oxidized twice as fast by ATII cells compared to fibroblasts.

Despite the many critical, energy-consuming functions of ATII cells, ATII cellular metabolism has not been studied in detail at the functional level. Estimates based on cellular oxygen consumption indicate that around 15% of oxygen consumed by ATII cells is dedicated to generating ATP to serve function of the Na⁺/K⁺ ATPase, indicating a substantial energetic commitment to ion and fluid transport (23) (although previous estimates concerning ATP consumption in mammalian cells in general were greater, approximately 40%) (24). The demand of other energy-consuming processes has not been addressed, although maintenance of surfactant production and homeostasis in particular is assumed to require considerable ATP *in vivo* for *de novo* protein and lipid synthesis and intracellular shuttling.

Classic Clark electrode studies of rat ATII cells showed that ATII consume oxygen, and provided rate estimates of approximately 3 pmoles/minute/ μ g protein (23). Recently, studies of metabolic flux have been performed using MLE-12, an immortalized mouse cell line used as a model for ATII cells. This work indicated a higher level of metabolic function with relatively rapid oxygen consumption and significant levels of extracellular acidification under ambient oxygen conditions. However, similar metabolic flux measurements have not been performed in primary ATII cells, and thus the usefulness of MLE-12 (and other MLE cell lines) as a metabolic model for primary cells is unknown (25).

1.4 Lactate as a metabolic substrate

1.4.1 Cellular Lactate Consumption

Lactic acid is produced as the end product of anaerobic glycolysis, and therefore lactate is generally considered as a metabolic waste product. Approximately 25%-50% of total lactate removal and turnover in the body is accomplished through gluconeogenesis in the liver, through which lactate is converted back to glucose. However, a comparatively larger proportion of lactate is metabolized through oxidation to pyruvate by cells in other tissues and subsequent use as a metabolic substrate to fuel mitochondrial energy production (26). Pyruvate generated from lactate oxidation serves as a primary metabolic substrate for heart muscle, wherein cardiomyocytes consume lactate produced by distant tissues and delivered via circulation. In brain and muscle tissue, highly oxidative cell types (neurons and red fibers) directly utilize lactate produced by neighboring glycolytic cells (astrocytes and white fibers) (27-29). This form of metabolic cooperation, in which oxidative cells utilize lactate generated as waste by glycolytic cells, is referred to as “**the intercellular lactate shuttle**” and plays a major role in removal of lactate in the body as well as local supply of metabolic substrate in tissues (Figure 1.2).

Cellular consumption of lactate requires conversion to pyruvate via the reverse activity of Lactate Dehydrogenase (LDH). Pyruvate is subsequently shuttled into the mitochondria to fuel tricarboxylic acid (TCA) cycle reactions, providing reducing equivalents necessary for mitochondrial electron transport and ATP production. To undertake this process, a cell must have active

mitochondria, a favorable lactate gradient into the cell, and must express monocarboxylate transport proteins (MCT) and LDH (26, 30).

Different isoforms of MCT and LDH favor lactate import (versus export) and oxidation (versus reduction), and these isoforms tend to be more highly expressed in cell types that can utilize lactate. Concerning MCT expression, the higher-affinity MCT1 and MCT2 transporters tend to be expressed in cells known to import lactate including skeletal muscle red fibers, neurons, and liver cells. The lower-affinity isoform MCT4 is expressed in cells that rely predominantly on glycolytic metabolism and is therefore more heavily associated with lactate efflux (31, 32). Likewise, differential expression of LDH isoforms has been found between cell types. LDH5 is composed entirely of four M subunits (LDH-M, encoded by the *LDHA* gene) and strongly favors the forward reaction that converts pyruvate to lactate. Accordingly, the LDH5 isoenzyme is generally expressed by highly glycolytic cell types. The other LDH isoforms contain at least one H subunit (LDH-H, encoded by the *LDHB* gene). The more H subunits in the complete LDH protein, the higher the tendency of the isoenzyme to facilitate the lactate-to-pyruvate conversion necessary for lactate consumption (33).

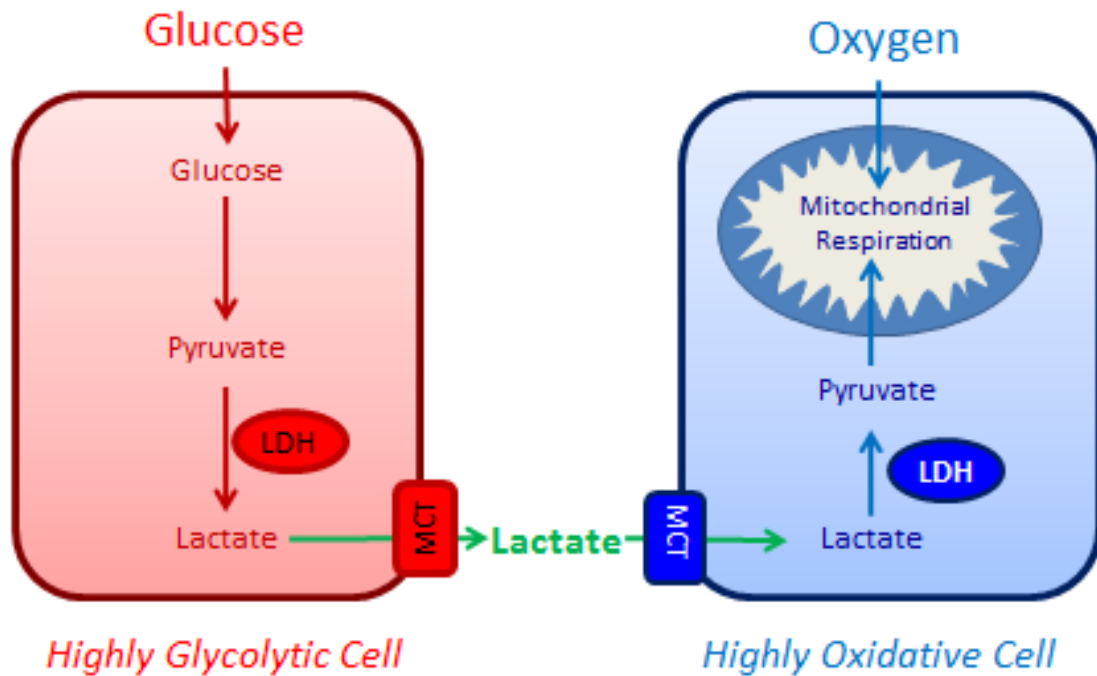


Figure 1.2: Intercellular lactate shuttling. In the cell-cell lactate shuttling scheme, anaerobic glycolysis and mitochondrial respiration are linked in distinct cell types within a tissue. Highly glycolytic cells meet their energy and charge balance needs via processing of glucose to lactate, which is extruded from the cell into the extracellular space. Highly oxidative neighboring cells import the extracellular lactate, and after conversion to pyruvate, use the monocarboxylate to fuel TCA cycle reactions and electron transport. Acetyl-coA derived from lactate may also be diverted from the TCA cycle for use in lipid synthesis.

1.4.2 Lactate metabolism in the lung

Studies of whole-lung metabolism in the isolated perfused lung indicated that lactate is oxidized to carbon dioxide in pulmonary tissue, suggesting that it could be used as substrate for mitochondrial ATP production. Experiments using labeled substrates demonstrated rapid generation of CO₂ from lactate precursor, even when glucose was provided simultaneously and at higher concentrations (17, 18). The presence of lactate reduced oxidization of glucose, indicating that, when available, lactate is utilized as a substrate for mitochondrial metabolism in lieu of glucose to some degree (17). Altogether, early studies of glucose and lactate metabolism in the isolated perfused lung model and in tissue slices indicated that lactate is not only produced by the lung, but is simultaneously utilized by the lung as metabolic substrate (11).

More recent work by Brooks and colleagues has demonstrated consistent net lactate removal from pulmonary circulation into lung tissue (30, 34). The cell type(s) responsible for lactate uptake and oxidation in the lung have yet to be determined, though experiments following the biochemical fate of labeled lactate observed preferential incorporation into lipids found in pulmonary surfactant (35, 36), implying a role for ATII cells. Furthermore, when lactate and glucose were both provided in whole lung perfusate, the acetyl moiety of synthesized lipid was composed almost exclusively of carbon derived from lactate precursor.

Study of isolated fetal rat alveolar epithelial cells demonstrated rapid lactate oxidization and reciprocal inhibition of oxidization between lactate and glucose (22). However, this has not been assessed in mature ATII cells, nor has

lactate oxidization been linked directly to pulmonary cell ATP generation. ATII cells have active mitochondria and a high energy demand, in addition to residing in an extremely well-oxygenated environment (37). Thus, the metabolism and physiological location of ATII cells indicate potentially favorable conditions for lactate oxidation.

1.5 Pulmonary hypoxia

The lung is normally exceptionally well-oxygenated compared to other body tissues, and the pulmonary parenchyma is unique among tissues in that it does not require vascular perfusion for oxygen delivery. The alveolar epithelium where ATII cells reside is estimated to experience oxygen conditions of approximately 100 mm Hg, or about 13% O₂ (38). By comparison, the renal cortex experiences O₂ levels of approximately 7-8% (39) or ~55 mm Hg, and the environment of the myocardium at rest is approximately 3-4% O₂ (40) or ~25 mm Hg.

While the alveolus is normally exposed to comparatively high oxygen levels, a variety of pathological conditions lead to decreased oxygen tensions in pulmonary tissue. Lung diseases that disrupt normal oxygen exposure include fibrotic diseases in which tissue remodeling limits oxygen permeation to the alveoli and gas exchange, including idiopathic pulmonary fibrosis (IPF) and cystic fibrosis (CF); and obstructive diseases that block portions of the lung from exposure to incoming O₂, including chronic obstructive pulmonary disease (COPD) (38). High altitude pulmonary edema (HAPE) results from travel to high

altitudes where atmospheric O₂ is comparatively low, with edema limiting gas exchange across the epithelial barrier and leading to reduced oxygen exposure to the alveolar epithelial cells themselves. In the case of lung cancer, tissue becomes hypoxic when vascular perfusion is limited within tumor masses.

In addition to pathological conditions associated with disease, the lung is exposed to low oxygen tensions during development. While in the adult lung a decrease in oxygen exposure represents hypoxic conditions for the tissue, low oxygen tensions are normal during development. *In utero* lung development occurs in oxygen levels well below those in the adult lung, estimated at approximately 1-5% (38). For the fetal lung, these low oxygen conditions are technically “normoxic”. Indeed, normal lung development appears to require this low oxygen environment, as pre-term exposure to atmospheric oxygen results in disruption of normal tissue development and is likely causative in the onset of neonatal lung diseases like bronchopulmonary dysplasia (BPD) and respiratory distress syndrome (RDS). Hypoxia-related signaling is required for normal alveolarization and development of the pulmonary surfactant system (41).

1.5.1 Clinical significance of decreased oxygen in pulmonary tissue

Pulmonary hypoxia is a contributing pathological factor in a variety of lung diseases. The cause of pulmonary hypoxia differs between diseases. In IPF, for example, onset of pulmonary hypoxia is the result of extensive tissue fibrosis and remodeling. COPD is also associated with development of pulmonary hypoxia;

however, in this case, airways become blocked due to severe inflammation. In HAPE, hypoxia develops due to pulmonary edema.

In response to pulmonary hypoxia, hypoxic pulmonary vasoconstriction (HPV) occurs in affected regions of the tissue (42). This decreases blood flow locally in an effort to conserve the gas exchange efficiency of the organ by limiting blood flow to poorly ventilated regions and increasing perfusion to unaffected regions of the lung. However, when disease results in widespread regions of hypoxia throughout the lung this can lead to severely limited pulmonary blood flow, poor overall perfusion, and greatly impaired gas exchange. Extensive vasoconstriction in the pulmonary tissue results in increased pulmonary arterial pressure. If this effect is severe and prolonged, it can lead to pulmonary arterial and right ventricular remodeling to accommodate the high pressure. In both COPD and IPF, patients presenting with pulmonary hypertension have particularly poor prognoses (43).

There remains debate about the degree to which pulmonary diseases result in truly hypoxic conditions in the lung tissue, primarily because it is extremely difficult to directly measure oxygen tension in patient lung tissue. However, in the case of IPF, stabilization of hypoxia-inducible factor transcription regulator proteins and downstream signaling has been demonstrated, suggesting that hypoxia does in fact occur and stimulate cellular hypoxia responses. There are mechanisms other than, or in addition to, true hypoxia through which HIF can become stabilized including generation of reactive oxygen species and other responses to stress, and these cannot be discounted as the cause of HIF

stabilization in disease. However, as HIF isoforms are currently considered to be the primary oxygen sensors in the lung and the main drivers of downstream responses, HIF stabilization indicates a “hypoxic” response at the cellular level, whether or not the tissue is in a state of true oxygen limitation.

1.5.2 Cellular Response to Hypoxia: General

In most cells, hypoxia causes physiological stress including loss of bioenergetic homeostasis and insufficient ATP levels, generation and accumulation of reactive oxygen species leading to DNA and protein damage, endoplasmic reticular stress, and even apoptosis. Without appropriate cellular adaptations to prevent or mediate these stressors, hypoxia can lead to cell death. Fortunately, cells are able to sense reduced oxygen tensions and respond accordingly to limit stress and damage. Generally, the response to hypoxia involves temporary cell cycle arrest, suppressed mitochondrial respiration, enhanced anaerobic glycolysis with lactic acid generation for ATP production, and reduction of ATP-consuming processes (44).

Metabolic changes are a fundamental component of the cellular response to hypoxia. In general, the hypoxic phenotype is characterized by a shift away from primary reliance on oxidative phosphorylation to enhanced glycolysis for maintenance of energy homeostasis. However, the typical response varies significantly by cell type, and depends largely on cell-specific function and energy demand, as well as the transient or chronic nature of exposure. AMP-activated kinase (AMPK), mTOR, the unfolded protein response (UPR), and other

signaling pathways are involved in mediating cellular metabolic homeostasis and response to stressors including oxygen limitation (45, 46). At the level of oxygen-sensing and initiation of response pathways, hypoxic responses are currently considered to be primarily mediated by the family of oxygen-sensitive hypoxia-inducible factor (HIF) transcription factor proteins.

The Hypoxia-Inducible Factor (HIF) family of transcriptional regulatory proteins is primarily responsible for mediating oxygen sensing and initiation of response pathways throughout the body. HIF transcription factors are heterodimeric proteins composed of a beta subunit (called HIF β or ARNT) and one of three different HIF α subunits, HIF1 α , HIF2 α , or HIF3 α . HIF heterodimers bind to HIF Response Element (HRE) sequences in DNA to enhance transcription of hypoxia-inducible genes. Control of HIF is achieved through post-translational, oxygen-dependent degradation of the alpha subunits. HIF α subunits are continuously transcribed and translated; however, when oxygen is available, prolyl-hydroxylase enzymes (PHD) hydroxylates HIF α at conserved proline residues. Hydroxylation promotes ubiquitination by Von Hippel-Lindau E3 ubiquitin ligase (VHL), which targets the protein for proteasomal degradation (47). Because oxygen is a substrate for PHD-mediated hydroxylation, PHD function is inhibited by hypoxia. In addition to this classic view of HIF stabilization in hypoxia, another mechanism of HIF stabilization involving ROS has been more recently elucidated. Under hypoxic conditions, mitochondria generate ROS from complexes of the electron transport chain that migrate to the cytosol where they inhibit PHD (48). Both mechanisms result in stabilization of HIF α subunits,

heterodimerization with beta subunits, and localization to the nucleus where they promote target gene transcription.

Multiple HIF isoforms regulate a wide variety of genes involved in directing cell energy metabolism under conditions of limited oxygen availability. The different HIF transcription factors (HIF1, 2, and 3) regulate transcription of overlapping, but different, sets of target genes containing HRE sequences. While both HIF1 and HIF2 regulate expression of some hypoxia-inducible genes including erythropoietin (EPO) and vascular endothelial growth factor (VEGF), other genes are specific targets of either HIF1 or HIF2. In the regulation of cellular metabolism in hypoxia, HIF1 and HIF2 play distinct roles (Figure 1.3). Genes associated with glycolysis and glucose uptake (including glucose transporters, pyruvate dehydrogenase kinase 1, and LDHA) are HIF1-specific targets, while HIF2 induces expression of genes associated with lipid storage, glycogen synthesis, and redox homeostasis. HIF2 also induces expression of PDK4 which, similar to PDK1, limits mitochondrial substrate availability.

Oxygen sensing and the coordinated response to hypoxia are primarily mediated by HIF stabilization and transcriptional control, but other pathways also contribute to hypoxic adaptation. The mTOR kinase signaling pathway controls cell growth, proliferation, and survival, and transcription and protein synthesis. The UPR also responds to hypoxia and together, these pathways control changes in protein translation and cellular metabolism. Transcriptional regulators besides HIFs induce expression of genes involved in the response to hypoxia. For example, PGC1 α can directly induce expression of VEGF, which is a HIF

target gene, independently of HIF activation. AMPK is a major modulator of metabolism that responds to cellular ATP deficit. The kinase is activated in response to changes in both cellular energy status and intracellular calcium, and has been shown to become activated in response to production of mitochondrial ROS in hypoxia (24). Under these conditions, different kinases act on AMPK resulting in phosphorylation and activation of AMPK. Activated AMPK generally shifts metabolism to favor glycolysis and contributes to down-regulation of ATP-consuming processes. AMPK activity is responsible for endocytosis of the Na⁺/K⁺ ATPase ion pump protein from the cell membrane under conditions of energy deficit, effectively conserving ATP by reducing pump activity. This is a rapid cellular response to conditions that induce energy deficit, including acute hypoxic exposure.

1.5.3 Cellular Response to Hypoxia: ATII Cells

Unlike the majority of cells in the body, ATII cells strongly express HIF2 α in addition to HIF1 α . Upon exposure to hypoxia, both HIF1 and HIF2 are immediately stabilized and translocate to the cell nucleus to regulate transcriptional responses. However, HIF1 expression in ATII cells peaks at approximately 8 hours of exposure, after which the level of HIF1 in the cell decreases steadily (49, 50). HIF2, on the other hand, remains stabilized and in the nucleus at a consistent level through 20 hours' exposure, suggesting that the long-term adaptation to hypoxia by ATII cells may be potentiated primarily by HIF2. This temporal difference in expression of the different isoforms has been

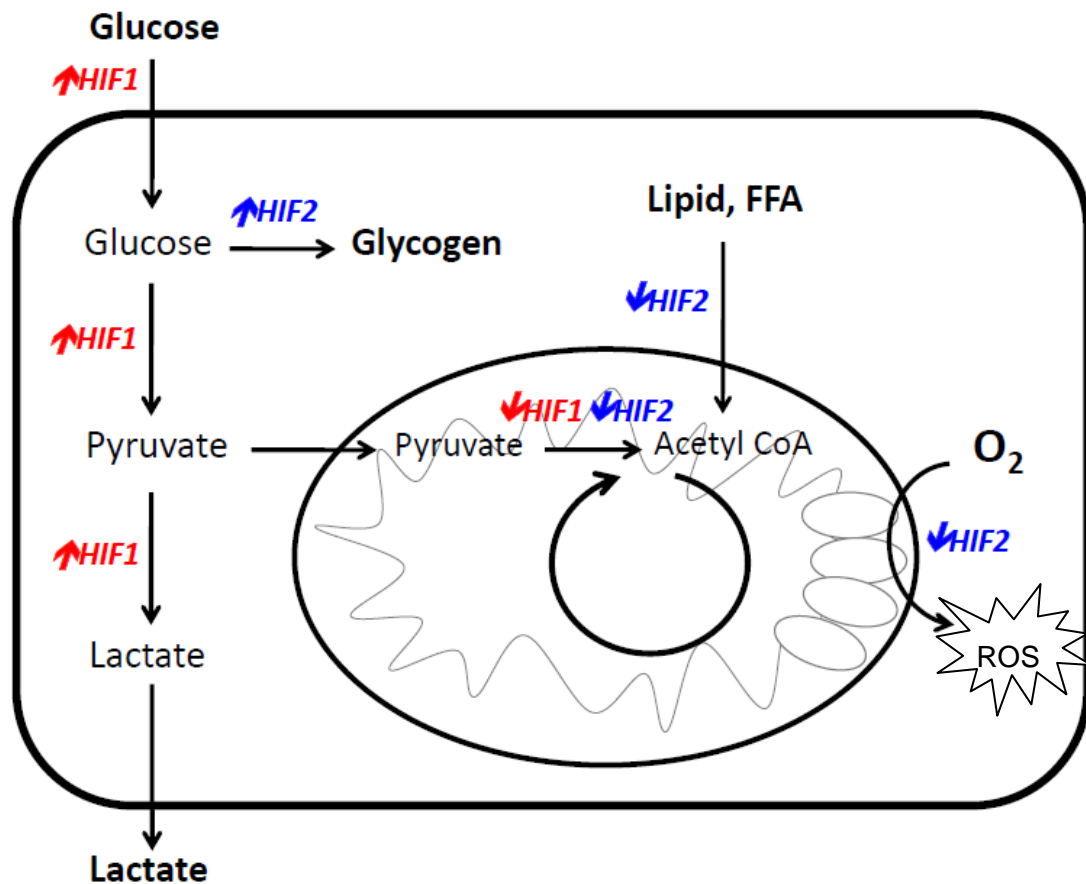


Figure 1.3: HIF1 and HIF2 regulate transcription of genes associated with overlapping but distinct roles in metabolism. HIF1 target genes include glycolytic enzymes and glucose transporters, as well as LDH. HIF2 enhances transcription of glycogenic enzymes and antioxidant enzymes including superoxide dismutase, and negatively regulates lipid β -oxidation. PDKs, which inhibit entry of pyruvate into the TCA cycle, are regulated by both HIF1 and HIF2. FFA, free fatty acids. *Adapted from Majmundar, Wong, and Simon, 2010 (46).*

investigated in the context of ATII cells, but may apply to other HIF2-expressing cell types as well. Previous investigations have detailed several ATII cell responses to short-term hypoxic exposure. These cellular processes include pro-angiogenesis signaling, generation of reactive oxygen species and activation of AMPK (51) and up-regulation of glucose transporters and localization to the cell membrane (52). Immediate metabolic responses include down-regulation of Na⁺/K⁺ ATPase pump, which normally mediates fluid and ion homeostasis across the alveolar epithelium. Reduced pump activity is achieved rapidly following hypoxic exposure by removal of the pump from the cell membrane via an AMP-kinase dependent mechanism. Despite this being a well-characterized response to hypoxia, metabolic analyses accounting for ATP allocation to Na⁺/K⁺ ATPase function have questioned the impact of this adaptation on ATP conservation, indicating that the energy savings achieved through this mechanism are relatively small (23).

The impacts of longer periods of hypoxia (ie, over 8 hours) are poorly characterized. Over extended exposure, HIF1 expression declines while HIF2 remains stable. Neither ATP levels (52) nor cell survival (23, 53) appear to be impacted, indicating robust hypoxia tolerance. Reduced citrate synthase concentrations following 24 hour exposure suggest decreased mitochondrial density (23) although these measurements were performed in A549, a cancer-derived, highly glycolytic cell line that has not been critically assessed as a model for metabolism of ATII. More detailed investigation of mitochondrial population dynamics in hypoxic ATII has not been performed.

ATII cell surfactant protein expression is reduced at the level of transcription in a HIF-responsive manner (49, 54). Additionally, findings from our laboratory and others have conclusively demonstrated that globin protein and associated globin regulatory proteins are expressed specifically in ATII cells (55, 56) and up-regulated at the level of transcription in response to HIF stabilization (49). This has been confirmed via immunohistochemical staining of tissue slices and also *in vivo*, with globins observed in the lung tissues and bronchoalveolar lavage fluid (BALF) obtained from long-term hypoxia-exposed rats (57). The function of hemoglobin in ATII cells under hypoxia has yet to be determined, but hypotheses include oxygen-sensing, scavenging of reactive oxygen and nitrogen species, and sequestration of oxygen within the cell.

1.6 Idiopathic Pulmonary Fibrosis

1.6.1 IPF overview

Idiopathic pulmonary fibrosis is a devastating lung disease characterized by the progressive formation of fibrotic scar tissue in the pulmonary interstitium. IPF affects up to an estimated 500,000 people in the USA, with approximately 50,000 new cases diagnoses each year. The disease is generally diagnosed in patients over the age of 50 and is more common in men than woman. IPF has no cure, with palliative care and lung transplantation being the only non-investigative courses of treatment, and is ultimately fatal with the median survival time of 3-5 years following diagnosis. In the progression of IPF, extensive fibrosis eventually

damages bronchioles and alveoli resulting in greatly impaired gas exchange and chronic oxygen deficiency that ultimately leads to death.

IPF is characterized as an interstitial lung disease, although the alveoli and peripheral airways are also heavily affected and substantial evidence points to the alveolar epithelium as the initial point of injury. It is classified as a chronic fibrosing, idiopathic interstitial pneumonia. Common clinical features include patient age greater than 50 years old, dry cough, exertional dyspnea, crackles on auscultation, and evidence of impaired gas exchange in pulmonary function tests (58). Radiologically, the disease is characterized by reticular and ground-glass opacities indicating dense fibrosis, and “honeycombing” of the lung where normal, saccular tissue has been thickened and dilated into large cystic airspaces. Fibrosis in IPF concentrates in subpleural regions and distal lung interstitium and alveolar tissue, relatively sparing the proximal, bronchiolar tissue. Characteristic honeycombing can also be observed histopathologically, in addition to areas of dense matrix deposition, infiltrating inflammatory cells, and fibroblastic foci containing proliferating myofibroblasts clustered locally atop the alveolar epithelium and disrupting the normally thin epithelial layer of the alveolar septae. The presence of organized fibrotic foci is a defining characteristic of IPF.

Environmental & Genetic Factors

Genetic predispositions including mutations in surfactant proteins A and C (59, 60), mucin protein 5B (61, 62), and telomerase (63) have been associated with both familial and non-familial IPF. *SPC* mutations related to IPF result in

surfactant proteins that do not fold properly in the ATII cells that produce them. This leads to activation of the Unfolded Protein Response (UPR) and associated endoplasmic reticulum stress, which causes mitochondrial dysfunction and ATII cell apoptosis. *MUC5B* encodes a mucin protein expressed by bronchial epithelial cells, and *MUC5B* polymorphisms have been associated with development of IPF (61). Telomerase is critical for ATII cell progenitor function, and mutations in the gene affect the ability of ATII cells to replicate and differentiate into ATI cells upon epithelial damage. Mutations in *hTERT*, the gene encoding telomerase, that impair function of the enzyme are present in a significant proportion of familial IPF cases.

Pathobiology of IPF

The current consensus is that IPF originates with injury to the alveolar epithelium. Although the injurious stimulus/stimuli are still unknown, senescence and/or apoptosis of ATII cells are thought to be the initiating factor (1, 64). ATII injury, senescence, and apoptosis generate a pro-fibrotic environment by secretion of factors that stimulate fibroblast conversion into an activated state, enhance extracellular matrix production, and recruit inflammatory cells to sites of injury. Additionally, the ability of surviving ATII cells to heal the damaged epithelium via cell proliferation and differentiation is impaired in IPF, wherein aberrant replication and differentiation by ATII cells leads to cell hyperplasia, loss of ATII cell phenotype, a decrease in fully-differentiated ATI cells, and potentially epithelial-to-mesenchymal transition (EMT) by ATII.

The cellular pathogenesis of fibrotic disease (as well as the normal wound-healing process) includes stimulation of normal fibroblasts and differentiation into the myofibroblast phenotype. Myofibroblasts are secretory, contractile mesenchymal cells that express markers of both fibroblasts and smooth muscle cells (65). Fibroblasts are stimulated by growth factors and cytokines to differentiate into the myofibroblast phenotype, which rapidly generates extracellular matrix components including collagen type I and II. The primary differences between fibroblasts and the differentiated myofibroblast include expression of alpha-Smooth Muscle Actin (α SMA), enhanced expression of collagen, increased contractility, and increased connections to the extracellular matrix and to other myofibroblasts (66). The enhanced secretory function of myofibroblasts that leads to excessive matrix deposition paired with reduced degradation makes myofibroblasts key cellular drivers of IPF pathogenesis downstream of alveolar epithelial injury. There is ongoing debate regarding the source of myofibroblasts in IPF lung, in that they may be the result of resident fibroblast differentiation and proliferation, recruitment of fibroblasts to sites of injury, or even the result of ATII cell EMT and adoption of a fibrogenic phenotype. Myofibroblasts concentrate into “fibroblastic foci” around sites of epithelial injury leading to localized areas of intense matrix deposition and tissue remodeling.

The major pro-fibrotic cytokine involved in stimulating recruitment, proliferation and differentiation of fibroblasts as well as inducing matrix production and deposition is transforming growth factor beta (TGF β) (67). TGF β is produced by a variety of pulmonary cell types including ATII cells and

stimulated fibroblasts, and plays an integral role in the development of IPF by continuously driving myofibroblast differentiation and stimulating matrix production. TGF β also affects ATII cell function directly, leading to ATII cell stress and apoptosis. The driving force of TGF β is highlighted by observations that the cytokine is consistently elevated in IPF lung from both human patients and mouse models, and that inhibition of TGF β resolves fibrosis in mouse models of IPF.

While originally thought to be a central component of IPF disease biology, inflammation is now considered a secondary event to epithelial injury and myofibroblast proliferation. This is altogether unlike COPD, in which inflammation is the primary driver of the disease leading to alveolar obstruction and hypoxia (64). Supporting this updated view of IPF pathogenesis are the observations that fibrosis is non-responsive to immune suppression including steroid treatment, and that the onset and clinical course of the disease after diagnosis is not associated with any major changes in inflammatory processes (68). However, epithelial damage does stimulate release of cytokines that recruit monocytes and neutrophils to injured tissue that do contribute to the pro-fibrotic environment. Inflammatory cells recruited to sites of damaged lung tissue produce ROS, TGF β , and cytokines including IL-1, all of which feed back into epithelial cell damage and myofibroblast stimulation. A feed-forward cycle of progressive, unresolved epithelial damage driving inappropriate fibrotic response appears to encapsulate the progression of the disease, but the cause of epithelial damage and the inability of the epithelial to heal are unknown. Thus, whereas

considerable progress has been made concerning the role of the fibroblast in IPF, epithelial dysfunction is still relatively undefined and is thus the focus of heavy investigation.

Progression of fibrosis leads to local epithelial tissue hypoxia, thickening of alveolar septae, and disrupted gas exchange. Eventually, when the disease becomes severe, blood flow to areas of poor gas exchange is reduced by the HPV response in an effort to improve gas exchange efficiency for the organ as a whole, which further aggravates the localized hypoxic conditions. The most common cause of mortality in IPF patients is respiratory failure, although death related to pulmonary hypertension and cardiac failure is also common.

1.6.2 Alveolar Epithelial Cells in IPF

Injury & Phenotypic Change

Despite the clear and integral role of fibroblasts in the progression of IPF, it is now widely accepted that the ultimate initiating event is injury to the alveolar epithelium, specifically ATII cells (1, 69). ATII cell senescence and apoptosis is increased in the IPF lung (70) and is likely a triggering event for the immunological and fibroblastic responses that follow. However, despite the evolution of this hypothesis that puts ATII cell damage at the onset of IPF pathogenesis, the molecular insult that results in ATII cell death in IPF remains unknown. Many different possible forms of injury to the alveolar epithelium are being examined in the initiation of IPF, including ROS generation (71), viral infections (72) autoimmunity (73), and aspiration of gastric contents (74).

In addition to senescence and apoptosis, the cellular phenotype of subpopulations of surviving ATII cells is altered in and around fibrotic foci. Regions of aggregated cuboidal cells form, indicating ATII cell hyperplasia. Hyperplastic ATII cells and populations that express ATII cell markers but have lost morphological characteristics of the ATII phenotype are also seen, suggested to be transitional phenotypes indicative of impaired differentiation to ATI cells (68). ATII hyperplasia and aberrant differentiation generates cells that express a variety of cell phenotype markers and do not effectively heal the wounded epithelial barrier.

Recent investigation has also demonstrated an EMT-like response by alveolar epithelial cells *in vitro* following exposure to TGF β . In multiple *in vitro* studies, exposed cells adopted altered cell morphology, expressed fibroblast markers and extracellular matrix proteins, and decreased epithelial cell markers (75, 76). This was later connected to ROS, in that exposure to ROS induces TGF β expression and EMT in model ATII cells, while inhibition of TGF β prevented ROS-induced EMT (77). Cells expressing both epithelial and fibroblastic markers have been observed in human tissue from IPF patients (78), suggesting that transition can occur between the two phenotypes. This evidence has inspired the hypothesis that both ATII cell loss and the prevalence of myofibroblasts in IPF tissue may be the result of TGF β -induced ATII cell EMT. Accordingly, preventing TGF β -induced EMT has been a focus of current research in treatment of IPF (79). However, this EMT hypothesis is heavily debated in IPF literature, based on inconsistency in histochemical labeling

studies to show co-localization of ATII and fibroblast markers, as well as labeling studies that fail to demonstrate myofibroblast generation from labeled ATII.

Surviving ATII cells in IPF lung, particularly those in proximity to fibroblastic foci, are primary sites of cytokine and growth factor production. IPF ATII cells produce TGF β , the main pro-fibrotic cytokine involved in converting fibroblasts to myofibroblasts and stimulating extracellular matrix deposition. ATII also play a critical role in activation latent TGF β stored in the extracellular matrix via integrin binding. $\alpha\beta6$ integrins are expressed on the surface of ATII cells, and their expression is up-regulated in IPF (80). These integrins bind to TGF β latency-associated peptides, which are bound to inactive TGF β in the extracellular matrix and prevents activation. When contraction of ATII cells is stimulated by binding of other mediators, the physical pulling of the integrin on the latency-associated peptide results in TGF β activation. Other factors released at sites of alveolar epithelial injury in IPF lung include tumor necrosis factor alpha (TNF α) and platelet-derived growth factor (PDGF) (68), which contributes to lung fibrosis by stimulating fibroblast proliferation and synthetic activity (81).

In summary, the epithelium and ATII cells specifically are the primary target of injury in the initiation of IPF. Following initial injury, aberrant response by ATII cells results in apoptosis, senescence, and phenotypic change including altered morphology and gene expression. These cells become important producers of pro-fibrotic growth factors and cytokines and may possibly contribute directly to the myofibroblast population through EMT. However, the

source of initiating injury to ATII cells and the nature of their chronic dysfunction is unknown.

Fibroblast-AEC interactions

In addition to matrix components, IPF lung fibroblasts produce extracellular signaling molecules that contribute to disease pathogenesis. TGF β is a critical signal for initiating conversion of fibroblasts into the myofibroblast phenotype, but it is also activated by myofibroblasts themselves (82). *In vitro* exposure to active TGF β has been shown to promote a variety of effects in alveolar epithelial cells including, epithelial-to-mesenchymal transition in alveolar epithelial type II cells (83), apoptosis (84), and ATII to ATI differentiation (85). Thus, TGF β may be a molecular mediator in both the early events of IPF that generate myofibroblasts and the prolonged, unresolved epithelial cell injury that progresses the disease.

Myofibroblasts produce reactive oxygen species, and several studies have demonstrated elevated ROS in the lungs of IPF patients (86, 87). Production is dependent on NADPH oxidase 4 (NOX4), which is up-regulated in myofibroblasts by exposure to TGF β and is highly expressed at fibroblastic foci (88). NOX4-dependent H₂O₂ generation plays a critical role in disease progression, as multiple mouse models of IPF showed resolution of fibrosis following NOX4 knockdown; therefore, ROS is a key component of the pro-fibrotic environment. While the exact contributions of ROS are under investigation, it has been shown that exposure to hydrogen peroxide induces cell death in alveolar epithelial cells

and prevents wound closure *in vitro* (89), demonstrating that exogenous ROS can cause epithelial injury. In the bleomycin-induced mouse model of IPF, NOX4 knockdown *in vivo* reduced epithelial cell apoptosis (88) and administration of the antioxidant enzyme superoxide dismutase suppressed fibrosis (90). Altogether, this evidence points to an important role for myofibroblast-produced ROS in the repetitive epithelial injury that characterizes the progression of IPF.

Immune Effector-AEC interactions

Epithelial injury at the initiation of IPF also initiates an immune response through several mechanisms. Platelets activated in response to wounding of the alveolar epithelium release TGF β and other growth factors that contribute directly to myofibroblast activation and matrix production (1). Injured epithelial cells themselves produce cytokines that recruit cellular inflammatory mediators, namely neutrophils and monocytes, which produce ROS. When inflammatory cells are not effectively cleared from the wounded tissue, as occurs in IPF, continued ROS production by these cells contributes to further injury (91). While the role of the innate immune system in IPF is less defined, cytokine secretion from T cells appears to play a role as well. In particular, IL-13 both directly stimulates fibroblast hyperproliferation and causes epithelial cell apoptosis (92), and IL-13 and IL-13 Receptor expression correlate with IPF disease severity (93).

1.6.3 Pulmonary cell metabolism in IPF

Despite the range of possible epithelial cell injuries that could conceivably lead to metabolic adaptation or dysfunction, the contribution of cellular metabolism to IPF has only relatively recently come under investigation. Recent work has discovered that lactic acid build-up occurs in IPF lung tissue, and further investigation demonstrated that an increased level of lactic acid contributes at the molecular level to the pro-fibrotic environment in IPF lung. Specifically, the decrease in extracellular pH associated with tissue lactic acid build-up activates TGF β from the extracellular milieu of the epithelium (94). TGF β is the primary signal leading to conversion of fibroblasts into the myofibroblast phenotype responsible for increased matrix deposition and fibrogenesis (95, 96). Therefore, processes that lead to a metabolic shift to enhanced glycolysis and/or a decrease in lactate removal from the extracellular space have the potential to drive pulmonary fibrosis via pH-mediated TGF β activation. The cellular source and cause(s) of elevated lactic acid in IPF is yet unknown, though TGF β -stimulated myofibroblasts have been shown to produce greater amounts of lactic acid than unstimulated fibroblasts *in vitro*.

A shift in LDH isoform expression has also been observed in IPF lung tissue, in conjunction with increased tissue lactate. Enhanced expression of the LDH5 isoenzyme occurs, localized in the approximate region of the alveolar epithelial cells near fibrotic foci (94), though the specific cells up-regulating LDH5 expression have not previously been determined. This isoform of the LDH enzyme most strongly favors the forward, lactate-producing reaction, and is often

expressed in highly glycolytic cells that favor lactic acid production from pyruvate over mitochondrial metabolism. In TGF β -stimulated myofibroblasts, up-regulated LDH5 expression was demonstrated to be influenced by HIF signaling, as overexpression of HIF1 lead to enhanced LDH5. This suggests that the localized hypoxia that occurs in IPF (or other factors that stabilize HIF, like ROS) may contribute to shifts in metabolic enzymes leading to overproduction of lactic acid. Follow-up studies to the discovery of elevated lactate generation in IPF lung tissue demonstrated improvement of fibrosis in mice treated systemically with a pharmacological LDH-inhibitor, further validating the influence of pulmonary cell glycolytic metabolism on the pro-fibrotic milieu.

Interestingly, neither lactic acid build-up, tissue acidification, nor LDH5 over-expression were found in tissue from patients with COPD, another hypoxia-associated lung disease. This indicates that the shift in metabolism and the insult(s) that initiates it may be unique to IPF, and not simply a consequence of onset of tissue hypoxia. Though both diseases are associated with pulmonary hypoxia, there are many differences in the two, most notably the injury to the ATII cells and subsequent fibrosis in IPF (versus mesenchymal cells and subsequent inflammation in COPD) (97). Thus, the specific metabolic rearrangements leading to lactic acid build-up in the lung appear to be somewhat unique to IPF, and not merely a consequent of pulmonary hypoxia. While elevated lactic acid has been noted also in lung tissue of patients with cystic fibrosis, this is thought to be a consequence of neutrophil accumulation and subsequent tissue necrosis and hypoxia, and not glycolytic change in pulmonary cells themselves (98, 99).

The contribution of ATII to lactic acid build-up in IPF lung is unknown, and metabolic function of ATII from IPF lung has never been measured. Several forms of alveolar cell injury under investigation in IPF could conceivably lead to mitochondrial impairment and metabolic change in ATII cells, potentially also leading to enhanced lactic acid generation. Oxidative stress is a possible underlying cause of fibrosis (100), and there are many different cellular and molecular mechanisms through which ROS generation and oxidative stress are thought to be enhanced in IPF. First, as discussed previously, both myofibroblasts and innate immune cells generate ROS directly, providing exogenous sources of ROS exposure to the lung epithelium. Second, intracellular sources of ROS are also likely enhanced in response to the extracellular conditions in IPF. Of particular interest to ATII cell metabolism, *in vitro* TGF β exposure leads to mitochondrial suppression and ROS generation by decreasing activity of complex IV of the electron transport chain (101). In this study, treatment and mitochondrial ROS generation resulted in cell cycle arrest senescence in a line of lung epithelial cells.

Complimentary to enhanced ROS, depletion of antioxidant defense enzymes is linked to IPF. Glutathione is reduced in cells composing fibrotic foci in human IPF lungs (102) and knockout mice for superoxide dismutase have increased fibrotic response to bleomycin treatment, while administration of antioxidant enzymes prevents fibrosis in the mouse model (100). Reduced expression of antioxidant defense enzymes in AEC has been linked *in vitro* to TGF β exposure.

From previous investigation, it is clear that a number of different conditions associated with IPF have potential to impact alveolar epithelial cell metabolism in IPF. This is of chief interest, given that recent study has identified metabolic changes in fibroblasts in the IPF lung and that the exact nature of epithelial cell dysfunction in IPF is unknown. Despite the implication based on molecular study that epithelial metabolism may be impacted in IPF, these observations have not been correlated to functional changes in overall alveolar epithelial cellular metabolism in IPF patients.

1.6.4 Need for assessment of human IPF patient samples

There is a critical need for basic science research utilizing human patient tissue obtained from IPF patients. At this time, there is no animal model available that faithfully replicates the unique human disease progression in IPF (103). For years, the most commonly-used animal model has been the bleomycin model of lung injury in mouse. Using this model, many breakthroughs in the molecular process of lung fibrosis have been made; however, the pathogenesis of the bleomycin-induced injury is different in critical aspects from IPF. Histologically, the models are quite different concerning the main sites of fibrosis: in the mouse model, fibrosis is often concentrated in the airways, while in human sub-pleural fibrosis dominates. Honeycombing, characteristic of human IPF, is variable in the mouse model. The organized pattern of layered myofibroblasts in parallel to the injured epithelium that is evident in fibroblastic foci in human disease is rarely observed the mouse, as is ATII cell hyperplasia. A portion of human patients

experience acute exacerbations of the disease, wherein clinical condition deteriorates over a matter of weeks; no model has been able to recapitulate this facet of disease progression. Furthermore, fibrosis self-resolves in mice over time, while in human spontaneous resolution does not occur. There is also strong dependency of fibrotic response to bleomycin on the strain of mouse exposed (104).

Not only is there a need to measure variables in human samples, but also to assess the metabolic function of ATII cells derived from IPF lung in general. While, as discussed, many molecular drivers of IPF have potential to alter cellular metabolism of the target epithelial cells, to our knowledge this has never been directly measured at the functional level in cells isolated from IPF lung. Recent work has measured cellular metabolism in myofibroblasts derived from IPF lung tissue, the first ever to connect previously noted molecular changes with a functional metabolic response with potential to impact not only the myofibroblasts themselves, but also the extracellular milieu by way of acidification and metabolite availability. While fibroblasts are central players in the disease, ATII cells are the proposed target of much of the injury and subsequent dysfunction in IPF. Thus, functional metabolic studies of human ATII derived from tissue samples from IPF lung are a natural, needed step in IPF investigation.

Despite the desperate need for novel research using human IPF patient samples, the reality is that lung tissue samples from human patients, those with and without IPF are severely limited. Investigation using patient samples can yield valuable, immediately translatable, and even highly personalized medical

findings; however, well-supported and reliable findings in human research will require assessment of many patient samples. Current efforts in tissue collection, preservation, and banking have expanded the availability of patient lung tissue samples, making fundamental cellular biology studies of human lung diseases feasible without the need to extrapolate from imperfect animal models of the disease. In the case of IPF, where no animal model to date faithfully recapitulates either the pathology or progression of the disease, access to human samples is of critical importance.

1.7 Overall significance and specific aims

Lung disease is a leading cause of death in the United States. Epithelial damage and cellular dysfunction are major features of lung disease, and in some cases defines the root cause of the disease, as in IPF. The role of cellular metabolic dysfunction has begun to be elucidated in many diseases including cancer, heart failure, ocular diseases, and renal disease; by comparison, investigation of cellular metabolism in the lung and its contribution to pulmonary disease pathogenesis is severely lacking.

In particular, idiopathic pulmonary fibrosis is associated with a variety of factors with the potential to influence cellular metabolism. Current theory regarding IPF pathogenesis considers ATII cell damage to be a critical initiating factor, but the role of ATII metabolism in the disease has not been examined. Local hypoxia, which develops in the pulmonary tissue in the pathogenesis of IPF and several other chronic lung diseases, has the potential to influence cellular

metabolism in the diseased lung. Oxygen exposure is a major factor known to influence cell metabolism throughout the body, however investigation of how local pulmonary hypoxia influences epithelial cell metabolism is lacking. Other insults that have potential to influence cell metabolism at the molecular level have also been defined as drivers of IPF including ROS and growth factors, but in most cases the connection between their molecular function, their impact on epithelial cell metabolism, and the influence of altered cellular metabolism on lung homeostasis has not been made. Contributing to this deficit is a general lack of understanding regarding the normal metabolic function of individual cell types in the healthy lung.

The body of work that follows examines the overall hypothesis that **conditions associated with hypoxia-related lung disease alter the normal metabolism of ATII cells**. We hypothesized that ATII cells are normally highly metabolic and dependent on oxidative mitochondrial metabolism to supply ATP for their many energy-demanding functions, and that under hypoxic conditions ATII cell mitochondrial function is suppressed while glycolysis is enhanced. To further extend this work we focus on the hypoxia-related disease IPF and examine metabolism of ATII isolated directly from patient samples.

The work presented herein serves the following aims:

Specific Aim 1: Establish a metabolic phenotype for primary and model ATII cells.

Specific Aim 2: Measure the impact of hypoxia on ATII cell metabolism.

Specific Aim 3: Examine the utilization of lactate as substrate for ATII cell metabolism.

Specific Aim 4: Examine metabolic function of ATII cells isolated from human IPF lung tissue.

Investigation of these aims involved use of ATII model cell lines and primary ATII cells isolated from mouse and human patient tissue samples. Metabolic function was assessed in vitro via metabolic flux assay to measure oxygen consumption and acid generation in response to a variety of experimental conditions including hypoxia, varied metabolic substrate availability, and exposure to mitochondrial inhibitors. Observations regarding metabolism at the function level were correlated with evaluations of gene and protein expression.

This body of work provides significant insight into the metabolic function of ATII cells. We define the metabolic phenotype of well-oxygenated ATII cells and show that ATII cells are capable of importing and utilizing lactate as substrate for mitochondrial ATP production, building on previous observations that lactate is taken up and oxidized in the lung and indicating a specific role for ATII in lung lactate homeostasis. We also define the metabolic strategy adopted by ATII in

response to low oxygen conditions, demonstrating that ATII cells are remarkably resistant to hypoxia and do not enhance glycolytic function in response, adapting instead through down-regulated ATP demand. Hypoxia impacts mitochondrial function in ATII cells, reducing mitochondrial oxidization regardless of substrate.

Finally, we connect these observations to the hypoxia-related lung disease IPF, in which we show that disrupted lactate homeostasis plays a role in the fibrotic process. ATII derived from human patient IPF lung tissue are less metabolic overall and relative reliance on glycolysis is enhanced, indicating that the ability of ATII to rapidly import and utilize lactate in the lung is impaired in IPF and may thus contribute to lactic acid build-up in this disease. We provide a hypothetical model of metabolic cooperation between ATII cells and neighboring cell types based on our findings, and suggest how altered ATII metabolism may contribute to lactic acid build-up in distal pulmonary tissue. In summary, the work presented here builds significantly on the current understanding of cellular metabolism in the lung, the metabolic response to hypoxia, and how ATII cell changes may contribute to hypoxia-related human diseases.

CHAPTER 2. ATII CELLS HAVE AN OXIDATIVE, HIGHLY METABOLIC PHENOTYPE

2.1 Introduction

Due to their physical location, the cells that line alveoli in developed mammalian lungs are normally exposed to a uniquely well-oxygenated environment of approximately 13% O₂ in non-diseased lungs (an approximate pO₂ of 100 mm Hg) as compared to about 5% (pO₂ of approximately 40 mm Hg) in peripheral blood (38). The mesh of pulmonary capillaries that cover each individual alveolus moves the entire cardiac output through the lung tissue for gas exchange, making the alveolar epithelium the only tissue apart from the heart itself that receives the full volume of blood (and the metabolic substrates it carries) on every single complete pass through the body.

ATII cells make up about 50% of the alveolar epithelial layer by cell number. They are the primary producers of pulmonary surfactant and also have important roles in ion and fluid transport (6-8) and innate immunity (105). Maintenance of surfactant homeostasis, which is essential for normal lung function, requires considerable metabolic investment by ATII cells for lipid and protein synthesis, packaging, secretion, and recycling (4). Fluid transport is performed via the action of ATPase ion pumps which have been estimated to require upwards of 15% of ATII energy supply (23), and the main innate immunity

functions of ATII cells depend upon surfactant protein production and secretion. ATII cells also serve as progenitor cells capable of repopulating ATI cells following physical damage or stress (9) and can rapidly repair epithelial wounding through cell replication and differentiation, cellular processes that require cellular energy in the form of ATP. Due to their many energy-consuming functions that are absolutely critical to support normal lung function, ATII cells are predicted to have a constant high demand for ATP. However, despite their unique position in the body and the necessity for ATII cells to maintain bioenergetic homeostasis in order for the lung to function properly, ATII cellular metabolism has not been thoroughly studied.

Historic studies of whole-lung metabolism demonstrated that the lung consumes oxygen, indicating mitochondrial respiration and ATP production. However, the lung was also shown to generate lactate under ambient oxygen conditions, indicating a degree of glycolytic glucose processing despite abundant available oxygen (21). These and other early studies elucidated whole-lung metabolism, but were limited in that they could not address the metabolic function of specific cell types in the lung. While glycolytic generation of lactic acid was initially considered to be a response to oxygen limitation, it is now understood that most cells generate some lactate without the pressure of oxygen limitation. The degree to which this occurs varies considerably by cell type, with some cells largely reliant on anaerobic metabolism of glucose to lactate to generate ATP and others primarily dependent on mitochondrial electron transport. Simultaneous real-time assessment of oxygen consumption and

lactate generation provides insight into the degree to which a specific cell type relies on anaerobic glycolysis versus mitochondrial function. These assessments have not been previously performed in primary ATII cells or using the predominant model for ATII cell biology, the MLE-15 cell line.

Part of the difficulty in studying ATII cell metabolism and ATII biology in general is the challenge of isolating a pure population of ATII from the lung, which is composed of an enormous variety of cell types, some of which do not have reliable cell-specific surface markers for use in cell isolation. Furthermore, primary ATII cells in culture rapidly differentiate into ATI cells, which phenotypically are very different from ATII cells in terms of both cell morphology and cell function. While there are multiple cell lines that have historically been utilized to model ATII cells in vitro including the human tumor-derived A549 and the MLE-12 and MLE-15 immortalized mouse lung epithelial lines, the utility of these cells in faithfully modeling ATII cellular metabolism is unknown. Here, we utilize modern cell-sorting techniques to isolate ATII cells from mouse lung and perform comparisons of basal, maximal, and overall relative oxidative and glycolytic function between primary cells and cultures of MLE-15, demonstrating for the first time that the MLE-15 line recapitulates the relative reliance on glycolysis versus oxidative function.

Confirming historical findings and predictions based on cell function, we find that ATII cells rapidly consume oxygen and extrude lactic acid under ambient O₂ conditions, indicating a highly metabolic phenotype. Approximately 50% of oxygen consumed is dedicated to mitochondrial ATP production. Almost all

extracellular acidification by MLE-15 can be accounted for by lactic acid production, implicating glycolytic output as the main driver of extracellular pH change by ATII. We quantify significant spare respiratory and glycolytic capacity, reserves of potential energy production above basal levels in culture. Overall we conclude that ATII cells are highly metabolic and oxidative under ambient O₂, and we provide a platform from which to study the impacts of modulators of ATII cellular metabolism.

2.2 Results

2.2.1 ATII cells consume oxygen rapidly to fuel mitochondrial ATP production.

Aerobic, mitochondrial energy production requires oxygen as an ultimate electron acceptor at the end of the electron transport chain. Cells that depend heavily on mitochondria to generate ATP consume oxygen at rapid rates, while oxygen consumption occurs more slowly in cell types that are more dependent on anaerobic glycolysis to generate ATP. In order to assess the aerobic function of ATII cells, extracellular flux analysis was performed to determine the oxygen consumption rate (OCR) of cells in culture. MLE-15 cells consumed oxygen at a rate of 12.7 ± 1.7 pmole O₂/min/μg protein. Primary mouse ATII cells consumed oxygen at a rate of 25.6 ± 1.4 pmol O₂/min/μg protein (Figure 2.1).

Oxygen may be consumed by cells to fuel mitochondrial ATP production, but there are also other functions that can contribute to total cellular oxygen consumption. Other processes that consume oxygen include proton leakage across the inner mitochondrial membrane and non-mitochondrial oxygen

consumption, which includes reactive oxygen species generation and cell surface oxygen consumption (106). The degree to which oxygen consumption is dedicated to mitochondrial ATP production can be determined by inhibiting mitochondrial ATP-synthase, which effectively blocks ATP production. This leads to a reduction in OCR from basal rates corresponding to the fraction that is coupled to ATP generation. Coupling of O₂ consumption to ATP synthesis was measured using MLE-15 cell cultures as a model for ATII. Inhibition of ATP-synthase via in-assay injection of the pharmacological inhibitor oligomycin A resulted in a 50% decrease in OCR from basal measurements (Figure 2.2). Therefore, approximately half of oxygen consumed by ATII cells is used as an electron acceptor facilitating ATP production.

2.2.2 ATII cells generate extracellular lactic acid.

Extracellular lactic acid is produced as a byproduct of anaerobic glycolysis, wherein pyruvate is converted to lactic acid and extruded from the cell as waste rather than being utilized by mitochondria to generate reducing equivalents for oxidative ATP generation. Efflux of lactic acid results in acidification of the extracellular milieu, which can be measured over time as a progressive drop in pH, and this value indicates the rate at which cells in culture perform anaerobic glycolysis. Primary mouse ATII cells produced extracellular protons at a rate of 48.8 +/- 3.4 pmole H⁺/minute/ug protein, while proton production rate (PPR) for MLE-15 cells was 25.5 +/- 4.4 pmole H⁺/minute/ug protein (Figure 2.3).

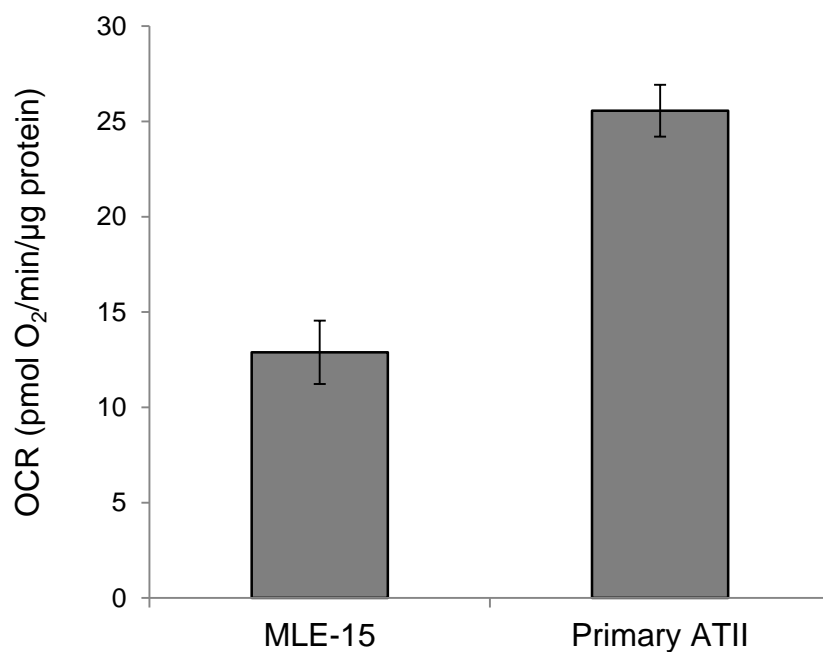


Figure 2.1: MLE-15 and primary ATII cells rapidly respire oxygen. OCR was measured for MLE-15 cells and primary mouse ATII cells using an XF24 Extracellular Flux Analyzer. For MLE-15 cultures, samples were assayed minimally in quadruplicate and plates run in triplicate. For primary cultures, a total of six individually-cultured wells were analyzed. MLE-15 and ATII were not compared statistically. Values are normalized to total protein of wells cultured in parallel. Error bars represent \pm SE.

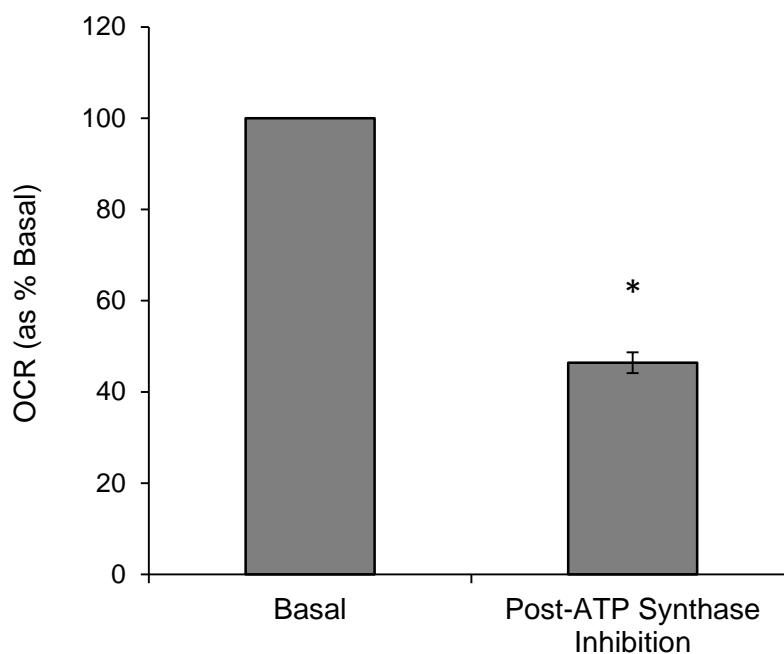


Figure 2.2: Approximately half of oxygen consumption by ATII cells is coupled to mitochondrial ATP production. The proportion of oxygen consumption dedicated to generation of ATP via oxidative phosphorylation was determined in MLE-15 cultures by measuring OCR before and after addition of oligomycin A, an inhibitor of ATP synthase, to assay media. For MLE-15 cultures, samples were assayed minimally in quadruplicate for each condition and plates run in triplicate. * indicates significant difference ($p < 0.05$) from basal measurements based on paired Student's T-Test. Values represent the percent decrease from basal values following inhibitor injection. Error bars represent \pm SE.

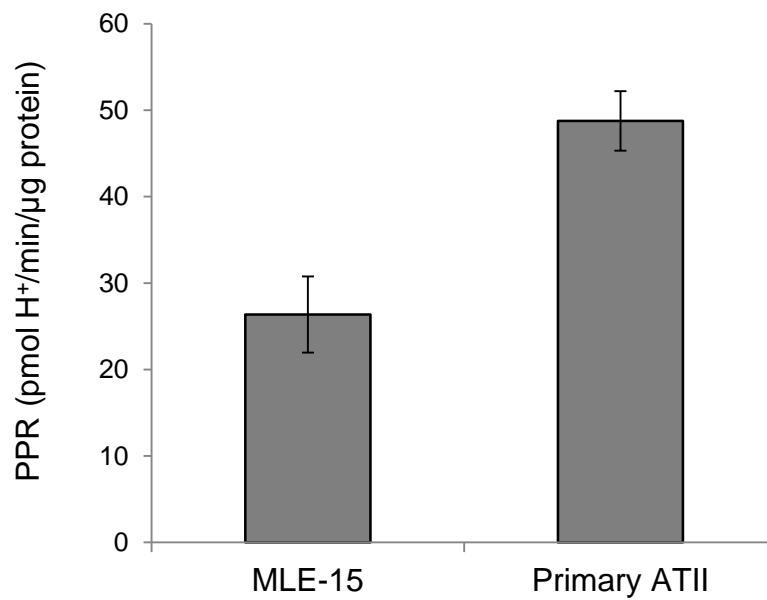


Figure 2.3: ATII cells have glycolytic function under ambient O₂. PPR was measured as an indicator of glycolysis in MLE-15 and primary ATII cells. Samples were assayed minimally in quadruplicate for each condition and plates run in triplicate. Error bars represent \pm SE. MLE-15 and ATII were not compared statistically.

2.2.3 ATII cells maintain spare respiratory and spare glycolytic capacities

The highest possible rates of mitochondrial function for intact cells can be measured by adding an ionophore compound, such as FCCP. The effect of this is rapid dissipation of the proton gradient across the mitochondrial inner membrane, forcing electron transport to be performed as quickly as possible in a futile attempt to re-establish the gradient necessary for ATP production. The difference between basal and uncoupled OCR measurements indicates the spare (or reserve) respiratory capacity of the cell, or the ability to perform respiration above basal level. To measure this maximal rate for ATII cells, FCCP was added to assay wells following basal measurements. OCR measurements following addition of FCCP indicated that uncoupled respiration rates for MLE-15 cultures was 175% of basal OCR. Uncoupled respiration in primary mouse ATII cells was approximately 150% of basal OCR (Figure 2.4A), demonstrating a significant reserve of potential mitochondrial functional capacity in both cell types.

An analogous situation exists for glycolytic function, in that inhibition of ATP synthesis from oxidative phosphorylation results in enhanced glycolytic output due to the cells' attempt to compensate for loss of mitochondrial ATP production. Addition of FCCP to assay wells thus stimulates enhanced PPR (spare glycolytic capacity) in parallel to enhanced OCR (spare respiratory capacity). Upon addition of FCCP to assay media, PPR increased to 133% of basal rates for primary ATII and 208% basal rates for MLE-15 (Figure 2.4B). This demonstrates that both cell types are operating at sub-maximal rates of anaerobic glycolysis.

2.2.4 MLE-15 cells recapitulate ATII relative reliance on mitochondrial respiration.

In terms of normalized OCR and PPR values, MLE-15 cells demonstrated lower function overall than primary mouse ATII cells. While these values alone are informative, it is the ratio of glycolytic and oxidative metabolic function that indicates the degree to which a cell type relies on either pathway and provides an indication of the metabolic phenotype. There was no statistical difference in the PPR/OCR for primary ATII cells and MLE-15, with values of 1.90 ± 0.04 moles H^+ /moles O_2 and 2.13 ± 0.29 moles H^+ /moles O_2 , respectively (Figure 2.5). The similarity of these values shows that, while MLE-15 cells are less metabolic than primary ATII cells, they recapitulate ATII metabolic function in terms of relative reliance on different metabolic pathways.

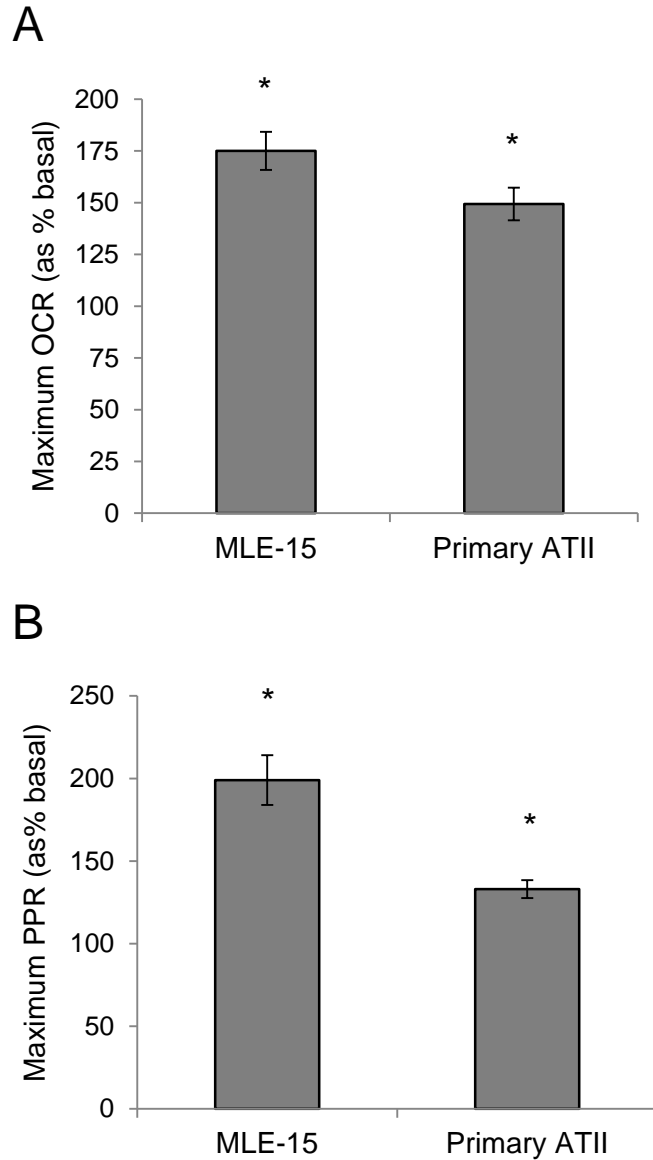


Figure 2.4: ATII cells have significant mitochondrial and glycolytic reserve capacity. To assess reserve capacity, OCR (A) and PPR (B) were measured in cultures of MLE-15 and primary ATII cells before and after addition of FCCP to assay media. For MLE-15, samples were assayed minimally in quadruplicate for each condition and plates run in triplicate. For primary cultures, a total of 6 single-well experiments for each condition. * indicates significant difference ($p < 0.05$) from basal measurements, based on Student's T-Test. Values represent the percent decrease from basal values following inhibitor injection. Error bars represent \pm SE.

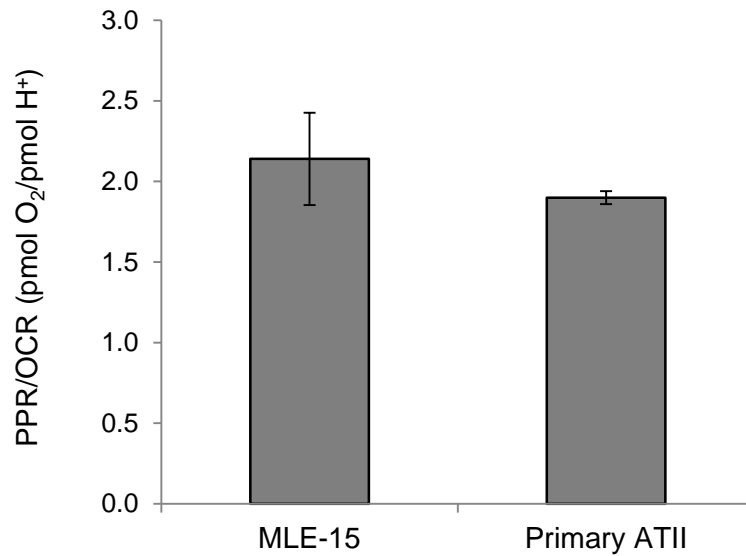


Figure 2.5: MLE-15 and primary ATII show similar relative reliance on oxidative versus glycolytic function. Basal PPR and basal OCR measurements were used to generate a PPR/OCR ratio for in MLE-15 and primary ATII cells. For MLE-15, samples were assayed minimally in quadruplicate for each condition and plates run in triplicate. For primary cultures, a total of six individual cultures were assessed. Error bars represent \pm SE.

2.3 Discussion

Through these studies, a metabolic phenotype has been defined for mouse ATII cells. MLE-15 and primary ATII cells rely heavily on oxidative phosphorylation to supply ATP, with MLE-15 consuming oxygen at basal rates in range of values reported for primary bovine aortic endothelial cells (3) and primary ATII respiring at rates nearly twice as rapid. Approximately 50% of oxygen consumption is coupled to mitochondrial ATP production. Primary ATII and MLE-15 also produced extracellular acid. As in the case of OCR, PPR measurements were approximately twice as high in primary ATII cells compared to MLE-15 cells. The transformed nature of the MLE-15 cell line, as well as the fact that MLE-15 stocks had been maintained in culture for many passages while primary ATII were used within days of the isolation and purification procedures, may account for these differences. Regardless, the relative reliance on oxidative versus glycolytic metabolism (as reflected by the ratio of basal proton production to O₂ consumption) is identical between cell type, indicating similar metabolic strategy for serving cell energy demand. Furthermore, this supports the use of MLE-15 cells as faithful models for primary ATII cells in terms of basal metabolism and metabolic response to stimuli.

Mouse ATII cells in culture demonstrated both spare respiratory capacity and spare glycolytic capacity. Maximal uncoupled respiratory capacity for MLE-15 cells is approximately 175% over basal metabolism, also within range of that previously reported for endothelial cells (just over 200% basal) but considerably lower than the 300% over basal reported for cardiomyocytes (3, 35). Primary ATII

cells maintain slightly less spare respiratory capacity (approximately 150% of basal), indicating that the primary cells were functioning closer to their maximal mitochondrial function at time of measurement. Uncoupling of respiration lead to an increase in lactic acid generation to approximately 200% of basal levels in MLE-15 and 140% of basal levels in primary ATII cells, indicating a similar degree of spare capacity to undergo glycolysis as for mitochondrial spare capacity for each cell type. In general, these data demonstrate that both cell types operate in culture at sub-maximal metabolic function, and supports the basal findings indicating that MLE-15 in culture are less metabolically active, potentially due to many passages in culture.

To gain a better understanding of the metabolic milieu of the alveolar epithelium, it is of chief interest to understand the metabolic function of other cells types that compose the alveolus and neighbor ATII cells. This degree of metabolic characterization has not been performed specifically for other alveolar cell types. It is likely that ATI cells have lower metabolic function than ATII cells, as they do not serve many of the energy-consuming functions that ATII cells fulfill. However, ATI cells do contain mitochondria, and may consume oxygen to fuel ATP production. Metabolic flux analysis has not been performed on fibroblasts derived from pulmonary tissue; however, measurements of Normal Human Dermal Fibroblasts (NHDF) showed lower metabolic function compared to mouse ATII cells. NHDF cells measured on the XF24 platform demonstrated OCR and ECAR values of approximately 100 pmole/min and 20 mpH/min, per 50,000 cells seeded into plates 16 or more hours prior to assay (107). This OCR

value is below the 350 pmole/min raw OCR values obtained for primary ATII cells at an approximate density of 75,000 cells/well. This concurs with prior investigation showing lower rates of substrate oxidization by fibroblasts compared to ATII (22).

The work presented here assessed metabolism in the presence of glucose and supplemented with glutamine as the sole available substrates for mitochondrial metabolism. However, studies of whole lung metabolism and limited investigation of fetal ATII cells suggest that other substrates may be oxidized, even preferentially, by ATII cells in the lung under physiological conditions. Several investigations of whole lung metabolism using the isolated perfused rat lung model reported high rates of lactate uptake and oxidation simultaneous with lactate production (17, 108). Lactate was also reported to be incorporated into lung lipids when provided in the perfusate in this model; as ATII cells are the primary producers of lipid in the lung to generate pulmonary surfactant, this likewise indicates that ATII cells may utilize lactate in addition to glucose under physiological conditions.

Variation in experimental protocols makes it difficult to compare these findings in ATII cells with flux data from other investigators using other cell types. Plating density, normalization strategy, proliferative capacity of the cell type, and assay timing vary widely between investigators and have major influence in how data is interpreted and compared. In this work, acidification is converted to PPR based on empirically calculated media buffering capacity, because even relatively minor alterations in assay media formulation can affect ECAR readings

and the media formulations differ based on the substrate or whether fetal bovine serum (FBS) has been added to the assay media. However, the majority of publications report ECAR values, which do not account for buffering capacity of different assay media formulations, and this makes comparison across studies difficult. Nonetheless, rough comparison of basal and maximal OCR values reported in publications or approximated from figures suggests that ATII cells are less metabolic than skeletal and heart muscle, but are otherwise in the upper echelon of cell phenotypes in terms of oxidative metabolic function (Table 1). On the other hand, primary ATII cells in culture demonstrated relatively lower spare respiratory capacity compared to other cell types. This may in part be due to the fact that they produce surfactant in culture; indeed, specific growth factors are added to primary ATII cell culture media that stimulate surfactant production in order to maintain the ATII cell phenotype and prevent differentiation. Thus, at the time of a metabolic flux measurement, the cells were actively performing at least one of their characteristic, highly energy-consuming functions and may require more of their total mitochondrial capacity to accomplish this. This would also help explain the different spare respiratory capacities of primary ATII and MLE-15 cells, which produce surfactant to a lesser degree.

Overall, we conclude ATII cells are highly metabolic in culture under ambient oxygen conditions, and are to a large degree dependent on mitochondrial ATP synthesis. This work quantifies for the first time the metabolic phenotype in terms of oxygen uptake and glycolytic output, as established by the PPR/OCR ratio, as well as demonstrating reserve mitochondrial and glycolytic

function. MLE-15 cells, while less metabolic overall, recapitulate the relative rates of lactic acid production and oxygen consumption observed in primary ATII cells, supporting their use as a model for further metabolic study.

Table 1: Comparison of mouse ATII OCR values to other metabolic cell types based on previously reported data. All data are previously reported or approximated from published reports; all data was obtained using the Seahorse Biosciences XF instrumentation.

CELL TYPE	Approximate cell number	Approximate OCR (pmol O₂/min)	Approximate reserve (% basal)	Reference
ATII Cells (<i>mouse primary</i>)	80,000	350	150%	<i>Lottes et al, 2014 (37)</i>
Primary Dermal Fibroblasts (<i>human</i>)	100,000	240	230%	<i>Moruzzi et al, 2014 (109)</i>
Aortic Endothelial Cells (<i>Bovine</i>)	60,000	150	220%	<i>Hill et al, 2010 (110)</i>
Cardiomyocytes (<i>neonatal mouse</i>)	50,000	400	400%	<i>Sridharan et al, 2008 (111)</i>
Neuron, Hippocampal (<i>mouse</i>)	50,000	250	200-300%	<i>Yao et al, 2011 (112)</i>
Muscle C2C12 Myoblasts (<i>mouse</i>)	10,000	250	200%	<i>Nicholls et al, 2010 (113)</i>

CHAPTER 3. CHRONIC HYPOXIA INDUCES METABOLIC ADAPTATION BY ATII CELLS

3.1 Introduction

In the pulmonary epithelium, ATII cells are normally exposed to relatively high levels of oxygen compared to the vast majority of cells in the body. In the healthy developed lung, the cells of the alveoli (including ATII cells) normally experience a well-oxygenated environment composed of approximately 13% oxygen (38). However, a number of diseases result in altered oxygen homeostasis in the pulmonary parenchyma and subject the alveolar epithelium to decreased oxygen availability. Conditions associated with development of pulmonary hypoxia include COPD, IPF, lung cancers, and edema (114). Additionally, the fetal lung develops normally in conditions of low oxygen *in utero* that would be considered “hypoxic” in the adult lung (115); indeed, low-oxygen conditions and hypoxia-associated signaling appear to play a critical role in normal lung development (116, 117). Determining the mechanisms through which the cells of the lung respond and adapt to decreased oxygen availability therefore holds significance for understanding both pulmonary health and disease.

Metabolic changes are critical for facilitating cell survival in response to hypoxia. In general, decreased oxygen tension results in a shift away from mitochondrial ATP production to enhanced glycolytic ATP production in order to maintain bioenergetic homeostasis. However, this response varies depending on cellular energy demand and function. While many down-stream pathways including AMP-activated protein kinase, mTOR, and others are involved in mediating metabolic change (45), oxygen-sensing and initiation of the signaling cascade that leads to adaptation is performed by members of the HIF family of oxygen-sensitive transcription factors. HIFs regulate expression of target genes in the response to hypoxia, many of which are involved in cellular metabolism. The three HIF isoforms regulate overlapping, but distinct, sets of target genes, and their expression varies depending on cell type; while most cells in the body express HIF1, HIF2 and HIF3 expression is isolated to specific cell populations in different tissues.

In the lung, HIF isoforms are critical components in alveolar development (41) and pulmonary surfactant production (117). ATII cells in particular demonstrate a unique pattern of HIF expression. While like most cells in the body they express HIF1, they also robustly express HIF2. Furthermore, while both isoforms are stabilized immediately in short-term hypoxia, longer exposure (greater than 8 hours) leads to a decline in HIF1 expression while HIF2 remains constant. The implication of a HIF2- versus HIF1-mediated response has yet to be determined; however, HIF2 expression specifically is critical for fetal

development of the lung structure and surfactant system, which occurs under low oxygen conditions.

Previous study of alveolar cell adaptation has focused predominantly on short-term exposures to hypoxia. Some elements of the response measured in mixed AEC and/or purified ATII cell populations have been identified including pro-angiogenic signaling, generation of reactive oxygen species and activation of AMPK (38, 118), up-regulation of glucose transporters and their localization to the cell membrane (52), and internalization and inactivation of Na⁺/K⁺-ATPase channels (24, 38). Some of these processes are expected to result in a decreased cellular ATP demand and, potentially, a shift to enhanced glycolytic glucose metabolism. However, the impacts of longer-term hypoxia are largely unknown. AECs exposed for 20 hours have been shown to have similar ATP levels to those cultured at 21% O₂ (52) and cell survival does not appear to be affected (53), but the mechanisms that mediate this remarkable resistant phenotype are not characterized and the enduring functional metabolic changes are unknown.

The work that follows characterizes the response of ATII cells to long-term (20 hour) hypoxia (1.5% O₂) at the level of metabolic function and investigates transcriptional-level change in genes associated with glucose metabolism. Furthermore, metabolic comparison is drawn between primary ATII cells derived from mouse lung and cultures of a standard ATII-like cell line, MLE-15, to assess their usefulness in modeling response to metabolic stressors.

3.2 Results

3.2.1 ATII cells maintain ATP homeostasis during long-term hypoxia.

ATP was measured in MLE-15 and primary mouse ATII cells exposed to 20 hours' hypoxia (1.5% O₂) compared to control cultures incubated in ambient oxygen to evaluate maintenance of ATP homeostasis. Following the exposure period, ATP levels in MLE-15 did not differ significantly between ambient oxygen and hypoxic culture conditions (Figure 3.1). Primary ATII cells maintained ATP at near-ambient levels, demonstrating a minimal (albeit significant) decrease in ATP. This demonstrates that both MLE-15 and primary ATII cells maintain energy balance after 20-hour exposure to hypoxia.

An additional set of MLE-15 cultures was exposed in parallel to the prolyl-hydroxylase inhibitor DMOG, which stabilizes HIF transcription factors in ATII cells under ambient conditions (49). In this manner, pharmacological prolyl-hydroxylase inhibition is used to mimic the HIF-driven effects of hypoxia. Similar to observations of hypoxic MLE-15, 20 hours of exposure to 250 μ M DMOG did not significantly change cellular ATP concentration.

3.2.2 Hypoxia suppresses oxidative metabolism in ATII cells.

In both MLE-15 and primary mouse ATII cells, 20-hour hypoxic exposure decreased oxygen consumption. MLE-15 and primary ATII cell basal OCR was decreased to 55% and 50% of rates observed for cells under ambient oxygen conditions, respectively (Figure 3.2). DMOG treatment also suppressed OCR in MLE-15.

MLE-15 and primary ATII cells maintained spare respiratory capacity following exposure to hypoxia or PHI (Figure 3.3). In terms of percentage above respective basal rates, reserve capacity was similar between treated cultures and those exposed to ambient O₂ conditions (approximately 175% for MLE-15 and 150% for primary ATII). Although similar in terms of percentage above basal OCR, due to the lower basal function in hypoxia- and PHI-treated cells absolute OCR maximal respiratory function was reduced by approximately 50% for both cell types. This ultimately demonstrates a similar degree of suppression of both basal and maximal oxygen consumption in response to hypoxia.

In MLE-15 cells, approximately 50% of oxygen consumed was dedicated to mitochondrial ATP generation regardless of hypoxia or DMOG exposure, as ATP synthase inhibition via oligomycin A injection elicited a similar, 50% drop in OCR for ambient O₂, hypoxic, and DMOG-exposed cells (Figure 3.4).

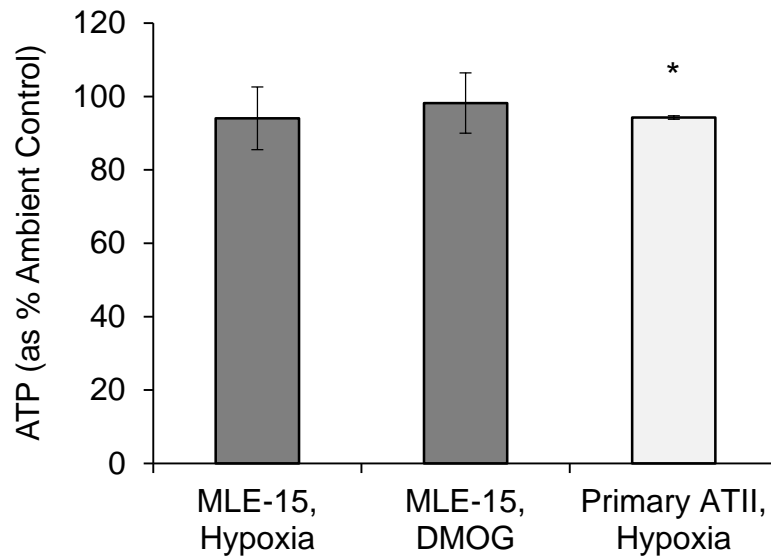


Figure 3.1: Hypoxia and PHI exposure do not alter steady-state ATP concentration in ATII cells. ATP was measured in MLE-15 cells (solid) and primary ATII cells (hatched) exposed for 20 hours to hypoxia (1.5% O₂) and compared to parallel control cultures exposed to ambient (21% O₂), as described in Methods. An additional set of MLE-15 cultures was exposed to the pharmacological hypoxia mimic DMOG. Samples were assayed in triplicate per plate using luminescent assay. Plates were run in quadruplicate for MLE-15, triplicate for primary ATII. * indicates p < 0.05 versus paired ambient culture control, assed via paired Student's T-Test.

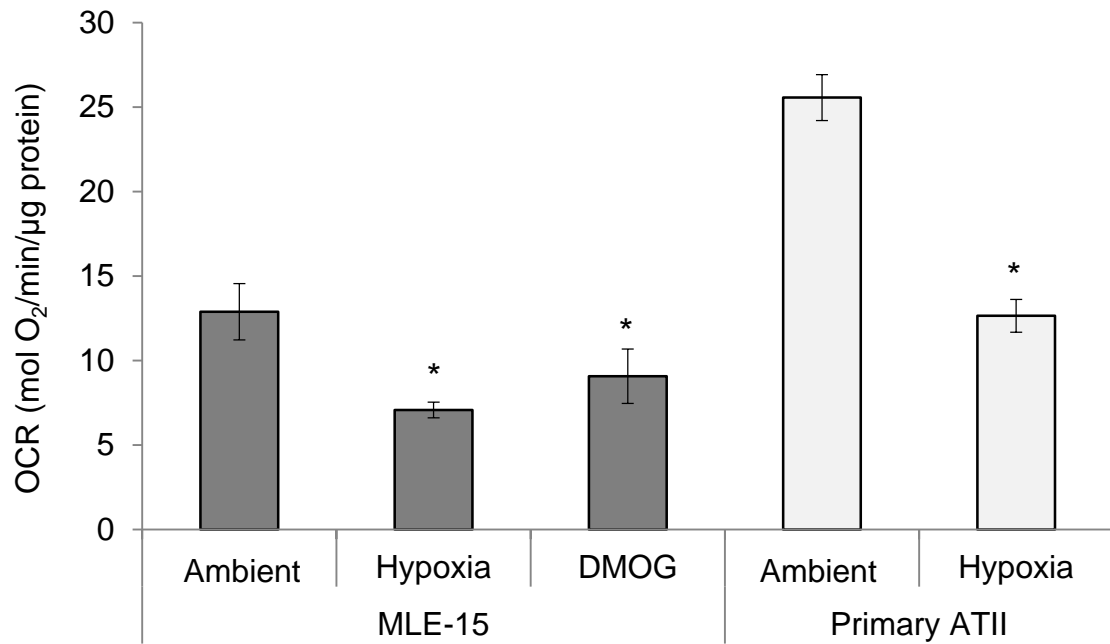


Figure 3.2: Hypoxia and PHI suppress cellular respiration. OCR was measured for MLE-15 cells and primary ATII cells cultured in ambient O₂ (21% O₂) or hypoxia (1.5% O₂). An additional set of MLE-15 cultures was exposed to PHI (250 micromolar DMOG). * indicates significant difference (p<0.05) between treatment group basal OCR and ambient control basal OCR based on ANOVA. Error bars represent ± SE.

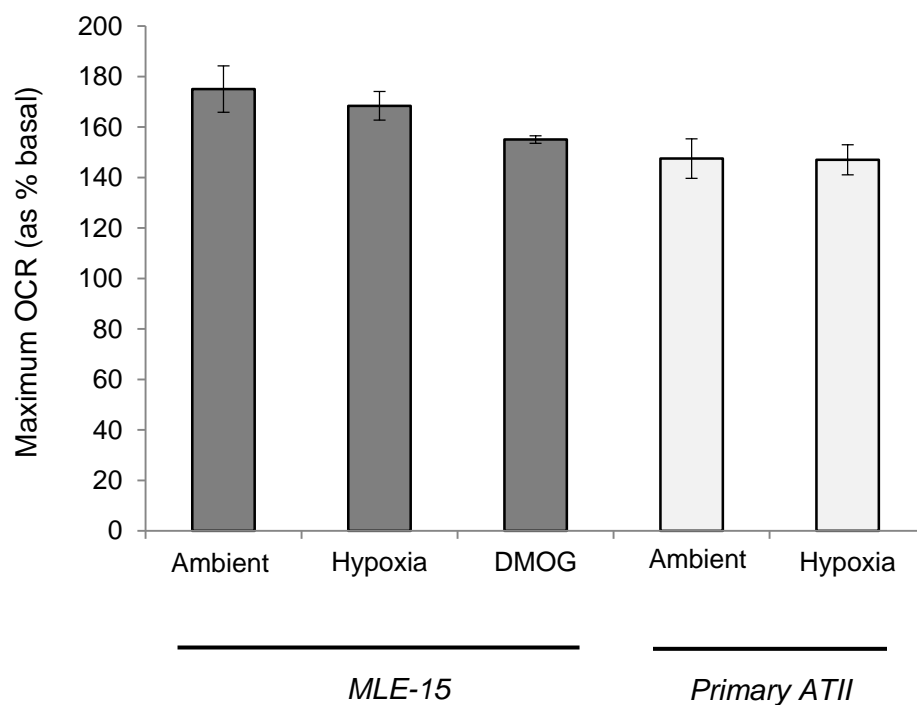


Figure 3.3: ATII cells maintain mitochondrial reserve capacity in hypoxia. Following the addition of FCCP to assay wells to stimulate maximal mitochondrial respiration, OCR was measured for MLE-15 cells and primary ATII cells cultured in 21% O₂ or hypoxia (1.5% O₂). An additional set of MLE-15 cultures was exposed to PHI (250 μM DMOG) under ambient conditions. No significance difference was detected between treatment conditions and respective ambient controls for either cell type based on ANOVA. Error bars represent ± SE.

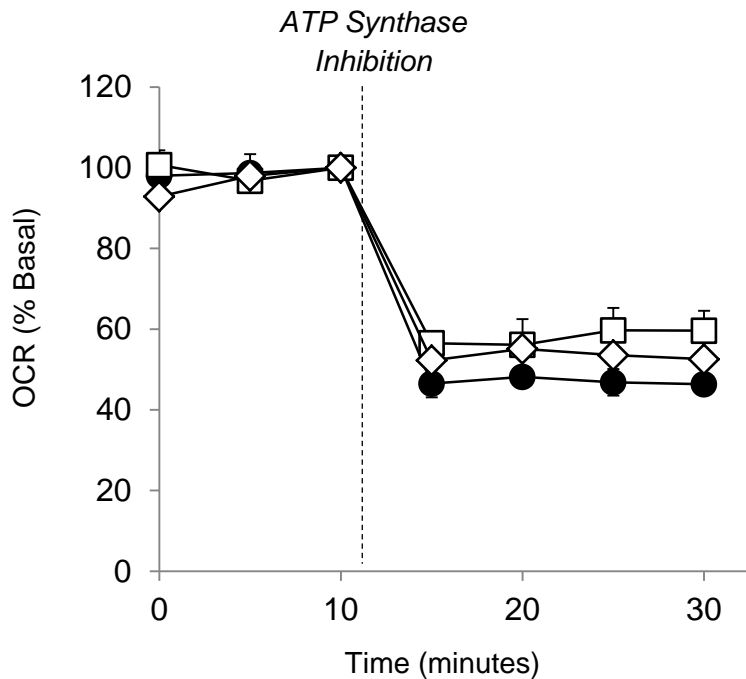


Figure 3.4: Hypoxia and PHI suppress basal do not affect coupling of oxygen consumption to mitochondrial ATP generation. The proportion of oxygen consumption dedicated to generation of ATP via oxidative phosphorylation was determined by measuring OCR before and after addition of oligomycin A, an inhibitor of ATP synthase, to assay media. OCR response to oligomycin A was measured in MLE-15 cultured in ambient O₂ (●), hypoxia (□) and DMOG (◇). For MLE-15 cultures, samples were assayed minimally in quadruplicate for each condition and plates run in triplicate. Error bars represent ± SE.

3.2.3 Hypoxia does not enhance glycolytic function in ATII cells.

Acid generation by primary mouse ATII and MLE-15 cells exposed to hypoxia was measured as an indicator of glycolytic metabolic function. PPR values did not differ significantly from basal ambient O₂ values for MLE-15, while primary ATII cell acid generation appeared to decrease from ambient O₂ values (Figure 3.5).

Lactate generation was measured using colorimetric assay to confirm findings from metabolic flux analysis and to determine whether media acidification could be accounted for by lactic acid generation. Media from MLE-15 cultures incubated in ambient oxygen or hypoxia was assayed for lactate concentration at several time points following 20-hour exposure. No significant difference was observed in the rate of lactate generation in terms of extracellular lactate concentration between ambient and hypoxic cultures, confirming extracellular flux analysis findings (Figure 3.6A). Similarly, there was no difference in intracellular lactate concentration (Figure 3.6B). Notably, the observed rate of extracellular lactate generation based on media concentration measurements over time was essentially similar to the rate of proton production as determined by flux analysis, indicating that acidification in both ambient oxygen and hypoxia is predominantly due to generation of lactic acid. Thus, lactic acid generation is the major determinant of extracellular pH by MLE-15 cells under ambient and hypoxic conditions.

Following basal measurements, maximal glycolytic rates were measured in cultures following addition of FCCP to assay media (Figure 3.7). MLE-15

underwent an increase in glycolysis following FCCP injection to approximately 200% of basal measurements in ambient oxygen, hypoxia and PHI. This indicates that the capacity to perform glycolysis was not affected by treatment. In primary ATII cells, FCCP stimulated PPR to a similar rate in both ambient O₂ and hypoxic cultures, although the increased PPR in these cells was 130% percent of basal primary cell rates.

3.2.4 Hypoxia enhances ATII cell relative reliance on glycolytic metabolism.

The relative reliance of cells on glycolytic versus oxidative means of energy production can be assessed based on the ratio of protons produced and oxygen consumed, or the PPR/OCR ratio. In response to hypoxic exposure, MLE-15 and primary ATII cells adopted an increased reliance on glycolysis as demonstrated by an increase in the PPR/OCR ratio for both cell types (Figure 3.8). However, as rates of glycolysis did not change in MLE-15 and appeared to decrease in response to hypoxia in mouse primary ATII, this “shift” to glycolysis was the effect of decreased OCR (and not increased PPR).

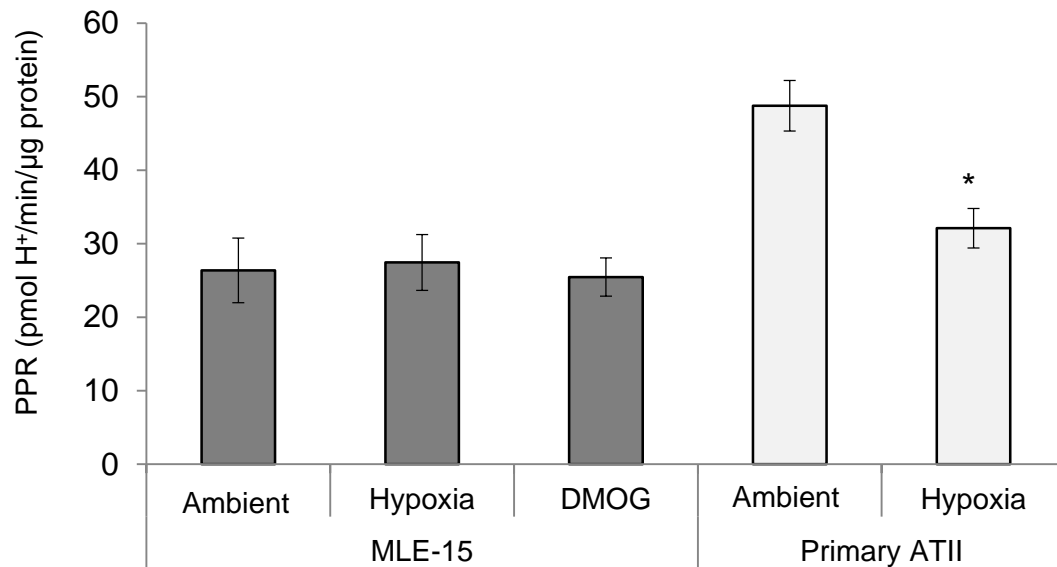


Figure 3.5: Hypoxia and PHI do not increase extracellular proton production. PPR was measured as an indicator of glycolysis in MLE-15 (dark) and primary ATII cells (light) exposed to hypoxia compared to ambient controls. An additional set of MLE-15 cultures was exposed to PHI (DMOG). For MLE-15, samples were assayed minimally in quadruplicate for each condition and plates run in triplicate. For primary cultures, a total of six single-well experiments for each condition. * indicates significant difference ($p < 0.05$) between treatment group and ambient, unexposed control. Error bars represent \pm SE.

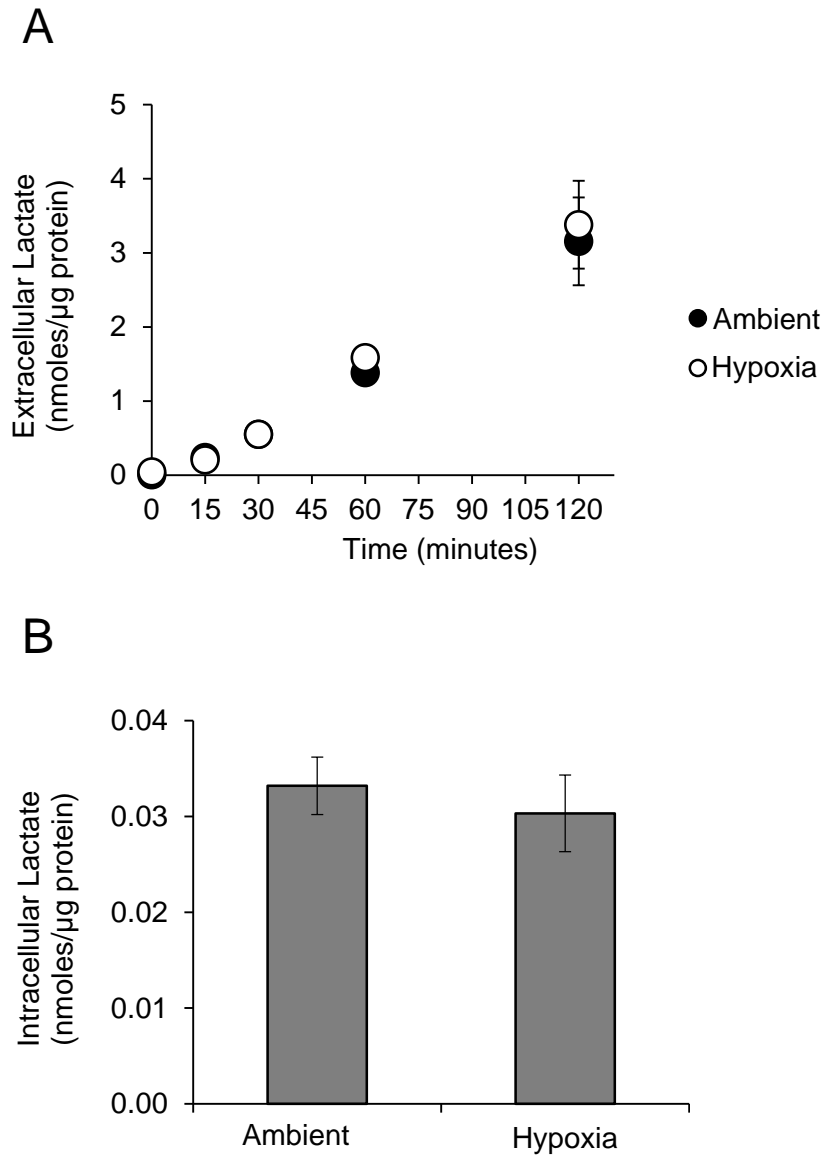


Figure 3.6: Hypoxia does not alter cellular lactate generation in MLE-15 cells. (A) Lactate was measured in media of MLE-15 cultures exposed to ambient O_2 (closed marker) and hypoxia (open marker). Time points indicate time passed after the addition of fresh media following 20-hour exposure. (B) Intracellular lactate was measured in cell homogenates immediately following collection of media samples at $t=120$ minutes in (A). Experiments were performed in triplicate. Error bars represent \pm SE.

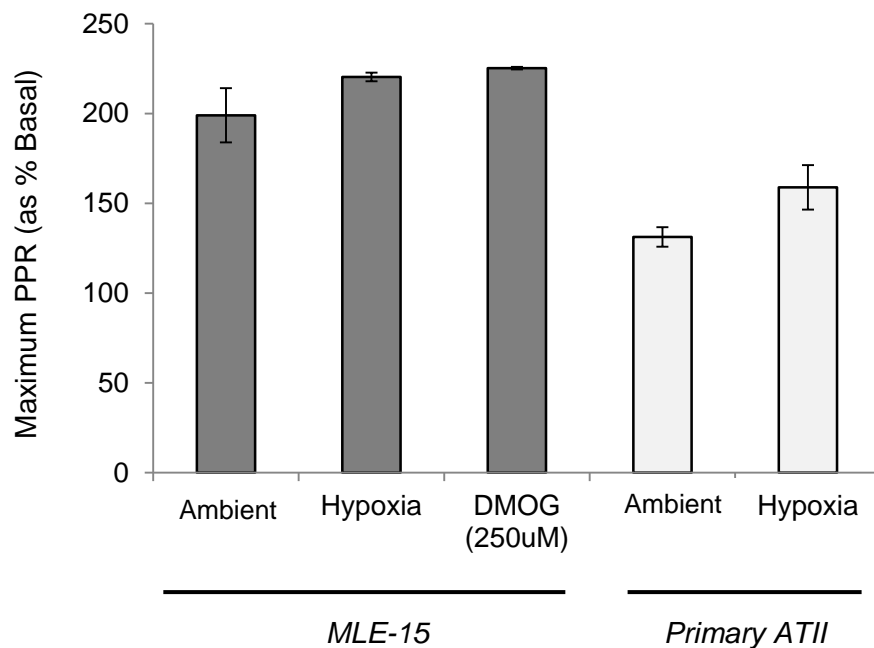


Figure 3.7: Hypoxia and PHI do not impact ATII cell glycolytic reserve. Following the addition of FCCP to assay wells to stimulate maximal mitochondrial respiration, PPR was measured for MLE-15 cells (dark bars) and primary ATII cells (light bars) cultured in ambient O₂ (21% O₂) or hypoxia (1.5% O₂). An additional set of MLE-15 cultures was exposed to PHI (250 μmolar DMOG). No significance difference was detected between treatment conditions and respective ambient, unexposed controls for either cell type based on ANOVA. Error bars represent ± SE.

3.2.5 Hypoxia induces changes in ATII mRNA expression of genes associated with glucose metabolism.

Previous work concerning ATII response to low oxygen tension has demonstrated a role for HIF proteins in directing the hypoxic response at the level of transcriptional change. Thus, to determine changes in gene expression occurring in long-term hypoxia, mRNA harvested from ambient- and hypoxia-cultured MLE-15 was subjected to a glucose metabolism-focused qPCR array. Many genes associated with glycolysis were collectively up-regulated by hypoxia (Table 2), including those that directly produce glycolytically-derived ATP (phosphoglycerate kinase, *Pgk1*) and those serving as master regulatory enzymes for the glycolytic pathway (phosphofructokinase, *Pfk1*). Enzymes responsible for phosphorylation (hexokinase 2, *Hk2*) and isomerization (phosphoglucomutase, *Pgm2*) of glucose, required for substrate entry into either glycolysis or glycogenesis, were up-regulated. Multiple other glycolytic genes were up-regulated as well, indicating that hypoxia may enhance the ability of MLE-15 to generate glycogen from glucose. No significant changes to TCA cycle enzymes or other pathways included in the array were observed, except for pyruvate dehydrogenase (*Pdk1*), which negatively regulates entry of pyruvate into mitochondrial metabolism and instead favors lactate generation via anaerobic reduction.

3.2.6 Hypoxia alters ATII metabolism to favor glycogen storage.

Based on the observation that hypoxia enhanced expression of metabolic enzymes associated with glycogen production, glycogen storage was assessed

in MLE-15 under hypoxic versus ambient oxygen conditions (Figure 3.8). In MLE-15 cultured at 21% (ambient) O₂, low levels of glycogen were observed. However, cultures exposed to hypoxia for 48 hours increased intracellular glycogen stores significantly. Exposure to PHI also significantly enhanced glycogen content of MLE-15 cultures.

To determine the effect of re-entry into ambient oxygen on stored glycogen, separate MLE-15 cultures were exposed to hypoxia for 48 hours, followed by incubation at 21% O₂ for an additional 24-hour period. In these cells, glycogen content returned to low near-ambient levels, suggesting that stored glycogen was mobilized and metabolized after oxygen levels were returned to 21%.

Table 2: Hypoxia-dependent differential gene expression in MLE-15 cells. Focused qPCR array was performed to assess changes in MLE-15 expression of genes associated with glucose metabolism in response to hypoxia. 3 cDNA were analyzed per condition. All genes meeting criteria of >2.0-fold change in gene expression and $P < 0.05$ (prior to rounding) are shown. Expression of all genes was increased after exposure to hypoxia vs. ambient O_2 . † indicates expression changes validated via targeted qPCR for selected genes. *TCA*, *tricarboxylic acid*.

Protein ID	Gene Name	Biological Process	Ref. Seq. ID	Fold Change Hypoxia vs. Ambient	p Value
Aldolase A, fructose-bisphosphate	<i>Aldoa</i>	Glycolysis	NM_007438	3.09	0.05
Enolase 1, α -nonneuron	<i>Eno1</i>	Glycolysis	NM_023119	3.17	0.03
Glucan (1,4- α), branching enzyme 1	<i>Gbe1</i>	Glycogenesis	NM_028803	6.81 [†]	0.001
Glucose phosphate isomerase 1	<i>Gpi1</i>	Glycolysis	NM_008155	3.91	0.04
Glycogen synthase 1, muscle	<i>Gys1</i>	Glycogenesis	NM_030678	5.27 [†]	0.04
Hexokinase 2	<i>Hk2</i>	Glycolysis/ glycogenesis	NM_198308	6.88 [†]	0.05
Pyruvate dehydrogenase kinase 1	<i>Pdk1</i>	Glycolysis/ TCA cycle	NM_172665	5.02 [†]	0.008
Phosphofructokinase, liver, B-type	<i>Pfkl</i>	Glycolysis	NM_008826	3.62	0.02
Phosphoglycerate kinase 1	<i>Pgk1</i>	Glycolysis	NM_008828	3.55 [†]	0.002
Phosphoglucosmutase 2	<i>Pgm2</i>	Glycolysis/ glycogen metabolism	NM_028132	4.51	0.02
Triosephosphate isomerase 1	<i>Tpi1</i>	Glycolysis	NM_009415	2.87	0.05

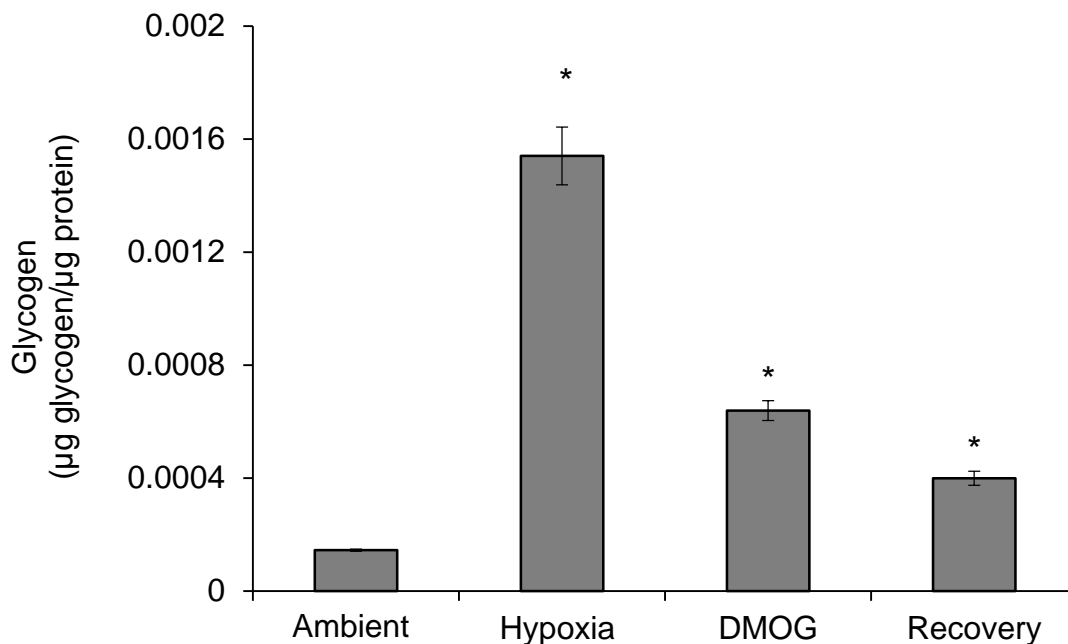


Figure 3.8: Hypoxia and PHI promote intracellular storage of glycogen, which is consumed upon recovery in ambient O₂. MLE-15 cultures were assayed for intracellular glycogen content using quantitative fluorimetric detection, as described in Methods. Samples were assayed in duplicate per assay plate and adjusted for sample glucose content; assays were run in triplicate. * indicates $p < 0.05$ versus ambient, unexposed control, determined via ANOVA followed by Tukey post hoc analysis. Error bars represent \pm SE.

3.3 Discussion

This work characterized the functional-level response of ATII cells to long-term hypoxia exposure in terms of impact on glycolytic and mitochondrial function, and linked these observations to molecular-level adaptation of glucose metabolism at the level of transcription. Hypoxia decreases mitochondrial respiration without enhancing anaerobic glycolysis and lactic acid generation. Despite this, ATP homeostasis is maintained, indicating that ATII cells primarily adapt to hypoxia through down-regulation of ATP-consuming processes, rather than enhanced glycolytic function to compensate for reduced mitochondrial ATP yield. These results support and extend previous observations that AECs adapt well to hypoxia in terms of avoiding cell damage and maintaining bioenergetic homeostasis (52).

Hypoxia suppressed OCR in both MLE-15 and primary ATII cells by approximately 50%. Previous respirometric measurements for rat ATII exposed to 2% O₂ demonstrated similar suppression in terms of percentage of ambient O₂ culture rates (23) using a different method to measure oxygen consumption. In respirometry studies, exposed rat ATII cells did not demonstrate enhanced anaerobic glycolytic processing of glucose, as measured by extracellular flux analysis and confirmed by direct measurement of lactate in culture media over time. This observation was not anticipated, and strongly suggests that down-regulation of ATP consuming processes (rather than enhanced lactic acid production) is the mechanism through which ATII adapt to reduced mitochondrial ATP production in hypoxia. This correlates well with clinical observations that

lactate production from the lung in patients with pulmonary conditions does not correlate with the degree of hypoxia, but rather with the extent of lung damage (119). Indeed, these authors proposed that this is the result of robust adaptation of healthy lung cells to hypoxia, a suggestion that is supported by the work presented here.

The observation that both basal and maximal respiratory rates are suppressed by hypoxia suggests that mitochondrial function is directly impacted to some degree. In other words, if decreased mitochondrial function were an effect only of reduced ATP demand, FCCP would be expected to stimulate similar maximal rates under hypoxic and ambient conditions. This, however, was not the case in these studies, as the addition of FCCP stimulated hypoxic A1II cell respiration only to the basal levels of cells cultured in ambient oxygen (approximately half the maximal rates of A1II cells cultured in ambient conditions). Direct suppression may be an effect of damage to components of the TCA cycle or electron transport chain, expression changes in mitochondrial enzymes, substrate limitation, or dynamic changes to the mitochondrial population via biogenesis and/or mitophagy. No significant changes were observed in expression of mitochondrial enzymes at the level of transcription, though this does not rule out protein-level expression changes. In the lung, the TCA cycle enzyme aconitase has been shown to be particularly sensitive to ROS generated under extremely hyperoxic conditions (85% O₂ and greater); as short-term hypoxia also generates ROS (38), damage to this or other mitochondrial components is possible. Substrate limitation to the mitochondria also provides

possible explanation for suppressed oxygen consumption, as enhanced expression of PDKs is expected to limit entry of pyruvate into the TCA cycle. The impact of hypoxia on ATII mitochondrial biogenesis and autophagy is unknown, and presents a significant direction for future investigation.

Despite suppressed mitochondrial function, glycolysis was not increased in ATII cells under hypoxia, as would be expected to maintain ATP production at levels comparable to cells cultured in ambient oxygen conditions. These findings strongly suggest that energy balance is maintained in hypoxia by reducing ATP turnover, rather than shifting to enhanced reliance glycolytic production. One mechanism that ATII cells reduce ATP demand is through down-regulation of Na⁺/K⁺ ATPase ion pump function. Rapidly following the onset of hypoxia, pump proteins are removed from the cell surface and degraded. However, respirometry measurements performed by Heerlein and colleagues suggests that the impact of this response on total ATP conservation is relatively small (23). Other mechanisms of ATP conservation in hypoxic ATII have yet to be elucidated, but may include reduced proliferative capacity and/or suppression of surfactant production, the latter being supported by the observation that surfactant protein expression is negatively controlled by hypoxia and HIF stabilization (49).

DMOG treatment of cells under ambient conditions resulted in metabolic responses similar to those observed in response to hypoxia, strongly suggesting that HIFs drive the observed metabolic adaptations observed here. HIFs are found ubiquitously throughout mammalian tissues, but ATII cells display a unique pattern of HIF stabilization in that they strongly express the HIF2 isoform. In the

lung, HIF2 expression is strictly limited to ATII cells and the vascular endothelium (120). Furthermore, while HIF1 is stabilized immediately, over time its expression is reduced, while HIF2 expression remains robust (49, 50). At the 20-hour time point utilized in these studies, the cellular concentration of stable HIF1 α is low, while HIF2 concentration is high. While the HIF1 isoform has been found to control transcription of many of the genes coding for glycolytic enzymes, HIF2 targets include genes involved in fatty acid storage, glycogen production, and anti-oxidant defense. HIF1 has been shown to drive apoptosis in ATII cells (121, 122) while HIF2 promotes anti-apoptotic pathways (123). HIF2 also plays critical roles in surfactant production (117) and alveolar development in the fetal lung (41).

Notably, the ATII cell response to PHI differs markedly from previously observed impacts on cardiomyocytes treated with the same concentration of DMOG. In cardiomyocytes, DMOG not only suppressed basal OCR, but completely abolished spare respiratory capacity (which is exceptionally high in untreated cardiomyocytes). Interestingly, inhibition of HIF1 mostly recovered spare capacity in these cells, indicating that HIF1 activity specifically suppressed mitochondrial function. In ATII, spare capacity was largely maintained in DMOG-treated cultures, demonstrating a fundamental difference between the cell types. This may be one effect of mounting a HIF2-, rather than HIF1-mediated response in ATII. Limiting HIF1 over longer-term exposure may be a strategy to preserve mitochondrial function. Given the importance of spare respiratory capacity for dealing with cell stress and promoting survival defined in neuronal metabolism

studies (124), uncovering how healthy ATII cells maintain mitochondrial function in hypoxia (and how this may be disrupted in disease) is an important step in understanding ATII cell biology. Further investigation will be necessary to determine how HIF1 versus HIF2 affects mitochondrial capacity.

Gapdh, *Hk2*, and other glycolysis-associated enzymes were up-regulated in terms of mRNA expression, confirming previous observations in AEC cultures (52). This is supported by proteomic work from our lab focused on elucidating the changes induced by hypoxia to the ATII cell proteome, which indicated that expression of several enzymes involved in the initial steps of the glycolytic pathway are up-regulated in hypoxia (37). However, glycolytic rates remained the same in MLE-15 cells and actually decreased in primary ATII cells under hypoxia. This report indicates that in unstressed, baseline conditions, the remaining mitochondrial function supplies sufficient ATP to meet reduced energy demand without the need to enhance glycolysis.

Previous study of hypoxia has demonstrated up-regulation of cell surface glucose transporters in AEC (52) and although we did not observe enhanced GLUT mRNA expression by MLE-15 at 20 hours' exposure, this has been more recently demonstrated in ATII cells in short-term (less than 8 hour) exposures. This highlights a possible key difference in the metabolic function of ATII in short-versus long-term exposure: at the onset of hypoxia, ATP levels drop due to immediate suppression of mitochondrial function, and the responses previously observed in association with hypoxia in these cells, including GLUT up-regulation (52) and phosphorylation of AMPK (24), are effects of the cellular effort to regain

bioenergetic homeostasis. Indeed, an initial drop in cellular ATP content has been shown in AEC challenged with anoxia. Based on our findings, these initial manipulations lead to re-established ATP levels by 20 hours' exposure. Thus, our observations represent the potentiated hypoxic response. We expect that the findings reported here regarding 20-hour exposure represent the conditions to which ATII are exposed in cases of IPF, COPD, and other chronic lung diseases associated with chronic hypoxia in distal lung regions.

Findings concerning glycogen storage suggest that in long-term hypoxia, glucose intake is at least in part dedicated to glycogen production (or other, non-glycolytic functions not assessed here). At 20 hours' exposure, increased glucose intake is not connected to increased flux through the anaerobic glycolytic pathway, as extracellular acidification is not increased in exposed cultures. This concurs with the conclusion that ATII adapt to hypoxia primarily by down-regulating ATP-consuming processes rather than increasing non-oxidative ATP production. Cultures exposed to hypoxia (1.5% O₂) and then allowed to incubate in ambient O₂ conditions showed lower glycogen content near that observed for cells cultured only under ambient O₂, indicating mobilization and metabolism of glycogen stored during the period of hypoxia. In skeletal muscle, glycogen storage was shown to occur downstream of hypoxia in a HIF-dependent manner (125), an effect that is supported in ATII by the observation that stabilization of HIF via DMOG treatment also induced glycogen storage. In the developing lung, glycogen storage is a critical component of the development of the surfactant system and generation of surfactant in preparation for breathing room air, and

both storage and utilization have been associated with HIF2 signaling (41). In MLE-15, glycogen storage thus recapitulates the physiology of premature ATII. The extent to which this occurs in the hypoxic adult lung is unknown.

In summary, this section of work quantifies the impact of hypoxia on ATII cell metabolic pathway function and capacity. Observations from functional-level assessment using flux assay and direct metabolite measurement are matched to transcriptional changes and previously-obtained data concerning the impact of hypoxia on the ATII proteome. Understanding how healthy human ATII cells response to hypoxia is clinically important, as a number of diseases associated with pulmonary hypoxia and in many of these cases the role of hypoxia in the disease progression is poorly understood.

CHAPTER 4. LACTATE SERVES AS SUBSTRATE FOR ATII CELL METABOLISM

4.1 Introduction

While the lung was originally thought to depend on glucose for energy production, a number of studies of whole lung metabolism demonstrated that other substrates are taken up into lung tissue from pulmonary circulation and oxidized. In these studies, lactate in particular was rapidly oxidized by the lung. Furthermore, lactate oxidation occurred at higher rates than oxidation of other substrates including glucose. Despite these early observations, lactate utilization by the lung has received little attention in modern investigation. While a balance of lactate production and consumption has been shown to be a critical component of tissue metabolism in heart, skeletal muscle, and most recently brain tissue, lactate metabolism has not been examined at the cellular and molecular level in the pulmonary tissue.

Lactic acid is classically considered a cellular waste product. In the process of anaerobic glycolysis, pyruvate is converted to lactate via the forward, reductive reaction of LDH and is extruded, with a single proton, from the cell into the extracellular milieu. A portion of lactate produced by cells of the body is carried via circulation to the liver, where it is oxidized back to pyruvate and used to re-generate glucose through the process of gluconeogenesis. However, this

process accounts for less than half of lactate oxidization during rest, and only 25% during exercise. A greater portion of lactate is oxidized by other cells elsewhere in the body, which can utilize lactate as a metabolic substrate through oxidization to pyruvate and subsequent use in mitochondrial energy production. Lactate oxidization for energy production occurs rapidly in cardiac tissue where it is consumed preferentially over glucose, particularly during exercise. In skeletal muscle, highly oxidative cells of the slow-twitch red fibers consume lactate produced by neighboring cells of the fast-twitch white fibers, which are heavily dependent on anaerobic glycolysis and produce large amounts of lactate (27, 28). Through the complimentary processes of anaerobic lactate production in one cell type and aerobic lactate oxidation in another, glycolysis and oxidative metabolism are inextricably linked.

Several previous studies demonstrated that, in addition to glucose, lactate is oxidized by lung tissue. Wolfe et al (17) used the isolated perfused rat lung model to demonstrate rapid oxidization of ^{14}C -labeled lactate by lung tissue. In this study, lactate oxidation occurred even when glucose was provided simultaneously and at higher concentrations in the perfusate. Later investigation by Fox and colleagues examining lactate use in isolated alveolar epithelial cells from fetal rat lung demonstrated rates of CO_2 generation from labeled lactate that were approximately 20 times the rate of glucose oxidation, the highest rate for any substrate tested (22). The presence of lactate decreased utilization of glucose and vice versa, indicating similar pathways of metabolic processing. Early studies found that lactate was incorporated into lung lipids, indicating a role

for AII in lactate oxidization, as AII cells are the primary synthesizers of lipid for production of pulmonary surfactant (18). Furthermore, lactate was preferentially incorporated into the acetyl moiety of synthesized lipids while glucose primarily composed the glycerol moiety, suggesting that lactate was processed preferentially by the mitochondria. Despite a strong body of evidence indicating that lactate is an important substrate in the lung and suggesting in particular that AII cells utilize lactate, lactate oxidation has not been examined in mature AII cells and has not been linked directly to energy production and homeostasis.

Lactate consumption for mitochondrial utilization requires, first, cellular import and second, conversion to pyruvate via the reverse, oxidizing reaction of LDH. Lactate transport both into and out of cells is mediated by a family of transport proteins, monocarboxylate transporters (MCTs) that can move lactate with a single proton down-gradient across cell membranes. There are four MCT isoforms, MCT1, 2, 3, and 4. All isoforms transport bi-directionally; however, some isoforms more heavily favor import versus export. MCT4, the lower-affinity member, is associated with more rapid lactate export and tends to be expressed in more highly glycolytic cells, including cells of the white muscle cells and brain astrocytes. MCT1, on the other hand, is associated with import and is found in cell types known to oxidize lactate for ATP production. MCT1 and MCT4 are expressed in the developing lung with MCT1 expression localized mainly to the maturing epithelium (126). Whole lung tissue from adult rat expresses MCT1, 2, and 4, however localization of expression to specific cell types has yet to be

examined (34). The importance of MCT-mediated lactate transport to ATII cell metabolism is unknown.

The ability to oxidize lactate once it is imported requires rapid mitochondrial activity and a high NAD⁺/NADH ratio to facilitate reverse activity of LDH (26). Based on our previous findings, ATII cells are highly metabolic with rapid rates of mitochondrial activity (37), and due to their physiological location in the lung epithelium, oxygen is readily available to fuel mitochondrial metabolism in the healthy lung. Furthermore, intracellular lactate levels are low, favoring import from a higher external concentration. These important facets of ATII cell metabolic function inspired the hypothesis that ATII cells import extracellular lactate and utilize it as substrate for mitochondrial energy production. Using extracellular flux assay technology to measure cellular metabolism of cells in culture, we show that primary and model ATII cells can rapidly oxidize lactate for use as substrate for ATP production. We provide evidence that lactate modulates glucose utilization in a dose-dependent manner when both substrates are provided simultaneously. Furthermore, using the addition of an inhibitor of MCT proteins, we directly demonstrate for the first time the importance of the transporter in ATII cell metabolism of both lactate and glucose. Additionally, expression of *Mct1* mRNA and protein is shown in ATII cell lysates, specifically identifying one pulmonary cell population that expresses the transporter. Cumulatively, this report provides evidence that ATII cells act as a “lactic acid sink” in the lung, removing lactate and protons from the extracellular milieu for use in maintaining their own bioenergetic homeostasis.

Finally, we investigate the effect of hypoxia on ATII cell lactate utilization. We and others have demonstrated that hypoxic exposure suppressed mitochondrial metabolism of glucose (23, 37), resulting in a more glycolytic phenotype. A variety of pulmonary diseases including IPF lead to development of pulmonary hypoxia and hypoxia-related signaling in the distal lung (73). Because lactate import and utilization depends ultimately on a high level of mitochondrial respiration, any condition that impairs mitochondrial function could be expected to reduce the capacity to consume lactate. Lactic acid build-up has been shown to occur in IPF lung tissue and contributes directly to the disease process (94), but the source of the excess lactate is unknown. This work is thus an important step forward in understanding the ATII functions that may be disrupted in, and contribute to, disease pathogenesis by developing a thorough understanding of lactate production, consumption, and balance in the healthy lung.

4.2 Results

4.2.1 Culture in lactate alone induces a highly oxidative ATII cell phenotype.

Compared to cells cultured in glucose, primary ATII and MLE-15 both showed elevated rates of oxygen consumption when cultured in lactate-formulated media (Figure 4.1). For both cell types, culture in lactate increased OCR by approximately 2-fold over glucose-grown cultures. PPR was low for both cell types, indicating low lactic acid production, expected due to the lack of glucose. Thus, in the presence of lactate and absence of glucose, ATII cell metabolism shifts into a highly oxidative phenotype.

Lactate utilization as substrate for mitochondrial ATP generation requires it to first be converted to pyruvate via the reverse, oxidative reaction of LDH. Thus, inhibition of LDH would be expected to decrease mitochondrial respiration of cells cultured in lactate by limiting the conversion to pyruvate, and thus the substrate necessary for mitochondrial NADH production. Inhibition of LDH using the competitive inhibitor oxamate resulted in a decrease in OCR by cells cultured in lactate (Figure 4.2) This provides further support for the conclusion that lactate, via LDH conversion to pyruvate, is utilized by MLE-15 for mitochondrial reactions. Conversely, LDH inhibition resulted in enhanced OCR in glucose-grown cells, possibly an effect of reducing the amount of pyruvate converted to lactate and thus increasing the substrate pool for mitochondrial metabolism and the need to regenerate NAD^+ .

4.2.2 Rapid respiration by mouse ATII grown in lactate is coupled to mitochondrial ATP production.

Inhibition of ATP synthase provides a measurement of the degree to which oxygen consumption is dedicated to ATP production through mitochondrial respiration. Upon inhibition of ATP-synthase during extracellular flux assay, oxygen consumption by lactate-cultured cells decreased from basal measurements by approximately 60%, indicating that approximately 60% of oxygen consumption was coupled to mitochondrial ATP production (Figure 4.3). This response to ATP synthase inhibition was similar to cells cultured in parallel in glucose, indicating a similar proportion of total basal OCR dedicated to ATP

synthesis. Considering that lactate-cultured MLE-15 had high basal OCR levels, this proportion represents approximately twice the amount of oxygen consumed for ATP synthesis by glucose-grown cells.

4.2.3 Respiration is performed at maximal capacity in mouse ATII cells cultured in lactate.

Addition of the respiratory chain uncoupling molecule FCCP results in an increase of oxygen consumption to maximal respiratory rates. FCCP exposure during metabolic flux assay resulted in OCR values approximately 180% of basal values for MLE-15 cultured in glucose; however, exposure to FCCP did not induce a significant increase above basal OCR for cells cultured in lactate (Figure 4.4). This demonstrates that cells cultured in lactate maintained minimal spare respiratory capacity, and therefore when lactate alone is available, cells perform respiration at near-maximum mitochondrial capacity.

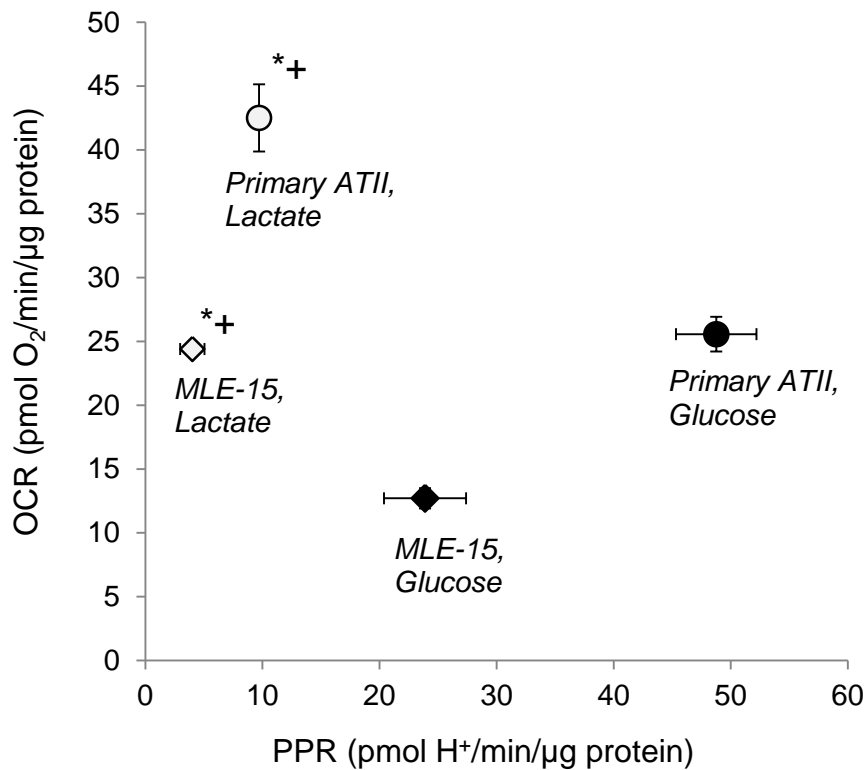


Figure 4.1: Culture in lactate shifts ATII cells into a highly oxidative metabolic state. OCR and PPR were measured for primary ATII cells (circle markers) and MLE-15 cells (diamond markers) cultured in either 5.5 mM glucose (shaded) or 5.5 mM lactate (open). For MLE-15 cultures, samples were assayed minimally in triplicate for each condition and plates run in triplicate. For primary cultures, a total of six single-well experiments were performed for each condition. * indicates significant difference ($p < 0.05$) from glucose condition OCR for each cell type; + indicates significance difference from glucose condition PPR for each cell type. Significance based on Student's T-Test. Error bars represent \pm SE.

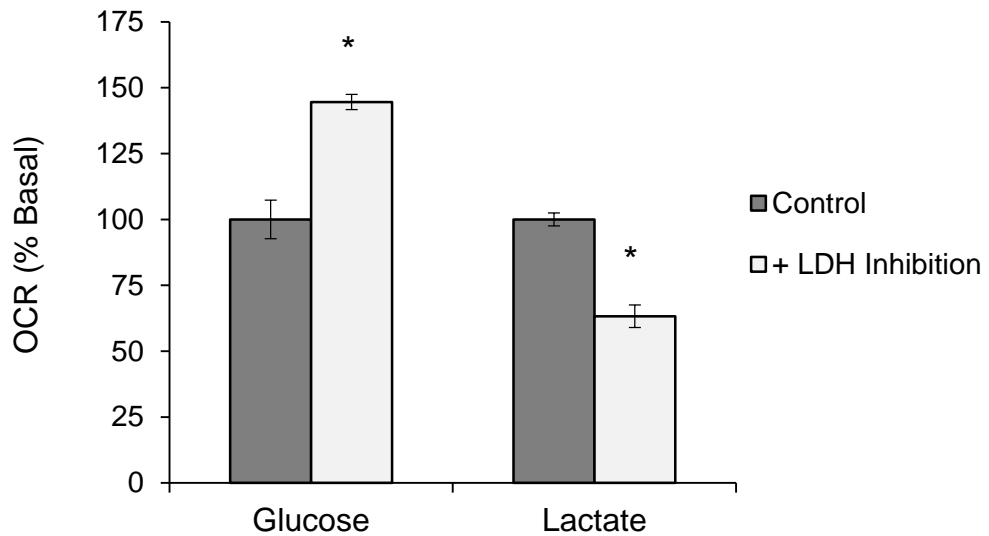


Figure 4.2: Inhibition of LDH reduces lactate-fueled respiration in MLE-15. OCR was measured for MLE-15 cells cultured in 5.5 mM glucose or 5.5 mM lactate and exposed to the LDH inhibitor oxamate. Oxamate was dissolved in assay media to a final concentration of 20 mM and added to culture wells 1 hour prior to assay; control wells received normal assay media. Data is represented as percentage of glucose or lactate controls unexposed to oxamate. n = 5 individually-cultured wells per condition. * indicates significant difference ($p < 0.05$) from unexposed controls based on Student's T-Test. Error bars represent \pm SE.

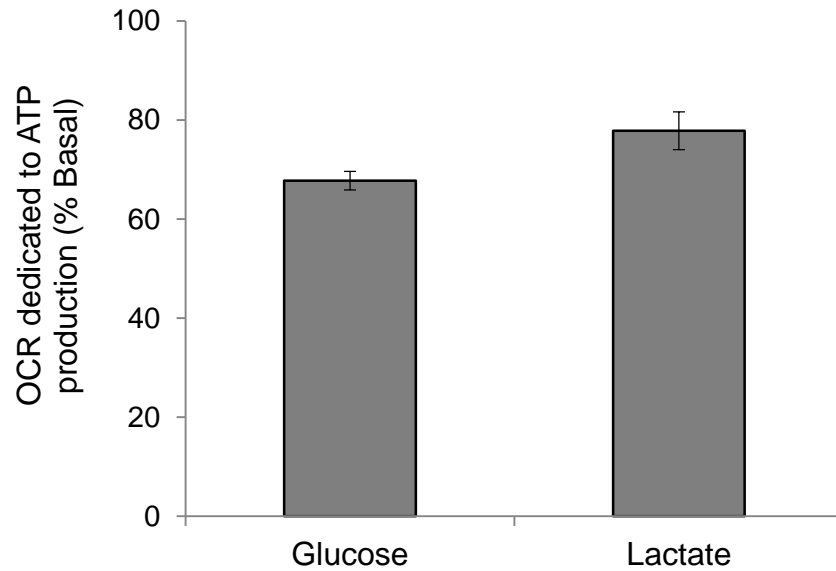


Figure 4.3: ATII cells utilize lactate for mitochondrial ATP production. The proportion of oxygen consumption dedicated to generation of ATP via oxidative phosphorylation was determined by measuring OCR before and after addition of oligomycin A, an inhibitor of ATP synthase, to assay media. OCR response to oligomycin A was measured in MLE-15 cultured in 5.5 mM glucose or 5.5 mM lactate. 5 independent cultures were measured per condition. Data represent percentage change from basal OCR measurements following ATP synthase inhibition. Error bars represent \pm SE.

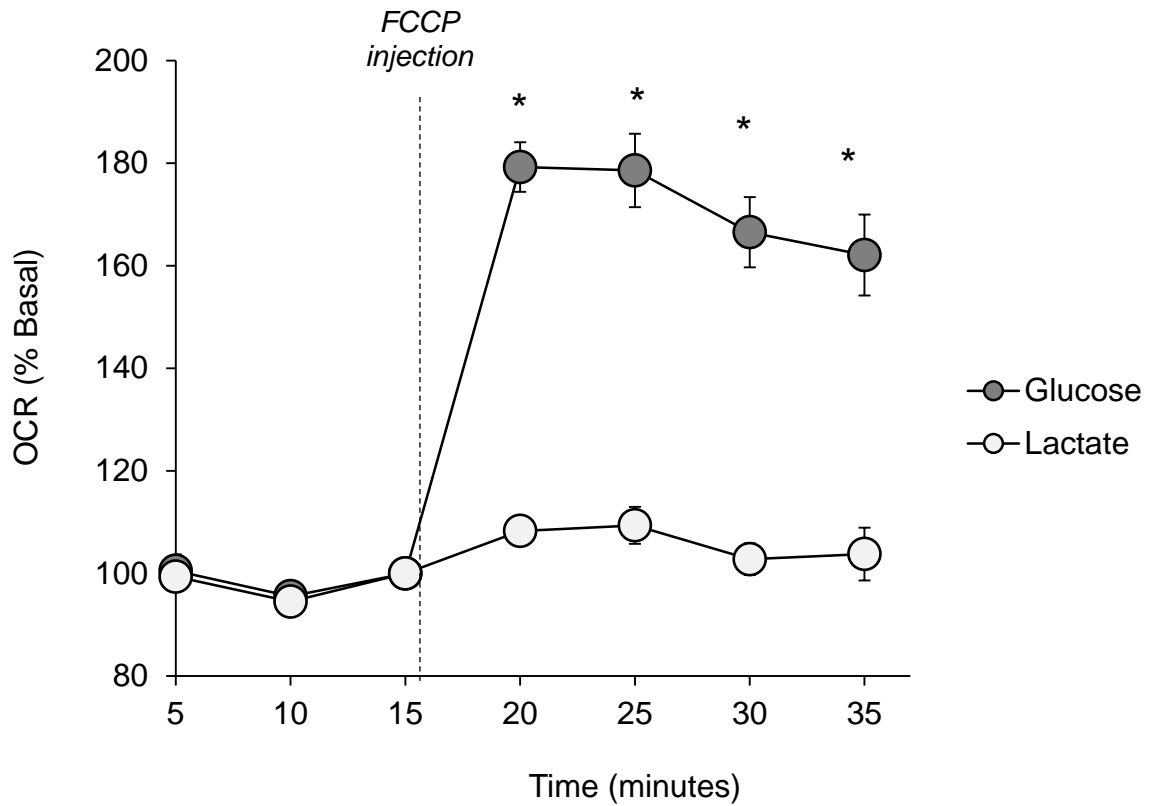


Figure 4.4: Mitochondrial respiration is performed at near-maximal rates in MLE-15 cells consuming lactate alone. Following measurements of basal respiration, FCCP was added to the assay media to measure uncoupled OCR in MLE-15 cells cultured in 5.5 mM glucose or 5.5 mM lactate. $n = 5$ individually-cultured wells per condition. Data represents percentage change from basal OCR values. * indicates significant difference ($p < 0.05$) from basal OCR for each condition, as determined by ANOVA and Tukey post hoc analysis. Error bars represent \pm SE.

4.2.4 Lactate availability alters glucose utilization.

To examine the impact of extracellular lactate availability on glucose metabolism, lactate was provided to MLE-15 in increasing concentrations in media formulated with 5.5 mM glucose and compared to media with glucose alone. At concentrations of 2.75 mM lactate and above, PPR was significantly decreased from the glucose-only condition in a dose-dependent manner (Figure 4.5). Conversely, OCR values did not differ significantly from glucose for any of the lactate concentrations examined.

4.2.5 Hypoxia suppresses ATII cell lactate respiration.

Following exposure of lactate-grown cultures to 1.5% O₂ for 20 hours, basal OCR of both primary ATII (Figure 4.6A) and MLE-15 cells (Figure 4.6B) decreased by 50% from ambient O₂ values. This degree of hypoxia-induced mitochondrial suppression is similar to that observed for control cultures grown in glucose in parallel.

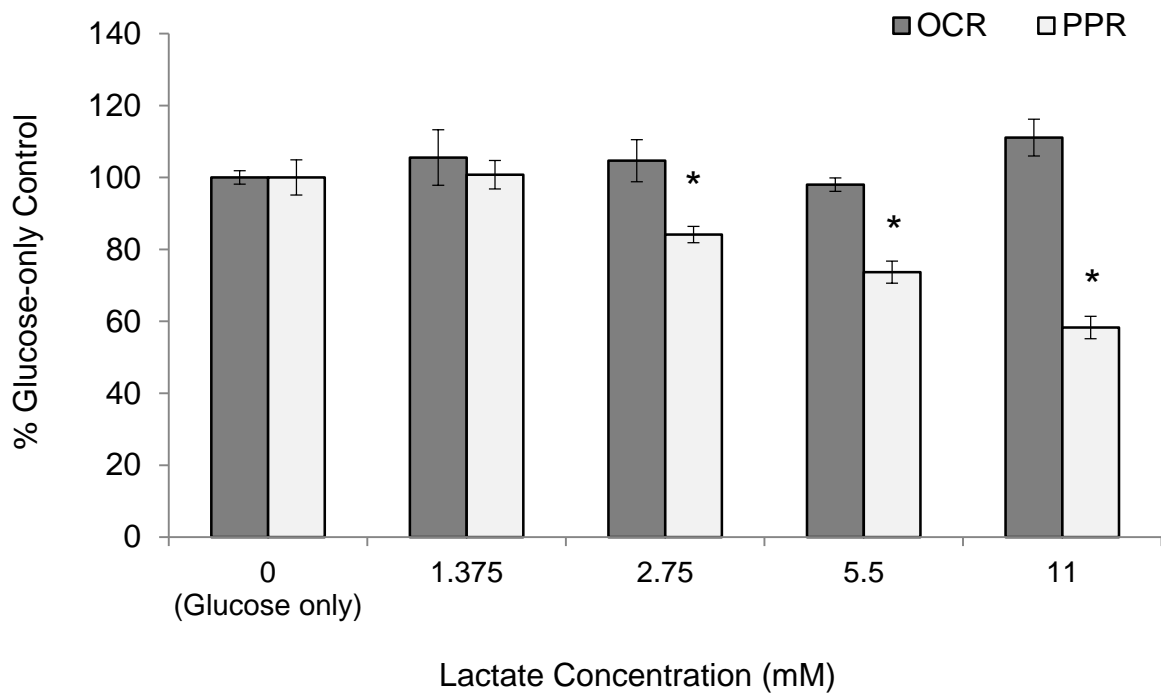


Figure 4.5: Extracellular lactate concentration regulates glycolytic output. OCR (dark bars) and PPR (light bars) were measured for MLE-15 cultured in 5.5mM glucose and increasing concentrations of lactate. Data is represented as % of glucose-only control. A total of 12 independent cultures were assessed for each condition. * indicates significant difference ($p < 0.05$) from glucose-only control, as determined via ANOVA followed by Tukey post hoc analysis. Error bars represent \pm SE.

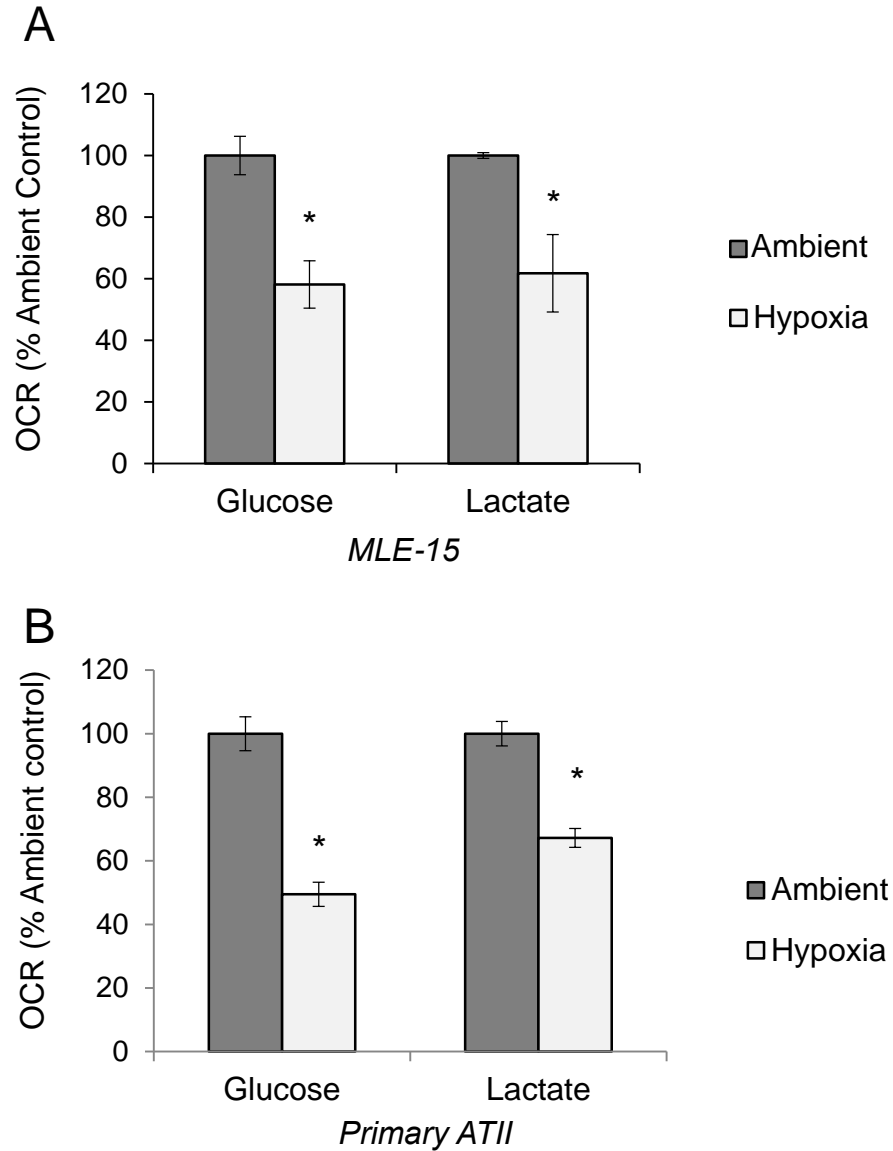


Figure 4.6: Exposure to hypoxia suppresses respiration of ATII cells cultured in glucose or lactate to a similar degree. OCR was measured for MLE-15 cells (A) and primary ATII cells (B) cultured in 5.5 mM glucose or 5.5 mM lactate and incubated in ambient O₂ (21% O₂) or hypoxia (1.5% O₂) for 20 hours. For MLE-15 cultures, samples were assayed minimally in triplicate for each condition and plates run in triplicate. For primary cultures, a total of 6 single-well experiments were performed for each condition. * indicates significant difference (p<0.05) from ambient O₂ OCR for each condition, as determined via Student's T-Test. Error bars represent ± SE.

4.2.6 ATII cell lactate consumption and export are dependent on MCT function.

MCT proteins control transport of lactate both into and out of cells. Lactate transport by MCTs can be inhibited pharmacologically using the compound alpha-4-hydroxycinnamate (CHC), which inhibits all MCT isoforms at the cytosolic membrane. Addition of CHC to both glucose- and lactate-grown MLE-15 cultures during metabolic flux assay resulted in decreased PPR from basal levels, demonstrating impaired lactic acid export (Figure 4.7A). Addition of CHC to both glucose- and lactate-grown MLE-affect OCR in glucose-grown cultures; however, in lactate-grown cultures, addition of CHC decreased OCR (Figure 4.7B) indicating that restricting lactate import reduced mitochondrial function. In summary, these data indicate that MCT function is necessary for both lactate export and lactate import and subsequent mitochondrial metabolism in ATII cells.

4.2.7 ATII cells express MCT1 in a non-hypoxia-inducible manner.

Expression of the monocarboxylate transporter isoform MCT1 is associated with co-import of lactate and protons into cells that oxidize lactate including cells of the heart and red skeletal muscle fibers. MCT1 protein expression was confirmed in MLE-15 lysates, with mouse skeletal muscle tissue lysate as a positive control (Figure 4.8). *Mct1* expression was assessed in lysates from MLE-15 and primary ATII cultures. Both cell types express *Mct1* mRNA (*cf. Figure 4.9A*). Based on Ct values observed in qPCR assays, *Mct1* mRNA is expressed by ATII cells at levels in the approximate range of *Gapdh*.

MCT1 has been shown to be hypoxia-inducible in some tissues, but not in others. In lysates from primary ATII and MLE-15 cells exposed to 1.5% O₂ for 20 hours, no significant difference in *Mct1* mRNA expression was observed (Figure 4.9A). Similarly, MCT1 protein concentration (Figure 4.9B) measured in MLE-15 cell lysates did not change in response to hypoxic exposure. This provides evidence that MCT1 is not responsive to hypoxia in ATII cells. However, *Mct1* mRNA expression was enhanced in MLE-15 cultured under ambient O₂ in lactate compared to those grown in glucose (Figure 4.10). This indicates that expression of the transporter is responsive to extracellular lactate availability, an observation that has been made in other tissues (27).

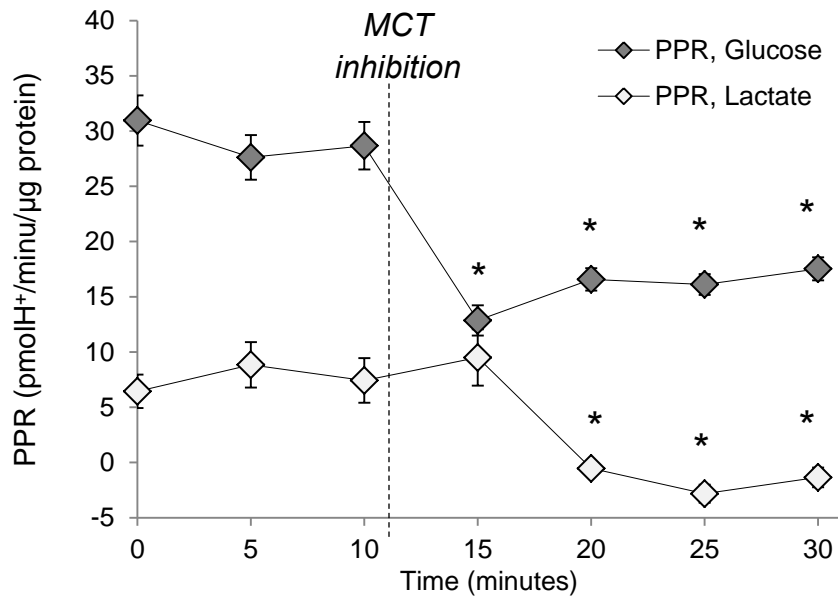
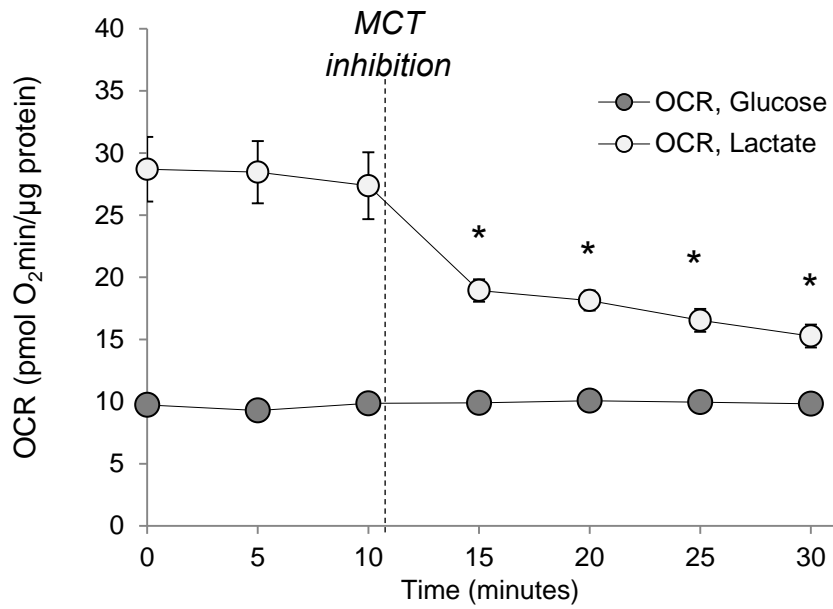
4.2.8 Lactate alone is sufficient to maintain ATP balance but not cell growth.

Culture in lactate in the absence of glucose did not disrupt the ability of MLE-15 cells to maintain energy balance, as intracellular ATP levels measured for lactate-grown cultures were statistically similar to those in glucose (Figure 4.11). This was true for culture in lactate under both ambient O₂ and hypoxic conditions.

While ATP level was similar cells cultured in lactate versus glucose, there was a dramatic difference in cell growth. In lactate alone, MLE-15 cells showed decreased rates of DNA synthesis compared to cells cultured in glucose. DNA synthesis in the combination of both lactate and glucose did not differ significantly from glucose-alone demonstrating that it is the absence of glucose, and not the presence of lactate, that impaired cell growth (Figure 4.12A). These

results were confirmed by cell counts taken over a period of 5 days, showing rapid increases in cell number in glucose alone and combined substrate but minimal increase in lactate alone (Figure 4.12B).

Figure 4.7: MCT transporter function mediates export and import of lactic acid by MLE-15 cells. PPR (A) and OCR (B) were measured for MLE-15 cells cultured in either 5.5 mM glucose (shaded) or 5.5 mM lactate (open). Following basal measurements, CHC was injected into assay wells to a final concentration of 10 mM to inhibit MCT proteins. n = 9 and 6 individually-cultured wells for glucose and lactate conditions, respectively. * indicates significant difference ($p < 0.05$) from basal (pre-injection) measurements, determined using ANOVA followed by Tukey post hoc analysis. A total of 9 independent cultures were assessed for each condition. Error bars represent \pm SE.

A**B**

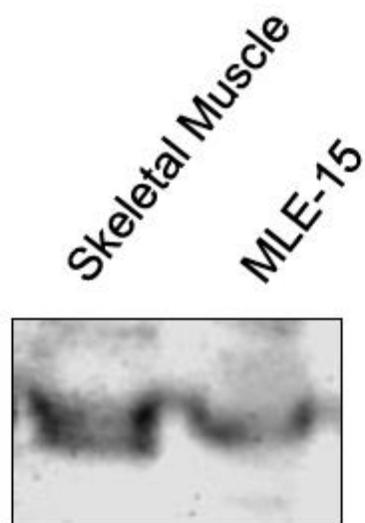


Figure 4.8: ATII cells express monocarboxylate transporter MCT1. MLE-15 cell lysates (approximately 25 μg total protein) was analyzed for MCT1 protein expression. Mouse skeletal muscle whole tissue lysate (approximately 12 μg total protein) serves as positive control for mouse MCT1 protein.

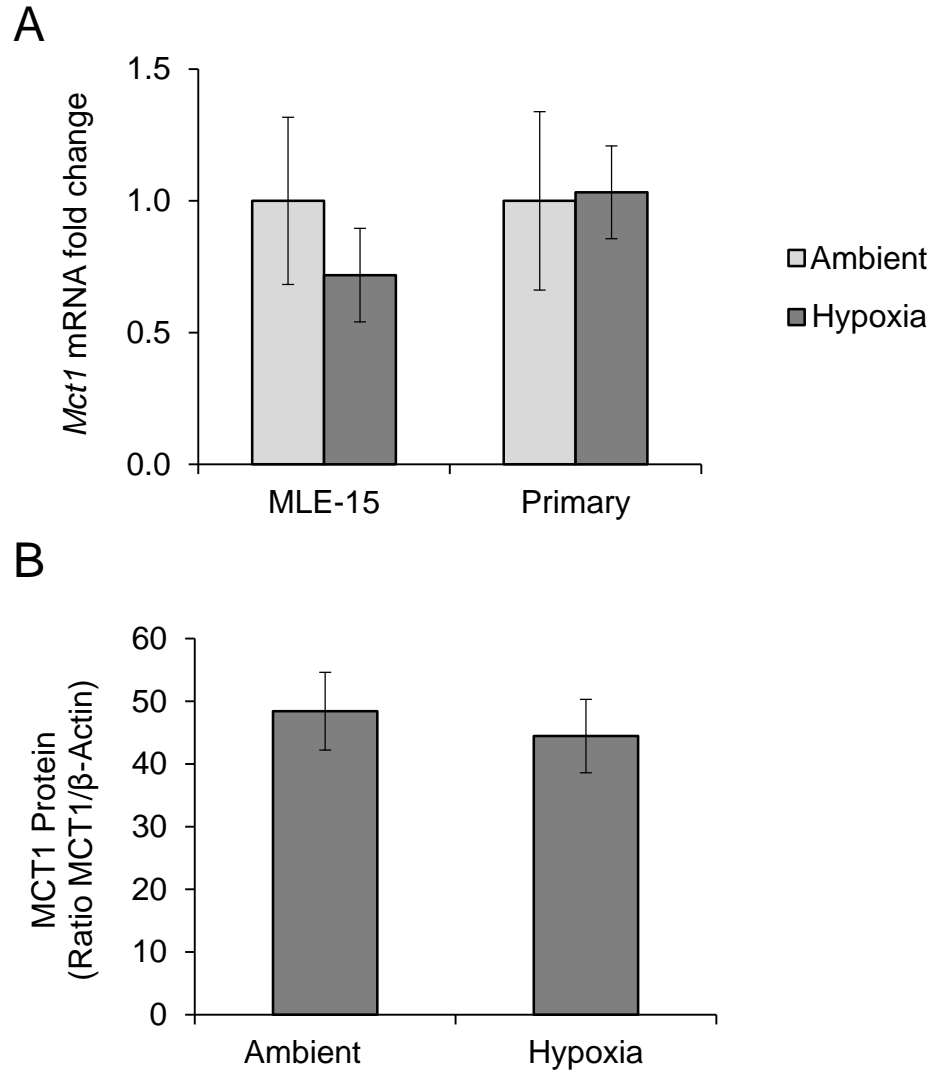


Figure 4.9: *Mct1* expression is not hypoxia-inducible in ATII cells. (A) Expression of *Mct1* RNA was measured in primary ATII cell and MLE-15 cells, cultured in ambient O₂ (21%) or hypoxia (1.5% O₂) for 20 hours, via qPCR. Fold change was calculated from delta-delta Ct values using beta-actin for normalization. (B) Expression of MCT1 protein was measured in MLE-15 lysates from cells cultured in ambient O₂ or hypoxia for 20 hours. Band densitometry was performed on blots to semi-quantitatively measure protein expression. Data represent the ratio of MCT1 band density to beta-actin band density for normalization. n = 3 lysates from individual cultures per condition. No significant difference (p < 0.05) was detected between conditions using Student's T-Test. Error bars represent ± SE.

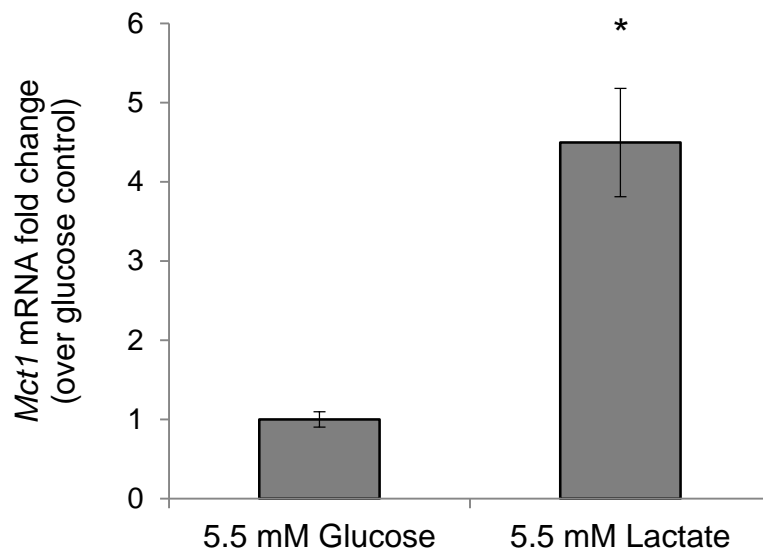


Figure 4.10: *Mct1* expression by MLE-15 is increased by culture in lactate. Expression of *Mct1* RNA was measured in MLE-15 cells, cultured in HITES formulated with 5.5 mM Glucose or 5.5 mM lactate via qPCR. Fold change was calculated from $\Delta\Delta C_t$ values using beta-actin for normalization. * indicates significant different ($p < 0.05$) from glucose-only control, based on Student's T-Test. Error bars represent \pm SE.

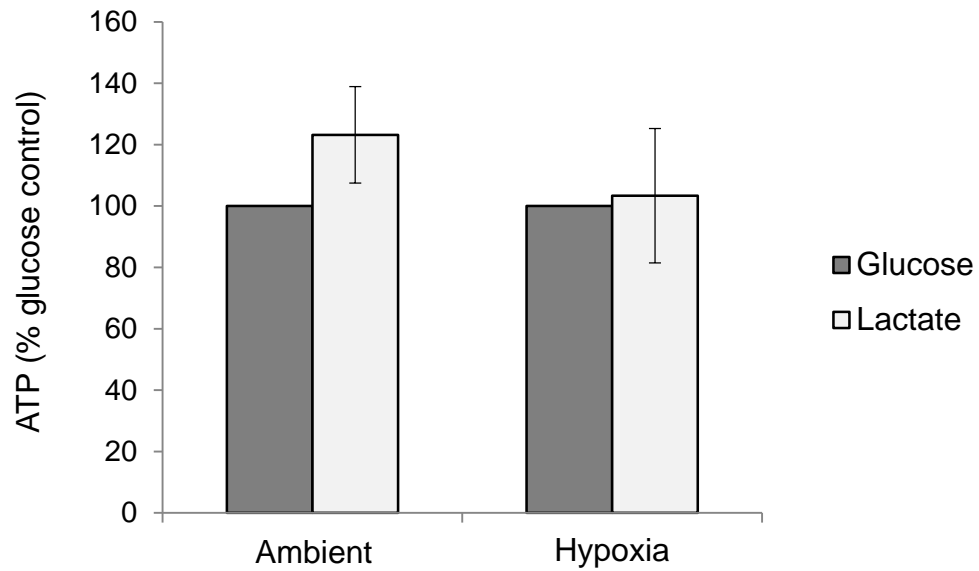
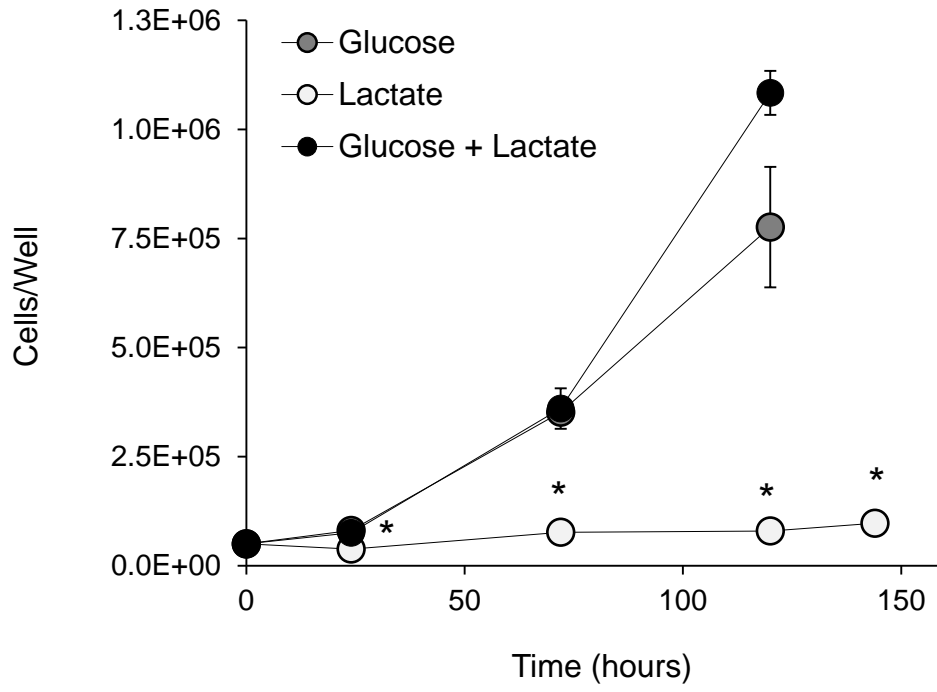


Figure 4.11: Lactate alone is sufficient to maintain MLE-15 cell ATP homeostasis. ATP was measured in MLE-15 cells cultured in media formulated with 5.5 mM glucose or 5.5 mM lactate. Samples were assayed in triplicate per plate using luminescent assay. Plates were run in triplicate. * indicates $p < 0.05$ versus ambient glucose control. Error bars represent \pm SE.

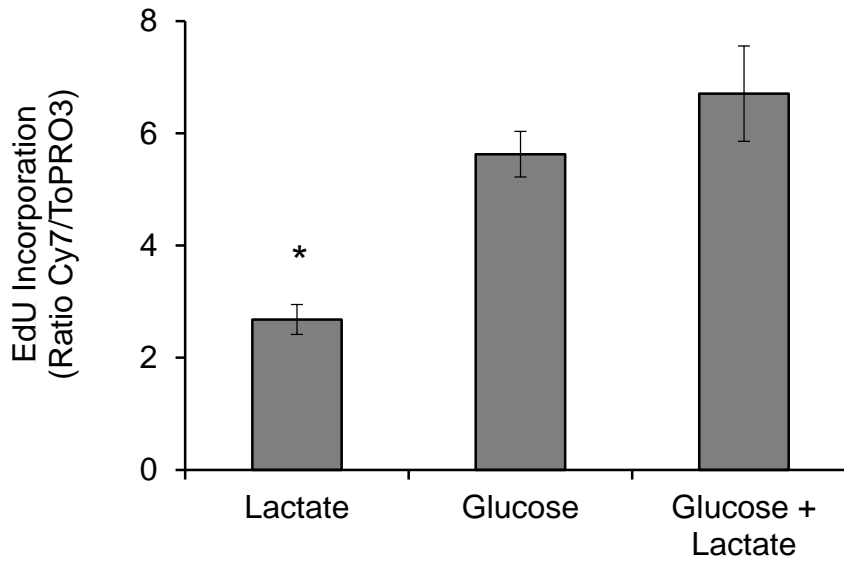
Figure 4.12: Lactate alone is not sufficient to maintain cell growth in MLE-15 cells.

(A) MLE-15 cell count in culture was assessed over a growth period of 6 days, or until cultures reached 100% confluence, for cultures grown in 5.5 mM glucose, 5.5 mM lactate, or 5.5 mM of both substrates. Data represent total cells per well determined via hemacytometer count of only cells excluding the vital dye trypan blue. $n = 3$ individually-cultured wells. * indicates significant different ($p < 0.05$) from glucose-only control. Error bars represent \pm SEM. (B) EdU incorporation into synthesized DNA was assessed fluorimetrically, as described in methods. Data represent fluorescent signal from Cy7 normalized to ToPRO3 signal for total DNA. $n = 3$ individual cultures of MLE-15. * indicates significant different ($p < 0.05$) from glucose-only control. Error bars represent \pm SE.

A



B



4.3 Discussion

Early metabolic studies in the 1970s and 1980s conclusively demonstrated that lactate is oxidized by lung tissue. Lactate oxidation was implicated as a potentially important process, both for generating cellular ATP and for providing precursor molecules for lipid synthesis. While these studies using the whole isolated perfused lung model provided significant insight into pulmonary metabolism, they were limited in their inability to provide information concerning the function of specific pulmonary cell types (11), of which there are many. Despite the ample evidence provided by these early studies that lactate is a potentially important substrate for lung metabolism, and despite heavy investigation of lactate consumption in brain and skeletal muscle, lactate oxidation in the lung has not been revisited using modern techniques. This report provides evidence that ATII cells import lactate from the extracellular space and utilize it as substrate for mitochondrial energy production. In this manner, ATII cells may serve as a “lactate sink” in the pulmonary tissue, consuming lactate carried in pulmonary circulation and extruded as waste from neighboring cells, thus preventing lactic acid build-up in the tissue and maintaining a physiological balance of lactate production and consumption. As lactic acid build-up has recently been implicated in the pathogenesis of IPF, maintaining this balance may be a critical, previously unknown role of ATII cells in healthy lung function.

A highly oxidative, minimally glycolytic phenotype was observed in cells cultured in lactate as compared to those cultured in glucose, resulting in a dramatic shift in metabolic phenotype. Oxygen consumption by lactate-grown

cultures occurred at approximately twice the rate of those in glucose. With lactate provided as metabolic substrate in the absence of glucose, respiration was performed at maximal rates of mitochondrial function as indicated by the absence of response to FCCP. The rapid rate of oxygen consumption by ATII cultured in lactate is dedicated largely to ATP production, as exposure of cultures to the ATP synthase inhibitor oligomycin A resulted in a decrease of approximately 70%. This degree of coupling is similar to that observed for cells cultured in glucose in parallel.

The observation that inhibition of LDH decreased OCR provides additional support for the conclusion that lactate is used as a precursor substrate for mitochondrial metabolism, as the lactate-to-pyruvate conversion necessary for entry into the TCA cycle is accomplished via the reverse reaction of LDH. Inhibition of this process decreases mitochondrial respiration by limiting available pyruvate. In glucose-grown cultures, LDH inhibition had the opposite effect, resulting in enhanced OCR above uninhibited levels. While ATII depend on mitochondrial metabolism to generate a large proportion of ATP, they do also simultaneously perform anaerobic metabolism of glucose, as evidenced by basal PPR rates. LDH inhibition decreases the amount of pyruvate converted to lactate, instead shuttling pyruvate into the oxidative metabolic pathway, which likely accounts for the modest increase in OCR in the glucose condition.

The data reported here demonstrate that lactate availability alters glucose utilization. When provided simultaneously with 5.5 mM glucose, lactate concentrations of 2.75 mM and higher lead to decreased acid generation. OCR

values did not change significantly with increasing concentrations of lactate. These findings demonstrate that glucose metabolism is altered by the presence of lactate, and supports previous findings from Fisher and Dodia that lactic acid generation and glucose consumption is reduced when lactate is present (127). As in that study, we suggest that the observed decrease in PPR is the result of increased lactate utilization, as lactate competes with glucose as a source of pyruvate for mitochondrial energy production. However, it is also possible that decreased PPR is alternatively the result of decreased lactic acid export, due to change in the extra- to intracellular lactate gradient. Further study will be necessary to determine the extent to which lactate is utilized as substrate when glucose is also present; however, this demonstrates that glucose metabolism is affected by the presence of lactate. Plasma lactate can exceed 20 mM in extreme cases of hypoxia or hypotension (128), and concentration in IPF lung are more approximately 2-fold greater than healthy lung (94); thus, modulation of glucose by extracellular lactate holds important implications for cell function in pulmonary disease.

For the first time, the importance of MCT proteins in mediating pulmonary cellular lactate transport is directly demonstrated. Inhibition using a pan-MCT inhibitor resulted in decreased flux of protons out of cells and into the extracellular environment, demonstrating the importance of MCT-mediated lactate export. Furthermore, in lactate-grown cultures, inhibition of MCT reduced oxygen consumption, demonstrating an effect on mitochondrial metabolism by limiting lactate transport into the cell. OCR was unaffected in MCT inhibition in

glucose-grown cells, as expected due to the fact that glucose is imported via its own set of transport proteins and MCT is not involved in mediating movement of glucose into the cell. Additionally, we demonstrate expression of the transporter isoform MCT1 by ATII cells. Expression of this MCT isoform is associated with lactate import in tissues known to oxidize lactate including cardiac muscle and skeletal muscle red fibers, and has been previously shown to be expressed in whole lung tissue. Here, MCT1 mRNA is found in MLE-15 and primary ATII, and protein expression confirmed in MLE-15, identifying ATII cells as one pulmonary population that expresses the transporter. This further supports the concept that ATII cells consume lactate and may serve as a sink for lactate in the lung. Exposure of rat fetal lung explants to CHC impairs alveolarization (126), indicating that MCTs play important, though yet undefined, roles in lung development. In combination with the work presented here, it appears that lactate transport and metabolism are critical components in proper lung development.

Use of lactate for mitochondrial metabolism is suppressed by hypoxia, as evidenced by a drop in OCR by approximately 50% following 20-hour exposure to 1.5% oxygen. This degree of change in response to hypoxic treatment is similar to the effect of hypoxia on oxidative metabolism in ATII cultured in glucose (23, 37). Hypoxia did not alter expression of *Mct1*, indicating that the gene is not hypoxia-inducible in these cells. Though *Mct1* is up-regulated in response to hypoxia in adipocytes, in skeletal muscle expression does not change, as observed here for ATII. As pulmonary hypoxia is associated with

multiple lung diseases, the impact of hypoxia on the ability of ATII to remove lactate, together with protons, from the extracellular space may contribute to lactic acid build-up. Indeed, lactic acid has been shown to increase in lung tissue in IPF and directly contribute to disease pathogenesis via pH decrease. Based on our findings, we propose that impaired lactate utilization contributes to the build-up of lactic acid in the extracellular space that occurs in certain pulmonary diseases, potentially in addition to enhanced acid generation by ATII or other cells. Here, only the effect of hypoxia on mitochondrial metabolism of lactate is investigated; however, we expect that any condition that inhibits respiration will limit lactate consumption.

Despite adopting a very different metabolic profile, cells cultured in lactate maintained ATP concentration. In fact, a statistically significant increase in ATP concentration was measured. Cells utilizing lactate in the absence of glucose cannot undergo glycolysis and thus lose glycolytically-derived ATP, and increased OCR to maximal levels under these conditions is possibly the result of compensating for this. While ATP homeostasis was maintained, lactate alone was insufficient to support cell growth, as measured by increase in cell count over time and relative rates of EdU incorporation into nascent DNA. This finding is not surprising, as glycolytic intermediates are required for DNA synthesis. Intermediate metabolites of glycolysis processed through the pentose phosphate pathway reactions generate ribose sugars, necessary for nucleotide synthesis. As lactate oxidation bypasses glycolysis, these products are not formed in the process of lactate consumption, limiting the availability of substrate for DNA

synthesis in cells cultured in alone. Culture in combined lactate and glucose did not inhibit DNA synthesis or increase in cell number, demonstrating that it is the absence of glucose, and not the presence of lactate, that mediates the effect. After 5 days of growth, a significant different was seen between glucose and combined substrate, with the combined condition showing greater cell number. Rates of EdU incorporation were not significantly different, although this variable was measured after only one day of culture; significant difference may also be observed in rate of synthesis given a longer period of growth. While this has not been examined in further detail, it may be the result of enhanced proliferation, reduced apoptosis, or both; further study will be necessary to determine how the presence of lactate influences either or both of these processes.

The capacity of ATII cells to consume lactate from the extracellular space has important implications for whole lung metabolism. Based on our findings, ATII cells in the lung may take up lactate produced by neighboring cells in a situation analogous to white-glycolytic and red-oxidative fiber metabolism in skeletal muscle tissue. Extracellular oxygen and proton flux has not been measured for ATI cells and pulmonary fibroblasts; however, in fibrotic lung disease, activated myofibroblasts generate high levels of lactic acid (94) and rough comparison of ATII flux measurements to those for normal human dermal fibroblasts indicate that ATII cells are more oxidative (107). ATII cells may also, or alternatively, utilize lactate delivered to the alveolus in pulmonary circulation, similar to the manner in which cardiac tissue consumes circulating lactate. Multiple investigators have demonstrated lactic acid uptake from pulmonary

circulation (34), oxidation (17, 18, 129) , and/or incorporation into lung lipids (18). In this manner, local metabolic cooperation between lung cell phenotypes may form a key component of normal alveolar tissue homeostasis, providing metabolic substrate for ATII cell energy and lipid production while also preventing lactic acid build-up in the healthy lung.

Likewise, dysregulation of local metabolic connection between cell types may lead to conditions associated with certain diseases. Recent investigation into pro-fibrotic processes that contribute to myofibroblast activation in idiopathic pulmonary fibrosis (IPF) have highlighted the importance of lactate balance in the lung. Kottman et. al. determined that not only is lactate elevated in the lungs of IPF patients, but lactic acid directly contributes to the process of tissue fibrosis (94). By lowering the local extracellular pH, lactic acid build-up leads to activation of latent TGF β *in vitro*, added directly to fibroblast culture media in that study. TGF β is the primary molecular signal responsible for initiating conversion of fibroblasts into the myofibroblast phenotype (130), and the study determined that increased lactic acid leads to enhanced myofibroblast conversion and matrix deposition. Increased lactate generation was associated with a shift to enhanced tissue expression of LDH5, the isoform most strongly favoring pyruvate-to-lactate conversion (and not the reverse). Altered expression was localized roughly to the epithelium near fibrotic centers, though the cell type(s) responsible have yet to be specifically identified. While it is now clear that lactic acid build-up is involved in IPF disease pathogenesis, the cells and molecular processes responsible for lactic acid build-up in the diseased pulmonary tissue are unknown. Based on our

findings here, it is rational to conjecture that altered ATII cell mitochondrial metabolism, and thus reduced ability to remove and consume lactate, is a contributing factor.

CHAPTER 5. ATII CELLS IN IPF LUNG ADOPT A GLYCOLYTIC METABOLIC PHENOTYPE

5.1 Introduction

Idiopathic pulmonary fibrosis is characterized by extensive formation of fibrous tissue, or scarring, in the pulmonary parenchyma associated with aberrant, pathological deposition of extracellular matrix by activated myofibroblasts. Despite the relatively well-defined role of the fibroblast in the progression of pulmonary fibrosis and IPF (66, 130), it is in fact the alveolar epithelium, specifically the ATII cell, that is now thought to be the primary site of damage that initiates the disease. In the current paradigm, damage to ATII cells leads to pro-fibrotic signaling from injured and apoptotic cells that stimulates fibroblast activation and conversion to the myofibroblast phenotype (69). Myofibroblasts produce excessive amounts of extracellular matrix material, and epithelial cell-fibroblast signaling results in further damage to the alveolar epithelium in a feed-forward mechanism that continuously stimulates myofibroblasts. Damaged epithelial cells also recruit both innate and adaptive immune system cell mediators including neutrophils, monocytes, and T cells, which further enhances the pro-fibrotic environment through cytokine signaling (92, 93, 131) and production of reactive oxygen species (91). Despite advances that have placed ATII cells as the central cellular targets of damage in

initiating the disease, the ultimate cause of the damage is unknown. Many potential sources are currently under investigation including environmental causes such as smoking and exposure to particulates; mutations in genes including *SPC* (59, 60), telomerase (63), and *MUC5B* (61, 62); gastroesophageal reflux disease (GERD) and exposure to gastric fluids (132); ER stress and the unfolded protein response (133); and viral infections (134). Ultimately, in most cases, generation of ROS is supposed to be at least part of the mechanism of damage involved in current hypotheses regarding epithelial damage in initiation of IPF (100, 135).

Altered cellular metabolism has not yet been directly assessed in IPF lung tissue. However, both the potential initiating insults and the known downstream pathogenesis events include mechanisms that could cause mitochondrial damage and alter cellular metabolism in epithelial cells. For instance, history of cigarette use is associated with development of IPF, and smoking is known to cause oxidative stress and mitochondrial ROS production and/or direct damage in a variety of tissues (136-138). Smoke exposure was recently shown specifically to decrease respiration in A1II cells of exposed mice (139). Asbestos, another particulate exposure also associated with IPF, damages mitochondrial DNA (mtDNA) leading to dysfunction and intrinsic mitochondrial apoptosis (140, 141).

Beyond endogenous generation of ROS by mitochondria in response to insult, exposure to exogenous hydrogen peroxide also generates damage in alveolar epithelial cells, suggesting that ROS production by myofibroblasts and

immune cells in IPF could alter ATII mitochondrial function. The robust mitochondrial function of ATII cells and their heavy reliance on oxidative phosphorylation for ATP generation under normal physiological conditions may make them a target susceptible to metabolic impairment as an initiating factor and/or a contributor to downstream pathogenesis in IPF.

TGF β , a growth factor intimately involved in IPF, may also lead to change in the metabolic status of ATII. TGF β is produced by multiple cells in IPF lung including myofibroblasts and ATII cells themselves, and has through recent investigation been linked to altered mitochondrial function including aberrant fission and fusion processes in the mink lung epithelial cell line (34) and organelle fragmentation in renal epithelial cells (33). TGF β stimulates ROS generation via activation of NADPH oxidase 4 (NOX4) and inhibits expression of antioxidant enzymes (38), and in mink lung epithelial cells leads to cell senescence associated with enhanced ROS generation and inhibition of electron transport system complexes (34).

IPF is associated with development of pulmonary hypoxia, yet another avenue through which ATII cell metabolism may be affected by the disease, as hypoxia leads to suppression of mitochondrial function in ATII cells. Formation of fibroblastic foci and scar tissue leads to thickening of the alveolar lining and reduced gas diffusion. This also affects the oxygen exposure of the alveolar epithelial cells themselves, which are normally exposed to approximately 13% oxygen. While there is debate regarding the extent to which the pathological conditions in the IPF lung subject pulmonary cells to reduced oxygen levels, it

has been shown that HIF signaling is stabilized and active in the IPF lung tissue. HIFs are the major inducers of the cellular hypoxic response, and it was demonstrated that pharmacological stabilization of HIFs using a prolyl-hydroxylase inhibition at 21% O₂ induced similar cellular adaptation as exposure to extreme hypoxia (1.5% O₂). Thus, regardless of whether true hypoxic conditions occur in the lung tissue in IPF, the noted HIF stabilization is likely to alter the metabolic function of ATII cells.

It has been recently demonstrated that lactic acid buildup occurs in the IPF lung. Tissue samples from IPF lung showed remarkably consistent elevation of lactate concentrations over 2-fold greater with a concurrent drop in tissue pH. The drop in pH associated with enhanced lactic acid contributes to the profibrotic environment of the IPF lung, in that lactic acid buildup lead to activation of latent TGF β and myofibroblast stimulation. The cellular source of the excess lactic acid is unknown. In the healthy lung, lactate is readily removed from the extracellular space and oxidized for use in energy production by ATII cells. However, any suppression of mitochondrial function will reduce the ability of ATII cells to remove lactate from the extracellular space to fuel their own metabolism. Reduced lactate consumption by ATII cells, paired with the observed up-regulation of lactic acid production from fibroblasts following conversion to myofibroblasts could disrupt normal lactate balance in the lung leading to extracellular build-up and tissue acidification that promotes fibrosis. Up-regulation of the LDH5 isoenzyme has been observed in and around fibroblastic foci of IPF lung, though the cell type in which LDH5 is up-regulated has not been specifically

determined. LDH5 favors the forward reaction of LDH that generates lactic acid from pyruvate, thus favoring a more glycolytic, acid-producing cellular phenotype.

The following work utilizes extracellular flux technology to measure cellular metabolism of ATII cells isolated from IPF patient lung, providing the first real-time, functional-level assessment of the cellular metabolic phenotype associated with a specific human pulmonary disease. While many elements of IPF pathophysiology have the potential to alter cellular metabolism and recent work suggests that glycolytic lactic acid production is enhanced in IPF lung, metabolism of cells isolated from diseased lung tissue have not been previously measured to assess the functional-level impact of the disease. Furthermore, there is a distinct need to assess cell function in IPF patient tissues because the currently available mouse models do not recapitulate many important facets of the pathological changes that occur in the human IPF lung. We report here that have low overall metabolic function and favor glycolysis. In further support of a metabolic shift in IPF ATII we find elevated levels of LDH protein, implicating ATII as one cell population contributing to the previously observed increase in LDH-M subunit expression in IPF alveolar lung tissue. Additionally, this work begins to address the role of TGF β and the extracellular milieu created by myofibroblasts in driving metabolic changes by exposing model ATII cells (MLE-15) to activated TGF β and myofibroblast-conditioned media and examining the resulting metabolism in vitro.

5.2 Results

5.2.1 ATII cells isolated from IPF lung have low overall metabolic function.

To examine mitochondrial metabolism in IPF, extracellular flux analysis was performed on ATII cells isolated from human IPF patient lung tissue samples and compared to ATII cells from a normal control sample of non-IPF patient lung, obtained from distal lung tissue donated from a deceased patient with cause of death unrelated to lung pathology. ATII isolated from IPF lung demonstrated low, but significant, OCR values compared to control tissue ATII (Figure 5.1). PPR (Figure 5.2) values were similar between normal and two of the IPF patient lung ATII preparations, while one patient showed elevated PPR.

ATII cells from IPF lung responded to FCCP injection with enhanced OCR and PPR, indicating both reserve respiratory and glycolytic capacities (Figure 5.3A and 5.3B). In terms of percentage increase above basal values, Patient 1 and Patient 3 maintained relatively greater spare capacities than Patient 2, with respiratory capacity similar to those observed previously for MLE-15. Patient 1 also showed remarkable glycolytic capacity, based on a glycolytic response to FCCP higher than any previously observed in ATII or MLE-15 cells. Patient 2 maintained respiratory and glycolytic capacity, albeit to a lesser degree than the others.

5.2.2 ATII cells from IPF lung demonstrate a glycolytic phenotype.

To assess the relative dependence on glycolytic versus oxidative metabolism in IPF lung-derived ATII, the ratio of PPR to OCR was calculated

from flux measurements. ATII isolated from all IPF patients showed relative glycolytic function higher than control lung ATII (Figure 5.4). A549 is an ATII-like cancer-derived line that is heavily reliant on glycolysis for ATP production (142) and here is shown as a human “positive control” for reliance on glycolysis. IPF patients showed PPR/OCR ratios approaching those measured in A549 cultures, with values greater than those observed here for healthy human control ATII, as well as those reported previously in this work for MLE-15 and primary mouse ATII (*cf.*, *Figure 2.6*). Increased PPR/OCR ratios indicate enhanced glycolytic relative to oxidative metabolism in IPF-derived ATII.

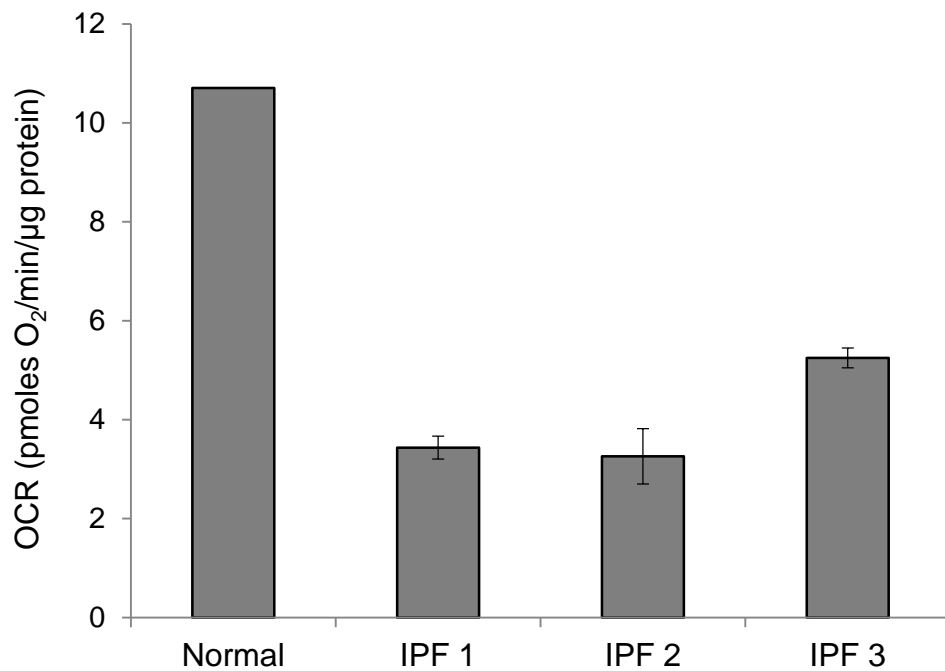


Figure 5.1: ATII cells isolated from IPF lung have low respiratory function compared to normal lung ATII. OCR was measured for primary ATII cells isolated from human patient lung using an XF Extracellular Flux Analyzer. For each patient, ATII cells were isolated from a single tissue sample, and samples were assayed minimally in quadruplicate. A single culture of non-IPF control lung ATII cells was analyzed for comparison. Values are normalized to total protein of wells cultured in parallel.

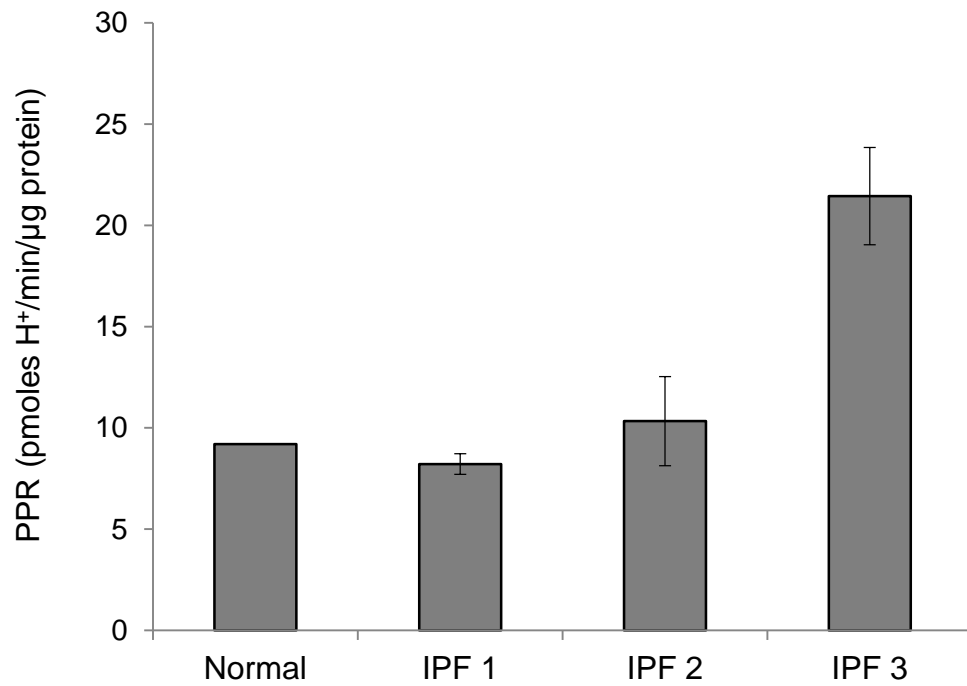


Figure 5.2: Glycolytic function of IPF ATII cells is maintained or elevated compared to control. PPR was measured for primary ATII cells isolated from human IPF patient lung. For each patient, ATII cells were isolated from a single tissue sample, and samples were assayed minimally in quadruplicate. A single culture of control lung ATII was analyzed. Values are normalized to total protein of wells cultured in parallel.

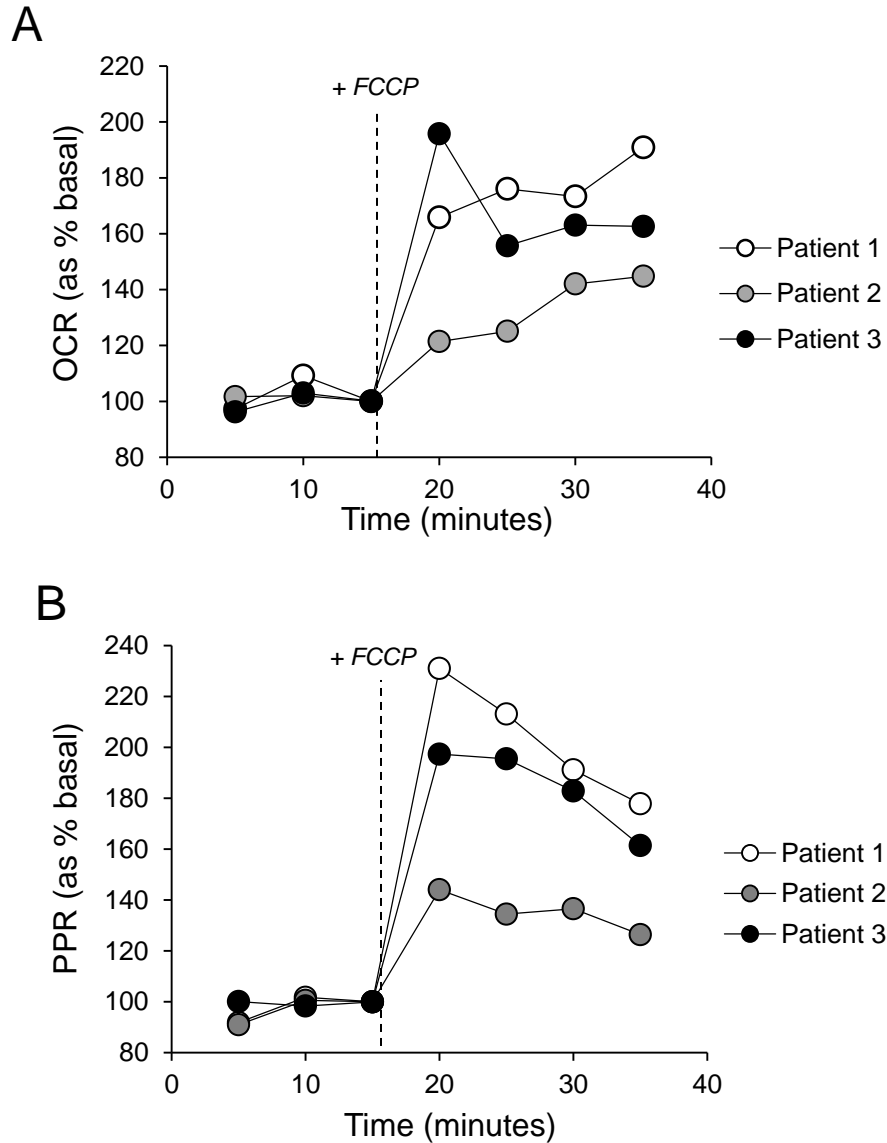


Figure 5.3: ATII cells isolated from IPF lung maintain reserve respiratory and glycolytic capacity. To assess reserve metabolic capacity, OCR (A) and PPR (B) were measured for primary ATII cells isolated from human IPF patient lung following addition of FCCP to assay media. For each IPF patient, ATII cells were isolated from a single tissue sample, and samples were assayed minimally in quadruplicate. A single culture of control lung ATII cells was analyzed. Data represent percentage increase above basal measurements following FCCP addition.

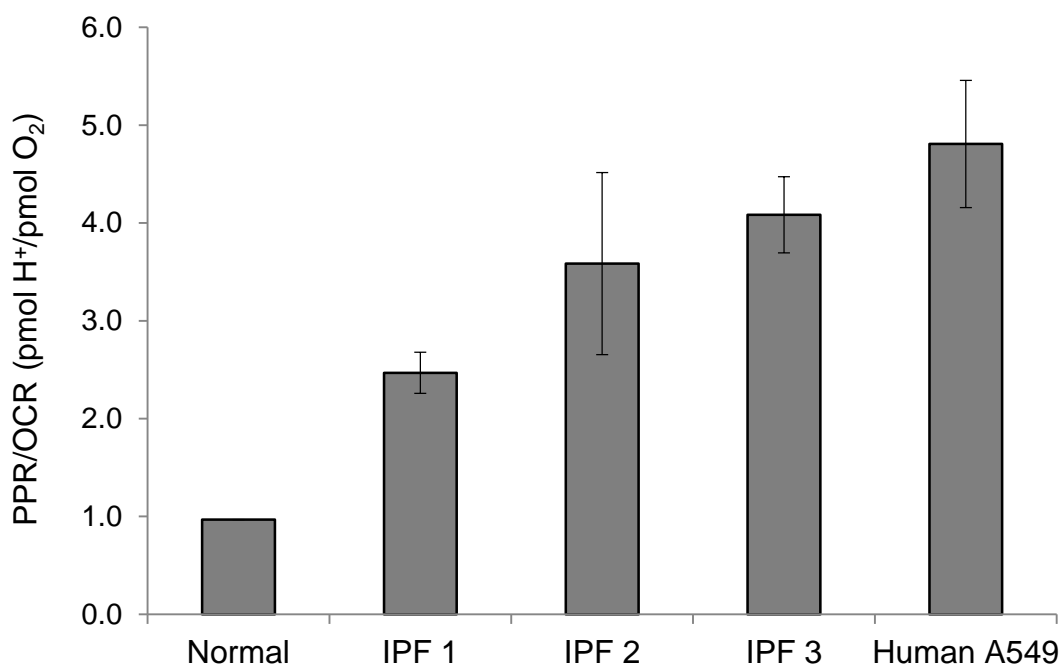


Figure 5.4: ATII from IPF lung rely more heavily on glycolysis than control lung ATII cells. OCR and PPR data were used to generate a PPR/OCR ratio, indicative of relative glycolytic versus oxidative metabolism. For each IPF patient, ATII cells were isolated from a single tissue sample, and samples were assayed minimally in quadruplicate. A single culture of non-IPF control lung ATII was analyzed. A549 were assayed minimally in quadruplicate per plate with plates run in triplicate.

5.2.3 IPF ATII cells express high levels of LDH protein.

LDH is a tetrameric enzyme composed of M and H subunits, and each isoenzyme is composed of a different ratio of LDH-M to LDH-H. Isoenzymes containing more LDH-M subunits more strongly favor the conversion of pyruvate to lactate over the reverse reaction. Of all the isoenzymes, LDH5 (composed of four LDH-M subunits) most strongly favors lactate production. LDH-M expression is enhanced in fibroblastic foci in IPF lung tissue, although the cell type responsible is unknown. To examine LDH expression in IPF ATII and address their contribution to the observed overexpression in the distal IPF lung, total LDH and LDH-M subunit protein was measured in lysates from one IPF patient (Patient 3) and compared to expression in lysates from the glycolytic A549 line as a human control. Both LDH-M and total LDH expression were increased in ATII from the IPF patient compared to human A549 (Figure 5.5). However, the ratio of LDH-M to LDH was comparable between human A549 and the patient sample, indicating that the altered expression was not specific to the LDH-M subunit, but rather to LDH in general.

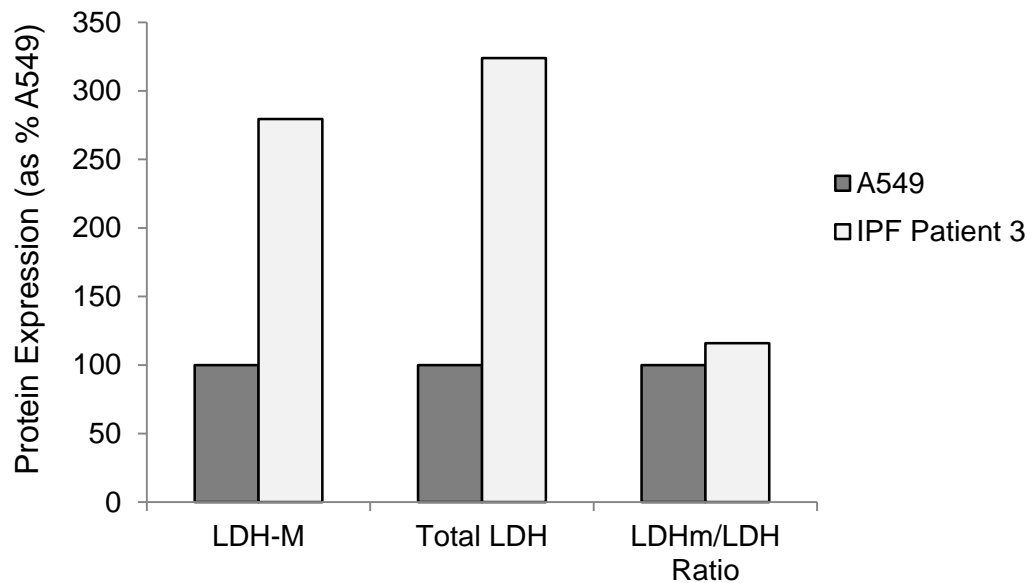


Figure 5.5: ATII cells from IPF lung express high levels of LDH protein. Total cell protein lysates from a single culture of A549 and ATII cell derived from human IPF lung tissue (Patient 3) were analyzed for LDH-M and total LDH via western blot. Expression was normalized to RNAPII as loading control using band densitometric quantification. Data represent densitometry readings normalized to RNAPII and expressed as percentage of normalized expression in A549 lysate.

Myofibroblasts at fibrotic foci secrete cytokines and growth factors that alter ATII cell function. One of these factors is TGF β . The following series of experiments sought to determine whether secreted factors from in vitro TGF β -stimulated myofibroblasts and/or TGF β alone directly contribute to generating the metabolic phenotype observed in human ATII cells derived from IPF lung tissue.

5.2.4 Treatment of MLE-15 with myofibroblast-conditioned media or TGF β decreases LDH protein expression.

To assess whether factors secreted by TGF β -stimulated myofibroblasts, or TGF β itself, induces enhanced expression of LDH in ATII cells, LDH-M and total LDH were measured in protein lysates from MLE-15 cells cultured with TGF β versus control, and MLE-15 cells cultured in TGF β -stimulated myofibroblast-conditioned media versus control. RNA Polymerase II (RNAPII) was assessed as a loading control and protein expression was quantified via band densitometry.

Both LDH-M and total LDH subunit content was decreased in response to myofibroblast-conditioned media and TGF β treatments (Figure 5.6A & 5.6B). Based on densitometric analysis, the degree of decrease was approximately 50% for both proteins, in response to both treatments. No difference was observed in the ratio of LDH-M to total LDH, indicating that expression of LDH was suppressed in general, versus specific down-regulation of the LDH-M subunit.

5.2.5 Neither TGF β -stimulated myofibroblast-conditioned media nor TGF β alter MLE-15 cell metabolism.

Oxidative and glycolytic function was measured in MLE-15 cells exposed to either myofibroblast-conditioned media or active TGF β to assess their role in generating the suppressed, glycolytic phenotype of ATII cells from IPF lung. Following 48-hour exposure, neither treatment altered OCR or PPR values (Figure 5.7 & 5.8).

5.2.6 TGF β does not affect the response of MLE-15 to hypoxia.

Hypoxic regions develop in IPF lung. Although we did not observe any change in oxidative or glycolytic function under ambient oxygen conditions, we next hypothesized that, due to the observed change in LDH and the multiple potential influences of TGF β on mitochondrial function, treatment might alter the cellular adaptation to hypoxia. However, MLE-15 treated with TGF β experienced a similar response to hypoxia as control (Figure 5.9). In both treated and control cultures, 20 hour exposure to hypoxia suppressed OCR by approximately 50%, with no significant change in PPR. This indicates that 48-hour exposure to TGF β did not influence the metabolic adaptation to hypoxia.

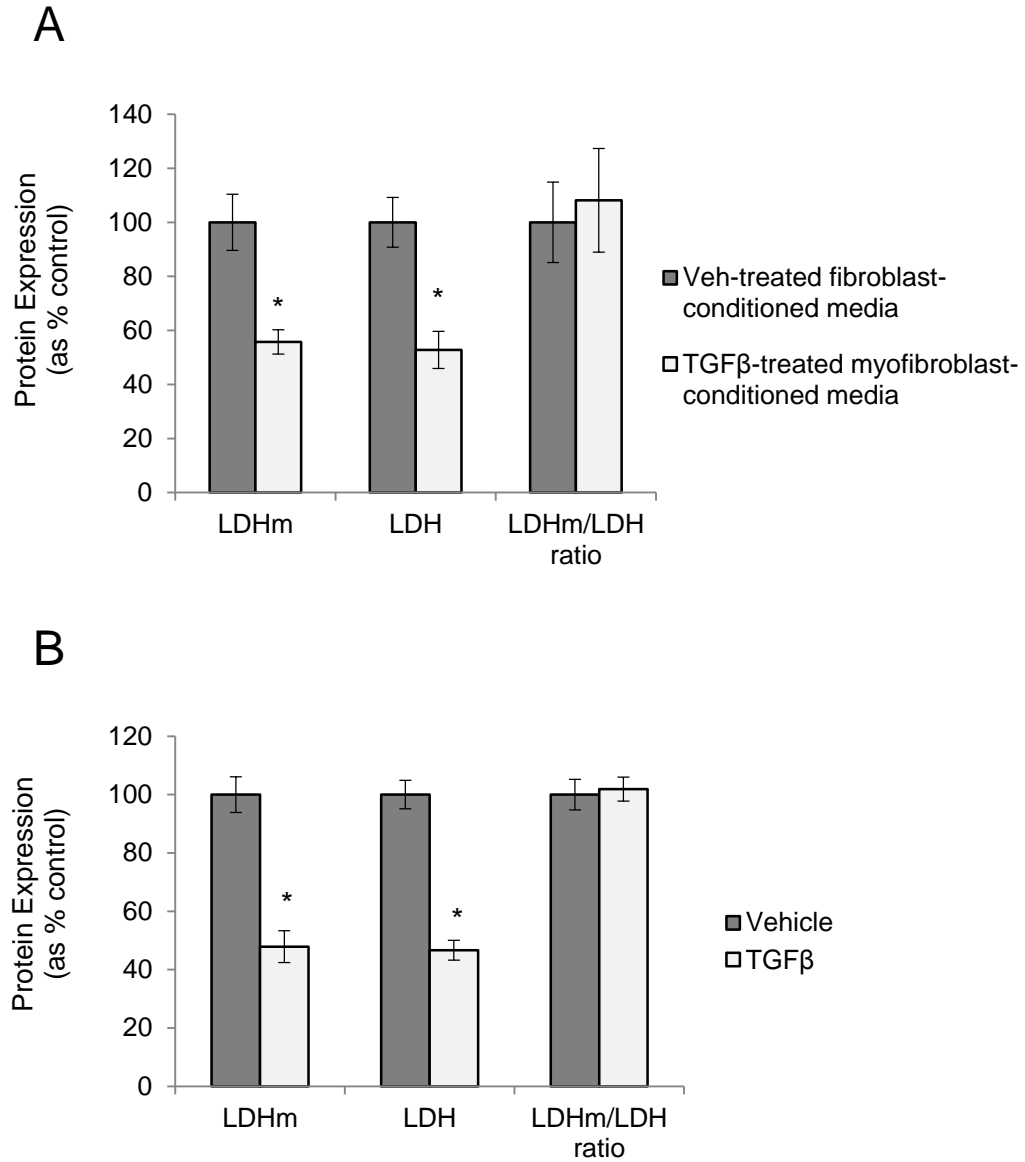


Figure 5.6: Treatment with myofibroblast-conditioned media or TGFβ decreases LDH expression in MLE-15. MLE-15 cultures were treated with myofibroblast-conditioned media (A) or TGFβ (B) for 48 hours. Total cell protein lysates were analyzed for LDH-M and total LDH via western blot and normalized to RNAPII as loading control using band densitometric quantification. * indicates significance from respective control, assessed via Student's T-Test. Error bars represent \pm SE.

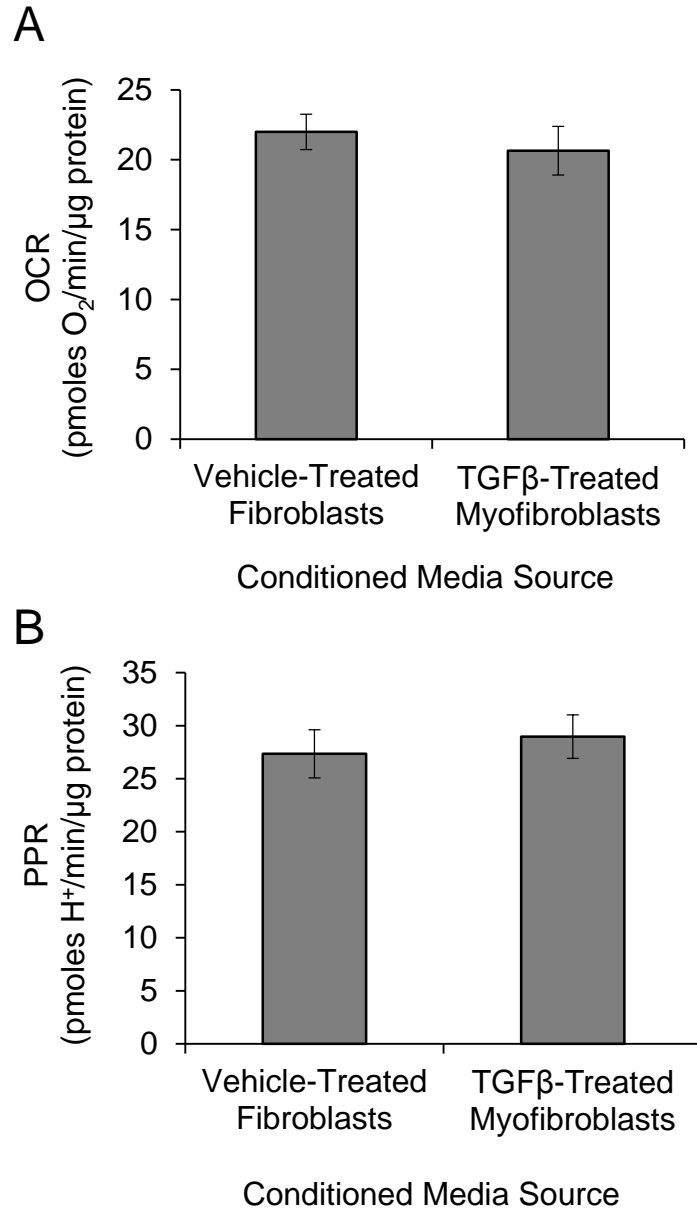


Figure 5.7: Treatment with myofibroblast-conditioned media does not influence glycolytic or oxidative function in MLE-15. Basal OCR (A) and PPR (B) were measured in cultures of MLE-15 cells treated with TGFβ-stimulated myofibroblast-conditioned media for 48 hours. No significant difference was detected between TGFβ-stimulated myofibroblast-conditioned media treatment and control via Student's T-Test. Error bars represent ± SE.

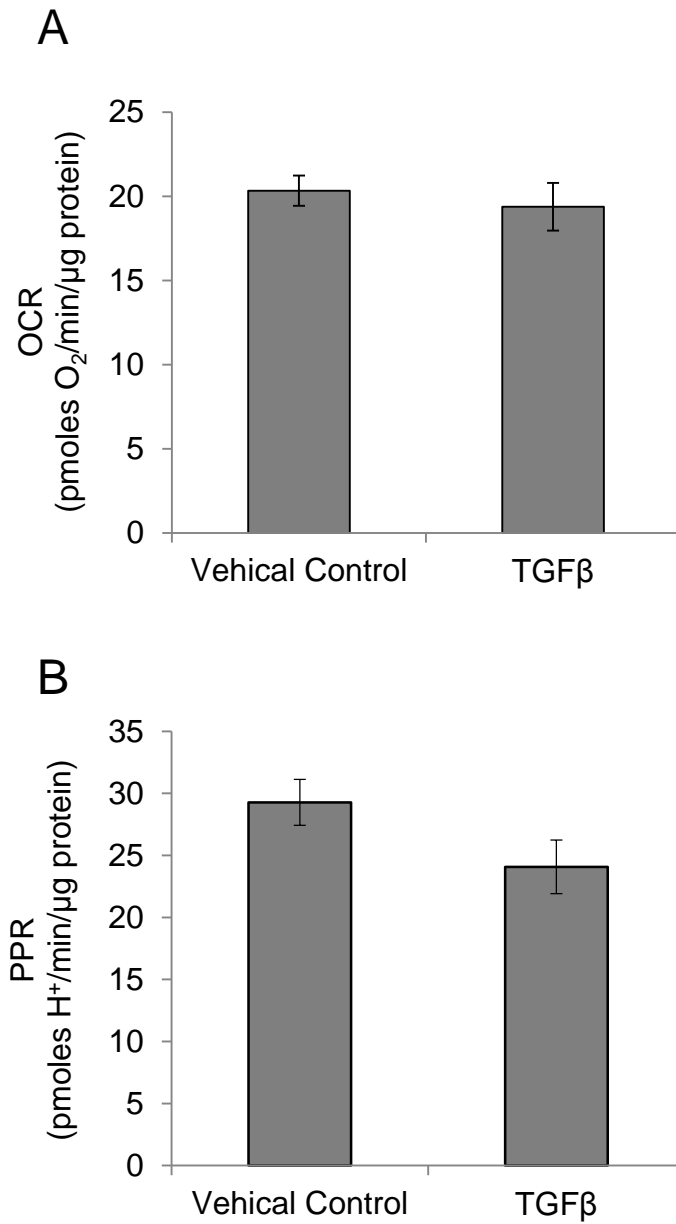


Figure 5.8: Treatment with TGFβ does not influence glycolytic or oxidative function in MLE-15. Basal OCR (A) and PPR (B) were measured in cultures of MLE-15 cells treated with TGFβ for 48 hours. No significant difference was detected between TGFβ treatment and control using Student's T-Test. Error bars represent \pm SE.

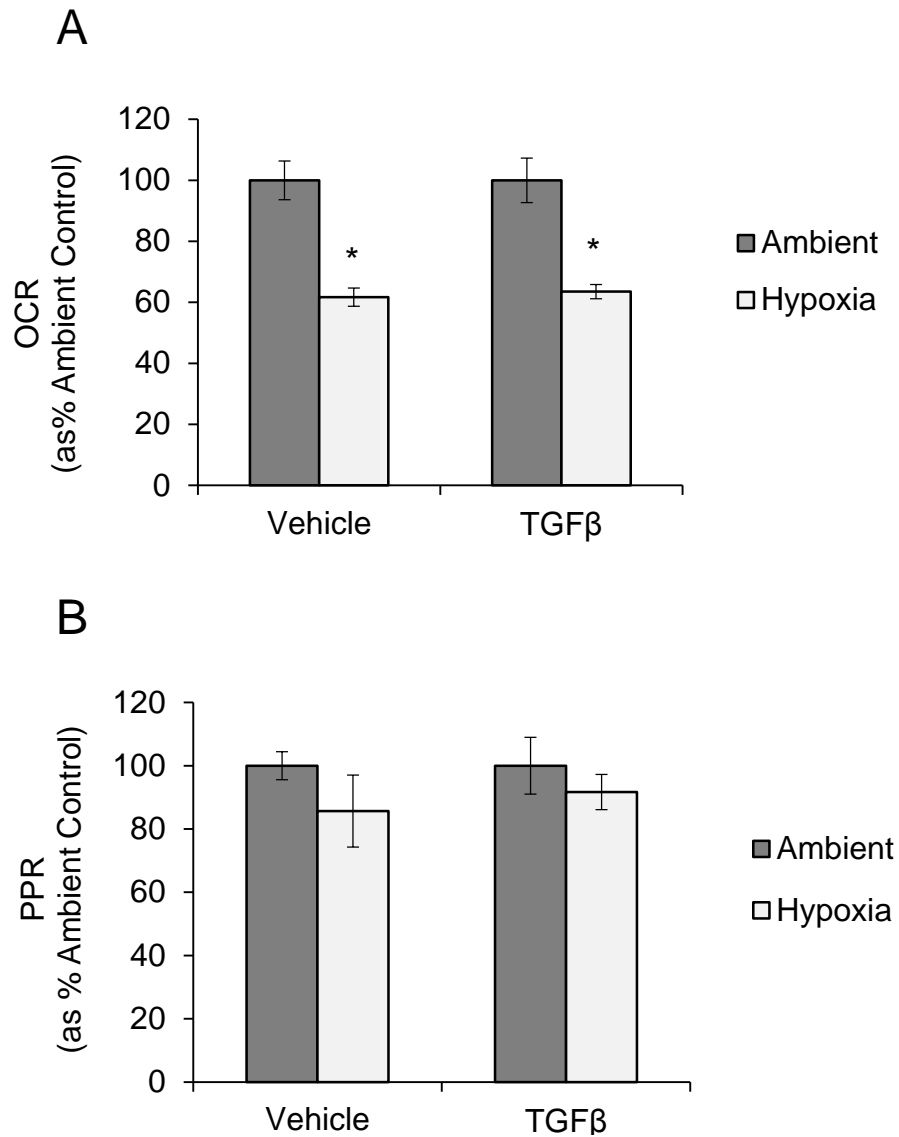


Figure 5.9: TGFβ treatment does not affect the MLE-15 metabolic response to hypoxia. OCR (A) and PPR (B) were measured in cultures of MLE-15 cells treated with TGFβ for a total of 48 hours and hypoxia (1.5% O₂) for 20 hours. Values represent percentage change in basal function compared to cultures grown in ambient O₂ (21%) in parallel. * indicates significant difference from ambient control; no difference was observed between hypoxic vehicle versus treated cultures, based on Student's T-Test. Error bars represent ± SE.

5.2.7 Exposure of MLE-15 to myofibroblast-conditioned media or TGF β induces morphological change.

While no measurable change in metabolism was found following TGF β and myofibroblast-media treatments, we noted morphological changes as early as 24 hours after exposure. ATII and ATII-like cells in culture have cuboidal morphology and grow in a tightly-connected monolayer with a “cobble-stone” appearance. At 48 hours, treated cells adopted a less cuboidal, more spread cell shape (Figure 5.10). These changes are reminiscent of an EMT-like response. Cells maintained little contact with neighboring cells, unlike the pattern of normal ATII cells in culture that reflects close connection with neighboring cells. Many cells showed cytoplasmic extensions. Vehicle- treated MLE-15 and those treated with unstimulated fibroblast-conditioned media showed similar morphology to MLE-15 cultured in normal HITES media with no exposure.

5.2.8 Exposure to myofibroblast-conditioned media or TGF β induces expression of fibroblast and ATI cell markers in MLE-15.

Based on the observation that TGF β and conditioned media exposure induced a change in morphology, lysates from treated and control cells were examined for changes in fibroblast markers and ATI markers to determine whether the change in morphology was associated with differentiation into a fibroblast or ATI cell phenotype (Figure 5.11). A small but statistically significant up-regulation was observed in expression of the ATI marker Aquaporin 5 (*Aqp5*) in response to both treatments. Pro-collagen 1a (*Pro-Col1a*) mRNA expression was up-regulated significantly in response to TGF β treatment, while expression

of Fibroblast-specific protein (*Fps*) did not change with either treatment. No change was observed in expression of the ATII cell marker Thyroid transcription factor (*Ttf*).

5.2.9 Exposure of ATII to myofibroblast-conditioned media or TGF β specifically enhances *Spc* mRNA expression.

In addition to fibroblast and ATI markers, surfactant protein expression was measured in lysates from MLE-15 exposed to conditioned media or TGF β versus control. *Spc* expression is specific to the ATII cell phenotype and *Spb* is expressed by lung secretory cells (including ATII). Surfactant expression is of interest for its value as a marker of the ATII cell phenotype, but also because genetic mutations in *Spc* are associated with IPF. In both experiments, *Spb* expression was similar between TGF β -treated cells versus control and myofibroblast conditioned media-exposed cells versus control. *Spc* mRNA expression was several-fold higher than respective controls in both cases (Figure 5.12).

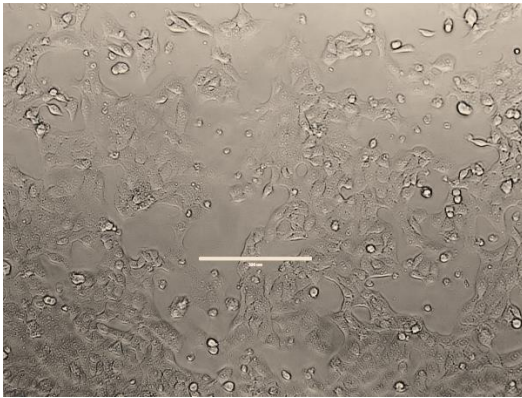
Figure 5.10: Treatment with TGF β or myofibroblast media alters MLE-15 cell morphology. MLE-15 Cultures were exposed to TGF β versus vehicle or TGF β -stimulated myofibroblast-conditioned media for 24 or 48 hours. Images were captured using a light microscope using the 20X objective. Representative images are shown.



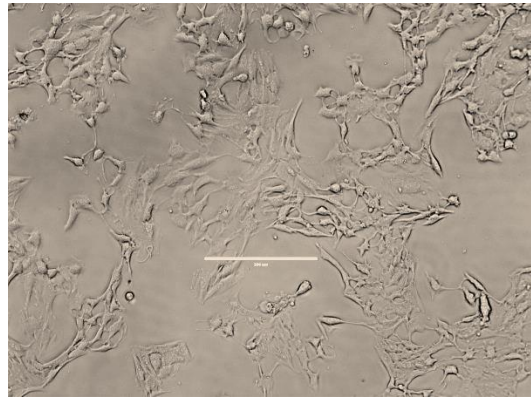
Vehicle-Treated MLE-15, 24 hours



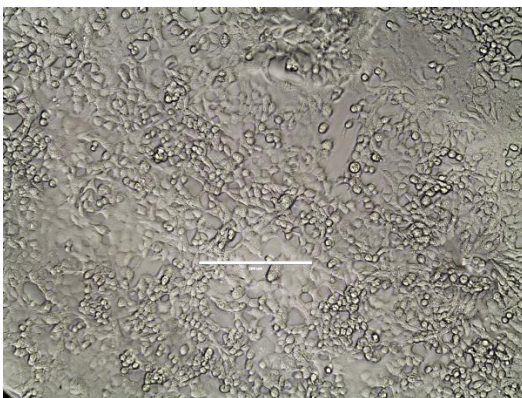
TGFβ-treated MLE-15, 24 hours



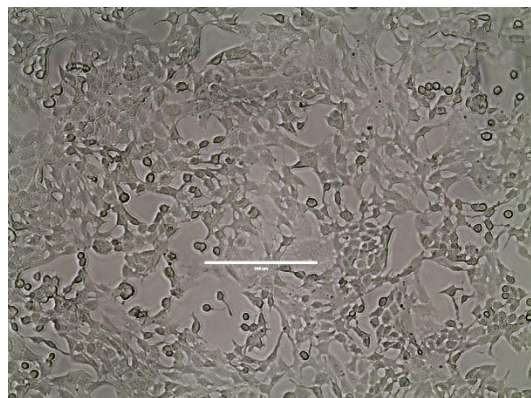
Vehicle-Treated MLE-15, 48 hours



TGFβ-treated MLE-15, 48 hours



Normal fibroblast-conditioned media-treated MLE-15, 48 hours



Myofibroblast-conditioned media-treated MLE-15, 48 hours

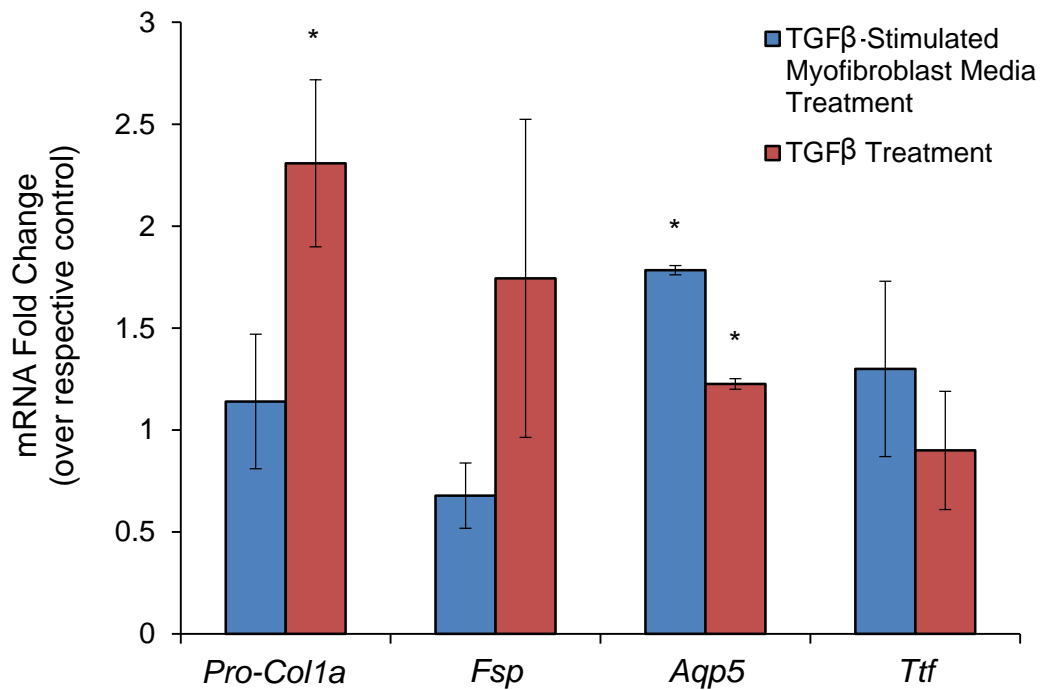


Figure 5.11: ATI and fibroblast marker gene expression is increased in MLE-15 exposed to myofibroblast-conditioned media or TGFβ. MLE-15 cultures were treated with myofibroblast-conditioned media (blue bars) or TGFβ (red bars) for 48 hours. cDNA generated from RNA lysates were analyzed for gene expression via qPCR analysis. Fold change values are based on $\Delta\Delta C_t$ calculations using RPL13 as a housekeeping gene for normalization. * indicates significant fold change ($p < 0.05$) from respective control based on analysis using Student's T-Test. Error bars represent \pm SE.

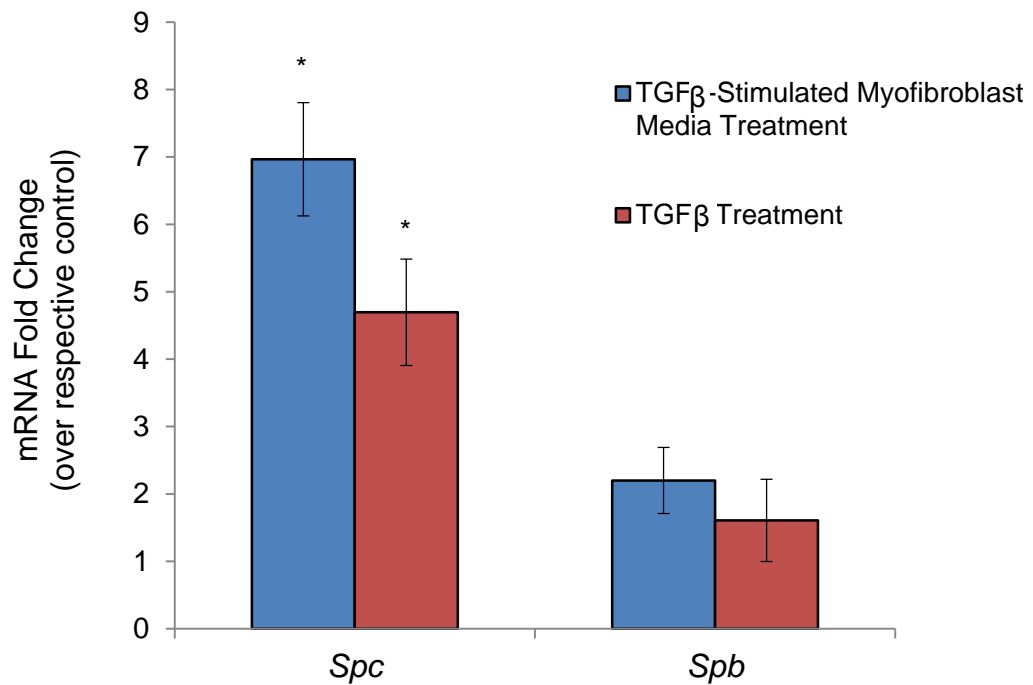


Figure 5.12: Exposure to myofibroblast-conditioned media or TGFβ increases *Spc*, but not *Spb* gene expression. MLE-15 cultures were treated with myofibroblast-conditioned media (blue bars) or TGFβ (red bars) for 48 hours. cDNA generated from RNA lysates were analyzed for gene expression via qPCR analysis. Fold change values are based on $\Delta\Delta C_t$ calculations using RPL13 as a housekeeping gene for normalization. * indicates significant fold change ($p < 0.05$) from respective control, assessed via Student's T-Test. Error bars represent \pm SE.

5.3 Discussion

The evidence presented here demonstrates that mitochondrial metabolism is impaired in ATII cells derived from IPF patient lung tissues. Oxidative metabolic function was low in IPF cells, compared to the higher OCR measurements of ATII cells from human control lung. Additionally, the remaining metabolic function was more reliant on anaerobic glycolysis than healthy lung ATII, as evidenced by an elevated PPR/OCR ratio for all IPF patient samples. IPF ATII more closely resembled the relative metabolic function of the highly glycolytic A549 in terms of OCR/PPR ratio (although both OCR and PPR individually were very low rates compared to those observed in A549 cells). Altogether, this evidence indicates that ATII cells in IPF lung adopt a glycolytic phenotype that is less metabolic overall.

The many ATP-requiring functions of ATII cells in the healthy lung result in a high energy demand that could not be served by the severely impaired metabolism of IPF ATII. Though ATP content of the cells was not measured here, without dramatic down-regulation of ATP-consuming processes, the energy demands normally placed on ATII cells could not be met by the remaining metabolic function. Many studies indicate that a large portion of surviving ATII cells in IPF undergo senescence, and the low OCR and PPR levels shown here potentially reflect this change. ATP-consuming functions that would be limited by low metabolism include surfactant production, ion pumping and fluid homeostasis, and, notably, progenitor function to repopulate both ATII and ATI cells in the alveoli. In the healthy lung, ATII cells can regenerate wounded tissue

through division and differentiation within a matter of hours (143), requiring cellular energetic investment. However, impaired wound healing and aberrant ATII progenitor function is a hallmark of IPF. Anomalous ATII cell replication and differentiation has been demonstrated repeatedly in IPF lung, including both abnormal hyperplasia as well as suppressed replication. As adequate cellular metabolism is critical for providing ATP and intermediate compounds for DNA synthesis and replication, we expect that metabolic suppression may be a factor in the inability of surviving ATII cells to participate in an appropriate wound healing process, leading to unresolved epithelial injury.

ATII from IPF lung showed high expression levels of LDH-M subunit protein and total LDH. Increased LDH-M expression has been recently noted in IPF tissue, with enhanced expression localized approximately to the region of the alveolar epithelium at fibroblastic foci (94). Other cells in the region of fibroblastic foci may also increase expression of LDH-M, particularly activated myofibroblasts as they have been shown in culture to increase both LDH-M expression and glycolysis in response to TGF β . However, the data reported here suggest that ATII cells also increase expression of LDH in IPF. The potential impacts of increased cellular LDH include enhanced lactic acid generation. Combined with decreased mitochondrial function, enhanced LDH likely results in shuttling of pyruvate preferentially into anaerobic conversion to lactate, leading to the high PPR/OCR ratio in IPF ATII cells. Reduced mitochondrial metabolism limits the ability of ATII to consume lactate, and this switch from lactate-consumer to

lactate-producer may contribute to the build-up of lactic acid and drop in lung tissue pH that occurs in IPF.

Although treatment with TGF β did not alter metabolic function in MLE-15 cells cultured in ambient oxygen, it did change LDH expression. Surprisingly, the change observed was in the opposite direction as anticipated; TGF β and myofibroblast media exposure effectively down-regulated LDH-M and total LDH expression by approximately 50%. The ratio of LDH-M to total LDH was not changed, indicating that LDH protein expression in general was effected with no specific change to LDH-M versus LDH-H expression. The healthy lung expresses primarily LDH3, composed of two subunits each of LDH-M and LDH-H. Thus, this pattern suggests down regulation of LDH expression without a shift in isoenzyme. Prior work by others has shown the opposite effect in fibroblasts, in which up-regulation of LDH-M protein was observed following treatment with similar concentrations of TGF β . The nature of the difference in response is unknown, but may represent a fundamental difference in the metabolic response of either cell type to TGF β . Indeed, TGF β has been shown to produce other opposing effects in fibroblasts versus ATII cells; for example, treatment leads to apoptosis resistance in fibroblasts, while in ATII apoptosis is induced by treatment.

Treatment of MLE-15 cells with myofibroblast-conditioned media and with active TGF β both resulted in altered cell morphology at 24 and 48 hours of exposure. Cells lost cuboidal morphology and close contact with neighboring cells in favor of a more elongated shape with outward cytoplasmic extensions

from the cell. Often, cells adopted a spindle-like shape, while a small number of cells grew larger and more spread out, reminiscent of ATI cell morphology. Altered cell morphology has been previously described in studies of TGF β effect on ATII and AEC, and have been associated with transcriptional and protein markers of EMT. This concurs with data showing enhanced MLE-15 expression of fibroblast marker *Pre-Col1a* mRNA in response to TGF β treatment, though more direct markers of EMT such as vimentin and α SMA were not assessed here. TGF β has also been implicated in ATII cell differentiation into ATI cells (85). While we observed significantly enhanced expression of the ATI cell marker Aquaporin 5, the increase was small. This likely reflects the homogeneity of the cell population following treatment; both fibroblast-like and ATI-like morphologies were found in treated cultures, with far less appearing with ATI-like characteristics.

Up-regulation of select fibroblast and ATI cell characteristics was not accompanied by down-regulation of ATII markers including *Ttf*, *Spb*, or *Spc* (in fact, analysis showed a concurrent up-regulation of ATII-cell specific *Spc*). This suggests that treated cultures adopted a transitional phenotype rather than full differentiation at 48 hours. Regardless, our findings provide some support for the conclusion that ATII cells can undergo EMT in response to TGF β ; however, the extent to which this occurs, if at all, *in vivo* is hotly debated. Proponents argue that TGF β -induced EMT by ATII Cells contributes to the large pool of fibroblasts in the lungs of IPF patients, a view supported by multiple *in vitro* observations like those reported here. However, *in vivo* labeling and immunohistochemistry studies

are conflicting regarding the co-localization of ATII and fibroblast markers. Our observations may be extended in the future using primary ATII cells, which are likely to be more sensitive to the effects of TGF β compared to the immortalized MLE-15 cell line.

Both treatments also unexpectedly induced up-regulation of *SPC* mRNA. This effect was specific, as *Spb* expression was unchanged, suggesting that up-regulation may be related to a downstream function other than enhanced production of complete surfactant. *Spc* is specifically expressed in ATII and in addition to its well-defined role in mediating lipid spreading in the biophysical function of pulmonary surfactant, mounting evidence suggests that *SPC* has innate immunological function as well (144). *Spc* is associated with suppression of inflammatory activity through multiple mechanisms including direct binding of LPS in the extracellular milieu and, in macrophages, inhibiting activation of Toll-Like Receptors (5). On the other hand, *Spc*-deficient mice experienced more severe fibrosis following bleomycin challenge, indicating a potential protective, anti-fibrotic role for *SPC* up-regulation in the human IPF lung (145). Of the genetic mutations associated with IPF, mutations in the human gene encoding *SPC* are some of the more commonly found. *SPC* mutations associated with IPF lead to protein aggregation, activation of the UPR, and ER stress leading to ATII cell apoptosis. Thus, enhanced expression of mutated *SPC* proteins would be predicted to aggravate ATII cell stress by generating more protein aggregates within the cell. This effect of TGF β exposure should be examined at the level of protein expression to determine whether enhanced *SPC* protein expression

occurs, and if enhanced SPC expression is accompanied by an increase in complete surfactant production. Future experiments will examine the effect of TGF β exposure on surfactant protein expression in primary ATII, as MLE-15 express these proteins but do not process, package, and secrete pulmonary surfactant in the same manner as primary cells.

Given the similarity in response to the two treatments, both in morphological change in the trends in mRNA expression, it is likely that the effects are due to a great degree, but not entirely, to active TGF β . In the myofibroblast-conditioned media, the presence of TGF β may be due either to the presence of remaining TGF β used originally to stimulate the fibroblasts, or to secretion of TGF β by the myofibroblasts. Regardless of the source in these experiments, TGF β is an undisputed element of the pro-fibrotic environment in IPF. Previous study has demonstrated that TGF β induces hallmarks of EMT in AEC exposed *in vitro* (146), although there is still intense debate regarding the contribution of EMT to the fibroblast population in IPF.

In summary, we demonstrate here that ATII cells isolated from IPF are metabolically suppressed, showing low oxidative metabolic function with high rates of glycolysis relative to mitochondrial function. A growing body of literature has examined various elements of the disease process that have potential to influence ATII cell metabolism, including ER stress; ROS production by fibroblasts, immune effectors, and ATII cells themselves; and even direct mitochondrial DNA damage downstream of TGF β signaling. However, these effects have not previously been linked to functional-level metabolic change in

ATII cells in patient lung tissue. The fact that ATII cells show suppressed mitochondrial metabolism holds important implications for their function in the affected lung tissue. This phenotype may contribute to the inability of ATII cells to appropriately respond to alveolar damage through replication and differentiation due to decreased ATP supply. Furthermore, impaired mitochondrial metabolism limits ATII cells' ability to import lactate and protons from the extracellular space, an observation reported elsewhere in this work concerning suppression of mitochondrial respiration in hypoxia. Therefore, reduced capacity to act as a sink for lactic acid in the lung potentially contributes to the build-up recently observed in IPF lung tissue. As the associated drop in pH is a direct driver of the disease pathogenesis through activation of TGF β in the extracellular milieu, we propose that reduced lactate consumption by ATII is an important factor in IPF progression.

CHAPTER 6. CONCLUSION AND DISCUSSION: AII CELL METABOLISM & METABOLIC CONTRIBUTION TO HYPOXIA-RELATED PULMONARY DISEASE

This body of work has investigated the metabolic phenotype of AII cells in health and hypoxia. The work presented here demonstrates that lactate is an important metabolic substrate for AII cell energy production, confirming and extending findings from landmark studies that suggested lactate consumption in pulmonary tissue. AII cells import and utilize lactate for use as substrate for mitochondrial ATP production, pointing to a critical role for AII metabolism in maintaining the normal balance of lactic acid in the pulmonary parenchyma by acting as a sink for lactate and protons. Hypoxia, and likely any insult that suppresses mitochondrial function, impairs this capability. Finally, these mechanisms are connected to the disease state of the epithelium in idiopathic pulmonary fibrosis: mitochondrial metabolism is suppressed in AII cells isolated from IPF lung tissue, and their ability to remove lactate from the extracellular space is reduced. As lactic acid build-up and tissue acidification may be causative forces in the development of the disease, the findings presented here hold significance for understanding the early events that contribute to the profibrotic environment that drives IPF progression. In summary, this work suggests

an important role for ATII cell metabolism in IPF and, potentially, other lung diseases related to pulmonary hypoxia.

6.1 ATII cell metabolic phenotype & adaptation to hypoxia

Based on the work presented here, ATII cells have a highly metabolic, oxidative cellular phenotype and depend on mitochondrial metabolism and oxygen consumption to maintain energy balance. We provide evidence that MLE-15 cells provide a useful *in vitro* model for primary ATII cell metabolism. Although MLE-15 cells appear to be less metabolic overall than primary mouse ATII cells, relative reliance on oxidative versus glycolytic function was similar between the cell types. Primary ATII cells operated closer to maximal metabolic capacity than MLE-15, and there are several reasons that this may be. First, MLE-15 cells are immortalized and have been cultured *in vitro* for many passages, while primary ATII cells were assayed within days of isolation. ATII cells serve many metabolically-demanding functions in the lung including surfactant production. While MLE-15 cells express the proteins involved in surfactant production and packaging, they do so to a lesser degree than primary ATII cells and generally produce little complete surfactant. We suspect that this leads to a lower energy demand in MLE-15, as they are not undergoing the same demanding functions as primary ATII cells. Furthermore, primary ATII cells were plated onto Matrigel and cultured with the growth factor keratinocyte growth factor (KGF), both of which are meant to maintain primary ATII cell functions.

ATII cell respiration is suppressed in hypoxia by decreased energy demand and direct suppression of mitochondrial function (indicated by the intermediate level of respiratory capacity). While ATII cells adopt a more glycolytic phenotype in response to hypoxia, it is likely due to decreased mitochondrial energy production and not to enhanced anaerobic glycolysis, as glycolytic output appeared to be similar to ambient conditions in MLE-15 and modestly decreased in ATII cells by hypoxic exposure.

Despite a lack of enhanced glycolytic output, we observed transcriptional-level adaption that seemingly would favor enhanced flux through glycolysis, as expression of several key glycolysis pathway enzymes were enhanced. The array findings reported here confirm and extend previous reports of expression change in genes involved in glucose metabolism in response to hypoxia. Several enzymes involved directly in glycolysis were up-regulated, including *Hk2* and *Gapdh*. Again, however, lactic acid generation was similar between cells cultured in ambient and oxygen and hypoxia (1.5% O₂). We propose that the observed pathway re-arrangements are part of the initial response to hypoxia, driven by HIF1 prior to its decline. Several early (<6 hours' exposure) responses to hypoxia in ATII cells have been determined including endocytosis of Na⁺/K⁺ ATPase via AMPK activity (24) and down-regulation of transporter expression, and enhanced glucose transporter expression and increased glucose influx (52). These studies show that HIF1 and non-HIF responders drive the initial response to hypoxia. HIF2 is also stabilized early and probably involved in the early response, but temporal control of HIF2 target genes has not been examined in short-term

hypoxia in ATII cells. Due to AMPK and HIF1 activity, the early response to hypoxia likely does involve enhanced glycolytic flux and lactic acid generation. Ouidir and colleagues demonstrated that ATP levels initially do decrease in AEC exposed hypoxia, and this probably drives an initial increase in glycolysis to restore ATP levels facilitated by enhanced expression of glycolytic enzymes (52). However, we demonstrate here that ATP concentrations return to levels comparable to those in ambient O₂ culture by 20 hours of exposure and that the lasting impact of hypoxia does not involve elevated glycolysis.

Glycogenic enzymes were up-regulated in response to hypoxia, and the consequence of this was confirmed at the functional level by measuring an increase in cellular glycogen content. This explains the fate of a portion of glucose consumed in hypoxia. Previous investigations have shown enhanced expression of glucose transporters and glucose uptake in hypoxic conditions. Our results indicate that enhanced glucose consumption serves the process of glycogen storage, and possibly other pathways of glucose metabolism not addressed here, rather than enhanced anaerobic lactate production. Glycogen production and storage is an important step in ATII maturation in the developing lung, and both storage and utilization of glycogen by ATII in the fetal lung have been associated with HIF2 signaling (41).

The maintenance of ATII spare respiratory capacity is an important component of the cell-specific response to hypoxia. MLE-15 cells maintained a mitochondrial reserve capacity slightly lower than cells in ambient culture in terms of percentage above basal, and reserve capacity was similar in primary

ATII under both conditions. Addition of the prolyl-hydroxylase inhibitor DMOG to MLE-15 elicited a similar response. Thus, in hypoxia and HIF stabilization under ambient O₂ conditions, ATII cells retain mitochondrial capacity above basal function. The concept of reserve capacity was originally elucidated in neuronal studies, in which it was shown that neuronal maintenance of mitochondrial reserve capacity is determinant in the ability of cells to respond to increased ATP demand without succumbing to stress. The importance of mitochondrial spare capacity in cells' ability to handle stress has been implicated in neurological disorders like Huntington's Disease in which electron transport chain dysfunction limits mitochondrial capacity (124), and has also been recently demonstrated to play a role in photoreceptor cell death induced by oxidative stress. Photoreceptor cells treated with reagents to induce cell stress lost reserve capacity prior to any indication of cell death, and the proportional reduction of reserve capacity correlated with the eventual degree of cell death observed (147). This highlights the importance of reserve capacity in response to cellular stressors, and maintenance of mitochondrial reserve may very well contribute to the remarkable tolerance of ATII cells under hypoxic environments.

The maintenance of some spare mitochondrial reserve by ATII cells exposed to hypoxia or DMOG is a very different response from that observed in cardiomyocytes, in which DMOG treatment completely abolished reserve capacity. While treatment resulted in suppressed basal oxygen consumption in both cell types, ATII maintained spare respiratory capacity while cardiomyocyte reserve was completely abolished (111). Maintenance of respiratory capacity in

particular may influence thus ATII cell resistance to stress in these conditions and result in exceptional resistance to hypoxia. However, the factors through which reserve capacity is maintained in ATII where it is lost in other cell types have not yet been determined.

Experimental knock-down of HIF1 expression in cardiomyocytes exposed to DMOG restored spare capacity, indicating a key role for HIF1 in “clamping” respiration at basal levels. MLE-15 cells likewise lose expression of HIF1 following 8 hour exposure, and maintain reserve in the absence of HIF1 at 20 hours. In this manner, loss of HIF1 in DMOG-treated cardiomyocytes recapitulated our observations of 20-hour DMOG treatment in MLE-15. This provides indirect support for the concept that the natural down-regulation of HIF1 by ATII in long-term hypoxia results in a unique adaptive response driven by HIF2. HIF2 drives expression of anti-oxidant enzymes, which may help prevent ROS build-up associated with mitochondrial function under hypoxic conditions, therefore supporting basal and spare mitochondrial function by preventing oxidative stress.

Because mitochondrial metabolism could not be stimulated to the levels of respiration observed in ambient O₂ culture, there is direct suppression partially limiting mitochondrial metabolism. This may reflect a change in mitochondrial population dynamics. Reduced citrate synthase has been observed in A549 cells (used as model ATII cells in that study) exposed to 24 hour hypoxia, suggesting reduced mitochondrial mass (23). This could conceivably result in the proportional suppression of basal respiration and reserve capacity. Further

analyses of mitochondrial population dynamics have not been performed in hypoxia-exposed ATII cells, and this represents a rich avenue for further study, initially through quantifying mitochondrial number and size, mtDNA content, and respiratory enzyme content; and secondarily through investigation of drivers of mitochondrial biogenesis (ie, PGC1 α -mediated transcription) and autophagy. Substrate limitation for mitochondrial respiration could also contribute to suppression of basal and reserve respiration. Array results detected up-regulation of PDK, which reduces pyruvate entry into the TCA cycle via phosphorylation of pyruvate dehydrogenase. This would serve to limit mitochondrial substrate availability and promote pyruvate metabolism to lactic acid by LDH. Substrate limitation due to enhanced PDK may be a mechanism through which mitochondrial function is reduced in hypoxia. Future pharmacological interference with PDK function under physiologic normoxia and hypoxia will help to elucidate the role that PDK plays in control of ATII mitochondrial metabolism under oxygen limitation.

The avoidance of enhanced lactic acid generation, maintenance of spare respiratory capacity, and overall robust resistance to hypoxic damage observed in ATII cells here and in previous works may be an effect of mounting a HIF2-mediated response and limiting HIF1, which as discussed leads to enhanced glycolysis and loss of spare respiratory capacity in other cell types. HIF2 expression is localized to a limited number of isolated cell populations in the body. In the lung, only ATII and vascular endothelial cells express this HIF isoform, while fibroblasts, macrophage, ATI cells, and cells composing non-

alveolar tissue do not. HIF2 regulates an overlapping but distinct set of genes related to control of cellular metabolism that seems to be associated with a storage-and-maintenance phenotype, involving glycogen storage and reduced lipid consumption in combination with enhanced antioxidant enzyme activity. Investigation of the consequences of HIF2 on the long-term response of ATII cells to hypoxia presents an interesting venture for future work. Efforts to knock-down HIF2 expression in MLE-15 utilizing RNA interference techniques are currently underway, with plans to assess metabolic function via similar flux assays to those reported here. As HIF2 has been implicated in helping to mediate the decrease in HIF1 over longer periods of hypoxia, we predict that HIF2 knock-down cells will maintain HIF1 over time in contrast to the pattern of expression in wild-type ATII cells. Flux assays using these cells will permit examination HIF2 α 's in reducing mitochondrial respiration without glycolytic compensation, as well as the potential role in maintaining cellular metabolic reserve.

Caveats & other considerations

True normoxia for the lung (and therefore, for ATII cells) is not ambient O₂ (21%). Rather, normal O₂ levels in the healthy mature lung are estimated in the range of 5-15% (depending on altitude, physical fitness, and the point of expiration/inspiration cycle, among other factors). Consequentially, in this work and in essentially all studies of hypoxia reported in the literature to date, control conditions do not accurately reflect the exposure of cells *in vivo*. Rather, 21% O₂

represents a mildly hyperoxic condition for ATII cells. Therefore, it is with some caution that we report here the “normal” phenotype of ATII cells, as well as the magnitude of change in response to hypoxic exposure. It is possible that ATII cell metabolism is different under physiologic normoxic conditions for the tissue, although this value is well above the estimated threshold at which mitochondrial metabolism is limited by O₂ availability. Although HIF stabilization is maximal at <1% O₂, stabilization does occur to some degree over the range of 1-21% in a graduated manner inversely proportional to oxygen concentration. Thus, exposure to normoxic conditions that truly mimic the *in vivo* oxygen exposure may lead to a different pattern of HIF stabilization and transcriptional control compared to ambient oxygen exposure. Subtle differences in HIF could conceivably influence metabolism, and may more robustly promote ATII cell-specific functions that occur in the healthy mammalian lung compared to the subtly hyperoxic ambient levels. Indeed, though metabolic flux has not yet been compared between ambient and normoxic oxygen exposures, preliminary experiments from our lab indicate that culture in 13% O₂ results in enhanced surfactant protein expression in MLE-15 cells, which in standard 21% O₂ culture produce surfactant at lower levels than primary cells. Alternatively, low-level HIF stabilization and other factors like the balance of stabilized isoforms and the negative regulation between HIF1 and HIF2 (and potentially HIF3) may prevent HIF-mediated effects on metabolism in the normoxic range of 8-15% O₂. This will be an extremely important avenue for investigation concerning fundamental ATII cellular biology. Experiments comparing metabolic flux of ATII cells across

graded oxygen concentrations are underway using primary ATII cells and MLE-15.

It is important to consider that other sources of extracellular proton production exist aside from glycolytic lactic acid generation. A major contributor to media acidification in culture is evolution of CO₂ due to respiration. Thus, even if a cell was solely reliant on mitochondrial respiration (i.e., under experimentally inhibited glycolysis), some degree of extracellular acidification could still be observed. Additionally, other acids may be released into the cytosol, contributing to PPR. Given our unexpected findings regarding the lack of PPR change in response to hypoxia exposure or PHI, we specifically measured lactate in the culture media of MLE-15 cells following culture in hypoxia versus ambient oxygen to determine whether the PPR observed in flux measurements in fact be attributed to lactic acid generation. Not only was no difference found in lactate production by MLE-15 cells under the different culture conditions, but also measured rates of lactate production over time that, when converted to comparable units, almost exactly matched the PPR data from flux experiments given that one proton is extruded per molecule of lactate. Using the 2-hour time point from lactate measurements, the rate of lactate generation is approximately 27 pmol H⁺/min/μg protein. This correlates extraordinarily well with the extracellular flux PPR values that ranged from approximately 22-32 pmol H⁺/min/μg protein, and provides strong support for conclusions based on PPR data indicating that lactic acid generation is the primary contributor to extracellular acidification by MLE-15 cells. Similar lactate measurements were

not performed using primary ATII cells, and we recognize that it is possible that primary ATII cells, particularly given their higher observed rate of respiration, may have other factors in addition to lactic acid generation contributing to PPR.

The fundamental studies reported here rely on mouse primary cells and the MLE-15 cell line. As with many studies that utilize mouse as a model organism, there remains uncertainty as to the suitability of mouse as a model for human cellular metabolism. The lungs in particular represent a critical point of species-specific differences between mouse and human, in that the respiratory rates of the organisms are vastly different. In addition, lung development in mice and humans progresses very differently, with human alveolarization occurring prior to birth in the relatively low-oxygen conditions of the in utero environment, while considerable development in mice occurs after birth. Thus, it is conceivable that the normal, basal rates differ between the species, as well as their response to hypoxia. The similarity of basal OCR rates in the single population of ATII cells from the normal human patient to those observed for MLE-15 cells is encouraging. However, this does indicate that OCR levels in the human primary ATII were lower than the mouse primary cells. Comparison of the PPR/OCR ratio provides an indication of relative reliance on glycolytic versus oxidative metabolic pathways. In terms of PPR/OCR ratio, the normal human ATII culture showed a ratio of approximately 1, indicating robust reliance on oxidative metabolism. In mouse primary cells, this ratio was approximately 2, indicating slightly more glycolytic production. As the human value reported here is based on a single culture, it is difficult to draw conclusions based on this data alone. Differences in

instrumentation may also contribute to this difference; analysis of mouse was performed using the XF24 instrument, while human samples were assayed using the XF96 platform. Anecdotally a slight increase was observed for OCR readings in MLE-15 cells assayed on the XF96 compared to the XF24, the effect of which would be a lower PPR/OCR ratio. Side-by-side comparison of mouse and human primary cells will resolve this issue for future study; however other species may better model the human lung and cellular metabolism. Pig lung more closely represents human in structure and developmental timing, and as a large mammalian species their respiratory rate is closer to that of humans. Numerous assessments of body metabolic rate in mammalian species have shown that basal body metabolic rate is a function of body size, supporting the use of larger mammals for modeling human metabolism (148). It is expected that planned extracellular flux analysis of A₁II isolated from cryopreserved pig lung tissue samples will closely mimic measurements in normal human A₁II, specifically supporting the use of pig for modeling fundamental human lung cell metabolism.

The observation that treatment with the PHI compound DMOG elicits similar results to hypoxia in terms of metabolic flux (and other measured parameters) suggests that HIF transcriptional control drives the observed effects of 20-hour hypoxia exposure. PHI has been previously shown by our lab to stabilize HIFs in MLE-15 cells in a similar manner to hypoxia: HIF1 and HIF2 are both stabilized early following PHI, whereas beyond 8 hours HIF1 expression declines while HIF2 remains stable. Using culture conditions similar to these earlier studies, we observed similar metabolic effects to hypoxia. However, as

HIF protein was not measured or manipulated directly, this work is limited in its ability to draw conclusions regarding the role of HIFs in general, as DMOG and other mechanisms of PHI can have off-target (non-HIF) effects. Also, despite similar culture conditions, without measuring HIFs directly we cannot conclusively say that the pattern of stabilization was identical to the prior studies. Furthermore, while previous work from this lab and others has identified HIF2 as the major isoform present in ATII cells in chronic (20 hour) hypoxia, it is not possible from the experiments performed here to determine how HIF1 versus HIF2 mediates the metabolic effects of long-term hypoxia in ATII cells.

To tease apart the contributions of HIF1 versus HIF2, it will be necessary to directly manipulate expression of either isoform in ATII cells. Work has been performed in hepatocytes, with the same goal of isolating the effects of HIF2 on hypoxia-induced lipid storage, using mice genetically engineered for knockdown of VHL/HIF1 or VHL/HIF2 (VHL knockdown leads to HIF stabilization regardless of oxygen exposure). Using a similar scheme, either by RNA interference in ATII cells or ATII cell isolation from lungs of knockdown mice, ATII cells expressing only HIF1 or HIF2 can be compared to wild-type. We hypothesize that ATII cells devoid of HIF2 and expressing only HIF1 would have a robust up-regulation of glycolytic acid generation in response to hypoxia (or DMOG) and loss of mitochondrial reserve, contrary to our observations in wild-type ATII but similar to the effects of hypoxia in other cell types that do not express HIF2. They may also demonstrate higher levels of apoptosis and cell death, as HIF2 mediates expression of SOD and other antioxidant enzymes that prevent mitochondrial

and cell damage. The different roles of HIF1 and HIF2 (and even HIF3) have recently come under investigation in lung development, during which the different isoforms appear to play different roles in development of lung structure and the surfactant system. Building on our findings to date concerning the metabolic response of ATII cells to hypoxia by identifying distinct roles of HIF isoforms will greatly inform these developmental studies.

6.2 Lactate shuttling in the alveolar epithelium

Lactate import and oxidization for use as fuel for mitochondrial electron transport require active mitochondria and rapid respiration, high NAD⁺/NADH ratios (which goes hand-in-hand with rapid electron transport), and a gradient of lactate favoring transport into the cell. Based on observations presented herein regarding the ATII metabolic phenotype and combined with previous observations of whole lung metabolism, lactate consumption by ATII cells was investigated in detail. The findings presented here provide support for the concept of an intercellular lactate shuttle in the lung, analogous to lactate shuttling that is known to occur between neighboring glycolytic and oxidative cell types in the brain and skeletal muscle.

By definition, cell-cell lactate shuttles require a cellular lactate source and lactate sink. This work has provided evidence that ATII cells serve as a lactate sink in the lung, utilizing extracellular lactate to fuel their own mitochondrial metabolism. Brooks et al have provided conclusive evidence that lactate is removed from blood across pulmonary circulation, indicating that blood flow

through alveolar capillary beds provides a likely source of lactate for ATII metabolism. Adjacent cells in the alveolar tissues may also provide a nearby source of lactate that directly feeds ATII. Metabolic flux has not specifically been measured in pulmonary fibroblasts using *in vitro* extracellular flux analysis for comparison. Flux measurements performed using human dermal fibroblasts indicate that they are less oxidative than mouse ATII cells, however whether this difference is truly due to cell-specific differences cannot be concluded, as species-specific differences in cellular metabolism may exist. Other measurements using isolated pulmonary fibroblasts showed that they generate extracellular lactate, and that stimulated pulmonary fibroblasts produce higher levels (94). ATI cells, which occupy the vast majority of the alveolar epithelial surface, contain mitochondria based on microscopic assessment but have long been considered to serve a relatively passive role in the lung, specifically as the primary site of gas exchange. Their metabolic phenotype is also unknown, but as terminally differentiated cells with limited ATP-demanding function, individual cells are most likely not very metabolic compared to individual ATII cells. On the other hand, given their expansive surface area, they may contribute significantly to local lactate production. Therefore, it remains to be seen whether neighboring ATI cells, fibroblasts, or other pulmonary cells provide lactate for ATII cell consumption. Flux analysis for comparison to ATII measurements and, eventually, cell type co-culture will be necessary to further define how local metabolic cooperation between cell types influences lung tissue homeostasis.

A critical role for MCT-mediated transport in ATII cell metabolism has been identified in these studies. MCT function mediates both export of lactic acid produced by anaerobic glycolysis and the import of lactate for conversion to pyruvate and subsequent use in mitochondrial reactions. MCT1, the isoform previously associated with import of lactate into oxidative cells of heart and skeletal muscle, is specifically expressed by ATII cells and is likely responsible for a significant amount of lactate uptake into pulmonary tissue. MCT1 expression is not affected by hypoxia in ATII at the level of mRNA or protein, a pattern which is similar to the gene's expression in muscle but is unlike the hypoxia-inducible expression observed in adipocytes. However, MCT expression does appear to be regulated by exposure to extracellular lactate, as culture in media formulated with lactate leads to increased concentration of MCT1 mRNA. The ability of lactate to stimulate MCT1 expression has previously been observed by Brooks and colleagues in other cells that oxidize lactate, and lead them to coin the term "lactormone" to describe the ability of lactate to regulate transcriptional responses. The manner in which lactate mediates these changes has not been investigated directly, but the observation that lactate can generate ROS suggests a mechanism through which cell responses may be initiated by lactate ultimately leading to expression changes (27).

Based on this work, we propose that ATII cells consume lactate from the pulmonary circulation and/or from the extracellular space produced by neighboring cells to fuel their own mitochondrial ATP production (Figure 6.1A). Under normal physiological conditions, lactate produced by neighboring glycolytic

cells (and/or delivered via pulmonary circulation) is removed from the extracellular space by ATII cells. Lactate is imported via MCT1 transport proteins, which favor monocarboxylate influx. Lactate is then converted to pyruvate through the activity of LDH. Reverse activity of LDH reduces NAD⁺ to NADH and oxidizes lactate to generate pyruvate. Pyruvate is rapidly used by ATII cell mitochondria to generate reducing equivalents via TCA cycle reactions, which in turn fuels electron transfer and oxidative ATP production. In this manner lactate build-up in the pulmonary tissue is avoided, with lactate instead being used to fuel ATP generation in ATII cell with high mitochondrial function and ATP demand.

Based on our findings, lactate serves as a metabolic substrate for mitochondrial metabolism. Surfactant production requires intermediates of mitochondrial metabolism to generate acetyl-CoA molecules for de novo lipid synthesis. Landmark studies that originally investigated the utilization of lactate by the lung found that, when provided in perfusate using the isolate perfused rate lung model, labeled lactate was rapidly incorporated into lung lipids. Furthermore, when lactate and glucose were provided simultaneously, lactate was preferentially incorporated into acetyl subunits of lung lipids, while glucose was incorporated primarily as glycerol moieties. This pattern provides support for lactate use in mitochondrial metabolism, but importantly demonstrates a specific role for lactate metabolism in surfactant production.

In accordance with findings presented here and those from previous studies using labeled lactate, we propose that mitochondrial lactate metabolism

by healthy ATII cells is an important component of normal surfactant production. Both lactate and glucose are consistently available to ATII cells *in vivo*; estimates from tissue samples have estimated total lactate at approximately 2 mM in healthy lung. In the local cellular milieu of ATII cells, this may be even higher due to glycolytic function of neighboring cells. Furthermore, the lung experiences comparatively low oxygen *in utero*, but high local lactate concentrations. Given elevated availability *in utero*, we expect that lactate serves as a critical substrate for energy and surfactant lipid production during late lung development.

It is notoriously difficult to maintain production and secretion of surfactant by ATII cells *in vitro*. In light of results reported here, this may be an effect of the substrate that is normally provided in culture; in general, primary ATII cells are cultured in high-glucose media (>11 mM) that is changed regularly. Extremely high levels of glucose and low levels of lactate potentially disrupts the normal surfactant production pathways by limiting lactate metabolism. Based on studies by Rhoades, Wolfe, and others that followed the fate of carbons from labeled lactate and showed incorporation into the acetyl moiety of lung lipids, lactate may be important in generating the lipid component of surfactant. As a transcriptional regulator or “lactormone” it could also play a role in controlling expression of the surfactant proteins as well. Studies are currently underway in this laboratory to assess the effect of lactate supplementation to culture media on surfactant protein gene expression in model and primary ATII cells, based on the hypothesis that lactate availability will enhance expression. The concept that lactate is both a substrate for ATII cell metabolism and a potential transcriptional

regulator holds significance for both surfactant homeostasis in the mature lung and regulation of alveolar development and surfactant production in the developing lung.

Caveats & other considerations

This work has shown that ATII cells can utilize lactate to fuel mitochondrial metabolism, and the finding that lactate, when provided simultaneously with glucose, alters glycolytic metabolism in a dose-dependent manner suggests that lactate is used simultaneously with glucose to fuel respiration. It is clear from these findings that the availability of lactate alters glucose metabolism, but despite previous evidence from whole-lung study that strongly supports use of lactate in place of some glucose for respiration, further study is necessary to definitively conclude that ATII cells consume lactate in the presence of glucose. To quantitatively assess the extent to which lactate is utilized when glucose is also present, it will be necessary to measure uptake of substrates using LC/MS to quantitate glucose and lactate removal from culture media over time.

Also unknown is the fate of lactate in the cell aside from TCA cycle metabolism to fuel electron transport. Previous work has indicated that lactate oxidized by lung tissue is readily incorporated into lung lipids. This suggests that a large portion of lactate consumed by ATII cells may be diverted from the TCA cycle and instead incorporated, as acetyl subunits, into surfactant lipid. Furthermore, when lactate and glucose are provided simultaneously, the acetyl moiety of lung lipids is almost entirely derived from lactate. Thus it is of interest to

determine the fate of lactate consumed by ATII, particularly to examine its incorporation into surfactant lipid. Nuclear Magnetic Resonance (NMR)-based metabolomic studies of culture media formulated with ¹⁴C-labeled substrates would be one approach to address these questions.

Intercellular lactate shuttles depend on the presence of both lactate producers and lactate consumers. While the early studies of lung lactate consumption measured utilization of lactate taken up from pulmonary circulation, these investigations, by nature of the whole-lung model, could not assess lactate shuttling between pulmonary cell types. Accordingly, further development of the concept of ATII cells as lactate scavengers in the lung will require a thorough understanding of metabolic function of other, neighboring pulmonary cell types, including fibroblasts and ATI cells. ATI cell metabolism has not been measured. Comparison of OCR values from ATII cells in this work to measurements from human dermal fibroblasts performed by others suggest that fibroblasts are less oxidative, although differences in species-specific cell metabolism may be a contributing factor. Future characterization of ATI and fibroblast metabolic function using XF technology for accurate comparison to our findings will greatly inform the concept of lactate shuttling in the lung, and of coordinated metabolism in lung tissue as a whole.

MCT1 protein expression was measured in MLE-15 lysates compared to mouse skeletal muscle as control. When protein isolated from skeletal muscle was probed with anti-MCT1 antibody, the resulting blot appeared to have two bands of very similar size in the appropriate size range for the MCT1 protein.

However, this second band was not apparent in lysates from MLE-15 cells. The nature of this discrepancy is unknown, and maybe an effect of alternative post-translational modifications, as there are multiple phosphorylation and ubiquitination sites in the MCT1 protein. Additionally, while MCT1 and MCT2 tend to be expressed in highly oxidative cell types in mouse and human, species differences have been noted regarding which isoform (MCT1 or MCT2) is more abundantly expressed. Here, only MCT1 expression was assessed. MCT2 protein has been found in whole lung protein lysates, and may be expressed alongside MCT1 in AII cells, contributing to the import of lactate.

CHC inhibits all MCT isoforms at the cytosolic membrane. Therefore, while the changes in metabolic flux following CHC addition demonstrate the importance of MCT to AII cell metabolism in general, this work does not differentiate between the different isoforms in terms of contribution to lactate output and/or input. An MCT1-specific inhibitor has been recently developed, and could be used to examine flux in response to MCT1 inhibition specifically. We expect that this form of inhibition would decrease respiration utilizing lactate, as this would inhibit the isoform strongly associated with lactate import. However, if other isoforms are also expressed by AII cells, they may compensate for loss of MCT1 function, as all MCTs transport lactate bi-directionally to some degree.

The intracellular location of lactate oxidation to pyruvate remains unknown. While LDH is predominantly located in the cytosol, it has also been found in peroxisomes and, more recently, in the mitochondria of rapidly respiring cells. There is ample evidence from studies of lactate shuttling in muscle and

brain tissue to support the existence of a “mitochondrial lactate oxidation complex” composed of LDH, MCT, cytochrome oxidase, and supporting structural proteins at the inner mitochondrial membrane. In this proposed scenario, lactate is imported into the mitochondria prior to oxidization, after which the oxidizing environment created by cytochrome c oxidase activity promotes conversion to pyruvate. Our work on AII cells cannot differentiate between cytosolic, peroxisomal, and mitochondrial lactate oxidization, and this remains an interesting question for future work. Assessing the presence and interaction (via co-immunoprecipitation) of LDH and MCT proteins in purified mitochondrial subcellular fractions will determine whether this complex exists in AII cells as in oxidative muscle and brain cell types. Additionally, measuring oxygen consumption of AII cell mitochondria purified and exposed to lactate as sole metabolic substrate will demonstrate the ability of mitochondria to utilize lactate directly. If there is measurable OCR linked to ATP production in mitochondria in the presence of lactate alone, this would provide strong support for a mitochondrial mechanism of lactate consumption.

6.3 AII metabolism in IPF lung

As discussed, many of the initial forms of injury to the epithelium that are under investigation have potential to alter mitochondrial function in epithelial cells, often acting ultimately through ROS production. However, prior to this work, metabolism of AII cells from IPF lung had not been directly assessed to determine the functional-level consequences. Only recently was metabolic

function of IPF fibroblasts explored to determine the consequences of myofibroblast activation. Based on our findings reported here, IPF ATII cell oxidative metabolism is suppressed compared to control cells isolated from normal control patient lung tissue, while glycolytic metabolism is relatively maintained or enhanced in the disease-conditioned ATII. Strikingly, IPF-derived ATII maintain reserve capacities, similar to those observed in the MLE-15 healthy ATII model cells. Though the nature of mitochondrial suppression is not determined in these studies, given their robust spare respiratory capacity it is unlikely that suppression of oxidative metabolism is the result of widespread direct damage to respiratory chain components.

Our comparison of IPF ATII to ATII from control lung bears resemblance to the metabolic effects of hypoxia on healthy ATII cells in many respects. Suppression of oxidative metabolism and maintained mitochondrial reserve capacity are important metabolic consequences of hypoxia detailed elsewhere in this work. IPF ATII cells showed maintained or elevated glycolytic function compared to control lung ATII, resulting in a shift to enhanced reliance on glycolysis. The impact of IPF on the PPR/OCR ratio was greater than the impact of hypoxia, indicating a more dramatic shift into glycolysis. This was also accompanied by enhanced expression of LDH, a well-established HIF1 target gene. Thus, HIF stabilization may play a role in mediating the metabolic changes observed here. However, it is important to note based on the work of others (94) that other pulmonary diseases associated with pulmonary hypoxia, such as COPD, do not appear to be affected by the same metabolic perturbations leading

to lactic acid build-up and tissue acidification that is observed in IPF. Thus, these consequences of the disease are potentially unique to IPF and not strictly related to development of pulmonary hypoxia.

Based on these findings, reduced ATII mitochondrial metabolism potentially contributes to lactic acid build-up in the IPF lung primarily by loss of their ability to act as a sink for lactate and protons. Sustained or enhanced glycolytic output may also contribute directly to increased lactic acid production in lung tissue. As demonstrated by Kottmann and colleagues, IPF myofibroblasts generate lactic acid at higher rates than normal fibroblasts (94). Conversely, based on our studies, IPF ATII cells have suppressed metabolic function. Both oxidative and glycolytic functions were low in IPF ATII, generating a relatively more glycolytic but overall less metabolic phenotype. As shown by the response of cells cultured in lactate to hypoxia, decreased mitochondrial function limits lactate removal from the extracellular space. Thus, while IPF ATII are not necessarily producing more acid than healthy ATII, they are removing less because the demand for substrate is reduced (Figure 6.1B). In this manner, complimentary metabolic dysfunction in fibroblasts and ATII cells leads to lactic acid build-up that contributes to pH-mediated TGF β activation, driving continued fibrosis and injury (Figure 6.1C).

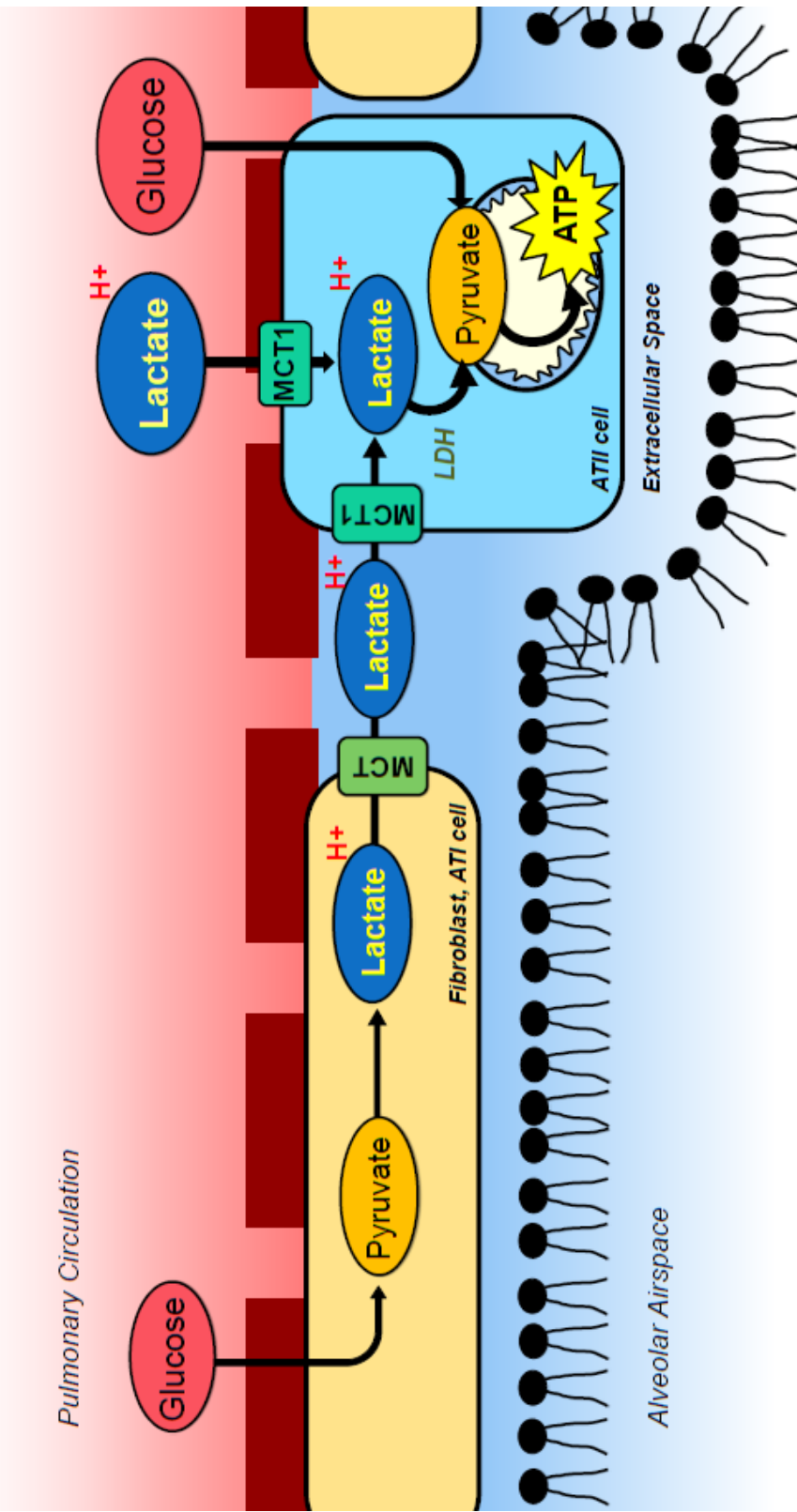
This work supports the concept that healthy ATII cells can potentially import and utilize, or “scavenge” excess lactate generated by activated fibroblasts; indeed, this cell-cell metabolic cooperation may be an element of normal wound repair in the alveolar epithelium, wherein controlled fibroblast

activation and myofibroblast differentiation occurs, while ATII proliferation and differentiation enhances energetic demand. However, metabolically-suppressed ATII are likely overwhelmed by the lactic acid generated by neighboring myofibroblasts, leading to acidification. This concept sets the stage for future co-culture studies to assess metabolism of healthy and IPF tissue-derived ATII and fibroblasts.

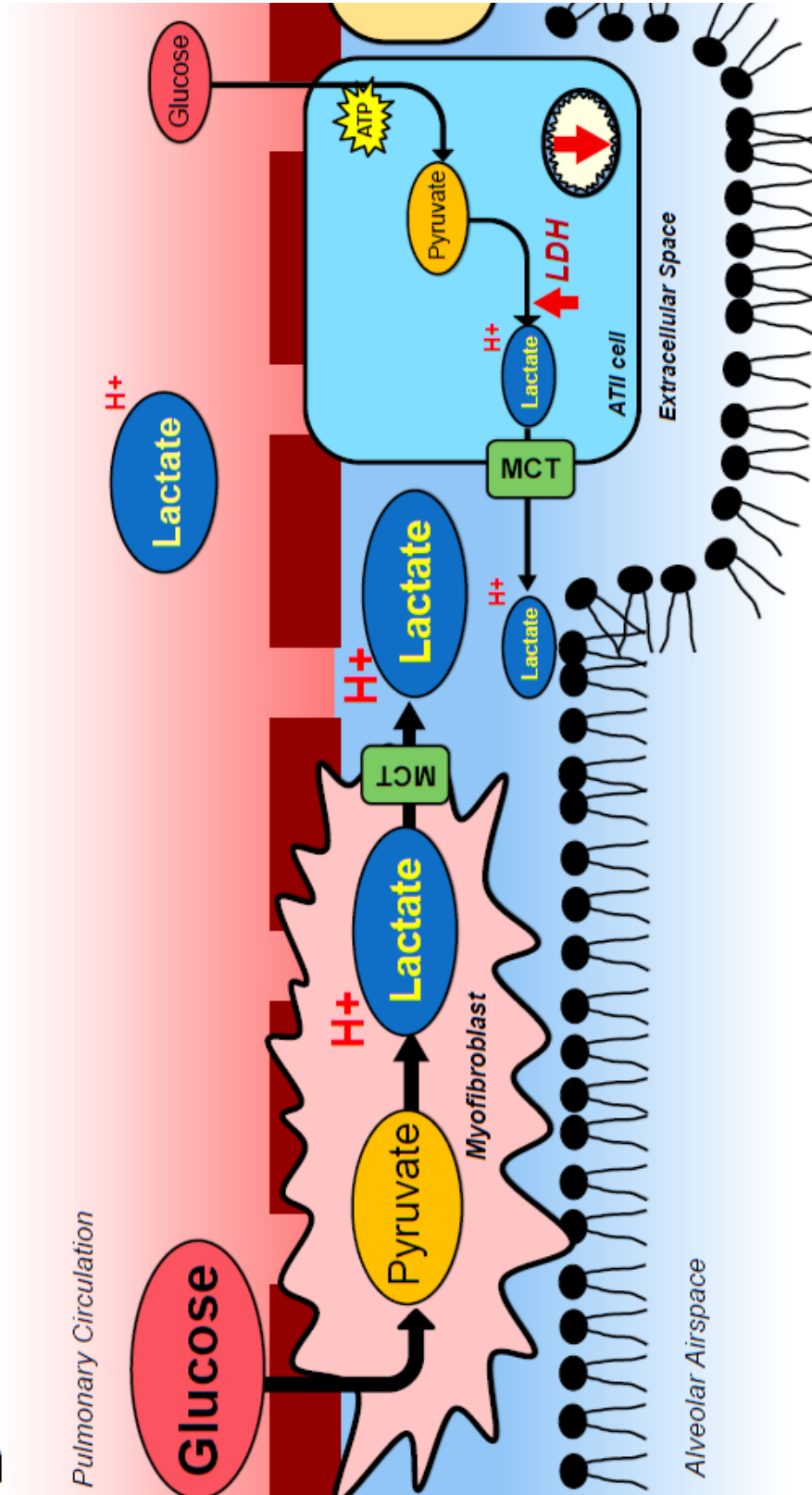
Signals from activated myofibroblasts may play a role in generating the suppressed phenotype of ATII cells. We did not observe a metabolic response in MLE-15 exposed to myofibroblast-conditioned media, but this may be in part due to the immortalized nature of the MLE-15 cell line. Furthermore, one of the primary mechanisms proposed through which myofibroblast activity negatively affects ATII cells at the molecular level is via ROS, which due to antioxidants in media and instability may be depleted in the conditioned media added to MLE-15. This further supports utilizing a co-culture system to examine metabolic cooperation and dysfunction between fibroblasts and ATII cells from healthy and IPF lung.

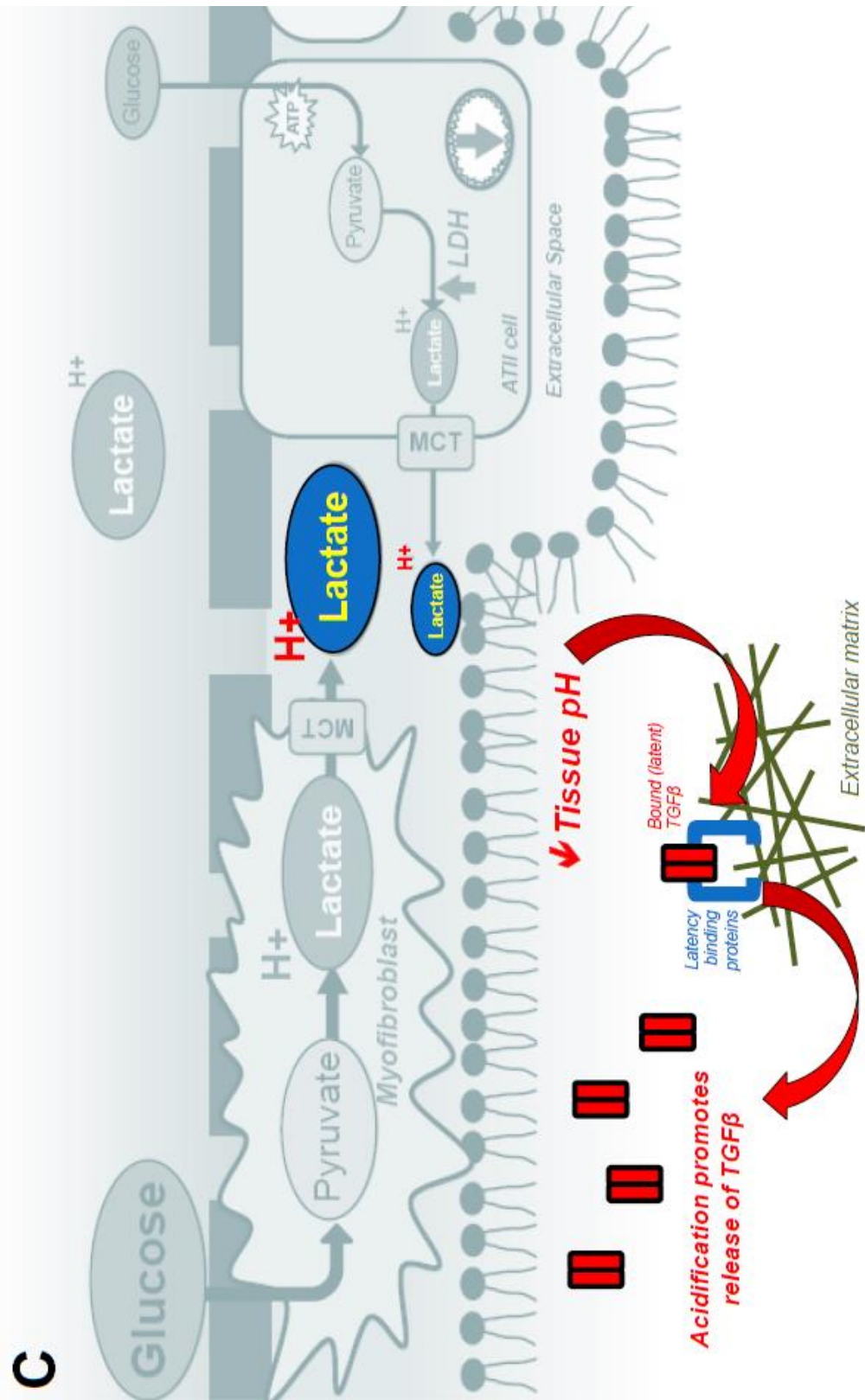
Figure 6.1: Hypothetical model of cellular metabolism in the alveoli in healthy and IPF lung tissue. (A) In healthy lung, lactate produced by neighboring glycolytic cells and/or delivered via pulmonary circulation is removed from the extracellular space by AII cells. Lactate is imported via MCT1 transport proteins, which favor lactate influx more heavily than other isoforms. Lactate is then converted to pyruvate through the activity of LDH. Reverse activity of LDH oxidizes lactate to generate pyruvate, which is rapidly used by AII mitochondria to generate reducing equivalents via TCA cycle reactions, which in turn fuels electron transfer and oxidative ATP production. In this manner lactate build-up in the pulmonary tissue is avoided, with lactate instead being used to fuel ATP generation in AII cell with high mitochondrial function and ATP demand. (B) In disease conditions associated with IPF, mitochondrial respiration is reduced in response to damage through processes including hypoxia-related signaling, ER and oxidative stress, or direct mitochondrial damage. This results in a shift toward a suppressed metabolism in AII cells that is more glycolytic and less capable of consuming lactate from the extracellular space. At the same time, myofibroblasts contribute to acid production in the alveolar epithelium, as demonstrated by Kottmann and colleagues. (C) Lowered pH due to lactic acid build-up leads to cleavage and release of TGF β from latency binding proteins in the extracellular matrix. Active TGF β in the extracellular milieu binds to receptors on the surface of pulmonary fibroblasts. Receptor binding leads to conversion of fibroblasts into myofibroblasts, the cells responsible for over-expression of extracellular matrix components and aberrant matrix deposition characteristic of IPF, as well as direct impacts on AII.

A



B





Caveats & other considerations

An important consideration in the critical assessment of this work is the small number of patient samples assessed. ATII isolated from three IPF patients were measured, and the OCR, PPR, and reserve capacities varied considerably between patients. Furthermore, only a single non-IPF lung tissue sample was used as normal control. The variation of ATII cellular metabolism between human subjects is unknown and, going forward, it will be critical to establish with confidence a normal metabolic phenotype for human ATII cells. In lieu of control samples from normal lung which are often difficult to obtain, ATII isolated from pig may potentially serve as a good control for healthy lung. Pig more closely resembles human in terms of lung structure, breathing rate, and overall metabolic rate compared to mouse, and study in the immediate future will characterize ATII derived from healthy pig lung for comparison to our single human control sample.

It is also important to note that the control sample used was taken from a deceased patient. While the cause of death was related to seizures and not lung disease, it is possible that the ATII isolated from this sample were permanently affected by the period of ischemia between time of death and tissue preservation, and in that case may not faithfully represent the function of healthy ATII in a living individual. This highlights the complications of obtaining control samples of normal tissue from human patients, perhaps one of the biggest barriers to patient-based lung disease research, and provides further support for finding a truly suitable model. Future study will determine if pig ATII can serve this purpose.

Because fibroblast-ATII cell communication and TGF β signaling are thought to be primary drivers of continued ATII cell injury and dysfunction in IPF, we anticipated that treatment with myofibroblast-conditioned media and/or TGF β would cause normal MLE-15 cells to adopt the metabolic phenotype observed in the IPF patient cells, characterized by decreased OCR, sustained or enhanced PPR, and a resulting increase in PPR/OCR ratio. However, no change in metabolic function was observed following either treatment. Instead, MLE-15 enhanced expression of fibroblast and ATI cell markers, suggesting partial differentiation over the 48 hour exposure, without impact to metabolism. It is possible that this effect is mediated by the immortalized nature of the MLE-15 cell line, which may result in a markedly different response to the treatments from the response of a primary ATII cell. This may also be an effect of exposure time; IPF develops over many years, while cultures in this study were exposed for a total of 48 hours. The gene expression changes and other effects of exposure may long precede any measureable metabolic changes. Additionally, the changes in metabolism observed in human IPF patient ATII may be mediated by other cells in the IPF lung. While the current paradigm in IPF research is focused on fibroblast-ATII cell interaction, immune cells and secreted factors have also been shown to play a role and specifically affect ATII cells. Finally, it is also possible that the source of ATII metabolic dysfunction is related to the original, as yet unknown, insult that damages the ATII cells and either directly initiates the disease or leaves the affected ATII cells susceptible to a subsequent stressor (or “second hit”). As discussed, many of the sources of injury proposed in IPF such

as smoking and ER stress have potential to influence ATII cell metabolism. The treatments performed here were intended to mimic elements of downstream signaling associated with later events in the disease process, without including the initial injurious stimulus.

Specific induction of *Spc* gene expression by TGF β and conditioned media treatments is a novel observation. The specific effects on *Spc* without a concurrent effect on *Spb* suggests that production of complete surfactant is not enhanced (although altered composition could also account for this observation). SPC protein is involved in immune function, specifically in suppressing macrophage activation by inhibiting TLR-mediated signaling. Additionally, human *SPC* mutations are associated with IPF. Our results indicate that TGF β or other secreted factors enhance *Spc* expression in mouse ATII model cells, which, if recapitulated in patient IPF ATII cells, holds considerable implications for a role in IPF. Enhanced SPC protein expression in response to fibroblast-generated stimuli may be a normal response intended to reduce inflammatory responses by tempering macrophage activation in the lung. Furthermore, enhanced expression of SPC in response may contribute to IPF in the case of *SPC* mutations: while normal levels of mutant SPC protein may be managed by the cell, enhanced expression could result in rapid protein build-up and aggregation leading to aggravated ER stress and ROS generation. It will be important to assess surfactant protein expression in response to these treatments in primary cells and IPF-derived ATII to better understand the significance of these findings.

Differences were observed between conditioned media treatment and TGF β treatment in terms of the degree of gene expression changes in MLE-15 cells, indicating that TGF β accounts for some, but not all, of the effects. Stimulated fibroblasts may themselves produce TGF β as well as a variety of other extracellular factors including other cytokines and ROS. Fibroblast-generated extracellular factors directly influence ATII cells and potentially mediate the effects on ATII transcription observed here. The role of other factors in conditioned media, aside from TGF β , in mediating the effects on transcription can be investigated by inhibiting TGF β receptors, activin receptor-like kinase (ALK). We anticipate that ALK inhibition would abolish the effects of TGF β treatment, but that conditioned media would still induce transcriptional effects (though potentially to a lesser degree than without ALK inhibition).

6.4 Targeting lactic acid production in treatment of IPF

Because lactic acid production contributes directly to the pro-fibrotic environment that converts and stimulates myofibroblasts, methods to limit lactic acid production have made an interesting target for therapy to prevent and/or resolve IPF. Genetic interference with LDHA expression in fibroblasts leads to decreased LDH activity and lactic acid generation, decreased TGF β signaling through downstream Smads, and dramatically decreased expression of α SMA and other markers of myofibroblast phenotype. Based on these observations, inhibition of lactic acid generation makes an appealing pharmacological target, and initial *in vitro* studies have indicated promise in the use of a naturally-derived

LDH inhibitor, Gossypol, to inhibit conversion of fibroblasts to myofibroblasts. While treatment of fibroblasts with TGF β alone stimulates rapid, robust differentiation to the myofibroblast phenotype, co-treatment with TGF β and the LDH inhibitor Gossypol limited expression of myofibroblast markers, Smad signaling downstream of TGF β , compared to cultures treated with TGF β alone (149). *In vivo* experiments using the bleomycin-induced fibrosis mouse model of IPF have also indicated the potential of Gossypol as a therapeutic treatment, as treatment of bleomycin-challenged mice with Gossypol via subcutaneous injection concurrently and for three weeks after bleomyin administration limited hydroxyproline content of lung tissue, a measure of lung collagen content indicative of the degree of fibrosis (150).

MCT presents a potential therapeutic target for reducing lactate overproduction in IPF. In MLE-15, pharmacological inhibition of MCT decreased lactic acid output and uptake, indicating an important role for MCTs in facilitating cellular metabolism. Limiting export of lactate may lead to metabolic impairment of glycolytic cells dependent on anaerobic metabolism. Accordingly, MCT is gaining attention as a target in the treatment of cancer (151). CHC inhibition of MCT has been evaluated as a therapy for treating gliomas, highly aggressive tumors of the central nervous system. *In vitro* findings showed that CHC treatment resulted in cell death in a highly glycolytic glioblastoma cell line, while treatment induced limited growth in a more oxidative line but did not affect cell viability (152). Low concentrations of CHC limited glucose uptake and acid generation by the highly glycolytic glioblastoma cells without impacting metabolic

function in more oxidative cells. In mice with glioblastoma, 40 mM CHC delivered to the brain via osmotic pump resulted in tumor necrosis with a portion of subjects achieving complete remission (153).

In IPF, lactic acid concentrates in the lung tissue. Although the cell type responsible for generating increased lactic is still under investigation, in vitro studies show that TGF β -stimulated myofibroblasts produce elevated lactic acid compared to normal fibroblasts (94). It is unlikely that enhanced lactic acid is due to output by ATII, as ATII cells isolated from IPF lung assessed in this work had low metabolic function in general and did not produce more lactic acid than those from healthy lung. Therefore, given their already low metabolic function, ATII cells in IPF lung may not be significantly affected by MCT inhibition. On the other hand, myofibroblasts rapidly generate lactic acid. MCT function has not yet been studied in fibroblasts, but whole lung tissue robustly expresses the MCT1, 2, and 4 isoforms, and given their widespread expression throughout the body, it is highly likely that fibroblasts and myofibroblasts depend on MCTs for lactate export. Relatively low doses of CHC may be sufficient to limit metabolism and lactic acid output by myofibroblasts, and thus prevent pH-mediated TGF β activation without altering metabolism of other, less glycolytic cells in the lung, including ATII.

In studies of CHC applied via infusion cannula to treat glioblastoma brain tumors in mice, treatment with relatively high doses did not lead to adverse neurological outcomes in control animals without tumors, and only slightly altered metabolite profiles of tissue near the site of application (153). The general lack of

metabolic impairment in normal brain cells surrounding glycolytic glioma is pertinent to the use of CHC in lung because, like ATII cells, neurons import and utilize as substrate lactate that is exported from nearby cells. Given the observation that high-dose CHC does not appreciably affect the neuron-astrocyte intercellular lactate shuttle or other off-target metabolic function in brain tissue suggests that it may be safely tested in the lung. Further investigation of the importance of lactate for normal ATII metabolism, as well as *in vitro* assessment of CHC treatment on normal fibroblasts and stimulated myofibroblasts will be necessary before CHC treatment is considered in mouse models of IPF. However, successful inhibition of fibrosis in the bleomycin mouse model with treatment of LDH-inhibitor Gossypol shows that preventing lactic acid build-up through metabolic manipulation is a feasible treatment strategy. Thus, MCT inhibition represents a potential target for reducing fibrosis by limiting lactic acid build-up, and general safety and efficacy have been demonstrated in previous mouse studies in other tissues.

Limiting lactic acid build-up represents a therapeutic possibility for limiting TGF β signaling in IPF lung by preventing its activation due to pH change. Other mechanisms to directly inhibit TGF β signaling are currently under heavy investigation in IPF treatment research, including administration of antibodies directed against TGF β to block receptor binding, and thus prevent the profibrotic, injurious downstream effects. Whereas these strategies are primarily intended to limit the effects of the cytokine once it has been activated, prevention of lactic acid build-up represents a different, complimentary strategy to limit

pathological TGF β activation. Strategies to regulate lactic acid metabolism such as LDH or MCT inhibition may provide an additional level to therapy directed at controlling TGF β -mediated damage when applied in combination with antibody-based treatment to scavenge active TGF β or pharmacological inhibition of downstream pathways. Moving forward, our work encourages evaluation of metabolic manipulation as a viable option for combination therapy in the treatment of IPF.

6.5 Beyond IPF: A role for lactic acid in bronchopulmonary dysplasia

Bronchopulmonary dysplasia (BPD) is a lung disease associated with preterm birth and one of the most common chronic lung diseases in children with 5,000-10,000 cases occurring in the US each year. The disease is characterized by poor alveolarization of the lung, including abnormally large alveoli and reduced number of alveoli. Clinically, there is distinction between what is referred to as “classic” versus “new” BPD. The original form of BPD that resulted from oxygen toxicity, high pressure and volume associated with mechanical ventilation was characterized by epithelial cell metaplasia, bronchial fibrosis, and vascular smooth muscle hypertrophy (154). With the use of steroids and administration of pulmonary surfactant, the “new” form of the disease is characterized primarily by impaired alveolarization. The molecular mechanisms are largely unknown, but recent hypotheses have focused on the role of oxygen toxicity.

Exposure of the premature lung to high levels of oxygen received during therapy certainly has potential to influence pulmonary cellular metabolism.

Hyperoxia has been shown repeatedly to stimulate ATII cell death via necrosis and/or apoptosis (155), in which mitochondrial production of ROS plays a critical role. More subtle changes have also been demonstrated in hyperoxia-exposed alveolar epithelial cells including mitochondrial swelling and ultrastructural changes, and alterations in LDH activity (156). At the molecular level, hyperoxia induces changes in expression and activity of metabolic enzymes including those associated with glycolytic flux (157). Aconitase, an enzyme involved in the TCA cycle and necessary for mitochondrial metabolism, has been shown in vitro and through in vivo studies of adult rat lung to be a molecular target of hyperoxia-induced damage (158, 159). In a primate model of BPD, lung aconitase activity negative correlated with inspired oxygen tension and exposure to 100% oxygen resulted in near-complete inhibition of enzyme activity (160). These findings show that mitochondrial dysfunction occurs in the pulmonary tissue as an effect of hyperoxia, and strongly suggest that metabolic changes contribute to or even underlie the impact of hyperoxia on the developing lung in BPD. Indeed, a more recent study of hyperoxia exposure in neonatal mice demonstrated impaired respiration, ATP production, and mitochondrial complex I activity in exposed mice; likewise, exposure of neonatal mice to a complex I inhibitor via subcutaneous injection recapitulated the effects of hyperoxia on pulmonary development (161). Importantly, this work indicated a critical role for mitochondrial respiration in normal lung development, and implicated mitochondrial dysfunction as a driver of BPD.

While the progressive, extensive fibrosis that characterizes IPF does not occur in BPD, relatively recent developments in BDP research have identified critical similarities to fibrotic lung disease (162), including the observation that TGF β signaling is a central driver of both diseases. In IPF, TGF beta is the critical growth factor that initiates conversion of fibroblasts into the myofibroblast phenotype and stimulates overproduction of extracellular matrix components, leading to the fibrotic scarring that characterizes the disease. TGF β signaling is required for normal development and injury repair (163); however, advances have recently demonstrated that increased levels of TGF β interferes with alveolarization during lung development, a characteristic of BPD. Overexpression of active TGF β in newborn mice and rats during the alveolarization period that, unlike humans, continues after birth, results in alveolar hypoplasia that closely resembles the pattern of disrupted development in BPD (164, 165). High therapeutic oxygen treatment is a common determinant of BPD in preterm infants, and hyperoxic exposure in neonatal rats and mice is a common model used in BPD studies. Hyperoxia is also thought to alter normal TGF β signaling in the exposed developing lung. Treatment of neonatal rats with hyperoxia enhances Smad3 and Smad7 phosphorylation downstream of TGF β signaling and increases α SMA and calponin expression (166), all of which are effects observed in IPF lung as a result of TGF β activation. Similarly, in neonatal mice treated with hyperoxia, specific TGF β receptors were up-regulated, Smad phosphorylation downstream of TGF β signaling was enhanced, and expression of TGF β -responsive genes were increased (167). Enhanced TGF β signaling

correlated with decreased BMP pathway signaling, the balance of which is critical for normal lung branching morphogenesis (168).

In humans, a study of preterm infants found that levels of active TGF β were elevated in endotracheal aspirates from very low birth weight premature infants, the patient category at most high risk for developing BPD (169). Collectively, these findings provide evidence that dysregulated TGF β signaling during the period of alveogenesis is involved in BPD pathogenesis, but the factors that enhance TGF β signaling in cases of BPD are unknown.

The work presented in this dissertation demonstrates that healthy, highly oxidative ATII cells consume lactate from the extracellular space for use in mitochondrial ATP generation. Prior studies demonstrated that lactate was rapidly oxidized by the prenatal lung and ATII cells derived from prenatal lung at rates of oxidation over 20-times those of glucose (108) Together, this points to lactate as a preferred metabolic substrate in the fetal lung and suggests that lactate is constantly imported into ATII cells during development to supply energy for expansion, differentiation, and alveogenesis. Investigation of MCTs in fetal lung showed MCT1 localization specifically in premature ATII cells, further supporting the idea that lactate provides an important substrate during development. The data presented here also demonstrate that pharmacological inhibition of mitochondrial ATP production (via FCCP or oligomycin A) in ATII cells leads to compensatory increase in glycolysis and extracellular acidification. In BPD, hyperoxia-mediated mitochondrial suppression may stimulate a similar

shift to enhanced lactic acid generation in an effort to compensate for loss of oxidative ATP generation from damaged mitochondria.

In this scenario, in a manner that mirrors acid-mediated activation in IPF to some degree, lactic acid build-up in BPD lung tissue may lead to enhanced TGF β activation and downstream signaling that interrupts normal alveolar development. Lactic acid concentration has not been assessed in BPD lung tissue or BALF, and metabolism has not been specifically measured in BPD lung cells or tissue as it has for IPF lung here and in other studies. Based on this new body of knowledge regarding the role of the balance of lactate consumption and production by ATII cells in health and disease, lactic acid overproduction represents both a potential contributor to pathogenesis and a novel target for therapy in prevention of BPD.

6.6 Final Comments

Over a century before the conception of the studies presented in this dissertation, pioneers in pulmonary physiology Bohr and Henriques made the following insightful observation regarding the function and metabolism of the lung as an organ:

...the lung is not only the place of excretion of carbonic acid...and the absorption of oxygen. This organ is also at the same time, to a variable degree, the place of the reverse phenomenon; that is to say, a process in which oxygen is consumed and carbonic acid formed. From: Datta and Stubbs, p.85 (11)

- C. Bohr & V. Henriques

The work presented herein has contributed to this early understanding by elucidating the functions of oxidative and glycolytic metabolism at the cellular level under conditions of health, hypoxia, and the disease IPF. Despite a flurry of investigation in the 1970s and 1980s that shed some light on the complex metabolic functions of the lung as a whole organ, limitations in the ability to assess metabolism at the cellular and molecular level of the lung hindered further understanding. Now, the studies presented here add dimension to our comprehension of metabolism in the critical ATII cells, as well as insight into how metabolic cooperation between pulmonary cell types may maintain metabolic homeostasis in the distal lung. Importantly, this report urges that lactate must be considered as more than simply a metabolic waste product in the lung; it is a

pertinent substrate for fueling ATP production, and potentially a signaling molecule to influence cell function at the level of transcription.

This work also represents a fundamental step in IPF research, performing the first metabolic analyses of cells isolated from human IPF patient lung tissue. As understanding of the pathobiology of IPF steadily grows, the realization that current models are, in many ways, insufficient grows as well, emphasizing the need to assess molecular pathology using patient tissue directly.

The models created from this body of work provide a foundation for exciting future studies. Cellular metabolism plays a role in IPF, and although the contribution of individual cell metabolism is just beginning to be elucidated, the work presented here indicates that future study focused on the metabolic cooperation of multiple pulmonary cell types in progression of IPF (and potentially other hypoxia-related pulmonary diseases) will be a major step, both in understanding the disease pathobiology and in developing therapies by targeting the metabolic contributions to lung dysfunction.

MATERIALS AND METHODS

Cell Isolation & Culture

The ATII model cell line mouse lung epithelial-15 (170) was provided as a generous gift from Dr. Jeffrey Whitsett (Children's Hospital Medical Center, Cincinnati, OH). MLE-15 is a line of cells derived from mouse pulmonary tumors. Cells were immortalized via the simian virus large tumor antigen under control of the surfactant protein-C promoter from the human SPC gene. This cell line recapitulates many of the defining characteristics of primary ATII cells including morphological features and expression of surfactant protein (49). MLE-15 stock cultures were maintained in a humidified incubator under ambient air (21% O₂) and 5% CO₂ at 37°C. Stock and experimental cultures were grown in HITES medium (RPMI 1640 with 10 µg/ml insulin, 10 µg/ml transferrin, 30 nM sodium selenite, 10 nM hydrocortisone, 10 nM β-estradiol) supplemented with 2mM Glutamax and 2% fetal bovine serum (Atlanta Biologicals, Flowery Branch, GA). All media and supplements were obtained from Invitrogen (Carlsbad, CA, USA) unless otherwise indicated.

Primary mouse ATII cells were isolated from a female C57B/6 mouse, approximately 6 weeks old. Animal was anaesthetized via intraperitoneal injection of tribromoethanol solution (125 mg/Kg; 15 µL of 2.5% Avertin per gram of body weight) and exsanguinated. Lungs were then perfused via injection of 10 mL of saline solution into the right atrium. The trachea was cannulated and lung filled with 3 mLs of dispase (Thermo Fisher Scientific, Waltham, MA) followed by

0.5 mL low melt agarose. Ice was applied directly to the chest cavity to solidify agarose, after which the lungs were removed. Lung tissue was incubated with dispase and DNase 1 (Sigma) and the resulting cell suspensions treated with red blood cell lysing buffer (Sigma) and filtered (100 to 40 to 20 μ m gauze). Remaining cells were collected via centrifugation, resuspended, and incubated on plates pre-coated with Donkey serum (BD Biosciences, San Jose, CA). ATII cells were panned from plates and cultured in small airway epithelial cell (SAEC) media (Lonza, Walkersville, MD) supplemented with 5% fetal bovine serum. ATII cell population purity was assessed by modified PAP stain to count cells positive for lamellar bodies and *SPB* gene expression was confirmed via qPCR.

Human IPF ATII cells were isolated from cryopreserved IPF lung tissue taken from lungs donated from IPF patients receiving transplants at the Medical University of South Carolina (Charleston, SC). Normal control ATII cells were isolated from the lungs of a 34 year-old male patient, deceased due to seizure. All human patient ATII cells used in these studies were isolated from cryopreserved tissue samples. The cryopreservation procedures and validation of tissue structural maintenance and cell viability has been reported elsewhere (171). Briefly, portions of diseased distal lung weighing approximately 0.5 grams were vacuum-expanded several times in cryopreservation medium to fully perfuse tissue. Perfused tissues were immediately frozen in liquid nitrogen and transferred to -80 degree Celsius for storage. To obtain viable cells from tissue, frozen vials of tissue were thawed in a 37 degree Celsius water bath, then minced into small portions using sterile forceps and scalpel. Tissue was then

transferred immediately into a dissociation solution composed of 1X dispase, 3 Units/mL elastase, 300 U/mL collagenase, 0.3 mg/mL DNase, 10 mM HEPES buffer, and antibiotic-antimycotic; placed into a 37 degree Celsius incubator; and allowed to incubate with gentle rocking for approximately 1 hour. After incubation, the suspension was combined with an equal volume of serum-free DMEM medium supplemented with 40 mM HEPES buffer at pH 7.4 and transferred to a petri dish. Remaining intact tissue portions were teased apart using sterile curved forceps, and the dish transferred back into the incubator for 15 minutes. The resulting suspension was then filtered through a pre-wetted 70 um cell strainer and serum added to the filtrate to 10%. Suspension was centrifuged for 10 minutes at 200x g to pellet cells.

ATII cells were isolated from pelleted human pulmonary cells using the MACS magnetic bead cell purification system (Myltenyi Bioscience, San Diego CA) according to manufacturer's protocols. Briefly, cells were labeled using primary antibodies against cell population-specific markers, attached to magnetic beads such that anti-bound cells are retained when passed over the magnetic bead sorting column. Three different sortings were performed as follows: first, cells were incubated with magnetic bead-bound antibody against Annexin V to remove apoptotic cells. The elution was discarded, and flow-thru from the first sort was incubated with magnetic bead-bound antibodies against CD35 to label endothelial cells, CD14 & CD45 to label immune cells, and an "Anti-Fibroblast" cell-specific antibody. Flow-thru from this sort contained target ATII cells. The final sort positively selected for ATII cells using magnetic-bead bound antibody

against CD326 (EpCAM), an ATII cell surface marker. Elution from the positive sort was plated directly into extracellular flux assay plates. A portion of the elution suspension was pelleted via centrifugation, resuspended in PBS, transferred to a glass microscope slide, and allowed to dry overnight for modified Papanicolaou staining to visualize lamellar bodies. Primary cells were plated and cultured in SAEC media supplemented with 5% FBS.

***In vitro* Exposures**

For hypoxia experiments, cells were plated at indicated densities and allowed to attach in an ambient O₂ (21% O₂) incubator for 1-2 hours. Cultures were then placed into a Bactron I Anaerobic Environmental Chamber (Sheldon Manufacturing, Cornelius, OR) with a humidified atmosphere of 1.5% O₂/5.0% CO₂ in N₂. Exposures were generally performed for 20 hours, with ambient control cultures kept in a humidified incubator under ambient O₂ (21% O₂) and 5% CO₂. For PHI experiments, 250 μM dimethyloxalyl glycine (DMOG) dissolved in DMSO was added directly to culture media.

For metabolic substrate experiments, cells were plated in normal HITES (11.1 mM glucose) media at indicated densities and allowed to attach. Media was then removed, plates were rinsed gently, and HITES media was replaced with the appropriate media formulation.

For TGFβ exposure, TGFβ reagent was provided as a generous gift from Dr. Ryan Kendall (Medical University of South Carolina, Charleston, SC). TGFβ in 4 mM hydrochloric acid plus 0.1% bovine serum albumin was added directly to

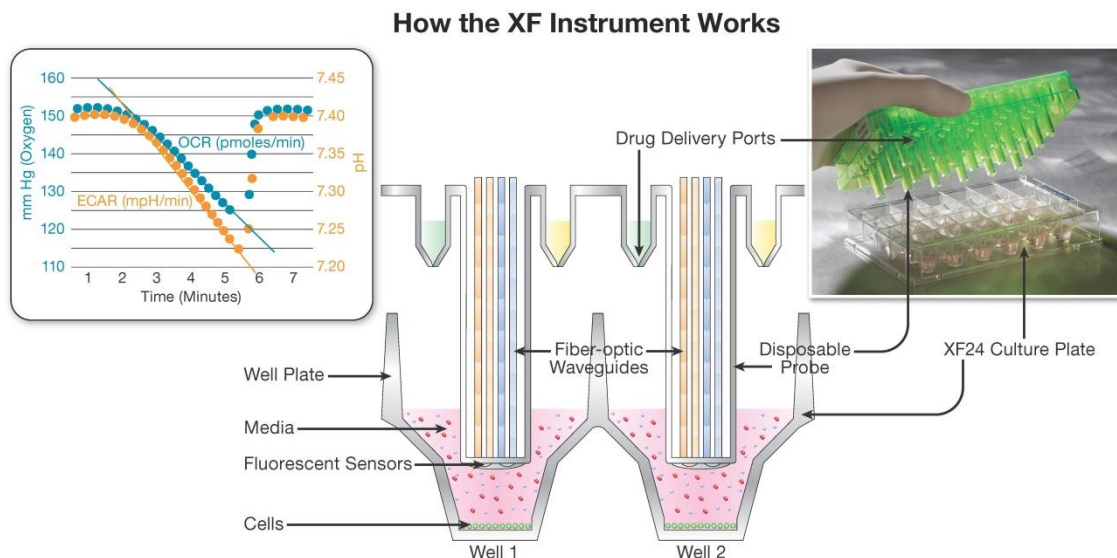
culture medium after plating to a final concentration of 5 ng/mL. Control cultures received an equal volume of vehicle only. For conditioned media exposures, cells were plated originally in HITES media formulated with 7.5 mM glucose. After attachment in an ambient oxygen incubator (1-2 hours), a volume of fibroblast-conditioned media equal to the volume of HITES used for plating was added to culture wells, resulting in a growth media composed of 1:1 HITES (7.5 mM glucose) and fibroblast-conditioned media. Conditioned media was a generous gift from Dr. Stanley Hoffman (Medical University of South Carolina, Charleston SC). Fibroblasts were cultured in HITES media formulated with 5.5mM glucose and exposed to either 10ng/mL TGF β in 4mM hydrochloric acid plus 0.1% bovine serum albumin or an equal volume of vehicle added directly to media. TGF β -stimulated fibroblasts adopted a myofibroblast phenotype, confirmed by the Hoffman lab via western blot for alpha-Smooth Muscle Actin and Collagen Type 1a in cell lysates. Original media was harvested after 72 hours in culture, centrifuged to remove cells, and frozen at -80 degrees Celsius prior to use.

Metabolic Flux Analysis

Metabolic XF analysis allows real-time measurement of oxygen consumption and acid generation by cells in culture. Changes in extracellular pH and oxygen concentration are measured over time in a small isolated volume of media, providing measurements of oxidative and glycolytic metabolic function *in vitro* (Methods & Materials Figure 1). In many of the experiments performed in this body of work, assessment of cellular O₂ consumption and acid generation of

near-confluent monolayer cells were assessed using a Seahorse Bioscience XF24 or XF96 instrument (Seahorse Bioscience, N. Billerica, MA). This technology also allows compounds to be injected directly into cell culture wells during flux assay, allowing real-time assessment of metabolic responses. Optimization of cell densities and inhibitor concentrations were performed prior to performing the experiments reported herein (see *Appendix A*). When plating cells for extracellular flux assays, the cell densities indicated in Table 3 were used to achieve approximately 90% confluence without cell piling or detachment.

Growth medium was removed prior to assay and replaced with unbuffered minimal assay medium (Seahorse Bioscience, Billerica, MD) at pH 7.4, supplemented with 11.1 mM glucose or indicated concentrations of glucose and/or lactate (as sodium lactate), 2 mM Glutamax, 10 µg/mL insulin, 10 µg/mL transferrin, and 40 nM sodium selenite. For experiments involving primary cells, assay media was formulated with 5.5 mM glucose and 5% FBS. Plates were incubated for 45 minutes to 1 hour in assay media prior to assay.



Methods & Materials Figure 1: Extracellular flux analysis using Seahorse Bioscience XF technology. Individual pH and oxygen probes are lowered into each well of a 24- or 96-well plate containing cells in monolayer culture, trapping a small volume of media above the cells. Change in media pH and oxygen are measured over multiple short measurement periods, providing multiple measurements representative of glycolytic and oxidative cell function. Injection ports allow compounds in solution to be injected during assay, thus providing real-time information on cellular metabolic responses. *Image courtesy of Seahorse Bioscience Image Gallery (Seahorse Bioscience, North Billerica, MA).*

Table 3: Mouse cell plating densities used for extracellular flux assays. The following cell densities were used to achieve approximately 90% confluent cell monolayers. Due to limited cell number following isolation procedures, human primary ATII cells were plated into 4 to 6 assay wells at maximal possible densities given yield for each individual experiment.

Instrument	Cell Type	Culture Period	Plating Density
XF24	MLE-15	20-24 hours	65,000
	Primary Mouse ATII	3-5 days	Approximately 50,000
XF96	MLE-15	20-24 hours	16,000
	MLE-15	48 hours	8,000

For basal oxygen-consumption rate (OCR) and proton production rate (PPR) determination, O₂ concentrations and pH were simultaneously measured during four 3-minute periods, each followed by a 2-minute mixing period. For measurements of mitochondrial reserve capacity and ATP coupling parameters, FCCP (carbonyl cyanide-p-trifluoromethoxy-phenylhydrazone) and Oligomycin A (Seahorse Bioscience, Billerica, MD) diluted in assay media were injected into separate wells to final concentrations of 0.5 μM and 1.5 μM, respectively. Injections are performed to measure the response to inhibitors in real-time after basal measurements in the absence of inhibitors have been made. Spare respiratory capacity and glycolytic capacities were calculated as the increase over basal OCR and PPR readings following FCCP injection. Coupling to ATP production was calculated as the decrease from basal OCR values following oligomycin A injection.

For experiments involving MCT inhibition, the pan-MCT inhibitor CHC (as stock dissolved in DMSO) was diluted in an aliquot of assay media at pH 7.4 and injected into assay wells following basal measurements to a final concentration of 10 mM CHC. Control wells received an equal volume of DMSO in assay media. For experiments involving inhibition of LDH, the competitive inhibitor oxamate (as sodium oxamate) was dissolved in assay media to a final concentration of 20 mM oxamate and brought to pH 7.4. Exposure was conducted concurrently with media change, prior to assay. Control cultures received normal assay media without oxamate. Cultures were incubated in assay media with or without oxamate for 1 hour prior to assay.

Raw OCR data was transformed via the “Level (Direct) AKOS” algorithm (172) using the Seahorse XF24 1.5.0.69 software package. The “Variable Technique” within the software was used to calculate PPR from measured rates of extracellular pH change with compensation for media buffering capacity measured for each media formulation.

ATP, Lactate & Glycogen Assays

ATP content of cultured cells was measured using the CellTitre Glo Luminescent cell viability assay (Promega, Madison, WI) as per manufacturer’s instructions. Cells (grown in parallel to metabolic flux assay cultures) were plated onto 96-well plates at a density of 5×10^3 cells/well and cultured for 20 hours in normoxia, hypoxia, or media containing 250 μ M DMOG.

Extracellular lactate production was measured using a probe-based assay (Lactate Colorimetric/Fluorimetric Assay Kit, BioVision, Milpitas, CA) according to manufacturer’s instructions. Cells were plated onto 6-well plates at densities of 5×10^5 cells/well and maintained in normoxic or hypoxic conditions for 20 hours. Cells were then rinsed twice with PBS, media replaced with modified HITES medium containing 0.5% fetal bovine serum, and culture plates returned to normoxic or hypoxic conditions. Culture media was sampled at time points 0, 15, 30, 60, and 120 minutes after media was replaced. Media samples were analyzed via colorimetric assay and cell lysates via fluorimetric assay. Total protein of cell lysates was determined via BCA assay for normalization.

Intracellular glycogen content was determined using a fluorimetric probe-based assay (Glycogen Assay Kit, BioVision, Milpitas, CA) as per manufacturer's instructions. MLE-15 cells were plated onto 6-well plates at densities of 2.5×10^5 cells/well. Ambient oxygen control cultures were maintained at 21% O₂ for 3 days. Hypoxia and DMOG treated cultures were allowed to incubate in ambient oxygen conditions for 20 hours, after which media was replaced and the cultures moved into treatment conditions (hypoxic chamber or media containing a final concentration of 250 μ M DMOG, respectively) for 48 h, after which the media was replaced and the cultures moved into ambient oxygen conditions for 20 hours. Glycogen values were corrected for sample glucose content and normalized to total cellular protein concentration. Analysis of significance between ambient control and treatment groups was performed via ANOVA with p values less than 0.05 being considered significant.

qPCR & Arrays

MLE-15 were seeded on 6-well culture plates at 1.5×10^5 cells/well. After 20 hours of exposure to experimental conditions, lysates from sample wells were pooled for each condition for RNA extraction using the RNeasy Mini Kit (QIAGEN Inc, Valencia, CA), followed by DNaseI digestion. cDNA synthesis was performed using 2 μ g total RNA, a mixture of random 9-mer and oligo-dT priming, and M-MuLV reverse transcriptase (reagents from New England Biolabs, Ipswich, MA). qPCR was performed on a Mastercycler RealPlex2 (Eppendorf, Hamburg, Germany) using iQ SYBR Green Supermix (BioRad, Hercules, CA). Ct values for

all genes of interest were normalized to a housekeeping gene for normalization. For TGF β and conditioned media treatment experiments, the Ribosomal Protein L13 (*RPL13*) was used for normalization; for hypoxia experiments, B-actin was used. Fold-change values for target genes between groups were calculated using $\Delta\Delta C_t$ analysis to determine expression-fold difference. Significance of differential expression was assessed via Student's T-Test of the replicate $2^{-\Delta C_t}$ values for each gene, with p values less than 0.05 considered significant. All oligonucleotide primers used in qPCR were synthesized by Integrated DNA Technologies (Coralville, IA) and are listed in Table 4.

Glucose Metabolism qPCR arrays for mouse (PAMM-006Z, SABiosciences, Valencia, CA) were performed according to manufacturer's instructions using 1 μ g total cDNA per array plate. Arrays were performed in triplicate using cDNA created from three individual cultures of MLE-15 for each condition. Ct values for all genes of interest were normalized to β -actin and hypoxanthine-ribosyl transferase (*HPRT*) averaged relative expression. Fold-change values for target genes between groups were calculated using $\Delta\Delta C_t$ analysis to determine expression-fold difference. Genes with greater than 2-fold difference between ambient and hypoxia groups are reported as differentially up- or down-regulated in response to hypoxia treatment. Significance of differential expression was assessed via Student's T-Test of the replicate $2^{-\Delta C_t}$ values for each gene, with p values less than 0.05 considered significant. Several genes were selected for independent validation of results; primers used for validation

were synthesized by Integrated DNA Technologies (Coralville, IA) and are listed in Table 4.

Table 4: Oligonucleotide primer sequences used in qPCR analyses. Oligonucleotide sequences were designed based on murine sequences found at the listed GenBank accession numbers. *Abbreviations: F, forward (sense); R, reverse (antisense).*

Organism	Gene Name	GenBank #	Primer pair sequence (5' to 3')
Mouse	Ribosomal Protein L13A	NM_009438.5	F: GAAGCAGATCTTGAGGTTACGG R: TATTGGGTTCCACACCAGGAGTC
	Hypoxanthine-ribosyl transferase	NM_013556.2	F: AGGCCAGACTTTGTTGGATTTG R: TTCAACTTGCCTCATCTTAGG
	Monocarboxylate Transporter 1	NM_009196.4	F: CACACATAACGATACTAGATTTGCG R: TAGGAGAAGCCAATAGAAATGAAGG
	Surfactant Protein B	NM_147779.1	F: TGCCAAGAGTGTGAGGATATTGTCCAC R: CCAGCTTGTCCAGCAGAGGGTTTG
	Surfactant Protein C	NM_011359.1	F: CCGGATTACTCGGCAGGTCCCAG R: ATGCCAGTGGAGCCGATGGAAAAGG
	Thyroid Transcription Factor	NM_009385.2	F: GCGCCATGTCTTGTCTACCTTGC R: GTCGTCCAGCAGTTTGGTCTTTGTG
	Aquaporin 5	NM_009701.4	F: ACTCACCGTCTTTGGTTCGTCCTC R: GTGGCAGTCGTTCTGCCTAATTCC
	Pre-Collagen 1a	NM_007742.3	F: ACATCCCTGAAGTCAGCTGCATACAC R: GTCTCCCTTGGGTCCCTCGACTC
Fibroblast Specific Protein	NM_011311.2	F: TAGCTTCCTGGGAAAAGGACAGATG R: CATCTGAGGAGTCTTCACTTCTCCG	
Human	Ribosomal 18s RNA	NR_003286.2	F: ATGAACGAGGAATCCCAGTAAG R: TAAACCATCCAATCGGTAGTAGC
	Surfactant Protein B	NM_000542.2	F: GGACATCGTCCACATCCTTAACAAGATG R: ATTGCTGCTCGGAGAGATCCTGTGTGTG

Western Blotting

For protein harvest from cell cultures, cells were lysed in modified RIPA lysis buffer (150 mM NaCl, 50 mM Tris pH 8, 1% Triton) plus 0.5% SDS, 1 mM phenylmethylsulfonyl fluoride, and protease inhibitor cocktail (Sigma). Quantification of protein samples was performed by Bichinoic Acid assay, using bovine serum albumin as standard. Protein aliquots were acetone precipitated and resolubilized in LDS sample buffer (Invitrogen, Grand Island NY). All separations were run under reducing conditions by adding 5% beta-mercaptoethanol to lysates added and incubating samples for 5 minutes at approximately 95 degrees Celsius.

Samples were separated by SDS-NuPAGE (polyacrylamide gel electrophoresis) Bis-Tris Minigels (Invitrogen) and blotted onto nitrocellulose membranes using Tris-Glycine buffer (Invitrogen). Blots were blocked for 2 hours in PBS containing 0.1% Tween 20 and 5% milk, then incubated with primary antibodies in phosphaste-buffered saline (PBS) containing 0.1% Tween 20 and 0.5% milk for 2-3 hours or overnight in 4 degrees Celsius. The following primary antibodies were used: polyclonal Goat anti-MCT1 (Santa Cruz, Dallas, TX), monoclonal Rabbit anti-B Actin (Sigma), polyclonal Rabbit anti-LDH (Santa Cruz), polyclonal Sheep anti-LDH5 (AbCAM, Cambridge, MA), monoclonal mouse anti-RNA Polymerase II (Santa Cruz). Donkey anti-goat and donkey anti-rabbit secondary antibodies (LI-COR, Lincoln, NE) attached to fluorophores of different emission wavelengths were used to visualize protein bands on a LI-COR Odyssey (LI-COR). Semi-quantitative band densitometry and normalization

was performed using Li-COR Image Studio™ 4.0 according to manufacturer's instructions. Anti-sheep antibody conjugated to peroxidase (Jackson ImmunoResearch Laboratories, West Grove, PA) was developed using the SuperSignal West Dura Extended Duration Substrate kit luminol and stable peroxide buffer (Thermo Scientific, Rockford, IL) and visualized on a Fluorchem 8900 Imager (Alpha Innotech Corporation, San Leandro, CA). Alpha Innotech Alpha Ease FC software was used for band densitometry of LDH-M blots.

EdU Incorporation

Relative rates of DNA synthesis were determined using EdU nucleotide analog incorporation followed by Cy-Dye staining as previously described (173). Cells were exposed to indicated media conditions for a total of 24 hours. EdU (Sigma) was prepared from a stock concentration of 25 mM dissolved in water and added to culture wells at hour 12 (for 12-hour total EdU exposure). For overnight exposure, EdU was added to a final concentration of 2 μ M. Cells were then fixed with 4% PFA, permeabilized with 0.5% Triton X-100, and incubated with labeling solution containing azide-conjugated Cy7 (Lumiprobe, Hallandale Beach FL) for 15 minutes at 37 degree Celsius. Each sample well was stained subsequently with ToPro3 (Invitrogen) nuclear stain for normalization. ToPro3 and Cy-7 were visualized and quantified using the plate array setting on a LiCor Odyssey Imager (LiCor). Readings from wells containing no cells were subtracted to account for background. Negative control wells were included that received only Cy7 or ToPro3.

Cell Counting

For experiments assessing cell growth and for plating in all other in vitro experiments, cells were lifted from culture dishes using trypsin (if necessary), centrifuged to pellet cells and remove trypsin, and resuspended in a known amount of media or PBS. An aliquot of cell suspension was mixed with the vital dye trypan blue in a 1:4 dilution and pipetted onto the hemacytometer. Cells excluding trypan blue were counted. For both calculating plating densities and measuring growth over time, live (trypan-blue excluding) cells only were considered.

Modified Papanicolaou staining & ATII cell count

Modified Papanicolaou staining was performed to assess the purity of ATII cell cultures. Following cell isolation procedures and/or immediately following assay measurements, cells were smeared onto a cleaned glass microscope slide and allowed to dry overnight at 4 degree Celsius. Slides were stained with Harris hematoxyline stain and “blued” via submersion in a 1:40 dilution of saturated lithium carbonate solution in water. Dehydration was performed via immersion in ethanol dilutions of 50%, 80%, 95%, and 100%, followed by 1:1 ethanol:xylene and finally 100% xylene. Slides were allowed to dry, then fixed with permount.

To assess ATII cell population purity, the percentage of cells with prominent blue inclusions (representing stained lamellar bodies) was determined. 200-400 total cells were counted per slide using a light microscope. For all included studies, purity was 95% or greater.

Statistics

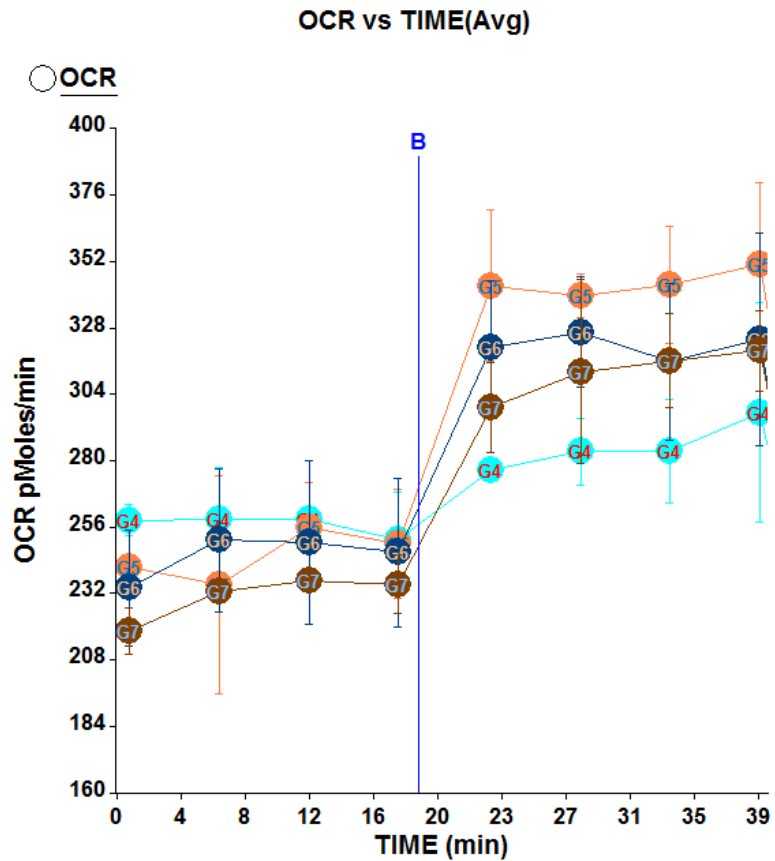
Student's T-test and ANOVA were used where indicated using GraphPad and the VassarStats ANOVA analysis tool. For all analyses, significance was defined as $p < 0.05$. When ANOVA was used and resulted in a significant F-ratio, Tukey HSD [0.05] post-hoc test was performed to determine significant differences among groups. All error bars shown represent +/- standard error.

APPENDIX A. OPTIMIZATION OF EXTRACELLULAR FLUX ASSAY

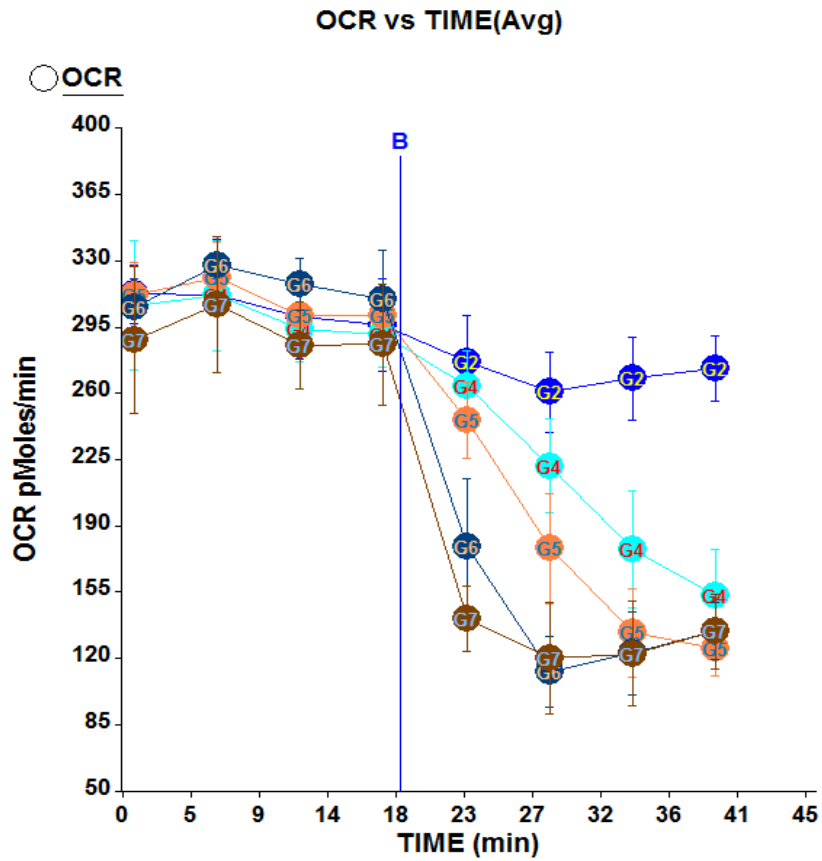
Prior to experimentation, optimization was performed using the MLE-15 and A549 cell lines concerning cell seeding density and mitochondrial inhibitor injection concentrations. All optimization was performed using 24-well plates designed for use on XF24 instruments; for XF96 experiments, densities and concentrations were scaled proportionally.

To determine optimal seeding densities for XF assay, cells were seeded at densities of 5, 7.5, and 10×10^5 cells per well. Cultures were allowed to incubate for approximately 24 hours prior to assay, after which wells were inspected for confluency. This indicated that greater than 5×10^4 but less than 7.5×10^4 cells per well should be used to obtain approximately 90% confluent monolayers without cell piling. Ultimately, assays reported here using the XF24 were performed using seeding densities of 6.5×10^4 cells per well.

Mitochondrial inhibitors can induce loss of mitochondrial membrane loss if used at high concentrations. Alternatively, low concentrations induce only partial response, leading to misinterpretation of data. Thus, for these experiments it was critical to determine the minimal concentrations of FCCP and oligomycin A needed to induce maximal response.



Appendix Figure A.1: Optimization of FCCP concentration for XF assay. After initial experiments using a wide range of FCCP concentrations indicated optimal concentration between 0.1 and 0.7 μM , MLE-15 were exposed to final concentrations of 0.3 (group G4), 0.45 (group G5), 0.6 (group G6), and 0.7 (group G7) μM FCCP as an injection at point B and the OCR response measured. Group G5 demonstrated the greatest response, thus 0.45 μM was optimal. This value was rounded to 0.5 μM FCCP for subsequent experiments.

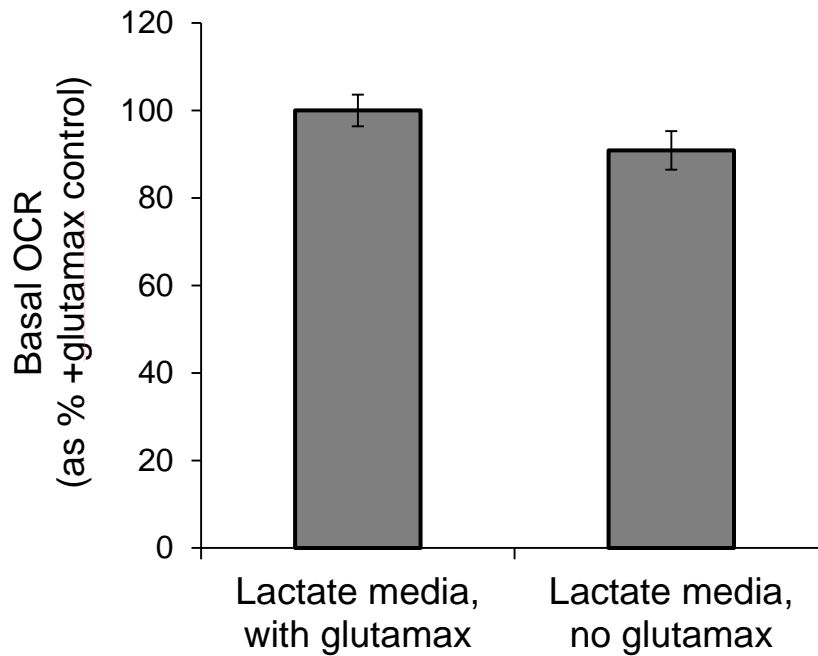


Appendix Figure A.2: Optimization of Oligomycin A concentration for XF assay. MLE-15 were exposed to final concentrations of 0.1 (group G2), 0.75 (group G4), 1.0 (group G5), 1.5 (group G6), and 3.0 (group G7) μM Oligomycin A as an injection at point B and the OCR response measured. Group G6 demonstrated the greatest response, thus 1.5 μM was optimal. This concentration was used for all subsequent studies.

APPENDIX B. GLUTAMAX-FREE CONTROL FOR METABOLIC ASSAY OF CELLS CULTURED IN LACTATE

Glutamax, the Glutamine-Alanine dipeptide, was added to cell culture and assay media for all experiments, even those targeted to assessing metabolism of lactate in the absence of glucose. The rationale for including Glutamax in the media formulations is based in the function of glutamine in mediation of oxidative stress, particularly important because some experiments required culture in hypoxic conditions which induces ROS generation and oxidative stress. However, the addition of Glutamax provides an additional oxidizable substrate besides lactate: glutamine can be oxidized directly by the TCA cycle, and alanine can be converted to lactate and pyruvate and thus can also provide oxidizable substrate to fuel mitochondrial metabolism.

In order to confirm that extracellular flux measurements were faithfully representing the effect of culture in lactate alone, follow-up control measurements were performed in MLE-15 cultures in lactate-formulated media with and without the addition of 2 mM Glutamax. The absence of Glutamax did not result in deviation from OCR levels observed in lactate-formulated media containing Glutamax.



Appendix Figure B.1: OCR in lactate-formulated media is not significantly affected by the absence of Glutamax. OCR was measured in MLE-15 cultured and assayed in media containing 5.5 mM lactate and formulated with or without 2 mM Glutamax. 6 individual cultures were measured per condition. No significant difference was measured between conditioned based on Student's T-Test. Error bars represent \pm SE.

APPENDIX C. COMPLETE RESULTS FOR PCR ARRAY

Table 5: Detailed results for glucose metabolism focused qPCR array using mRNA obtained from MLE-15 cultured in hypoxia versus ambient O₂. Focused qPCR array was performed to assess changes in MLE-15 expression of genes associated with glucose metabolism in response to hypoxia. Per condition, 3 individual cDNA were analyzed. All genes assessed are shown; genes with greater than 2-fold difference between ambient and hypoxia groups and having a p value <0.05 are represented in bold type. * AVG ΔC_t values are the average normalized values obtained from three independent arrays for both hypoxia and ambient groups. Down-regulation in hypoxia versus ambient is indicated by negative fold-regulation value.

† Expression of this gene was low (average threshold cycle > 30) in either the hypoxia or ambient sample, but higher in the other sample (cycle < 30). ‡ Expression of this gene was low (average threshold cycle > 30) in both hypoxia and ambient samples, and the p-value for the fold-change is either unavailable or > 0.05. § Expression of this gene was very low or undetected (average threshold cycle is either not determined or greater than the defined cut-off of 35) in both samples, making this fold-change result erroneous and uninterpretable. Gene Array: SA Biosciences PCR Array Catalog #PAMM006. Abbreviations: GOI, gene of interest; HKG, housekeeping gene.

Gene Symbol	RefSeq ID	* AVG ΔC_t (C _t (GOI) - Ave C _t (HKG))		$2^{-\Delta\Delta C_t}$		Fold Change	p value	Fold Up- or Down- Regulation
		Hypoxia	Ambient	Hypoxia	Ambient	Hypoxia/ Ambient		Hypoxia/ Ambient
Pdp2	NM_001024606	7.04	7.24	7.6E-03	6.6E-03	1.15	0.967	1.15
Pdpr	NM_198308	6.43	6.72	1.2E-02	9.5E-03	1.22	0.550	1.22
Acly	NM_134037	2.23	2.14	2.1E-01	2.3E-01	0.94	0.784	-1.06
Aco1	NM_007386	9.56	9.13	1.3E-03	1.8E-03	0.74	0.531	-1.35 †
Aco2	NM_080633	2.09	2.12	2.4E-01	2.3E-01	1.02	0.976	1.02
Agl	NM_001081326	10.69	11.47	6.1E-04	3.5E-04	1.73	0.387	1.73 ‡
Aldoa	NM_007438	-3.49	-1.86	1.1E+01	3.6E+00	3.09	0.054	3.09
Aldob	NM_144903	11.96	12.39	2.5E-04	1.9E-04	1.34	0.881	1.34 ‡
Aldoc	NM_009657	0.26	2.57	8.4E-01	1.7E-01	4.97	0.082	4.97
Bpgm	NM_007563	6.38	4.83	1.2E-02	3.5E-02	0.34	0.069	-2.93
Cs	NM_026444	2.39	2.13	1.9E-01	2.3E-01	0.84	0.421	-1.19
Dlat	NM_145614	4.13	3.58	5.7E-02	8.4E-02	0.68	0.494	-1.47
Dld	NM_007861	2.64	2.42	1.6E-01	1.9E-01	0.86	0.541	-1.16

Table 5--continued

Gene Symbol	RefSeq ID	* AVG ΔC_t (C _t (GOI) - Ave C _t (HKG))		$2^{-\Delta\Delta C_t}$		Fold Change	p value	Fold Up- or Down- Regulation
		Hypoxia	Ambient	Hypoxia	Ambient	Hypoxia/ Ambient		Hypoxia/ Ambient
Dlst	NM_030225	3.92	3.27	6.6E-02	1.0E-01	0.64	0.228	-1.57
Eno1	NM_023119	-1.43	0.23	2.7E+00	8.5E-01	3.17	0.030	3.17
Eno2	NM_013509	2.22	5.25	2.1E-01	2.6E-02	8.15	0.124	8.15
Eno3	NM_007933	4.56	3.63	4.2E-02	8.1E-02	0.53	0.236	-1.90
Fbp1	NM_019395	11.14	13.47	4.4E-04	8.8E-05	5.00	0.187	5.00 ‡
Fbp2	NM_007994	9.58	9.75	1.3E-03	1.2E-03	1.13	0.892	1.13 ‡
Fh1	NM_010209	2.86	2.75	1.4E-01	1.5E-01	0.92	0.617	-1.08
G6pc	NM_008061	13.53	14.51	8.4E-05	4.3E-05	1.97	N/A	1.97 ‡
G6pc3	NM_175935	4.65	4.99	4.0E-02	3.1E-02	1.27	0.537	1.27
G6pdx	NM_008062	3.69	3.75	7.8E-02	7.5E-02	1.04	0.745	1.04
Galm	NM_176963	7.99	8.17	3.9E-03	3.5E-03	1.13	0.935	1.13
Gapdhs	NM_008085	9.97	10.74	1.0E-03	5.9E-04	1.71	0.258	1.71 ‡
Gbe1	NM_028803	1.41	4.18	3.8E-01	5.5E-02	6.81	0.001	6.81
Gck	NM_010292	13.91	14.99	6.5E-05	3.1E-05	2.12	N/A	2.12 ‡
Gpi1	NM_008155	-1.43	0.54	2.7E+00	6.9E-01	3.91	0.039	3.91
Gsk3a	NM_001031 667	3.29	3.00	1.0E-01	1.2E-01	0.82	0.736	-1.22
Gsk3b	NM_019827	7.11	7.42	7.3E-03	5.8E-03	1.24	0.326	1.24
Gys1	NM_030678	1.29	3.69	4.1E-01	7.8E-02	5.27	0.039	5.27
Gys2	NM_145572	13.91	13.82	6.5E-05	6.9E-05	0.94	N/A	-1.06 ‡
H6pd	NM_173371	6.95	6.41	8.1E-03	1.2E-02	0.69	0.762	-1.46
Hk2	NM_013820	2.18	4.97	2.2E-01	3.2E-02	6.88	0.051	6.88
Hk3	NM_001033 245	12.83	13.72	1.4E-04	7.4E-05	1.84	0.176	1.84 ‡
ldh1	NM_010497	4.18	3.76	5.5E-02	7.4E-02	0.75	0.507	-1.34
ldh2	NM_173011	2.22	2.29	2.1E-01	2.0E-01	1.05	0.824	1.05
ldh3a	NM_029573	3.31	2.52	1.0E-01	1.7E-01	0.58	0.129	-1.73
ldh3b	NM_130884	3.72	3.38	7.6E-02	9.6E-02	0.79	0.772	-1.27
ldh3g	NM_008323	2.65	2.43	1.6E-01	1.9E-01	0.86	0.581	-1.17
Mdh1	NM_008618	1.49	1.46	3.6E-01	3.6E-01	0.98	0.836	-1.02
Mdh1b	NM_029696	13.91	14.59	6.5E-05	4.1E-05	1.60	N/A	1.60 §
Mdh2	NM_008617	1.30	1.00	4.1E-01	5.0E-01	0.81	0.165	-1.23
Ogdh	NM_010956	13.48	14.05	8.7E-05	5.9E-05	1.48	0.441	1.48 ‡
Pck1	NM_011044	13.48	13.98	8.7E-05	6.2E-05	1.41	0.491	1.41 ‡
Pck2	NM_028994	2.92	3.85	1.3E-01	6.9E-02	1.91	0.290	1.91
Pcx	NM_008797	5.31	5.83	2.5E-02	1.8E-02	1.43	0.355	1.43
Pdha1	NM_008810	3.39	3.19	9.6E-02	1.1E-01	0.87	0.593	-1.14
Pdha2	NM_024221	2.80	2.77	1.4E-01	1.5E-01	0.98	0.754	-1.02
Pdk1	NM_172665	2.89	5.21	1.4E-01	2.7E-02	5.02	0.008	5.02
Pdk2	NM_133667	6.88	6.55	8.5E-03	1.1E-02	0.80	0.346	-1.26
Pdk3	NM_145630	3.92	4.91	6.6E-02	3.3E-02	2.00	0.015	2.00
Pdk4	NM_013743	13.48	15.18	8.7E-05	2.7E-05	3.23	N/A	3.23 ‡
Pfkl	NM_008826	6.27	8.12	1.3E-02	3.6E-03	3.62	0.023	3.62

Table 5--continued

Gene Symbol	RefSeq ID	* AVG ΔC_t ($C_t(\text{GOI}) - \text{Ave } C_t(\text{HKG})$)		$2^{-\Delta\Delta C_t}$		Fold Change	p value	Fold Up- or Down-Regulation
		Hypoxia	Ambient	Hypoxia	Ambient	Hypoxia/ Ambient		Hypoxia/ Ambient
Pgam2	NM_018870	10.39	10.49	7.4E-04	6.9E-04	1.07	0.679	1.07 ‡
Pgk1	NM_008828	-2.29	-0.46	4.9E+00	1.4E+00	3.55	0.002	3.55
Pgk2	NM_031190	13.91	15.51	6.5E-05	2.1E-05	3.04	N/A	3.04 §
Pgm1	NM_025700	5.05	4.99	3.0E-02	3.1E-02	0.96	0.779	-1.04
Pgm2	NM_028132	0.98	3.15	5.1E-01	1.1E-01	4.51	0.020	4.51
Pgm3	NM_028352	5.56	5.21	2.1E-02	2.7E-02	0.79	0.508	-1.27
Phka1	NM_173021	7.29	7.15	6.4E-03	7.1E-03	0.91	0.706	-1.10
Phkb	NM_199446	6.06	6.16	1.5E-02	1.4E-02	1.08	0.703	1.08
Phkg1	NM_011079	11.62	11.35	3.2E-04	3.8E-04	0.83	0.911	-1.20 ‡
Phkg2	NM_026888	5.25	5.53	2.6E-02	2.2E-02	1.21	0.803	1.21
Pklr	NM_013631	13.96	14.41	6.3E-05	4.6E-05	1.37	N/A	1.37 §
Prps1	NM_021463	3.31	2.92	1.0E-01	1.3E-01	0.76	0.348	-1.31
Prps1l1	NM_029294	N/A	15.22	N/A	2.6E-05	N/A	N/A	N/A §
Prps2	NM_026662	5.58	5.30	2.1E-02	2.5E-02	0.82	0.691	-1.21
Pygl	NM_133198	12.53	14.46	1.7E-04	4.4E-05	3.81	0.234	3.81 ‡
Pygm	NM_011224	9.64	10.20	1.3E-03	8.5E-04	1.47	0.537	1.47 ‡
Rbks	NM_153196	9.05	8.33	1.9E-03	3.1E-03	0.61	0.389	-1.65 †
Rpe	NM_025683	4.31	4.42	5.1E-02	4.7E-02	1.08	0.717	1.08
Rpia	NM_009075	5.51	5.29	2.2E-02	2.6E-02	0.86	0.606	-1.16
Sdha	NM_023281	3.75	3.38	7.5E-02	9.6E-02	0.77	0.497	-1.29
Sdhb	NM_023374	3.53	3.06	8.7E-02	1.2E-01	0.72	0.112	-1.39
Sdhc	NM_025321	2.08	2.05	2.4E-01	2.4E-01	0.98	0.826	-1.02
Sdhd	NM_025848	2.39	2.30	1.9E-01	2.0E-01	0.94	0.734	-1.07
Sucla2	NM_011506	4.29	4.11	5.1E-02	5.8E-02	0.88	0.483	-1.14
Suclg1	NM_019879	4.72	3.92	3.8E-02	6.6E-02	0.58	0.063	-1.73
Suclg2	NM_011507	10.56	10.69	6.6E-04	6.1E-04	1.09	0.940	1.09 ‡
Taldo1	NM_011528	3.19	2.45	1.1E-01	1.8E-01	0.60	0.100	-1.67
Tkt	NM_009388	1.32	1.71	4.0E-01	3.1E-01	1.30	0.803	1.30
Tpi1	NM_009415	-1.92	-0.40	3.8E+00	1.3E+00	2.87	0.054	2.87
Ugp2	NM_139297	2.97	3.82	1.3E-01	7.1E-02	1.80	0.150	1.80
Gusb	NM_010368	5.72	4.35	1.9E-02	4.9E-02	0.39	0.083	-2.58
Hprt	NM_013556	2.24	2.51	2.1E-01	1.8E-01	1.20	0.092	1.20
Hsp90a b1	NM_008302	-0.20	-0.37	1.2E+00	1.3E+00	0.89	0.985	-1.13
Gapdh	NM_008084	-4.96	-3.01	3.1E+01	8.1E+00	3.85	0.163	3.85
Actb	NM_007393	-2.04	-2.13	4.1E+00	4.4E+00	0.94	0.836	-1.07

LIST OF REFERENCES

1. Camelo A, Dunmore R, Sleeman MA, Clarke DL. The epithelium in idiopathic pulmonary fibrosis: Breaking the barrier. *Front Pharmacol*. 2014 Jan 10;4:173.
2. Wright JR, Dobbs LG. Regulation of pulmonary surfactant secretion and clearance. *Annu Rev Physiol*. 1991;53:395-414.
3. Agassandian M, Mallampalli RK. Surfactant phospholipid metabolism. *Biochim Biophys Acta*. 2013 Mar;1831(3):612-25.
4. Ridsdale R, Post M. Surfactant lipid synthesis and lamellar body formation in glycogen-laden type II cells. *Am J Physiol Lung Cell Mol Physiol*. 2004 Oct;287(4):L743-51.
5. Glasser SW, Witt TL, Senft AP, Baatz JE, Folger D, Maxfield MD, et al. Surfactant protein C-deficient mice are susceptible to respiratory syncytial virus infection. *Am J Physiol Lung Cell Mol Physiol*. 2009 Jul;297(1):L64-72.
6. Mason RJ, Williams MC, Widdicombe JH. Fluid and electrolyte transport across monolayers of alveolar type II cells in vitro. *Am Rev Respir Dis*. 1983 May;127(5 Pt 2):S24-8.
7. Matalon S. Mechanisms and regulation of ion transport in adult mammalian alveolar type II pneumocytes. *Am J Physiol*. 1991 Nov;261(5 Pt 1):C727-38.
8. Vivona ML, Matthay M, Chabaud MB, Friedlander G, Clerici C. Hypoxia reduces alveolar epithelial sodium and fluid transport in rats: Reversal by beta-adrenergic agonist treatment. *Am J Respir Cell Mol Biol*. 2001 Nov;25(5):554-61.
9. Hoffman AM, Ingenito EP. Alveolar epithelial stem and progenitor cells: Emerging evidence for their role in lung regeneration. *Curr Med Chem*. 2012;19(35):6003-8.
10. Tierney DF. Intermediary metabolism of the lung. *Fed Proc*. 1974 Nov;33(11):2232-7.
11. Datta H, Stubbs WA, Alberti KG. Substrate utilization by the lung. *Ciba Found Symp*. 1980;78:85-104.
12. Levey S, Gast R. Isolated perfused rat lung preparation. *J Appl Physiol*. 1966 Jan;21(1):313-6.

13. Weber KC, Visscher MB. Metabolism of the isolated canine lung. *Am J Physiol.* 1969 Oct;217(4):1044-52.
14. Bassett DJ, Fisher AB. Metabolic response to carbon monoxide by isolated rat lungs. *Am J Physiol.* 1976 Mar;230(3):658-63.
15. Williamson JR. Glycolytic control mechanisms. I. inhibition of glycolysis by acetate and pyruvate in the isolated, perfused rat heart. *J Biol Chem.* 1965 Jun;240:2308-21.
16. Bassett DJ, Fisher AB, Rabinowitz JL. Effect of hypoxia on incorporation of glucose carbons into lipids by isolated rat lung. *Am J Physiol.* 1974 Nov;227(5):1103-8.
17. Wolfe RR, Hochachka PW, Trelstad RL, Burke JF. Lactate oxidation in perfused rat lung. *Am J Physiol.* 1979 Mar;236(3):E276-82.
18. Rhoades RA, Shaw ME, Eskew ML, Wali S. Lactate metabolism in perfused rat lung. *Am J Physiol.* 1978 Dec;235(6):E619-23.
19. Felts JM. Biochemistry of the lung. *Health Phys.* 1964 Dec;10:973-9.
20. Shaw ME, Rhoades RA. Substrate metabolism in the perfused lung: Response to changes in circulating glucose and palmitate levels. *Lipids.* 1977 Nov;12(11):930-5.
21. Longmore WJ, Mourning JT. Lactate production in isolated perfused rat lung. *Am J Physiol.* 1976 Aug;231(2):351-4.
22. Fox RE, Hopkins IB, Cabacungan ET, Tildon JT. The role of glutamine and other alternate substrates as energy sources in the fetal rat lung type II cell. *Pediatr Res.* 1996 Jul;40(1):135-41.
23. Heerlein K, Schulze A, Hotz L, Bartsch P, Mairbaurl H. Hypoxia decreases cellular ATP demand and inhibits mitochondrial respiration of a549 cells. *Am J Respir Cell Mol Biol.* 2005 Jan;32(1):44-51.
24. Gusarova GA, Trejo HE, Dada LA, Briva A, Welch LC, Hamanaka RB, et al. Hypoxia leads to na,K-ATPase downregulation via ca(2+) release-activated ca(2+) channels and AMPK activation. *Mol Cell Biol.* 2011 Sep;31(17):3546-56.
25. Das KC. Hyperoxia decreases glycolytic capacity, glycolytic reserve and oxidative phosphorylation in MLE-12 cells and inhibits complex I and II function,

but not complex IV in isolated mouse lung mitochondria. *PLoS One*. 2013 Sep 2;8(9):e73358.

26. Brooks GA. Lactate shuttles in nature. *Biochem Soc Trans*. 2002 Apr;30(2):258-64.

27. Brooks GA. Cell-cell and intracellular lactate shuttles. *J Physiol*. 2009 Dec 1;587(Pt 23):5591-600.

28. Hashimoto T, Brooks GA. Mitochondrial lactate oxidation complex and an adaptive role for lactate production. *Med Sci Sports Exerc*. 2008 Mar;40(3):486-94.

29. Hashimoto T, Hussien R, Brooks GA. Colocalization of MCT1, CD147, and LDH in mitochondrial inner membrane of L6 muscle cells: Evidence of a mitochondrial lactate oxidation complex. *Am J Physiol Endocrinol Metab*. 2006 Jun;290(6):E1237-44.

30. Johnson ML, Hussien R, Horning MA, Brooks GA. Transpulmonary pyruvate kinetics. *Am J Physiol Regul Integr Comp Physiol*. 2011 Sep;301(3):R769-74.

31. Halestrap AP. The SLC16 gene family - structure, role and regulation in health and disease. *Mol Aspects Med*. 2013 Apr-Jun;34(2-3):337-49.

32. Halestrap AP, Price NT. The proton-linked monocarboxylate transporter (MCT) family: Structure, function and regulation. *Biochem J*. 1999 Oct 15;343 Pt 2:281-99.

33. Draoui N, Feron O. Lactate shuttles at a glance: From physiological paradigms to anti-cancer treatments. *Dis Model Mech*. 2011 Nov;4(6):727-32.

34. Johnson ML, Emhoff CA, Horning MA, Brooks GA. Transpulmonary lactate shuttle. *Am J Physiol Regul Integr Comp Physiol*. 2012 Jan 1;302(1):R143-9.

35. Patterson CE, Koniki MV, Selig WM, Owens CM, Rhoades RA. Integrated substrate utilization by perinatal lung. *Exp Lung Res*. 1986;10(1):71-86.

36. Sheehan PM, Yeh YY. Pulmonary surfactant lipid synthesis from ketone bodies, lactate and glucose in newborn rats. *Lipids*. 1985 Dec;20(12):835-41.

37. Lottes RG, Newton DA, Spyropoulos DD, Baatz JE. Alveolar type II cells maintain bioenergetic homeostasis in hypoxia through metabolic and molecular adaptation. *Am J Physiol Lung Cell Mol Physiol*. 2014 Mar 28.

38. Schumacker PT. Lung cell hypoxia: Role of mitochondrial reactive oxygen species signaling in triggering responses. *Proc Am Thorac Soc.* 2011 Nov;8(6):477-84.
39. Schumacker PT, Cain SM. The concept of a critical oxygen delivery. *Intensive Care Med.* 1987;13(4):223-9.
40. Gayeski TE, Honig CR. Intracellular PO₂ in individual cardiac myocytes in dogs, cats, rabbits, ferrets, and rats. *Am J Physiol.* 1991 Feb;260(2 Pt 2):H522-31.
41. Huang Y, Kempen MB, Munck AB, Swagemakers S, Driegen S, Mahavadi P, et al. Hypoxia-inducible factor 2alpha plays a critical role in the formation of alveoli and surfactant. *Am J Respir Cell Mol Biol.* 2012 Feb;46(2):224-32.
42. Pitsiou G, Papakosta D, Bouros D. Pulmonary hypertension in idiopathic pulmonary fibrosis: A review. *Respiration.* 2011;82(3):294-304.
43. Weitzenblum E, Chaouat A, Canuet M, Kessler R. Pulmonary hypertension in chronic obstructive pulmonary disease and interstitial lung diseases. *Semin Respir Crit Care Med.* 2009 Aug;30(4):458-70.
44. Hochachka PW, Buck LT, Doll CJ, Land SC. Unifying theory of hypoxia tolerance: Molecular/metabolic defense and rescue mechanisms for surviving oxygen lack. *Proc Natl Acad Sci U S A.* 1996 Sep 3;93(18):9493-8.
45. Jezek P, Plecita-Hlavata L, Smolkova K, Rossignol R. Distinctions and similarities of cell bioenergetics and the role of mitochondria in hypoxia, cancer, and embryonic development. *Int J Biochem Cell Biol.* 2010 May;42(5):604-22.
46. Majmundar AJ, Wong WJ, Simon MC. Hypoxia-inducible factors and the response to hypoxic stress. *Mol Cell.* 2010 Oct 22;40(2):294-309.
47. Kaelin WG, Jr, Ratcliffe PJ. Oxygen sensing by metazoans: The central role of the HIF hydroxylase pathway. *Mol Cell.* 2008 May 23;30(4):393-402.
48. Klimova T, Chandel NS. Mitochondrial complex III regulates hypoxic activation of HIF. *Cell Death Differ.* 2008 Apr;15(4):660-6.
49. Grek CL, Newton DA, Spyropoulos DD, Baatz JE. Hypoxia up-regulates expression of hemoglobin in alveolar epithelial cells. *Am J Respir Cell Mol Biol.* 2011 Apr;44(4):439-47.

50. Uchida T, Rossignol F, Matthay MA, Mounier R, Couette S, Clottes E, et al. Prolonged hypoxia differentially regulates hypoxia-inducible factor (HIF)-1alpha and HIF-2alpha expression in lung epithelial cells: Implication of natural antisense HIF-1alpha. *J Biol Chem*. 2004 Apr 9;279(15):14871-8.
51. Mungai PT, Waypa GB, Jairaman A, Prakriya M, Dokic D, Ball MK, et al. Hypoxia triggers AMPK activation through reactive oxygen species-mediated activation of calcium release-activated calcium channels. *Mol Cell Biol*. 2011 Sep;31(17):3531-45.
52. Ouiddir A, Planes C, Fernandes I, VanHesse A, Clerici C. Hypoxia upregulates activity and expression of the glucose transporter GLUT1 in alveolar epithelial cells. *Am J Respir Cell Mol Biol*. 1999 Dec;21(6):710-8.
53. Vadivel A, Alphonse RS, Etches N, van Haaften T, Collins JJ, O'Reilly M, et al. Hypoxia-inducible factors promote alveolar development and regeneration. *Am J Respir Cell Mol Biol*. 2014 Jan;50(1):96-105.
54. Ito Y, Ahmad A, Kewley E, Mason RJ. Hypoxia-inducible factor regulates expression of surfactant protein in alveolar type II cells in vitro. *Am J Respir Cell Mol Biol*. 2011 Nov;45(5):938-45.
55. Bhaskaran M, Chen H, Chen Z, Liu L. Hemoglobin is expressed in alveolar epithelial type II cells. *Biochem Biophys Res Commun*. 2005 Aug 12;333(4):1348-52.
56. Newton DA, Rao KM, Dluhy RA, Baatz JE. Hemoglobin is expressed by alveolar epithelial cells. *J Biol Chem*. 2006 Mar 3;281(9):5668-76.
57. Olmeda B, Umstead TM, Silveyra P, Pascual A, Lopez-Barneo J, Phelps DS, et al. Effect of hypoxia on lung gene expression and proteomic profile: Insights into the pulmonary surfactant response. *J Proteomics*. 2014 Apr 14;101:179-91.
58. Travis WD, Costabel U, Hansell DM, King TE, Jr, Lynch DA, Nicholson AG, et al. An official american thoracic society/european respiratory society statement: Update of the international multidisciplinary classification of the idiopathic interstitial pneumonias. *Am J Respir Crit Care Med*. 2013 Sep 15;188(6):733-48.
59. Chibbar R, Shih F, Baga M, Torlakovic E, Ramlall K, Skomro R, et al. Nonspecific interstitial pneumonia and usual interstitial pneumonia with mutation in surfactant protein C in familial pulmonary fibrosis. *Mod Pathol*. 2004 Aug;17(8):973-80.

60. Thomas AQ, Lane K, Phillips J, 3rd, Prince M, Markin C, Speer M, et al. Heterozygosity for a surfactant protein C gene mutation associated with usual interstitial pneumonitis and cellular nonspecific interstitial pneumonitis in one kindred. *Am J Respir Crit Care Med.* 2002 May 1;165(9):1322-8.
61. Hunninghake GM, Hatabu H, Okajima Y, Gao W, Dupuis J, Latourelle JC, et al. MUC5B promoter polymorphism and interstitial lung abnormalities. *N Engl J Med.* 2013 Jun 6;368(23):2192-200.
62. Stock CJ, Sato H, Fonseca C, Banya WA, Molyneaux PL, Adamali H, et al. Mucin 5B promoter polymorphism is associated with idiopathic pulmonary fibrosis but not with development of lung fibrosis in systemic sclerosis or sarcoidosis. *Thorax.* 2013 May;68(5):436-41.
63. Tsang AR, Wyatt HD, Ting NS, Beattie TL. hTERT mutations associated with idiopathic pulmonary fibrosis affect telomerase activity, telomere length, and cell growth by distinct mechanisms. *Aging Cell.* 2012 Jun;11(3):482-90.
64. Chilosi M, Poletti V, Rossi A. The pathogenesis of COPD and IPF: Distinct horns of the same devil? *Respir Res.* 2012 Jan 11;13:3,9921-13-3.
65. Hinz B, Phan SH, Thannickal VJ, Galli A, Bochaton-Piallat ML, Gabbiani G. The myofibroblast: One function, multiple origins. *Am J Pathol.* 2007 Jun;170(6):1807-16.
66. Phan SH. The myofibroblast in pulmonary fibrosis. *Chest.* 2002 Dec;122(6 Suppl):286S-9S.
67. Sheppard D. Transforming growth factor beta: A central modulator of pulmonary and airway inflammation and fibrosis. *Proc Am Thorac Soc.* 2006 Jul;3(5):413-7.
68. Selman M, Pardo A. Idiopathic pulmonary fibrosis: An epithelial/fibroblastic cross-talk disorder. *Respir Res.* 2002;3:3.
69. Sakai N, Tager AM. Fibrosis of two: Epithelial cell-fibroblast interactions in pulmonary fibrosis. *Biochim Biophys Acta.* 2013 Jul;1832(7):911-21.
70. Plataki M, Koutsopoulos AV, Darivianaki K, Delides G, Siafakas NM, Bouros D. Expression of apoptotic and antiapoptotic markers in epithelial cells in idiopathic pulmonary fibrosis. *Chest.* 2005 Jan;127(1):266-74.

71. Waghray M, Cui Z, Horowitz JC, Subramanian IM, Martinez FJ, Toews GB, et al. Hydrogen peroxide is a diffusible paracrine signal for the induction of epithelial cell death by activated myofibroblasts. *FASEB J*. 2005 May;19(7):854-6.
72. Tsukamoto K, Hayakawa H, Sato A, Chida K, Nakamura H, Miura K. Involvement of epstein-barr virus latent membrane protein 1 in disease progression in patients with idiopathic pulmonary fibrosis. *Thorax*. 2000 Nov;55(11):958-61.
73. Tzouvelekis A, Harokopos V, Paparountas T, Oikonomou N, Chatziioannou A, Vilaras G, et al. Comparative expression profiling in pulmonary fibrosis suggests a role of hypoxia-inducible factor-1alpha in disease pathogenesis. *Am J Respir Crit Care Med*. 2007 Dec 1;176(11):1108-19.
74. Perng DW, Chang KT, Su KC, Wu YC, Wu MT, Hsu WH, et al. Exposure of airway epithelium to bile acids associated with gastroesophageal reflux symptoms: A relation to transforming growth factor-beta1 production and fibroblast proliferation. *Chest*. 2007 Nov;132(5):1548-56.
75. Willis BC, Liebler JM, Luby-Phelps K, Nicholson AG, Crandall ED, du Bois RM, et al. Induction of epithelial-mesenchymal transition in alveolar epithelial cells by transforming growth factor-beta1: Potential role in idiopathic pulmonary fibrosis. *Am J Pathol*. 2005 May;166(5):1321-32.
76. Kasai H, Allen JT, Mason RM, Kamimura T, Zhang Z. TGF-beta1 induces human alveolar epithelial to mesenchymal cell transition (EMT). *Respir Res*. 2005 Jun 9;6:56.
77. Gorowiec MR, Borthwick LA, Parker SM, Kirby JA, Saretzki GC, Fisher AJ. Free radical generation induces epithelial-to-mesenchymal transition in lung epithelium via a TGF-beta1-dependent mechanism. *Free Radic Biol Med*. 2012 Mar 15;52(6):1024-32.
78. Coward WR, Saini G, Jenkins G. The pathogenesis of idiopathic pulmonary fibrosis. *Ther Adv Respir Dis*. 2010 Dec;4(6):367-88.
79. Chen YL, Zhang X, Bai J, Gai L, Ye XL, Zhang L, et al. Sorafenib ameliorates bleomycin-induced pulmonary fibrosis: Potential roles in the inhibition of epithelial-mesenchymal transition and fibroblast activation. *Cell Death Dis*. 2013 Jun 13;4:e665.

80. Horan GS, Wood S, Ona V, Li DJ, Lukashev ME, Weinreb PH, et al. Partial inhibition of integrin $\alpha(v)\beta6$ prevents pulmonary fibrosis without exacerbating inflammation. *Am J Respir Crit Care Med*. 2008 Jan 1;177(1):56-65.
81. Hetzel M, Bachem M, Anders D, Trischler G, Faehling M. Different effects of growth factors on proliferation and matrix production of normal and fibrotic human lung fibroblasts. *Lung*. 2005 Jul-Aug;183(4):225-37.
82. Zhou Y, Hagood JS, Lu B, Merryman WD, Murphy-Ullrich JE. Thy-1-integrin $\alpha v \beta 5$ interactions inhibit lung fibroblast contraction-induced latent transforming growth factor- $\beta 1$ activation and myofibroblast differentiation. *J Biol Chem*. 2010 Jul 16;285(29):22382-93.
83. Willis BC, Liebler JM, Luby-Phelps K, Nicholson AG, Crandall ED, du Bois RM, et al. Induction of epithelial-mesenchymal transition in alveolar epithelial cells by transforming growth factor- $\beta 1$: Potential role in idiopathic pulmonary fibrosis. *Am J Pathol*. 2005 May;166(5):1321-32.
84. Solovyan VT, Keski-Oja J. Proteolytic activation of latent TGF- β precedes caspase-3 activation and enhances apoptotic death of lung epithelial cells. *J Cell Physiol*. 2006 May;207(2):445-53.
85. Zhao L, Yee M, O'Reilly MA. Transdifferentiation of alveolar epithelial type II to type I cells is controlled by opposing TGF- β and BMP signaling. *Am J Physiol Lung Cell Mol Physiol*. 2013 Sep 15;305(6):L409-18.
86. Psathakis K, Mermigkis D, Papatheodorou G, Loukides S, Panagou P, Polychronopoulos V, et al. Exhaled markers of oxidative stress in idiopathic pulmonary fibrosis. *Eur J Clin Invest*. 2006 May;36(5):362-7.
87. Lenz AG, Costabel U, Maier KL. Oxidized BAL fluid proteins in patients with interstitial lung diseases. *Eur Respir J*. 1996 Feb;9(2):307-12.
88. Hecker L, Vittal R, Jones T, Jagirdar R, Luckhardt TR, Horowitz JC, et al. NADPH oxidase-4 mediates myofibroblast activation and fibrogenic responses to lung injury. *Nat Med*. 2009 Sep;15(9):1077-81.
89. Geiser T, Ishigaki M, van Leer C, Matthay MA, Broaddus VC. H_2O_2 inhibits alveolar epithelial wound repair in vitro by induction of apoptosis. *Am J Physiol Lung Cell Mol Physiol*. 2004 Aug;287(2):L448-53.
90. Tanaka K, Ishihara T, Azuma A, Kudoh S, Ebina M, Nukiwa T, et al. Therapeutic effect of lecithinized superoxide dismutase on bleomycin-induced

pulmonary fibrosis. *Am J Physiol Lung Cell Mol Physiol*. 2010 Mar;298(3):L348-60.

91. Wynn TA, Ramalingam TR. Mechanisms of fibrosis: Therapeutic translation for fibrotic disease. *Nat Med*. 2012 Jul 6;18(7):1028-40.

92. Borowski A, Kuepper M, Horn U, Knupfer U, Zissel G, Hohne K, et al. Interleukin-13 acts as an apoptotic effector on lung epithelial cells and induces pro-fibrotic gene expression in lung fibroblasts. *Clin Exp Allergy*. 2008 Apr;38(4):619-28.

93. Murray LA, Argentieri RL, Farrell FX, Bracht M, Sheng H, Whitaker B, et al. Hyper-responsiveness of IPF/UIP fibroblasts: Interplay between TGFbeta1, IL-13 and CCL2. *Int J Biochem Cell Biol*. 2008;40(10):2174-82.

94. Kottmann RM, Kulkarni AA, Smolnycki KA, Lyda E, Dahanayake T, Salibi R, et al. Lactic acid is elevated in idiopathic pulmonary fibrosis and induces myofibroblast differentiation via pH-dependent activation of transforming growth factor-beta. *Am J Respir Crit Care Med*. 2012 Oct 15;186(8):740-51.

95. Gu L, Zhu YJ, Yang X, Guo ZJ, Xu WB, Tian XL. Effect of TGF-beta/smads signaling pathway on lung myofibroblast differentiation. *Acta Pharmacol Sin*. 2007 Mar;28(3):382-91.

96. Evans RA, Tian YC, Steadman R, Phillips AO. TGF-beta1-mediated fibroblast-myofibroblast terminal differentiation-the role of smad proteins. *Exp Cell Res*. 2003 Jan 15;282(2):90-100.

97. Chilosi M, Poletti V, Rossi A. The pathogenesis of COPD and IPF: Distinct horns of the same devil? *Respir Res*. 2012 Jan 11;13:3,9921-13-3.

98. Worlitzsch D, Meyer KC, Doring G. Lactate levels in airways of patients with cystic fibrosis and idiopathic pulmonary fibrosis. *Am J Respir Crit Care Med*. 2013 Jul 1;188(1):111.

99. Kottmann R, Phipps R, Sime P. Reply: From idiopathic pulmonary fibrosis to cystic fibrosis: Got lactate? *Am J Respir Crit Care Med*. 2013 Jul 1;188(1):111-2.

100. Cheresh P, Kim SJ, Tulasiram S, Kamp DW. Oxidative stress and pulmonary fibrosis. *Biochim Biophys Acta*. 2013 Jul;1832(7):1028-40.

101. Yoon YS, Lee JH, Hwang SC, Choi KS, Yoon G. TGF beta1 induces prolonged mitochondrial ROS generation through decreased complex IV activity with senescent arrest in Mv1Lu cells. *Oncogene*. 2005 Mar 10;24(11):1895-903.

102. Cantin AM, Hubbard RC, Crystal RG. Glutathione deficiency in the epithelial lining fluid of the lower respiratory tract in idiopathic pulmonary fibrosis. *Am Rev Respir Dis.* 1989 Feb;139(2):370-2.
103. Moore BB, Hogaboam CM. Murine models of pulmonary fibrosis. *Am J Physiol Lung Cell Mol Physiol.* 2008 Feb;294(2):L152-60.
104. Schrier DJ, Kunkel RG, Phan SH. The role of strain variation in murine bleomycin-induced pulmonary fibrosis. *Am Rev Respir Dis.* 1983 Jan;127(1):63-6.
105. Mason RJ. Biology of alveolar type II cells. *Respirology.* 2006 Jan;11 Suppl:S12-5.
106. Herst PM, Berridge MV. Cell surface oxygen consumption: A major contributor to cellular oxygen consumption in glycolytic cancer cell lines. *Biochim Biophys Acta.* 2007 Feb;1767(2):170-7.
107. Zhang J, Khvorostov I, Hong JS, Oktay Y, Vergnes L, Nuebel E, et al. UCP2 regulates energy metabolism and differentiation potential of human pluripotent stem cells. *EMBO J.* 2011 Nov 15;30(24):4860-73.
108. Fox RE, Hopkins IB, Cabacungan EB, Tildon JT. The role of glutamine as an energy source in the developing rat lung. *J Nutr.* 1996 Apr;126(4 Suppl):1131S-6S.
109. Moruzzi N, Del Sole M, Fato R, Gerdes JM, Berggren PO, Bergamini C, et al. Short and prolonged exposure to hyperglycaemia in human fibroblasts and endothelial cells: Metabolic and osmotic effects. *Int J Biochem Cell Biol.* 2014 Aug;53:66-76.
110. Dranka BP, Hill BG, Darley-Usmar VM. Mitochondrial reserve capacity in endothelial cells: The impact of nitric oxide and reactive oxygen species. *Free Radic Biol Med.* 2010 Apr 1;48(7):905-14.
111. Sridharan V, Guichard J, Li CY, Muise-Helmericks R, Beeson CC, Wright GL. O(2)-sensing signal cascade: Clamping of O(2) respiration, reduced ATP utilization, and inducible fumarate respiration. *Am J Physiol Cell Physiol.* 2008 Jul;295(1):C29-37.
112. Yao J, Chen S, Mao Z, Cadenas E, Brinton RD. 2-deoxy-D-glucose treatment induces ketogenesis, sustains mitochondrial function, and reduces

pathology in female mouse model of alzheimer's disease. PLoS One. 2011;6(7):e21788.

113. Nicholls DG, Darley-Usmar VM, Wu M, Jensen PB, Rogers GW, Ferrick DA. Bioenergetic profile experiment using C2C12 myoblast cells. J Vis Exp. 2010 Dec 6;(46). pii: 2511. doi(46):10.3791/2511.

114. Shimoda LA, Semenza GL. HIF and the lung: Role of hypoxia-inducible factors in pulmonary development and disease. Am J Respir Crit Care Med. 2011 Jan 15;183(2):152-6.

115. Lee YM, Jeong CH, Koo SY, Son MJ, Song HS, Bae SK, et al. Determination of hypoxic region by hypoxia marker in developing mouse embryos in vivo: A possible signal for vessel development. Dev Dyn. 2001 Feb;220(2):175-86.

116. Saini Y, Harkema JR, LaPres JJ. HIF1alpha is essential for normal intrauterine differentiation of alveolar epithelium and surfactant production in the newborn lung of mice. J Biol Chem. 2008 Nov 28;283(48):33650-7.

117. Compennolle V, Brusselmans K, Acker T, Hoet P, Tjwa M, Beck H, et al. Loss of HIF-2alpha and inhibition of VEGF impair fetal lung maturation, whereas treatment with VEGF prevents fatal respiratory distress in premature mice. Nat Med. 2002 Jul;8(7):702-10.

118. Mungai PT, Waypa GB, Jairaman A, Prakriya M, Dokic D, Ball MK, et al. Hypoxia triggers AMPK activation through reactive oxygen species-mediated activation of calcium release-activated calcium channels. Mol Cell Biol. 2011 Sep;31(17):3531-45.

119. Routsis C, Bardouniotou H, Delivoria-Ioannidou V, Kazi D, Roussos C, Zakynthinos S. Pulmonary lactate release in patients with acute lung injury is not attributable to lung tissue hypoxia. Crit Care Med. 1999 Nov;27(11):2469-73.

120. Wiesener MS, Jurgensen JS, Rosenberger C, Scholze CK, Horstrup JH, Warnecke C, et al. Widespread hypoxia-inducible expression of HIF-2alpha in distinct cell populations of different organs. FASEB J. 2003 Feb;17(2):271-3.

121. He XY, Shi XY, Yuan HB, Xu HT, Li YK, Zou Z. Propofol attenuates hypoxia-induced apoptosis in alveolar epithelial type II cells through down-regulating hypoxia-inducible factor-1alpha. Injury. 2012 Mar;43(3):279-83.

122. Krick S, Eul BG, Hanze J, Savai R, Grimminger F, Seeger W, et al. Role of hypoxia-inducible factor-1alpha in hypoxia-induced apoptosis of primary alveolar epithelial type II cells. *Am J Respir Cell Mol Biol*. 2005 May;32(5):395-403.
123. Wagner KF, Hellberg AK, Balenger S, Depping R, Dodd-O J, Johns RA, et al. Hypoxia-induced mitogenic factor has antiapoptotic action and is upregulated in the developing lung: Coexpression with hypoxia-inducible factor-2alpha. *Am J Respir Cell Mol Biol*. 2004 Sep;31(3):276-82.
124. Yadava N, Nicholls DG. Spare respiratory capacity rather than oxidative stress regulates glutamate excitotoxicity after partial respiratory inhibition of mitochondrial complex I with rotenone. *J Neurosci*. 2007 Jul 4;27(27):7310-7.
125. Pescador N, Villar D, Cifuentes D, Garcia-Rocha M, Ortiz-Barahona A, Vazquez S, et al. Hypoxia promotes glycogen accumulation through hypoxia inducible factor (HIF)-mediated induction of glycogen synthase 1. *PLoS One*. 2010 Mar 12;5(3):e9644.
126. Granja S, Morais-Santos F, Miranda-Goncalves V, Viana-Ferreira M, Nogueira R, Nogueira-Silva C, et al. The monocarboxylate transporter inhibitor alpha-cyano-4-hydroxycinnamic acid disrupts rat lung branching. *Cell Physiol Biochem*. 2013;32(6):1845-56.
127. Fisher AB, Dodia C. Lactate and regulation of lung glycolytic rate. *Am J Physiol*. 1984 May;246(5 Pt 1):E426-9.
128. Luft FC. Lactic acidosis update for critical care clinicians. *J Am Soc Nephrol*. 2001 Feb;12 Suppl 17:S15-9.
129. Patterson CE, Rhoades RA. Substrate utilization in the perinatal lung. *Am J Physiol*. 1989 Dec;257(6 Pt 1):L318-30.
130. Gharaee-Kermani M, Hu B, Phan SH, Gyetko MR. Recent advances in molecular targets and treatment of idiopathic pulmonary fibrosis: Focus on TGFbeta signaling and the myofibroblast. *Curr Med Chem*. 2009;16(11):1400-17.
131. Wynn TA. Integrating mechanisms of pulmonary fibrosis. *J Exp Med*. 2011 Jul 4;208(7):1339-50.
132. Lee JS, Song JW, Wolters PJ, Elicker BM, King TE, Jr, Kim DS, et al. Bronchoalveolar lavage pepsin in acute exacerbation of idiopathic pulmonary fibrosis. *Eur Respir J*. 2012 Feb;39(2):352-8.

133. Noble PW, Barkauskas CE, Jiang D. Pulmonary fibrosis: Patterns and perpetrators. *J Clin Invest*. 2012 Aug 1;122(8):2756-62.
134. Molyneaux PL, Maher TM. The role of infection in the pathogenesis of idiopathic pulmonary fibrosis. *Eur Respir Rev*. 2013 Sep 1;22(129):376-81.
135. Kliment CR, Oury TD. Oxidative stress, extracellular matrix targets, and idiopathic pulmonary fibrosis. *Free Radic Biol Med*. 2010 Sep 1;49(5):707-17.
136. Kunchithapautham K, Atkinson C, Rohrer B. Smoke exposure causes endoplasmic reticulum stress and lipid accumulation in retinal pigment epithelium through oxidative stress and complement activation. *J Biol Chem*. 2014 May 23;289(21):14534-46.
137. Aravamudan B, Kiel A, Freeman M, Delmotte P, Thompson M, Vassallo R, et al. Cigarette smoke-induced mitochondrial fragmentation and dysfunction in human airway smooth muscle. *Am J Physiol Lung Cell Mol Physiol*. 2014 May 1;306(9):L840-54.
138. Guo L, Li L, Wang W, Pan Z, Zhou Q, Wu Z. Mitochondrial reactive oxygen species mediates nicotine-induced hypoxia-inducible factor-1alpha expression in human non-small cell lung cancer cells. *Biochim Biophys Acta*. 2012 Jun;1822(6):852-61.
139. Agarwal AR, Yin F, Cadenas E. Short-term cigarette smoke exposure leads to metabolic alterations in lung alveolar cells. *Am J Respir Cell Mol Biol*. 2014 Aug;51(2):284-93.
140. Kim SJ, Cheresh P, Williams D, Cheng Y, Ridge K, Schumacker PT, et al. Mitochondria-targeted Ogg1 and aconitase-2 prevent oxidant-induced mitochondrial DNA damage in alveolar epithelial cells. *J Biol Chem*. 2014 Feb 28;289(9):6165-76.
141. Liu G, Beri R, Mueller A, Kamp DW. Molecular mechanisms of asbestos-induced lung epithelial cell apoptosis. *Chem Biol Interact*. 2010 Nov 5;188(2):309-18.
142. Wu M, Neilson A, Swift AL, Moran R, Tamagnine J, Parslow D, et al. Multiparameter metabolic analysis reveals a close link between attenuated mitochondrial bioenergetic function and enhanced glycolysis dependency in human tumor cells. *Am J Physiol Cell Physiol*. 2007 Jan;292(1):C125-36.

143. Kasper M, Haroske G. Alterations in the alveolar epithelium after injury leading to pulmonary fibrosis. *Histol Histopathol.* 1996 Apr;11(2):463-83.
144. Chroneos ZC, Sever-Chroneos Z, Shepherd VL. Pulmonary surfactant: An immunological perspective. *Cell Physiol Biochem.* 2010;25(1):13-26.
145. Lawson WE, Polosukhin VV, Stathopoulos GT, Zoia O, Han W, Lane KB, et al. Increased and prolonged pulmonary fibrosis in surfactant protein C-deficient mice following intratracheal bleomycin. *Am J Pathol.* 2005 Nov;167(5):1267-77.
146. Willis BC, Liebler JM, Luby-Phelps K, Nicholson AG, Crandall ED, du Bois RM, et al. Induction of epithelial-mesenchymal transition in alveolar epithelial cells by transforming growth factor-beta1: Potential role in idiopathic pulmonary fibrosis. *Am J Pathol.* 2005 May;166(5):1321-32.
147. Perron NR, Beeson C, Rohrer B. Early alterations in mitochondrial reserve capacity; a means to predict subsequent photoreceptor cell death. *J Bioenerg Biomembr.* 2012 Oct 23.
148. Hulbert AJ, Pamplona R, Buffenstein R, Buttemer WA. Life and death: Metabolic rate, membrane composition, and life span of animals. *Physiol Rev.* 2007 Oct;87(4):1175-213.
149. Trawick E, Phipps R, Sime P, Kottmann R. Lactate dehydrogenase inhibitor gossypol inhibits lung fibroblast to myofibroblast differentiation. Poster presented at: American Thoracic Society International Conference. 2014 May 16-21; San Diego, CA.
150. Kottmann R, Owens K, Narrow W, Lyda E, Phipps R, Sime P. The lactate dehydrogenase inhibitor gossypol inhibits bleomycin induced pulmonary fibrosis. Poster presented at: American Thoracic Society International Conference. 2014 May 16-21; San Diego, CA.
151. Doherty JR, Cleveland JL. Targeting lactate metabolism for cancer therapeutics. *J Clin Invest.* 2013 Sep 3;123(9):3685-92.
152. Miranda-Goncalves V, Honavar M, Pinheiro C, Martinho O, Pires MM, Pinheiro C, et al. Monocarboxylate transporters (MCTs) in gliomas: Expression and exploitation as therapeutic targets. *Neuro Oncol.* 2013 Feb;15(2):172-88.
153. Colen CB, Shen Y, Ghoddoussi F, Yu P, Francis TB, Koch BJ, et al. Metabolic targeting of lactate efflux by malignant glioma inhibits invasiveness and induces necrosis: An in vivo study. *Neoplasia.* 2011 Jul;13(7):620-32.

154. O'Brodovich HM, Mellins RB. Bronchopulmonary dysplasia. unresolved neonatal acute lung injury. *Am Rev Respir Dis*. 1985 Sep;132(3):694-709.
155. Pagano A, Barazzone-Argiroffo C. Alveolar cell death in hyperoxia-induced lung injury. *Ann N Y Acad Sci*. 2003 Dec;1010:405-16.
156. Bin-Jaliah I, Dallak M, Haffor AS. Effect of hyperoxia on the ultrastructural pathology of alveolar epithelium in relation to glutathione peroxidase, lactate dehydrogenase activities, and free radical production in rats, *rattus norvigicus*. *Ultrastruct Pathol*. 2009;33(3):112-22.
157. Allen CB, Guo XL, White CW. Changes in pulmonary expression of hexokinase and glucose transporter mRNAs in rats adapted to hyperoxia. *Am J Physiol*. 1998 Mar;274(3 Pt 1):L320-9.
158. Gardner PR, Nguyen DD, White CW. Aconitase is a sensitive and critical target of oxygen poisoning in cultured mammalian cells and in rat lungs. *Proc Natl Acad Sci U S A*. 1994 Dec 6;91(25):12248-52.
159. Yan LJ, Levine RL, Sohal RS. Oxidative damage during aging targets mitochondrial aconitase. *Proc Natl Acad Sci U S A*. 1997 Oct 14;94(21):11168-72.
160. Morton RL, Ikle D, White CW. Loss of lung mitochondrial aconitase activity due to hyperoxia in bronchopulmonary dysplasia in primates. *Am J Physiol*. 1998 Jan;274(1 Pt 1):L127-33.
161. Ratner V, Starkov A, Matsiukevich D, Polin RA, Ten VS. Mitochondrial dysfunction contributes to alveolar developmental arrest in hyperoxia-exposed mice. *Am J Respir Cell Mol Biol*. 2009 May;40(5):511-8.
162. Warburton D. Developmental responses to lung injury: Repair or fibrosis. *Fibrogenesis Tissue Repair*. 2012 Jun 6;5(Suppl 1 Proceedings of Fibroproliferative disorders: from biochemical analysis to targeted therapies Petro E Petrides and David Brenner):S2.
163. Buckley S, Shi W, Barsky L, Warburton D. TGF-beta signaling promotes survival and repair in rat alveolar epithelial type 2 cells during recovery after hyperoxic injury. *Am J Physiol Lung Cell Mol Physiol*. 2008 Apr;294(4):L739-48.
164. Gauldie J, Galt T, Bonniaud P, Robbins C, Kelly M, Warburton D. Transfer of the active form of transforming growth factor-beta 1 gene to newborn rat lung

induces changes consistent with bronchopulmonary dysplasia. *Am J Pathol*. 2003 Dec;163(6):2575-84.

165. Vicencio AG, Lee CG, Cho SJ, Eickelberg O, Chuu Y, Haddad GG, et al. Conditional overexpression of bioactive transforming growth factor-beta1 in neonatal mouse lung: A new model for bronchopulmonary dysplasia? *Am J Respir Cell Mol Biol*. 2004 Dec;31(6):650-6.

166. Dasgupta C, Sakurai R, Wang Y, Guo P, Ambalavanan N, Torday JS, et al. Hyperoxia-induced neonatal rat lung injury involves activation of TGF- β and wnt signaling and is protected by rosiglitazone. *Am J Physiol Lung Cell Mol Physiol*. 2009 Jun;296(6):L1031-41.

167. Alejandre-Alcazar MA, Kwapiszewska G, Reiss I, Amarie OV, Marsh LM, Sevilla-Perez J, et al. Hyperoxia modulates TGF-beta/BMP signaling in a mouse model of bronchopulmonary dysplasia. *Am J Physiol Lung Cell Mol Physiol*. 2007 Feb;292(2):L537-49.

168. Liu J, Tseu I, Wang J, Tanswell K, Post M. Transforming growth factor beta2, but not beta1 and beta3, is critical for early rat lung branching. *Dev Dyn*. 2000 Apr;217(4):343-60.

169. Lecart C, Cayabyab R, Buckley S, Morrison J, Kwong KY, Warburton D, et al. Bioactive transforming growth factor-beta in the lungs of extremely low birthweight neonates predicts the need for home oxygen supplementation. *Biol Neonate*. 2000 May;77(4):217-23.

170. Wikenheiser KA, Vorbroker DK, Rice WR, Clark JC, Bachurski CJ, Oie HK, et al. Production of immortalized distal respiratory epithelial cell lines from surfactant protein C/simian virus 40 large tumor antigen transgenic mice. *Proc Natl Acad Sci U S A*. 1993 Dec 1;90(23):11029-33.

171. Baatz JE, Newton DA, Riemer EC, Denlinger CE, Jones EE, Drake RR, et al. Cryopreservation of viable human lung tissue for versatile post-thaw analyses and culture. *In Vivo*. 2014 Jul-Aug;28(4):411-23.

172. Gerencser AA, Neilson A, Choi SW, Edman U, Yadava N, Oh RJ, et al. Quantitative microplate-based respirometry with correction for oxygen diffusion. *Anal Chem*. 2009 Aug 15;81(16):6868-78.

173. Ranall MV, Gabrielli BG, Gonda TJ. Adaptation and validation of DNA synthesis detection by fluorescent dye derivatization for high-throughput screening. *BioTechniques*. 2010 May;48(5):379-86.

BIOGRAPHY

Robyn was born and raised in Juneau, Alaska, and graduated from the University of Kansas in 2008 with a Bachelor's Degree in Biodiversity, Ecology, & Evolutionary Biology. While she had long held a deep passion for marine science and oceanography, in the final semesters of her undergraduate education she became increasingly interested in biomedical science. Wishing to combine these interests into one graduate experience, she discovered the MUSC Marine Biomedicine & Environmental Sciences program and matriculated in 2010.

As a member of the Baatz lab, Robyn has been dedicated to understanding the complex contributions of cellular metabolism to lung disease, with additional research interests in neonatal lung development and diseases of prematurity. As a student at MUSC she has been invested in a variety of professional pursuits including teaching and mentoring at the undergraduate and graduate levels with the College of Charleston Biology Department and the Summer Undergraduate Research Program at MUSC, and involvement in outreach activities focused on educating the public about the inextricable overlap between human and environmental health. Most recently, she has extended her interests into the clinical realm, working as part of a team researching the effects of Vitamin D supplementation during pregnancy.

Beyond the lab, classroom, and clinic, Robyn and her husband James live the good life in James Island SC.